

GPO PRICE \$ \_\_\_\_\_  
CFSTI PRICE(S) \$ \_\_\_\_\_  
Hard copy (HC) 7.00  
Microfiche (MF) 2.00  
# 653 July 65

N66 37361  
(ACCESSION NUMBER)  
372  
(PAGES)  
CR-66173  
(NASA CR OR TMX OR AD NUMBER)  
(THRU)  
1  
(CODE)  
31  
(CATEGORY)

MISSILE & SPACE SYSTEMS DIVISION  
DOUGLAS AIRCRAFT COMPANY, INC.  
SANTA MONICA/CALIFORNIA

Distribution of this report is provided in the interest of  
information exchange. Responsibility for the contents  
resides in the author or organization that prepared it.



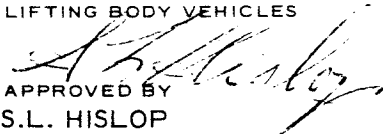
PHASE II STUDY OF HEAD-END STEERING  
FOR A SIMPLIFIED MANNED SPACE VEHICLE

MARCH 1966

DOUGLAS REPORT SM-51872

PREPARED FOR NATIONAL AERONAUTICS  
AND SPACE ADMINISTRATION, LANGLEY  
RESEARCH CENTER, LANGLEY FIELD,  
VIRGINIA, CONTRACT NO. NAS1-5451

PREPARED BY  
G.M. FULLER  
PROJECT ENGINEER  
LIFTING BODY VEHICLES

APPROVED BY   
S.L. HISLOP  
PROGRAM MANAGER  
LIFTING BODY VEHICLES

APPROVED BY   
R.J. GUNKEL  
DIRECTOR  
ADVANCE MANNED SPACECRAFT SYSTEMS  
ADVANCE SYSTEMS AND TECHNOLOGY

**DOUGLAS MISSILE & SPACE SYSTEMS DIVISION**

## ABSTRACT

The Phase II study of head-end steering for a simplified manned space vehicle was conducted by the Douglas Aircraft Company, Inc., for the National Aeronautics and Space Administration's Langley Research Center (NASA-LRC), under Contract NAS1-5451. This study was motivated by a continuing NASA interest in the reduction of costs and system complexity for manned space operations.

The Phase I study resulted in a manned space vehicle concept which had as a baseline the logistics support of a space station in low Earth orbit at an altitude of 300 nmi. The spacecraft configuration featured (1) an HL-10 lifting body with the capability of transporting up to 11 passengers and 2 crewmen; (2) a booster steering and in-orbit maneuvering propulsion system located in the HL-10; (3) design maximum cargo provisions for up to 5,000 lb. in the HL-10 and up to 18,750 lb. in the cargo-module adapter; and (4) a 3-stage solid-propellant booster system. The 3-stage booster consisted of 260-in. diameter 1st and 2nd stages and a 156-in. diameter 3rd stage. Steering thrust vector control was accomplished entirely from the HL-10 spacecraft.

Key questions identified in the Phase I study were the basis for the objectives of the Phase II study. The two broad objectives were (1) to refine and optimize the system concept developed in the Phase I study, and (2) to perform a first order comparison of the improved vehicle with other system concepts in a manner which would isolate the performance and cost effects of steering technique, launch vehicle propulsion, and the spacecraft configuration.

The conclusions drawn from the results of the Phase II study are grouped according to the three major task areas: vehicle refinement and optimization, system definition, and comparative studies.

## PREFACE

This document is submitted to the National Aeronautics and Space Administration's Langley Research Center in response to Contract No. NAS 1-5451. It presents a report by the Douglas Aircraft Company, Inc. , on the Phase II study of head-end steering for a simplified manned space vehicle. A summary of this report may be found in Douglas Report SM-53104.



## CONTENTS

Section 1	INTRODUCTION AND SUMMARY	1
	1.1 Vehicle Refinement and Optimization	2
	1.2 System Definition	3
	1.3 Comparison Studies	4
Section 2	BACKGROUND	9
	2.1 Economic Analyses	9
	2.2 System Concept	15
	2.3 The Phase I Study	17
Section 3	DISCUSSION OF TECHNICAL AND ECONOMIC ANALYSES	25
	3.1 Vehicle Refinement and Optimization	25
	3.2 System Description	118
	3.3 Comparative Studies	146
Section 4	CONCLUSIONS	323
	4.1 Vehicle Refinement and Optimization (Section 3.1)	323
	4.2 System Definition (Section 3.2)	324
	4.3 Comparison Studies (Section 3.3)	324
Section 5	RECOMMENDATIONS FOR FUTURE STUDY	325
	5.1 Vehicle Refinement and Optimization (Section 3.1)	325
	5.2 System Definition (Section 3.2)	325
	5.3 Comparison Studies (Section 3.3)	325
	5.4 Additional Study Steps	326
Section 6	REFERENCES	327

## FIGURES

1-1	Manned Space Vehicle Comparisons	7
2-1	Economic Risk	10
2-2	Development Engineering Costs	11
2-3	Distribution of Direct Operating Costs	12
2-4	Distribution of Direct Operating Costs (No Spacecraft)	13
2-5	Effect of Reusability--100,000-lb Spacecraft	14
2-6	The System Concept	16
2-7	Phase I Study--Possible Arrangement Spacecraft	20
2-8	HES-2G Spacecraft	21
2-9	Phase I Study--Booster Motors	22
2-10	Phase I Study--Resultant Vehicle Configuration	23
2-11	Phase I Study Summary--Economic Feasibility Cost Effectiveness	24
3-1	Major Study Task Areas	26
3-2	Performance Capability, HES-2G	28
3-3	Crew-Cargo Arrangement, HES-2G	29
3-4	Phase II Solid-Propellant Theoretical Performance	31
3-5	First-Stage Nozzle Optimization Effect on Specific Impulse	32
3-6	First-Stage Nozzle Optimization Effect on Mass Fraction	32
3-7	First-Stage Nozzle Optimization Effect of Expansion Ratio	33
3-8	First-Stage Nozzle Optimization Effect of Nozzle Divergence	34
3-9	Third-Stage Characteristics ( $W_{p_3} = 526,100 \text{ lb}$ )	35
3-10	Third-Stage Optimization ( $W_{p_3} = 526,100 \text{ lb}$ )	35

3-11	Third-Stage Characteristics ( $W_{P_3} = 250,000 \text{ lb}$ )	36
3-12	Third-Stage Nozzle Optimization ( $W_{P_3} = 250,000 \text{ lb}$ )	36
3-13	Effect of Third-Stage Propellant Weight on Maximum Control Thrust	38
3-14	Effect of Stage Velocity Distribution on Total Motor Cost	39
3-15	Typical Third-Stage Control Thrust Histories	41
3-16	Effect on Regressivity on Control Requirements	42
3-17	Control Engine Geometry for Maximum Yaw Steering Moment--Configuration I	46
3-18	Steering Engine Step Throttling	47
3-19	Yaw-Control Moment Effectiveness Differential Throttling	48
3-20	Effects of Differential Throttling	50
3-21	Aerodynamic Pitch Moments--Phase I, HES-2G	57
3-22	Aerodynamic Yaw Moments--Phase II, Configuration I--Total Yaw Moment	58
3-23	Aerodynamic Pitch Moments--Phase II, Configuration I--Total Pitch Control	59
3-24	Effect of Off-Optimum Pitch Fins	61
3-25	Effect of Pitch Fin Planform Shape, Yaw Fin-- $R = 2.0$ , $b/2 = 8.0 \text{ ft}$	62
3-26	Effect of Yaw Fin Planform Shape, Pitch Fins-- $R = 4.0$ , $b/2 = 12.0 \text{ ft}$	63
3-27	Effect of Aerodynamic Phenomena on Optimum Fin-Span Selection	64
3-28	First-Stage Composite Control-Thrust Requirements--Configuration I	66
3-29	The Escape Problem	72
3-30	Escape Rocket Sizing Chart, Pad Abort	73
3-31	Effect of TNT Equivalence on Payload, Launch Pad Abort	75
3-32	Pad Abort Recovery Profile	78
3-33	Spacecraft Range Capability, Pad Abort	79
3-34	Relative Separation Distance, Abort Escape at Maximum Dynamic Pressure	82
3-35	Ground Trace of Flight Path, Maximum Dynamic Pressure Abort	83

3-36	Flight Conditions--Escape and Turn Phase, Maximum Dynamic Pressure Abort	84
3-37	Ground Trace of Flight Profile, Maximum Dynamic Pressure Abort	85
3-38	Flight Conditions, Maximum Dynamic Pressure Abort	86
3-39	Steering-Failure Mode, Maximum Dynamic Pressure Abort	88
3-40	EI Distribution--Configuration I	92
3-41	Bending Mode Shapes--Configuration I, $t = 0$	93
3-42	Bending Mode Shapes--Configuration I, $t = 70$ sec	94
3-43	Flexible Vehicle Control System Model	95
3-44	Vehicle Time Response to Unit $\theta$ Step Command Configuration I, $t = 0$	98
3-45	Vehicle Time Response to Unit $\theta$ Step Command Configuration I, $t = 70$ sec	99
3-46	Nyquist Diagram--Configuration I, $t = 0$	101
3-47	Nyquist Diagram--Configuration I, $t = 70$ sec	101
3-48	Nyquist Diagram--Configuration I, $t = 0$	102
3-49	Nyquist Diagram--Configuration I, $t = 70$ sec	103
3-50	Nyquist Diagram--Configuration I, $t = 0$	104
3-51	Nyquist Diagram--Configuration I, $t = 70$ sec	105
3-52	Nyquist Diagram--Configuration I, $t = 0$	106
3-53	Nyquist Diagram--Configuration I, $t = 70$ sec	107
3-54	Nyquist Diagram--Configuration I, $t = 0$	108
3-55	Nyquist Diagram--Configuration I, $t = 70$ sec	109
3-56	Stage Velocity Optimization	111
3-57	Control Thrust History, Phases I and II	112
3-58	Relation of Wind Profiles and Wind Profile Envelopes	116
3-59	System Operations	119
3-60	Spacecraft Dissassembled for Shipment in C-5A	122
3-61	Configuration I Spacecraft Adapter and Launch Vehicle Master Flow Chart	124
3-62	Conceptual Ground Handling Plan--Configuration I Space System	125
3-63	Launch Vehicle Processing Time	127
3-64	New Spacecraft Processing Time	130

3-65	Used Spacecraft Processing Schedule	132
3-66	Prelaunch and Launch Countdown Phases	134
3-67	Recovery Site Key Sequence Time	139
3-68	Recovery Site Events and Detail Operations, Configuration I Spacecraft	140
3-69	Refurbishment Model	142
3-70	Spacecraft--Configurations I, II, VII, VIII Extended MORL Mission	152
3-71	Spacecraft--Configurations III, IV, V LORL Mission	153
3-72	Spacecraft--Configuration VI LORL Mission	154
3-73	Reliability Model	155
3-74	Reliability Time Bases	157
3-75	Cost Model	158
3-76	Average Cost of Solid-Propellant Motors	162
3-77	Primary Thrust Vector Control Techniques	165
3-78	General Arrangement--Configuration I	169
3-79	Control Thrust History--Configuration I	173
3-80	Trajectory Characteristics--Configuration I	175
3-81	Trajectory Characteristics--Configuration I	176
3-82	General Arrangement--Configuration II	183
3-83	Trajectory Characteristics--Configuration II	188
3-84	Trajectory Characteristics--Configuration II	189
3-85	General Arrangement--Configuration III	196
3-86	Trajectory Characteristics--Configuration III	198
3-87	General Arrangement--Configuration IV	205
3-88	Control Thrust History--Configuration IV	207
3-89	Trajectory Characteristics--Configuration IV	209
3-90	Trajectory Characteristics--Configuration IV	210
3-91	General Arrangement--Configuration V	214
3-92	Trajectory Characteristics--Configuration V	219
3-93	Trajectory Characteristics--Configuration V	220
3-94	General Arrangement--Configuration VI	225
3-95	Control Thrust History--Configuration VI	228
3-96	Trajectory Characteristics--Configuration VI	231
3-97	Trajectory Characteristics--Configuration VI	232

3-98	General Arrangement--Configuration VII	238
3-99	Control Thrust History (First Stage)-- Configuration VII	242
3-100	Trajectory Characteristics--Configuration VII	244
3-101	Trajectory Characteristics--Configuration VII	245
3-102	General Arrangement--Configuration VIII	250
3-103	Trajectory Characteristics--Configuration VIII	255
3-104	Trajectory Characteristics--Configuration VIII	256
3-105	Effect of Steering Technique on Gross Vehicle Size--Extended MORL Mission	262
3-106	Effect of Steering Technique on Gross Vehicle Size--LORL Mission	271
3-107	Effect of Launch Vehicle Propulsion on Gross Vehicle Size--LORL Mission	279
3-108	Effect of Launch Vehicle Propulsion on Gross Vehicle Size--Extended MORL Mission	286
3-109	Effect of Spacecraft Configuration on Gross Vehicle Size--LORL Mission	296
3-110	Effect of Total System Concept on Gross Vehicle Size--LORL Mission	306
3-111	Summary--Phase II, Extended MORL Mission Vehicles	314
3-112	Summary--Phase II, LORL Mission Vehicles	315
3-113	Building Block Approach to Payload Increase	322

## Section 1

### INTRODUCTION AND SUMMARY

The Phase II study of head-end steering for a simplified manned space vehicle was conducted by the Douglas Aircraft Company, Inc., for the National Aeronautics and Space Administration's Langley Research Center (NASA-LRC), under Contract NAS 1-5451. This study was motivated by a continuing NASA interest in the reduction of costs and system complexity for manned space operations. The study period extended from July 1965 to February 1966.

The two objectives of the Phase I study, which was completed in December 1964, were (1) to define a system concept which stressed simplicity in the expendable components and reusability in those systems that were recovered and (2) to perform a first-order evaluation of technical and economic feasibility for the system concept.

The Phase I study resulted in a manned space vehicle concept which had as a baseline the logistics support of a space station in low Earth orbit at an altitude of 300 nmi. The spacecraft configuration featured (1) an HL-10 lifting body with the capability of transporting up to 11 passengers and 2 crewmen; (2) a booster steering and in-orbit maneuvering propulsion system located in the HL-10; (3) design maximum cargo provisions for up to 5,000 lb in the HL-10 and up to 18,750 lb in the cargo-module adapter; and (4) a 3-stage solid-propellant booster system. The 3-stage booster consisted of 260-in. diam 1st and 2nd stages and a 156-in. diam 3rd stage. Steering thrust vector control was accomplished entirely from the HL-10 spacecraft.

The results of the Phase I study indicated that the head-end steering system concept possessed the following attributes:

1. Technical feasibility.
2. The potential for a sizable reduction of operations costs.
3. Significant reduction in launch pad occupancy time.
4. Faster response times.

Several key questions were identified at the end of the Phase I Study:

1. How much system optimization is possible?
2. What is the relative reliability inherent in the system concept?
3. What part of the total cost reduction potential could be attributed to the following:
  - A. Head-end steering?
  - B. Launch vehicle propulsion?
  - C. Spacecraft configuration?

Therefore, the objectives undertaken in the Phase II study were (1) to refine and optimize the system concept developed in the Phase I study, and (2) to perform a first order comparison of the improved vehicle with other system concepts in a manner which would isolate the performance and cost effects of steering technique, launch vehicle propulsion, and the spacecraft configuration.

The conclusions drawn from the results of the Phase II study are grouped according to the three major task areas: vehicle refinement and optimization, system definition, and comparative studies.

#### 1.1 VEHICLE REFINEMENT AND OPTIMIZATION

Refinement of the vehicle concentrated on improvement of the aerodynamic representation of the vehicle and on the evaluation of spacecraft/launch vehicle compatibility. Optimization was pursued only in those areas where it was clear that major reductions could be made in vehicle size. Cost optimizations were not pursued except to indicate the direction that future studies should take. Furthermore, the scope of the study was limited to investigations of the launch vehicle and steering system. Other areas are subsequently discussed in this report under "Recommendations for Future Work."

The following conclusions are presented to indicate major study results within the scope of vehicle refinement and optimization:

1. The use of a regressive thrust-time profile in the third stage, together with an improved step throttling program for the steering engines, resulted in overall weight reduction of 900,000 lb, or 14% with reference to the vehicle defined at the end of the Phase I study.



2. Selection of the launch vehicle tail fin size for producing minimum steering control moments proved to be sensitive to fin plantform shape in the transonic and supersonic regimes of the ascent trajectory.
3. Control system design requirements are state-of-the-art. Satisfactory gain and phase margins are characteristic of the techniques examined in this study. The first bending mode frequency at the most critical time in the flight (at liftoff) is slightly less than 1 cps or approximately the same as Saturn V.
4. The particular level of TNT equivalence specified for abort escape design analyses did not produce significant abort escape system weight penalties.
5. Escape from incipient first-stage motor failures on the launch pad is feasible and the spacecraft may be recovered with a normal horizontal landing at Patrick AFB.
6. Escape from incipient first-stage motor failures at the condition of maximum dynamic pressure is feasible, and the spacecraft may be recovered with a normal horizontal landing at Patrick AFB. This is true also for the case of a steering system failure.
7. Recovery from a high-altitude abort situation produces the most severe dynamic pressure and normal acceleration environment for the spacecraft. Mission ascent profiles used in these analyses for vehicle optimization, however, result in abort recovery dynamic pressures which are less than  $1,200 \text{ lb/ft}^2$  and, in normal accelerations, less than 6 g's.

## 1.2 SYSTEM DEFINITION

The system definition studies were structured to produce better information on the operating characteristics of the head-end steering system concept than was available during the Phase I study. It was desired to provide some clarification of those areas of operations exhibiting significant reductions in complexity and to provide an improved base for predicting total operation cost. The following conclusions summarize the results of this segment of the study:

1. The use of the solid-propellant launch vehicle propulsion with head-end steering will result in significant savings in launch pad occupancy times when compared to all-liquid-propulsion types employing conventional steering.
2. Transportation of the spacecraft from recovery site to refurbishment site in the Super-Guppy aircraft is feasible.
3. Primary refurbishment tasks would be accomplished at the launch site location.

4. Refurbishment analyses made for the 44-ft HL-10 spacecraft employing an all-ablative, double wall thermo-protection system resulted in costs slightly over 10% of spacecraft procurement costs per refurbishment. This cost is that required to bring the spacecraft to the same condition as a new spacecraft when received at Cape Kennedy.

### 1.3 COMPARISON STUDIES

The third major task area was concerned with providing a group of model systems, a comparison of whose characteristics could be used to isolate the performance and cost effects of steering technique, launch vehicle propulsion, and spacecraft configuration. The characteristics of the model systems and the types of comparisons are shown in Table 1-1.

Configuration I is the head-end steering system concept evolved in the Phase I study and refined and optimized in the Phase II study. Configuration II employs secondary liquid injection in the booster motor nozzles for steering control. Through a comparison of Configurations I and II, the effect of steering technique was isolated. Both Configurations I and II were required to perform the extended Manned Orbital Research Laboratory (MORL) mission with a direct ascent to a 300-nmi circular orbit rendezvous.

The next group of four vehicles (Configurations III, IV, V, and VI) was required to perform the Large Orbital Research Laboratory (LORL) mission with a space station rendezvous at 260 nmi, employing a Hohman transfer from a 105-nmi parking orbit. The characteristics of these vehicles were selected to enable a separate identification of performance and cost effect resulting from steering technique, launch vehicle propulsion, and spacecraft configuration and from the combined effect of all three of these characteristics.

The third group of vehicles (Configurations VII and VIII) has mission requirements which are nearly the same as for Configurations I and II. They differ, however, in that the design orbital altitude is 100 nmi and they possess somewhat lower in-orbit maneuvering capability. This third group was structured to permit a comparison of an all-solid-propellant launch vehicle and a launch vehicle consisting of a solid-propellant first stage and a high-energy liquid upper stage, the S-IVB.

Table 1-1

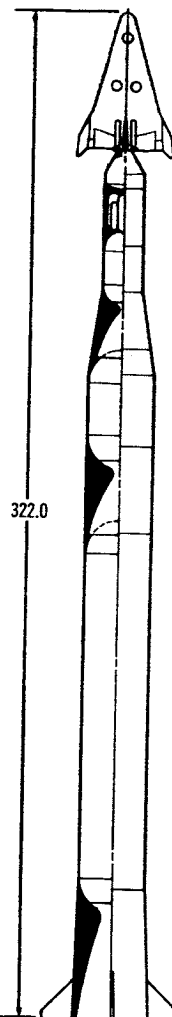
## COMPARATIVE STUDY VEHICLE DESCRIPTION

Configuration	Spacecraft Type	Booster Type	Steering Technique	Mission Description	Type of Comparison
GROUP A					
I	HL-10	Solid	HES	Extended MORL	Effect of Steering Technique
II	HL-10	Solid	PTVC	Extended MORL	
GROUP B					
III	BALLOS	Liquid (Saturn IB)	PTVC	BALLOS-LORL	Effect of L/V Propulsion Effect of Steering Technique Effect of Spacecraft
IV	BALLOS	Solid	HES	BALLOS-LORL	
V	BALLOS	Solid	PTVC	BALLOS-LORL	
VI	HL-10	Solid	HES	BALLOS-LORL	
GROUP C					
VII	HL-10	Solid - First Stage	HES - First Stage	Extended MORL	Effect of Steering Technique and Upper Stage Propulsion
VIII	HL-10	Liquid - Second Stage Solid	PTVC - Second Stage HES	Extended MORL	

Figure 1-1 is presented to clarify the major system characteristics and the comparison data generated in the study. These data resulted in the following conclusions applicable to manned space vehicles performing logistics missions in low Earth orbit:

1. The performance and cost effectiveness of the head-end steering technique were found to be sensitive to the spacecraft configuration employed.
  - A. Head-end steering integrated with a lifting-body type of spacecraft results in a vehicle which is more cost effective, reliable, and has quicker launch response time than a vehicle which uses conventional thrust vector control techniques.
  - B. Head-end steering when used with a ballistic type of spacecraft results in a vehicle which is less cost effective and less reliable than when conventional steering techniques are employed.
2. The use of lifting body spacecraft significantly reduces space recovery costs for missions requiring high orbit inclinations.
3. Launch vehicles employing all-solid-propellant stages are more cost effective than those employing all-liquid propulsion.
4. A high-energy liquid upper stage when used with a solid-propellant first stage results in a launch vehicle that is competitive in cost and performance with a vehicle which incorporates solid-propellant motors in all stages.
5. The combined effect of all-solid-propellant booster motors, head-end steering, and a lifting body spacecraft results in a vehicle that is twice as cost effective as one which uses all-liquid propulsion, conventional steering, and a ballistic type spacecraft.

A brief examination of all eight vehicles shown in Figure 1-1 indicates some interesting similarities. For instance, the first-stage propellant requirements for Configurations VI, VII, and VIII are nearly the same. The first-stage motor size of VI is smaller by 7.6% than that of VII. The first stage of VIII is 11.8% larger than that of VII. This suggests the incorporation of a first stage designed for the payload class of Configuration VII (96,000 lb ) and used for a configuration similar to VI, with a potential payload capability somewhat in excess of 46,000 lb. Use of this same first stage for Configuration VIII is feasible, but with a small degradation in payload.



MODEL DESIGNATION	I
MISSION	EXT. MORL
CARGO, MAXIMUM (LB)	37,400
NO. OF MEN, MAXIMUM	13
MANEUVER CAPABILITY, BASELINE (FT/SEC)	5,820
GROSS WEIGHT, LIFTOFF (LB)	5,727,830
NUMBER OF STAGES	3
LAUNCH VEHICLE PROPULSION	ALL-SOLID
TYPE OF STEERING	HES
POTENTIAL RELIABILITY REL. TO VI	.986
FIRST FLIGHT COST	59.07/58.99
EXPENDABLE HARDWARE	17.53
SPACECRAFT	38.54
LAUNCH SUPPORT	2.00
RECOVERY SUPPORT *, 30°/90°	1.00/0.92
SUBSEQUENT FLIGHT COST	
(A) 30° ORBIT - 10% REFURB. COST	25.43
(B) 30° ORBIT - EST. REFURB FROM NASA INDUSTRY STUDIES	25.70
(C) 90° ORBIT - 10% REFURB. COST	25.35
(D) 90° ORBIT - EST. REFURB. FROM NASA INDUSTRY STUDIES	25.62
SUBSEQUENT FLT. COST RELATIVE VI	1.49/1.49
(ORBIT - 30°/90°)	
24-HR WAIT TIME	

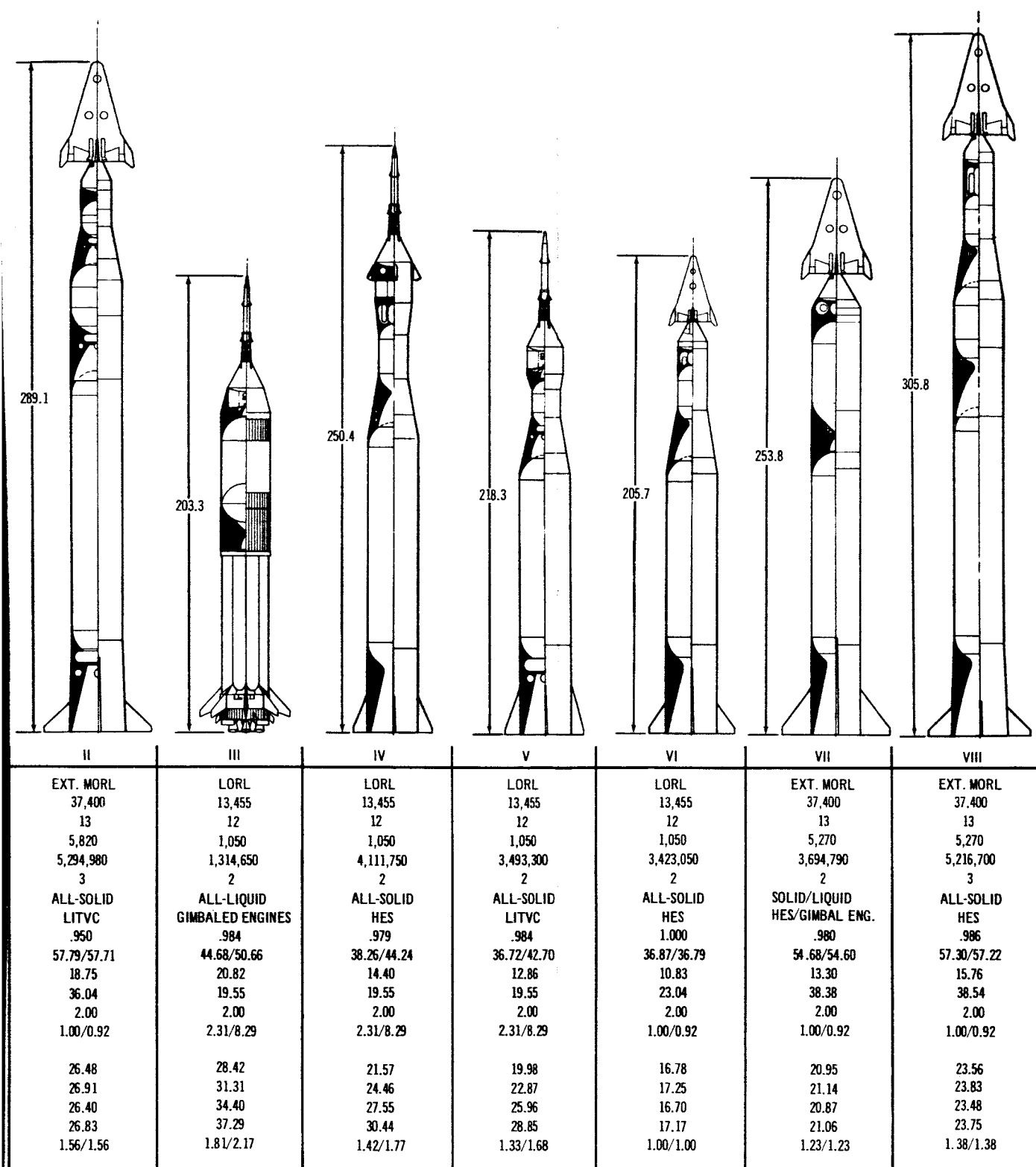


Figure 1-1. Manned Space Vehicle Comparisons

The gross second-stage weight of the S-IVB of Configuration VII (269,070 lb) and the gross third-stage weight of Configuration VIII (307,740 lb) would permit use of the S-IVB as the third stage of Configuration VIII. A significant increase in payload would result.

## Section 2

### BACKGROUND

It is the purpose of this section to discuss several salient economic characteristics of current space launch systems and to show how these characteristics suggested the unique features of the space launch system concept which is the principal subject of this study. The major concern of this study is with manned systems, and it is within this context that the following discussion has developed.

#### 2.1 ECONOMIC ANALYSES

One understood and accepted characteristic of space launch systems is that they are expensive, and that they will tend to become more expensive is an inevitable conclusion if we examine the trends in other aerospace systems of the past. For instance, Figure 2-1 shows the historical development cost increase for transport aircraft. The first time period shown represents the development period of pre-World War II propeller driven aircraft. The 1946 to 1955 time period includes the DC-6's, DC-7's, and Constellation aircraft. High subsonic jet transports were introduced in the 1956 to 1965 time period and will influence, to some extent, the projected future periods of aerospace transport development. The last period shown in this figure is the 1966 to 1975 period, where we may expect to see supersonic and very large subsonic transports developed.

It is interesting to note that, as the aircraft size doubles from period to period, the development costs increase threefold. Size is certainly a factor, but does not explain the total cost increase. Other factors are at work, such as more severe operating requirements, increased demand for greater flexibility in operations, and nontechnical influences.

When costs proceed upward with time at the rate shown, it is clear that there must be fewer programs initiated. Consequently, increased emphasis must be given to developing a high degree of mission flexibility within a given system concept.



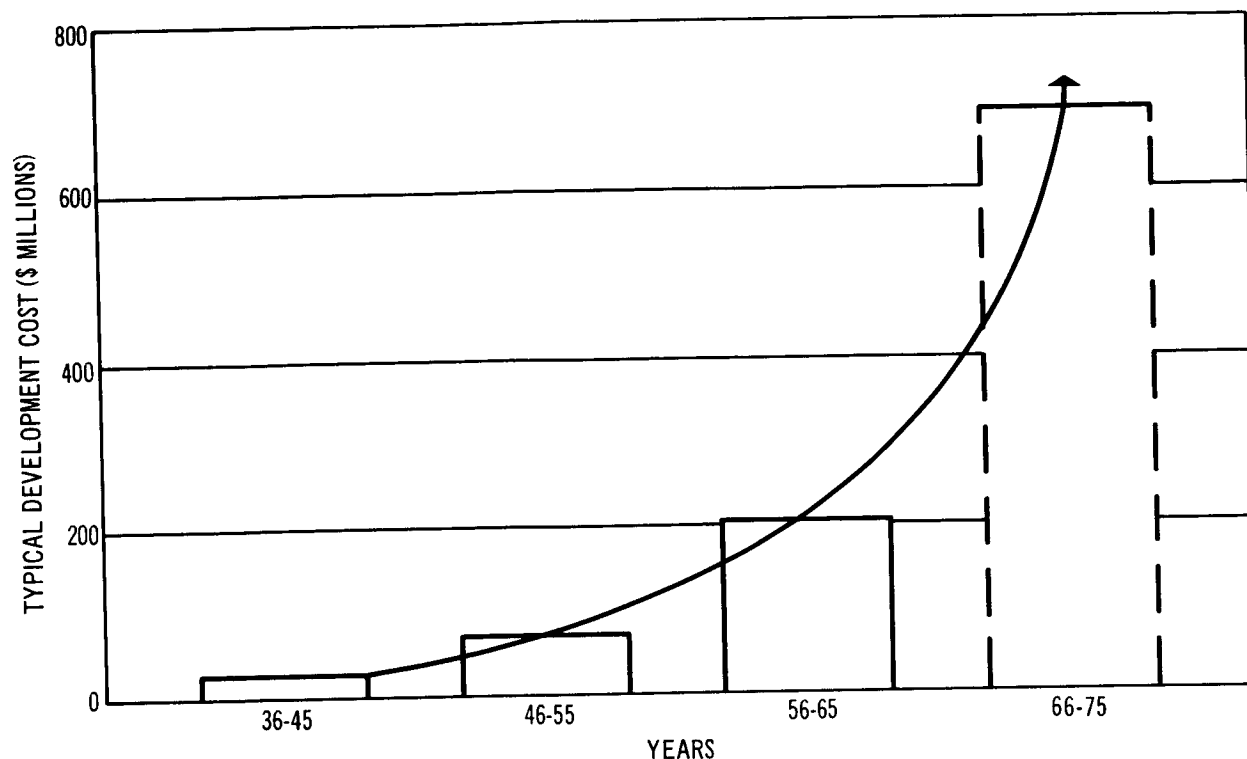


Figure 2-1. Economic Risk

While aircraft have been carrying men from almost the point of inception, the introduction of humans into space vehicles is recent and occurred some time after successful unmanned space missions. It is apparent that significant increases in research, development, test and evaluation (RDT&E) costs for a space vehicle are incurred by the inclusion of man into the system. Figure 2-2 shows this effect on engineering man-hour requirements to develop a number of current and projected space systems. The difference between the upper and lower curves may be attributed not only to man-rating the system, but to providing those additional subsystems required to support man in a space environment and to utilizing his unique capabilities. It will be noted that there is a four-fold increase in engineering man-hour requirements for the integration of man into the system, independent of vehicle size. A not insignificant factor here is the provision for the safe recovery of man back on Earth.

As pointed out earlier, when space systems become more expensive, we have a right to demand that they become more useful, that is, they become more cost effective. One potentially powerful lever for reducing costs is through the

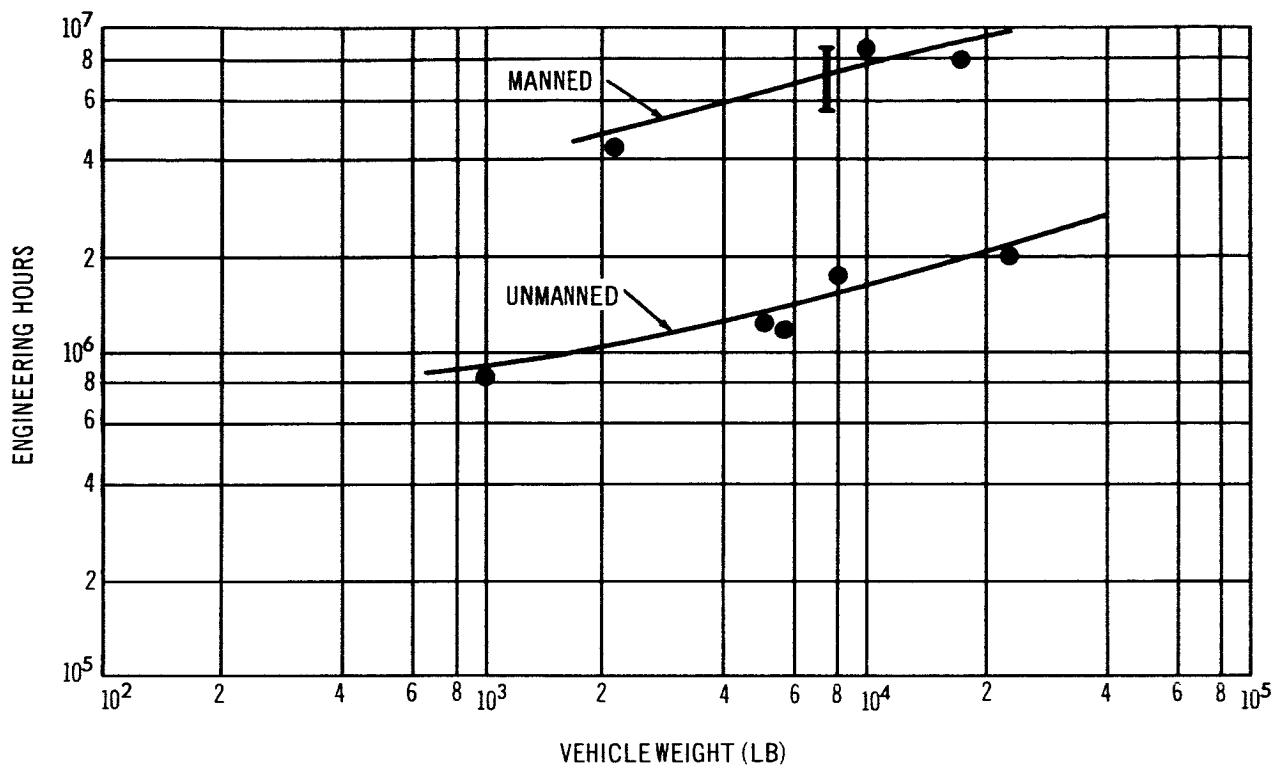


Figure 2-2. Development Engineering Costs

incorporation of reusability in the system concept, not as an after thought, but as a well integrated objective at the inception of the design. Two factors are important at this point: (1) the operational time period and (2) the total number of flights in the program. Determination of these two factors will provide the answer to the question of whether or not it pays to recover and reuse all of the space vehicle system.

For the purpose of this study, a time period has been postulated coincident with the introduction of a manned space station representing the next step beyond the Manned Orbital Laboratory (MOL) program. It is assumed that such a space station will require at least 4 flights a year for 5 years; this could increase ultimately to 20 flights a year if ancillary missions are performed.

For this type of mission environment, it is necessary to examine the distribution of direct operating cost elements in a space vehicle system. Figure 2-3 shows this distribution as a function of spacecraft weight and for the cost elements of launch vehicle procurement, launch support, and recovery support.

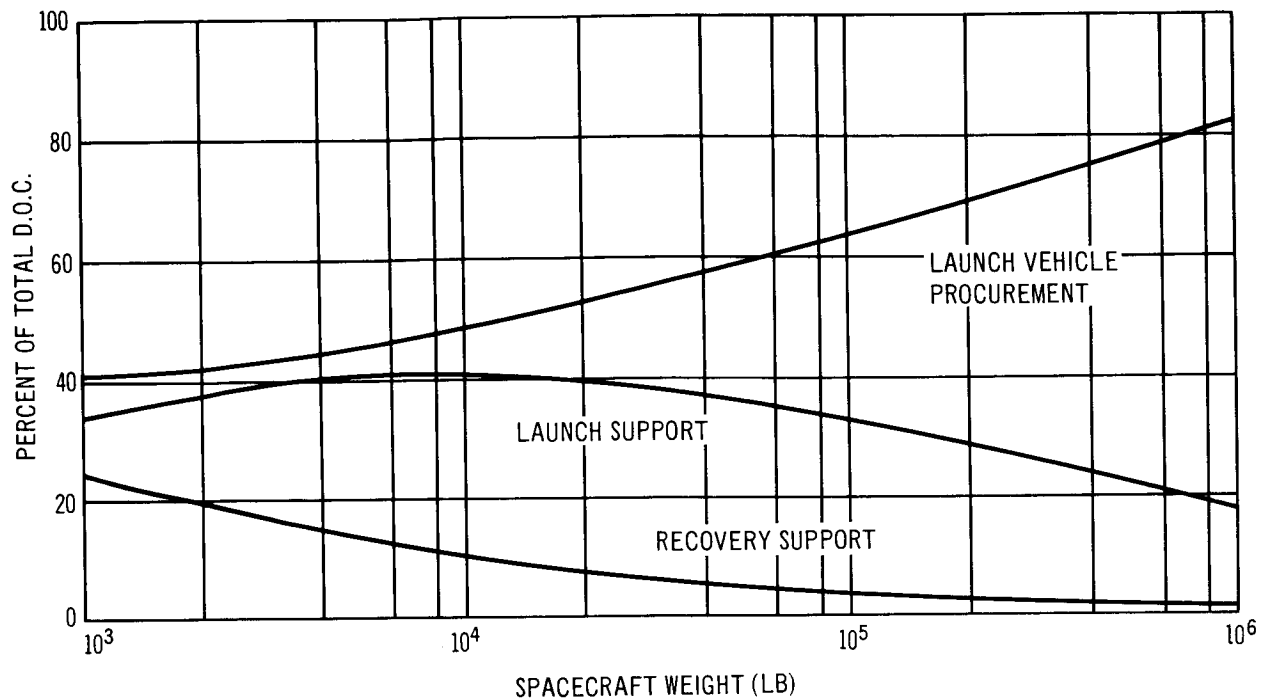


Figure 2-3. Distribution of Direct Operating Costs (No Spacecraft)

These elements are typical of those considered when launch vehicle costs are of prime consideration. The cost information used here is based on published data for Thor, Atlas, the Titan III-C series, Saturn IB, and Saturn V. Clearly, the launch vehicle costs predominate for spacecraft sizes larger than 8,000 lb.

If the cost of the spacecraft procurement is introduced, the effect on the distribution of operating costs is as shown in Figure 2-4. The cost data for the spacecraft are based on Mercury and Gemini costs for spacecraft weights less than 10,000 lb. Projected manned spacecraft costs are used for vehicles up through sizes corresponding to a passenger capacity of 12 men. They then reflect a diminishing cost per pound as the vehicles are configured to carry more and more bulk cargo and fuels. The predominant effect of the spacecraft is certainly maintained into regions of 1,000,000 lb. of spacecraft weight.

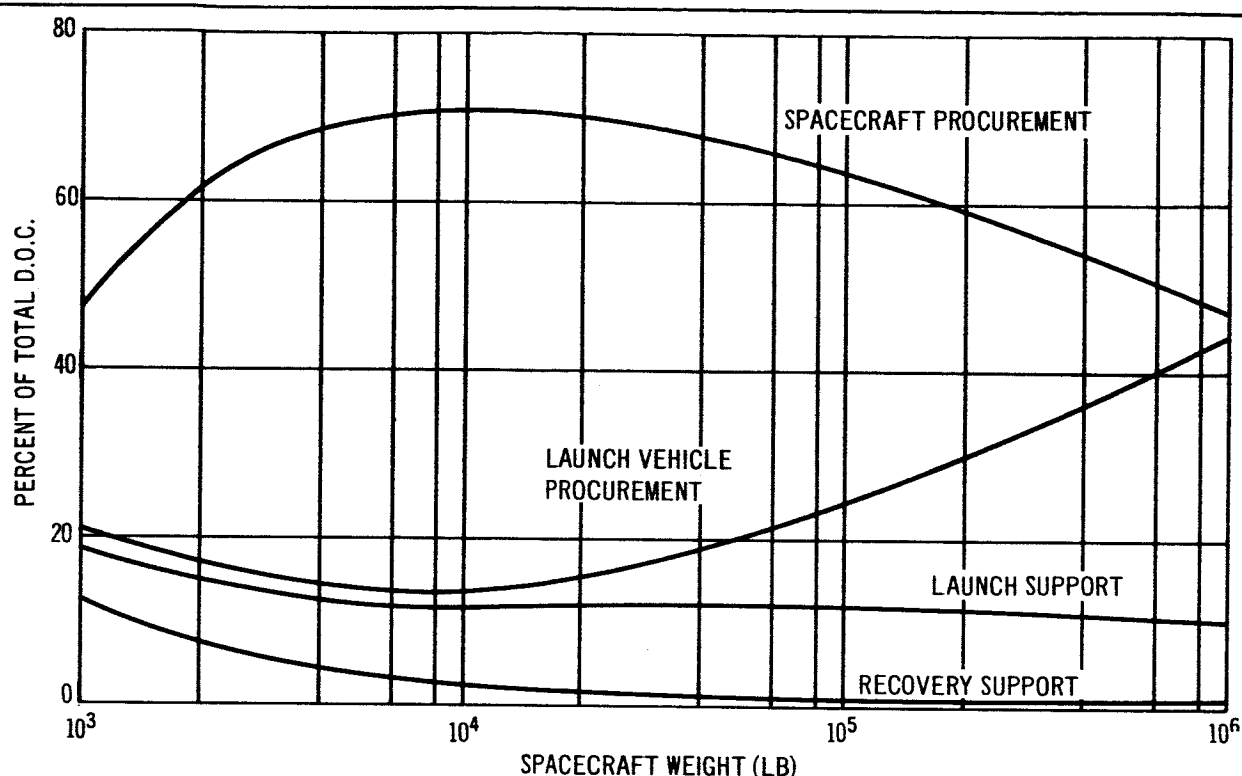


Figure 2-4. Distribution of Direct Operating Costs (With Spacecraft)

Relating the data of Figure 2-4 to the factors of concern in this study, it is clear that the region of interest is for spacecraft sizes in the range of 30,000 to 100,000 lb. In this region, several factors are important:

1. The largest fraction, by far, of the directing operating costs of a manned space vehicle system is in the spacecraft procurement.
2. The recovery techniques of manned spacecraft are well known and actual experience in these techniques is a reality.

The degree to which reusability is warranted in a space transportation system is a function of the state of our technology at any particular time and the potential savings which may be realized. Consideration will now be given to the accrued cost savings achievable through the incorporation of reusability by first examining reusability of the spacecraft only, and then examining the reusability of both spacecraft and launch vehicle. The data presented in Figure 2-5 are based on cost equations which express the ratio of direct operating costs for a fully expendable system to the direct operating costs of a system featuring various degrees of reusability. Two examples are shown in Figure 2-5: (1) that of a

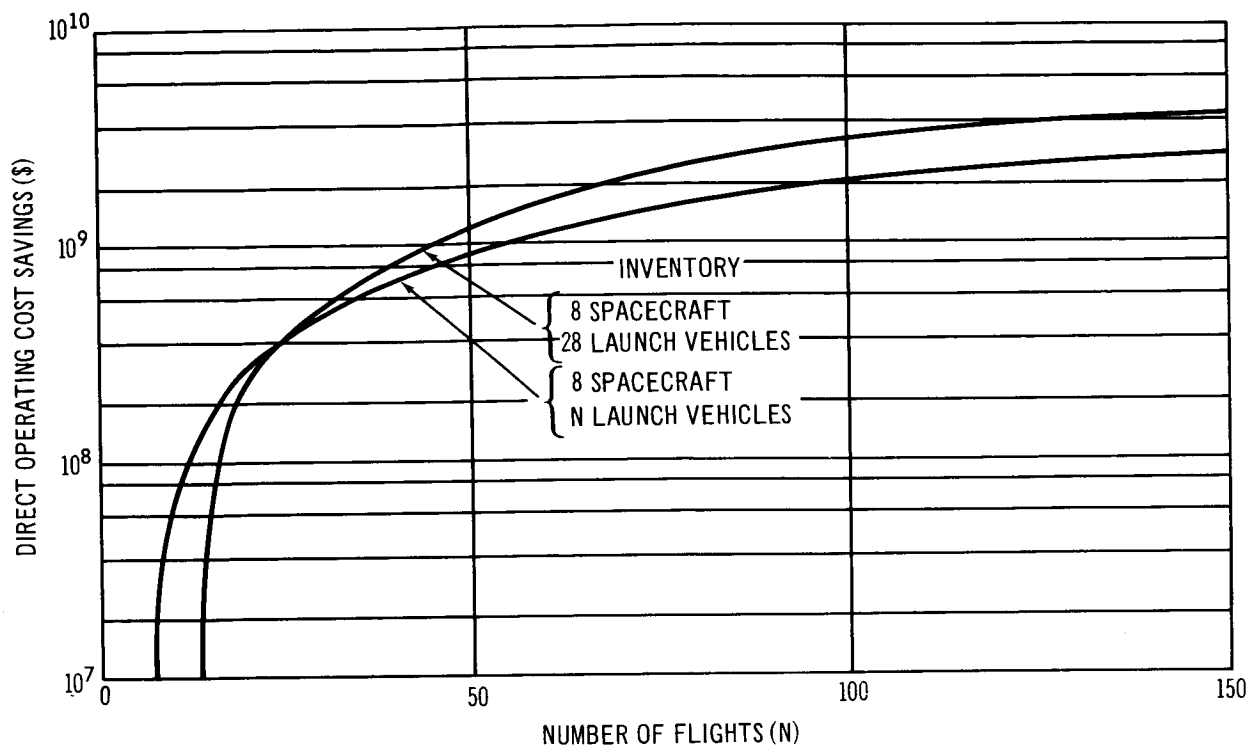


Figure 2-5. Effect of Reusability – 100,000-lb Spacecraft

spacecraft inventory of 8 vehicles and an expendable launch vehicle and (2) that of a spacecraft inventory of 8 vehicles and a reusable launch vehicle inventory of 28. The spacecraft weight is 100,000 lb, and the distribution of direct operating cost elements is the same as shown in Figure 2-4. Refurbishment costs were assumed to be 10% of the hardware procurement costs. First unit hardware costs of the reusable spacecraft are assumed to be the same as those for the expendable spacecraft. It will be noted that the accrued savings for the reusable launch vehicle system exceed those of the expendable launch vehicle system at approximately 30 flights. The crossover point is, of course, sensitive to the assumptions made on the refurbishment cost of the launch vehicle and spacecraft and on the size of the inventory.

For the case of the reusable spacecraft and expendable launch vehicle, the accrued savings reach \$1 billion in 54 flights and \$2 billion in 102 flights. A portion of these savings may be required to offset any difference in RDT&E between the expendable and reusable spacecraft.

## 2.2 SYSTEM CONCEPT

The results of the economic analyses discussed briefly in the preceding section suggest several characteristics that would be desirable in a cost-effective, manned space vehicle system. Such a system would be expected to be operational in a time period coincident with a post-MOL space station and for flight frequency requirements of from 4 to 20 missions/year into low Earth orbit.

These characteristics are as follows:

1. A simplified low-cost expendable launch vehicle.
2. A manned, recoverable, and reusable spacecraft capable of performing a variety of missions.
3. Simplified launch and recovery operations.

A simplified, low-cost expendable launch vehicle suggests the use of solid-propellant motors with fixed nozzles. After development, the large motors can be procured for costs from about \$1.30/lb of total motor weight in the large 260-in. sizes to between \$4 and \$5/lb in the smaller 156-in. sizes. The use of fixed-nozzle motor configurations permits utilization of near optimum expansion ratios without exceeding the case diameter envelope and requires the addition of a steering capability, preferably at a single location. To realize a single-point steering system location, a region must be selected in either the upper stage of the launch vehicle or in the spacecraft. The final selection of a location would depend, of course, on the spacecraft configuration and a detailed steering analysis.

The selection of a crew module or re-entry spacecraft configuration is dependent on the tradeoff in development cost and vehicle re-entry maneuvering capability, since the latter offers large reductions in the complexities of recovery operations and entry acceleration environment.

The system concept selected for the Phase I study is shown in Figure 2-6. The launch vehicle consists of all-solid-propellant motors with fixed nozzles. The spacecraft configuration is a lifting body of the NASA HL-10 type, producing lift-to-drag ratios of slightly over 1.0 in the hypersonic speed regime. Steering is performed at the head-end of the vehicle through two alternative configurations. The steering configuration, shown together with the total launch vehicle, consists of two fully gimballed liquid-propellant rocket engines located at the

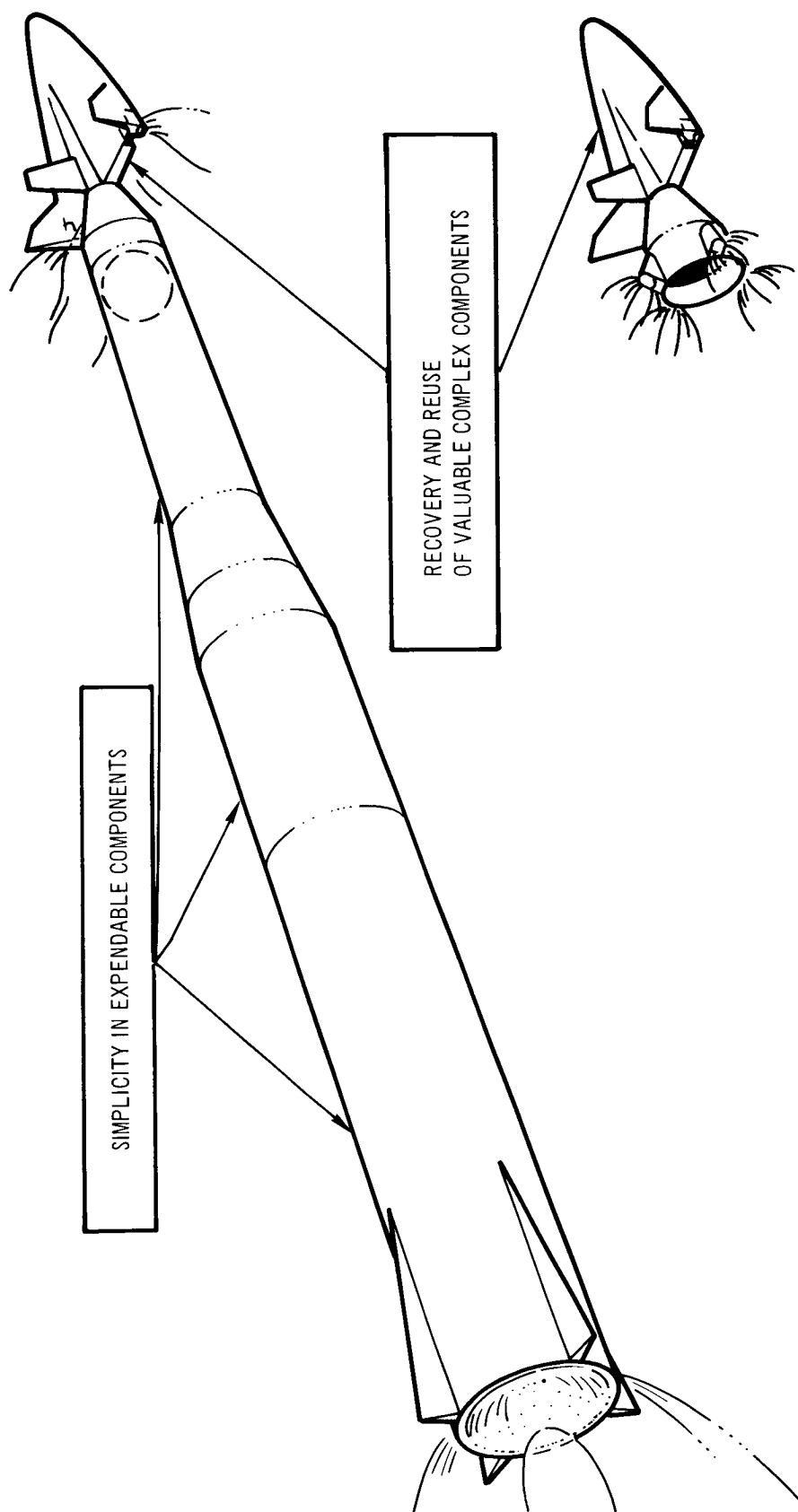


Figure 2-6. The System Concept

outer trailing edge region of the HL-10 spacecraft. These two engines provide all of the pitch, yaw, and roll control for the entire vehicle during the ascent phase of the mission. For this configuration, the steering system, not including the propellant tankage, is recoverable and reusable. The alternate configuration shown in the lower right part of Figure 2-6 incorporates four steering engines, positioned in 90° increments around the periphery of a steering system module. Two of the four engines provide pitch control, two provide yaw control, and all four provide roll control. This steering system is nonrecoverable. The development of these concepts through a first order feasibility evaluation (the Phase I study) is summarized in the following section.

### 2.3 THE PHASE I STUDY

This section will discuss the Phase I study objectives, guidelines, and major study results. A more extensive treatment of these study data may be found in Reference 1.

The Phase I study objectives were twofold. The first objective was to define the size and performance characteristics of the major system components of the system concept. The second objective was to perform a first order evaluation of the technical and economic feasibility of the system concept.

It was desired to define a mission model which, by its challenging nature, would provide as broad a base as possible for establishing feasibility. The mission selected was the extended MORL logistic resupply mission. This mission requires the transporting of 6 crewmen to the space station every 90 days, together with a maximum of 19,000 lb of consumable supplies and experiments. This cargo weighs 23,750 lb when packaged for shipment to the space station. An additional mission requirement was imposed in order to increase the mission flexibility. This was the requirement for 4,000-fps in-orbit maneuvering capability for the spacecraft. This capability was designed for the cargo/personnel loading of 6 space-station crewmen and 5,000 lb of cargo. Increased cargo loadings required an off-loading of in-orbit maneuvering propellants.

The space station orbit used for the baseline mission was at an altitude of 300 nmi and an inclination of 31°. The launch site was located at Cape Kennedy.



A mission duration of 7 days was selected for the design of spacecraft subsystems and costing was based on 5-year operational program with a nominal flight frequency of 10 flights/year. The NASA HL-10 configuration was chosen by the NASA-Langley Research Center as the spacecraft with a structural design criterion of 10-psi max. overpressure existing during the abort phases.

The launch vehicle consisted of all-solid-propellant motors and steering rocket engines located at the head-end of the vehicle. These steering engines use a storable liquid propellant. Maximum acceleration was limited to 10 g's during boosted flight; the hazard level of the all-solid motors was stipulated at 2%. Additional study goals were to (1) maintain simple stage interfaces, (2) recover the steering engines, (3) recover a significant fraction of the cargo, (4) preserve the external contour definition of the HL-10 spacecraft, (5) modularize the cargo, and maximize the use of the steering engines for post-ascent propulsion functions. The baseline maneuvering requirements are listed in Table 2-1 and reflect the incorporation of the parallel launch technique to permit a larger plane phasing launch window.

Table 2-1  
MANEUVERING REQUIREMENTS—BASELINE MISSION

Maneuver	Impulsive Velocity Requirement, $\Delta V$ (fps)
Vernier injection control*	80
Plane change during coast	1,110
Coast to 300-nmi apogee	0
Rendezvous (including injection)	600
Dock	0**
Separate	0**
Deorbit and coast	460
Re-enter and descend	0**
Approach and land	0
	2,250
Discretionary maneuvers capability	4,000
Total required	6,250
*Injection conditions will result in a 300-nmi apogee	
**Provided by attitude control system ( $\Delta V$ equivalent of 250 fps)	

The spacecraft arrangements that were analyzed in the Phase I study are shown in Figure 2-7. Factors considered in these arrangements were: (1) placement of crew and passengers, (2) location and distribution of cargo, (3) placement of steering and maneuver rocket engines, (4) location of steering propellant, and (5) location of maneuver propellants.

Configuration of the HES-2G spacecraft was selected as the baseline for further evaluation principally because it offered the broadest base for establishing the feasibility of head-end steering. Figure 2-8 shows a cutaway perspective sketch of the HES-2G spacecraft. The mission capability of the spacecraft is shown in Table 2-2.

At the end of the Phase I study, the launch vehicle consisted of three stages whose principal characteristics are shown in Figure 2-9. The total vehicle is shown in Figure 2-10.

Table 2-2  
MISSION CAPABILITY — BASELINE VEHICLE

Total Cargo Unpackaged (lb)	Impulsive Velocity ( $\Delta V$ )	Mission Description
29,900	1,140	Max. cargo with min. $\Delta V$ . Rendezvous at 300-nmi circular orbit, $i = 31^\circ$
19,000	2,860	Extended MORL resupply rendezvous at 200-nmi orbit, $i = 28.7^\circ$
0	6,530	Extended MORL - rescue search capability is $\Delta i_{REL} = 13.8^\circ$ (9 passengers)
8,400	4,920	Rendezvous with space station launched at max. azimuth of $40^\circ$ at ETR at 200-nmi altitude ( $53^\circ$ inclination)
23,000	2,190	Polar orbit (minimum energy ascent)
0	6,880	Maximum altitude of 2,000-nmi
0	6,880	Multiple rendezvous with 4 equally-spaced coplanar targets at 860 nmi, $i = 28.5^\circ$
0	6,880	Reconnaissance with one over-fly assurance, $i = 78.5^\circ$

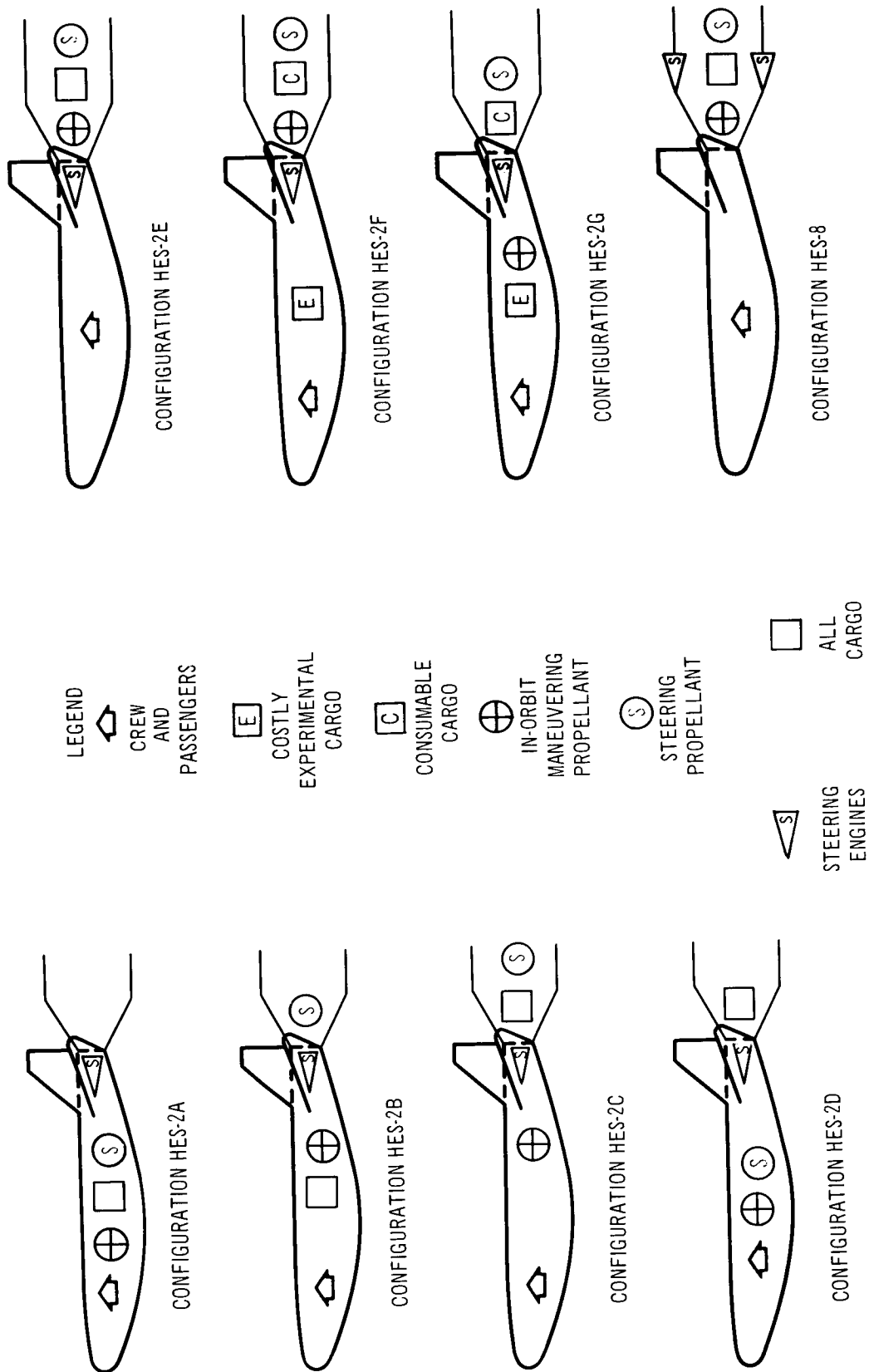


Figure 2-7. Phase I Study—Possible Arrangements—Spacecraft

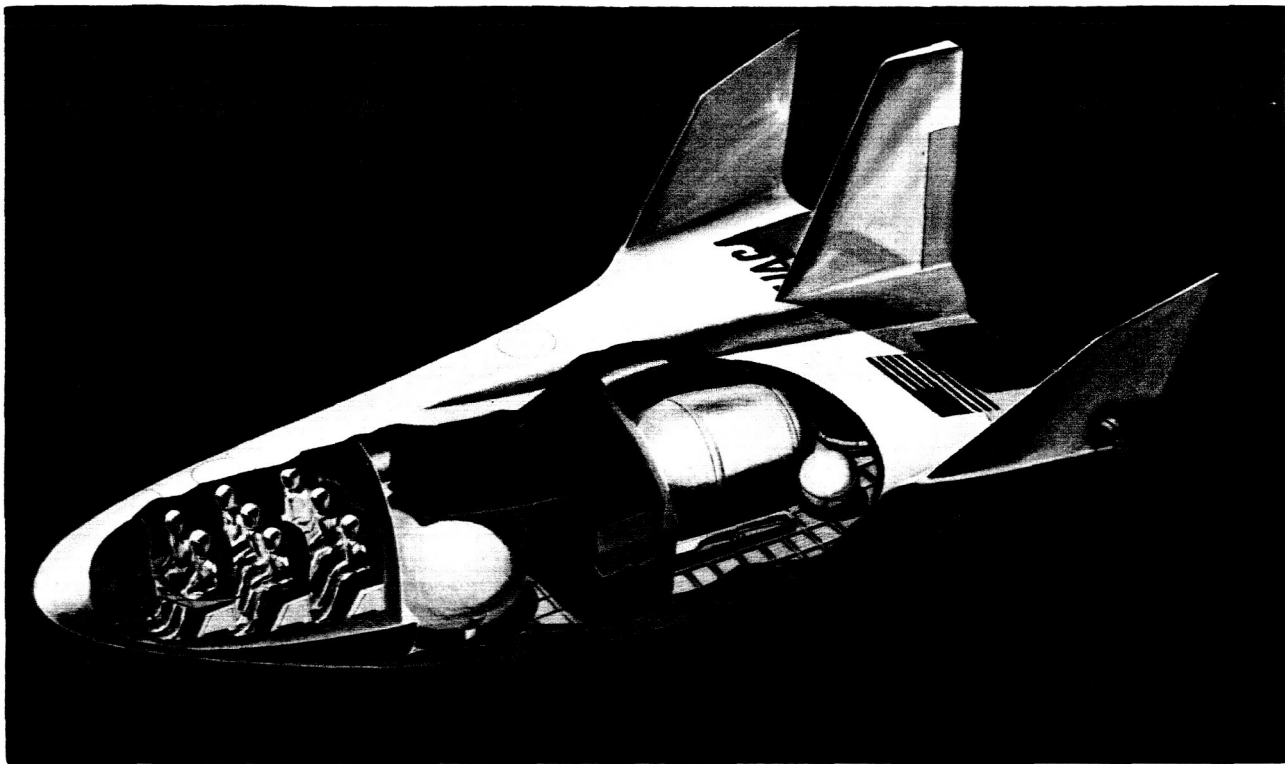


Figure 2-8. HES-2G Spacecraft

First order cost comparisons of the vehicle, as developed in the Phase I study, are shown in Figure 2-11. These data were based on published data for the launch vehicles, Titan III-C, Saturn IB, and 260-in. solid/S-IVB and represent first flight hardware procurement costs only. Estimated payload costs were included, together with estimates of useful load based on manned logistic mission vehicles. The purpose of establishing these comparative data was to make a first order evaluation of the economic feasibility of the Phase I study system concept employing head-end steering and solid-propellant booster motors.

While the accuracy of the data of Figure 2-11 may be questioned, a sufficiently large cost effectiveness potential was indicated for the solid-boosted launch vehicle to warrant additional study and verification.

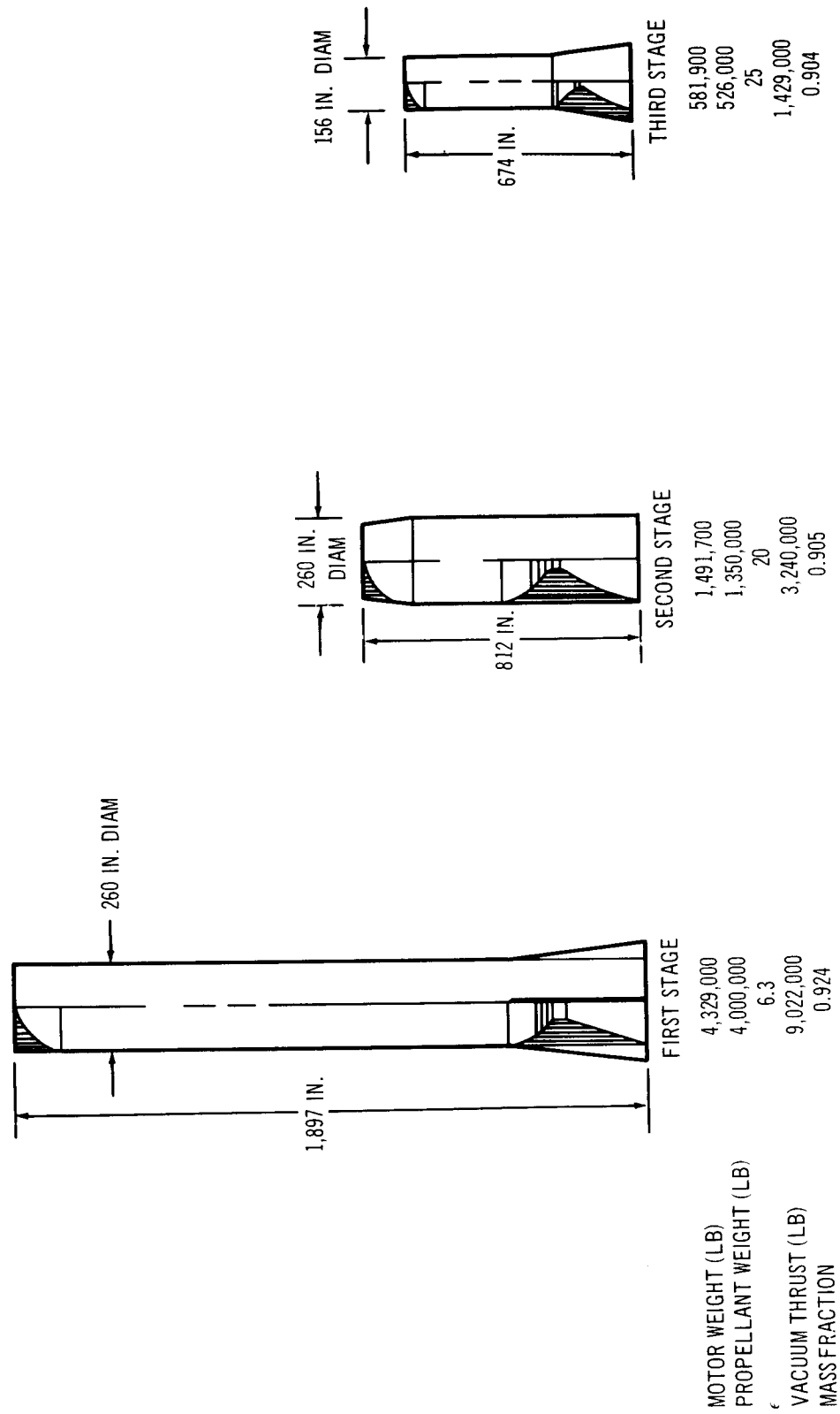


Figure 2-9. Phase I Study-The Booster Motors

HES-2G (1.2-0.4-0)

THRUST/WEIGHT  
@ LIFTOFF = 1.25

GROSS WEIGHT  
@ LIFTOFF = 6,651,600

PAYLOAD WEIGHT  
TO 100 N. MI. = 106,000 LB.

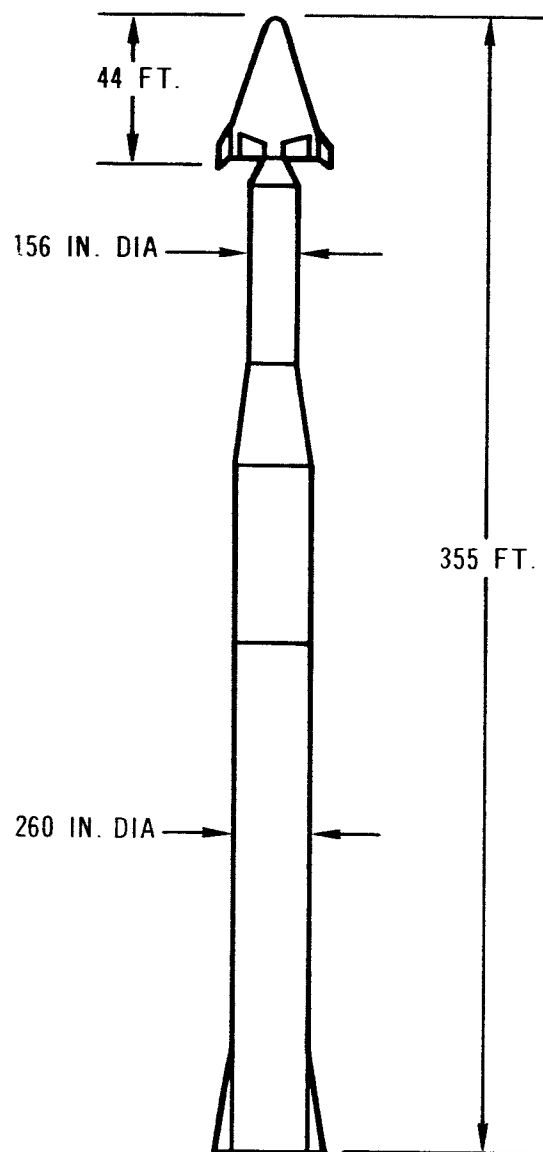


Figure 2-10. Phase I Study Resultant Vehicle Configuration

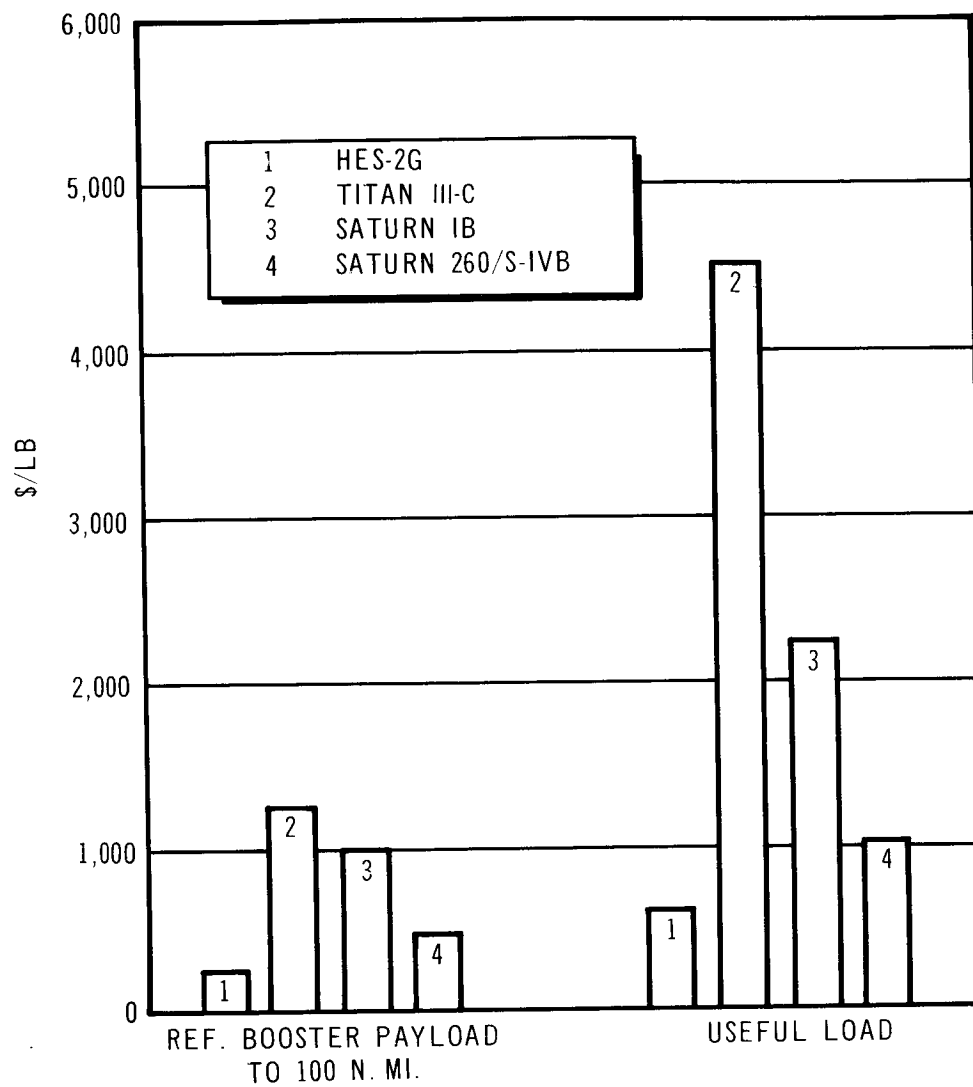


Figure 2-11. Phase I Study Summary – Economic Feasibility Cost Effectiveness

### Section 3

## DISCUSSION OF TECHNICAL AND ECONOMIC ANALYSES

This section presents the major study tasks in terms of objectives, mission requirements and guidelines, technical approach, and study results. At the end of each major task area, specific conclusions and recommendations for future work are presented. Conclusions and recommendations from a broader system perspective are presented in Sections 4 and 5.

The major study tasks are described in Figure 3-1. The study guidelines are discussed within each major task area whose titles are as follows:

- Vehicle Refinement and Optimization (Section 3. 1)
- System Definition (Section 3. 2)
- Comparison Studies (Section 3. 3)

These task areas had specific objectives which were to answer three major questions raised at the end of the Phase I study:

- How much system optimization is possible?
- What is the relative reliability inherent to the system concept?
- What part of the total cost reduction potential can be attributed to head-end steering, launch vehicle propulsion, and spacecraft propulsion?

The objectives of the Phase II study were to (1) refine and optimize the technical and operational aspects of the system concept developed in the Phase I study, and (2) to compare the refined and optimized head-end steering system concept with other current and projected system designs in such a manner that would permit isolation of the effects of steering technique, launch vehicle propulsion, and spacecraft configuration.

### 3.1 VEHICLE REFINEMENT AND OPTIMIZATION

This section concerns the optimization of the Configuration I vehicle (HES-2G of the Phase I study) and the investigation of technical questions arising during and



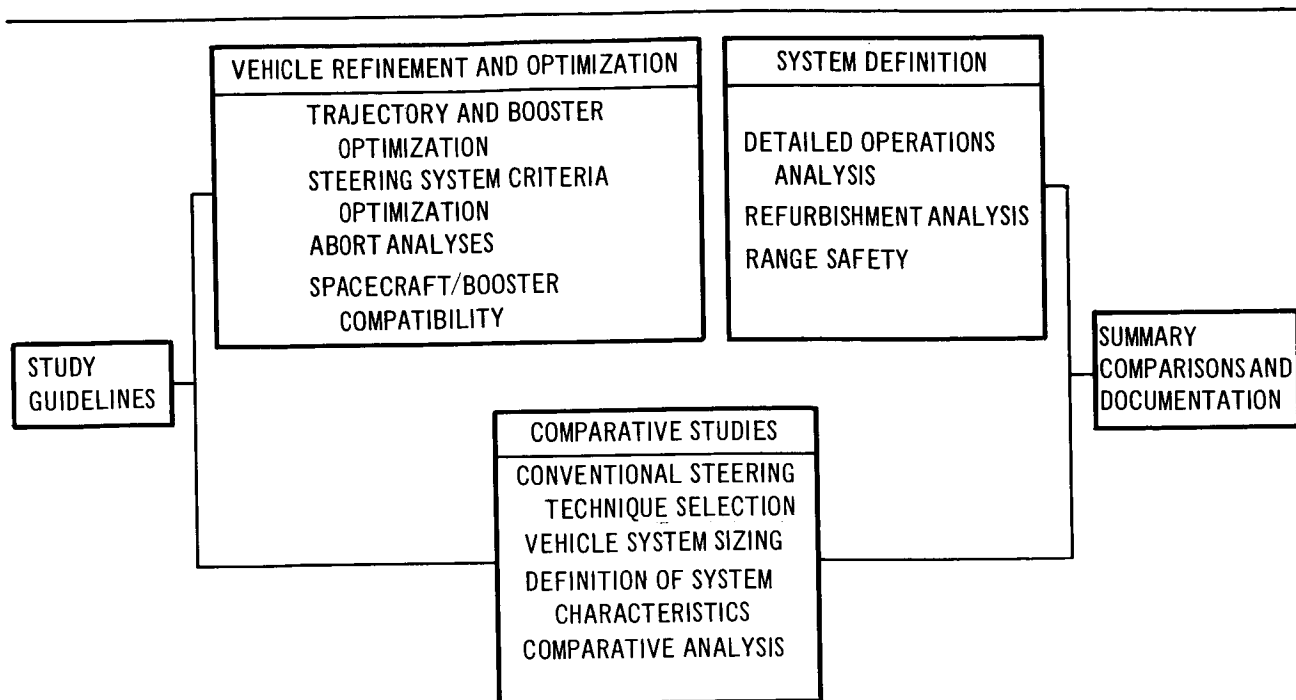


Figure 3-1. Major Study Task Areas

at the end of Phase I regarding the size of the steering system, abort requirements, and compatibility of spacecraft and booster. The degree of optimization that was possible within the budget limitations of the study was, of course, limited. Major effects, however, were identified and evaluated.

### 3.1.1 Mission Requirements and Guidelines

The baseline mission requirements selected for the Phase I study were used throughout the refinement and optimization analyses performed in the Phase II study. The primary mission is the resupply of men and cargo to an extended MORL type of space station. This is a 9-man space station requiring a rotation of six men on a 90-day basis. Projected cargo requirement at the time of the Phase I study indicated a maximum of 19,000 lb on the 90-day rotation schedule. The packaged weight of this cargo was 23,750 lb. The baseline rendezvous conditions are a circular orbit at 300 nmi inclined at 31°. The ascent profile used in sizing the energy requirements for the spacecraft was based on a parallel launch technique and direct ascent to the rendezvous orbital altitude. To enable the spacecraft to perform other missions requiring less cargo and a

larger in-orbit maneuvering capability, the spacecraft was specified to have an impulsive velocity capability of 4,000 fps for a cargo load of 5,000 lb. The energy budget characteristics are described in Section 2 and tradeoff between cargo and impulsive velocity is shown in Figure 3-2.

The flexibility in the distribution of men and cargo is shown in Figure 3-3 and the specific mission capability has been discussed in Section 2 of this report.

The solid-propellant motor characteristics were changed to reflect current propellant performance estimates and available motor weight data. The solid-propellant characteristics used for all motor sizing is presented in Section 3.1.4. The hazard classification in terms of TNT equivalence is treated parametrically instead of the fixed value of 2% used in the Phase I study.

The solid-propellant motor thrust misalignment and eccentricity characteristics used in determining control moment requirements were also held at the same values used in the Phase I study. These characteristics are discussed in more detail in Section 3.1.3.

The steering engine used in Phase II studies is the same type as used in Phase I. The gimbal deflection limits are maintained at the same values and the propellant type,  $N_2O_4$  and MMH, is the same. As steering requirements were changed as a result of launch-vehicle size changes, the thrust levels and  $I_{sp}$ 's were analyzed and adjusted accordingly.

### 3.1.2 Trajectory and Booster Optimization

Potential reductions in vehicle size through optimization of the HES-2G booster and flight trajectory, as indicated by results of the Phase I study, were assessed in the Phase II Head-End Steering study. Those areas investigated and reported on include booster motor nozzle optimization, stage velocity distribution, thrust-time history shaping, and booster trajectory reshaping. The Phase I HES-2G spacecraft and mission were used for these studies. Where investigations of the effects of changes on steering requirements were necessary, booster payloads were adjusted accordingly while holding crew size, cargo size, and in-orbit maneuvering capability constant.

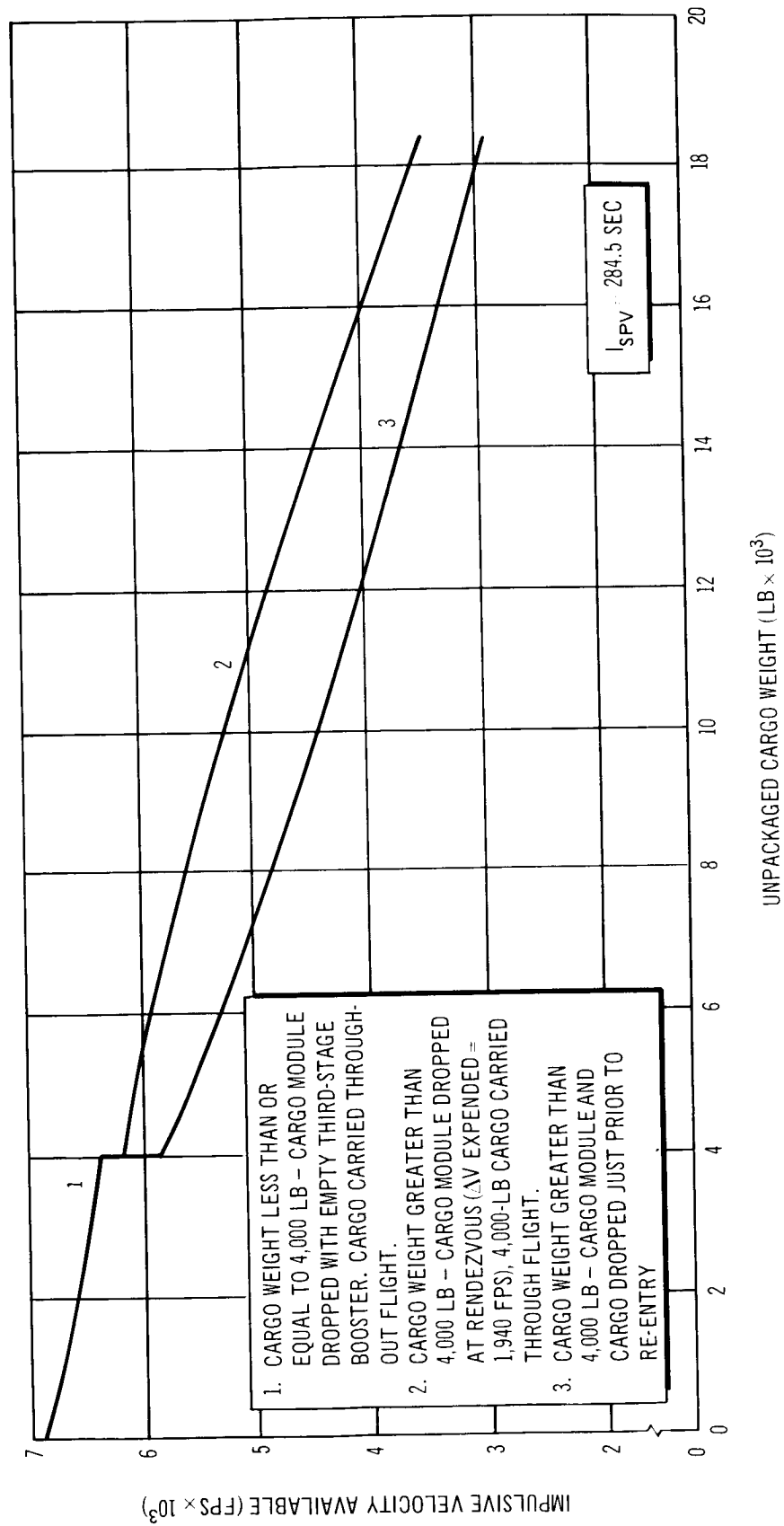


Figure 3.2 Performance Capability, HES-2G

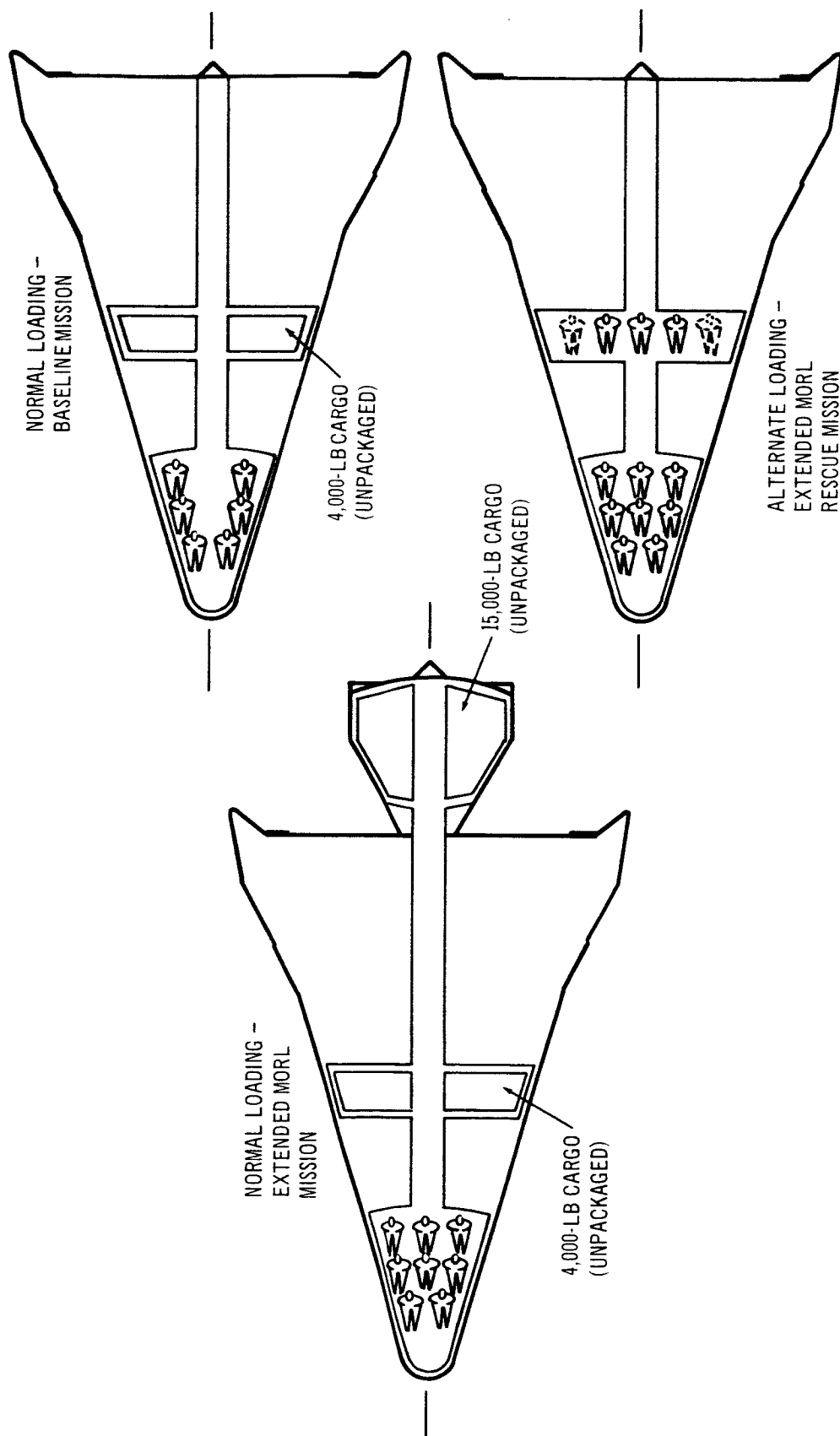


Figure 3-3. Crew-Cargo Arrangement, HES-2G

The solid propellant selected for all Phase II booster sizing and costing work was the HC type of aluminized, composite propellant made by the Thiokol Chemical Corporation. No effort was made to optimize propellant type on the basis of cost for use in these studies, the selection being based primarily on the higher energy available from this type of propellant; cost trends were developed, however, as described in Section 3.1.2.2. The propellant characteristics consistent with this choice are shown in Table 3-1.

### 3.1.2.1 Booster Motor Nozzle Optimization

Nozzle expansion ratio, the ratio of exit area to throat area, has a large effect on the specific impulse attained from a given motor. A curve showing the effect of expansion ratio on vacuum specific impulse for the reference propellant is shown in Figure 3-4. Inherent to an increase in expansion ratio for a given motor, however, is an increase in nozzle weight and a probable increase in motor skirt or interstage weight. Since impulsive velocity (hence, payload capability) is directly related to motor specific impulse and inversely related to stage inert weight, a tradeoff study is required to optimize expansion ratio with respect to vehicle performance.

Table 3-1  
SOLID-PROPELLANT CHARACTERISTICS USED IN PHASE II STUDY

Typical of Thiokol Chemical Corporation HC-Type Propellant	
Type: Composite, Polybutadiene, Carboxylly Termination	
Standard specific impulse (optimum expansion, 1,000 psia $\rightarrow$ 14.7 psia, 0° half-angle)	255 sec
Specific heat ratio	1.16
Characteristic velocity (theoretical)	5379.4 fps
Combustion efficiency	0.96
Nozzle efficiency	0.98
Burn rate (1,000 psia)	0.3 in. /sec
Burn-rate exponent, n	0.38
Propellant density	0.0655 lb/in <sup>3</sup>

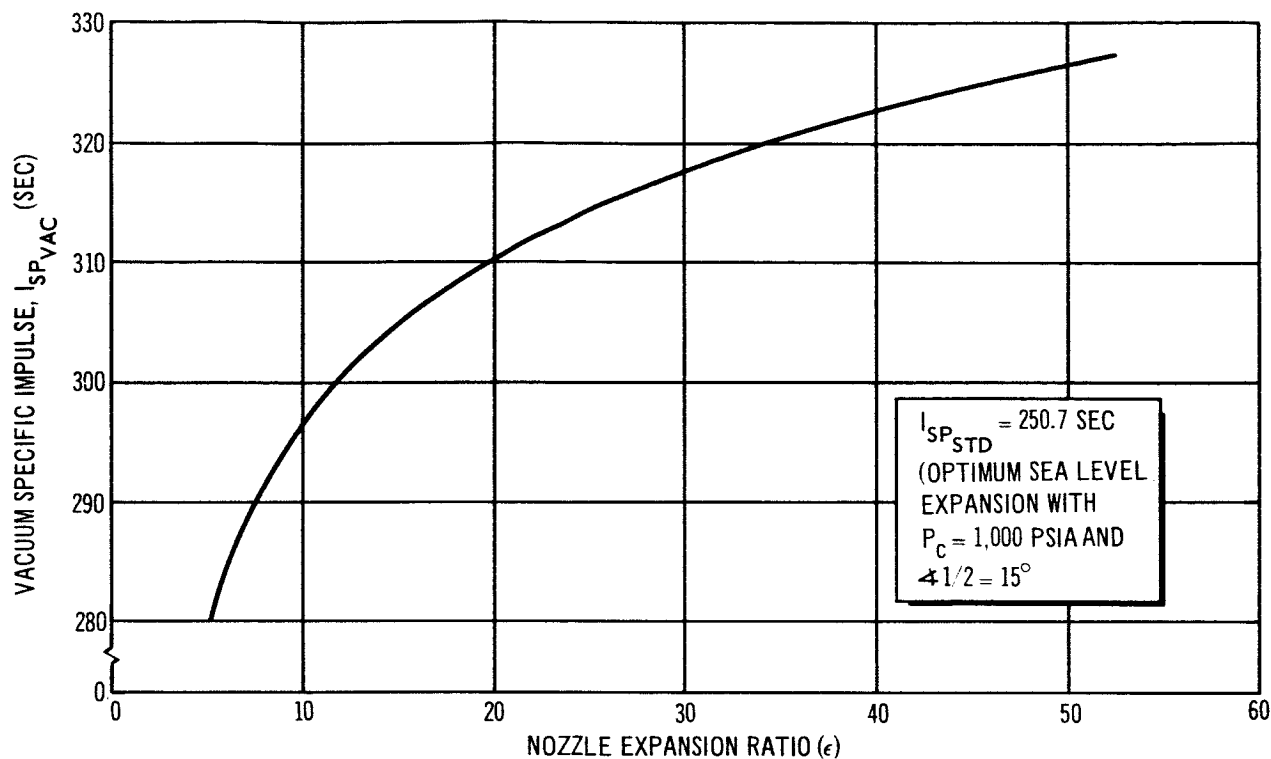


Figure 3-4. Phase II Solid-Propellant Theoretical Performance

Booster nozzle expansion ratios used for the Phase I HES-2G were the maximum expansion ratios permitted by skirt and interstage diameters for the first- and second-stage motors. The first-stage aft skirt was a full length, 260-in. diam cylinder extending the full length of the nozzle. The resultant first- and second-stage expansion ratios were 6.3:1 and 20:1, respectively. The third-stage nozzle expansion ratio was arbitrarily set at 25:1.

A first-stage nozzle optimization study was performed with expansion ratio and nozzle divergence half-angle as independent variables, with the effects of delivered specific impulse, nozzle weight and first-stage aft skirt weight on vehicle total growth factor taken into account. Growth factor is defined as the ratio of vehicle weight at lift-off to payload weight above the third stage. Conical nozzles were used for the first stage. The specific impulse considered was the time-averaged specific impulse delivered for the Phase I HES-2G trajectory. The effect of nozzle expansion ratio and divergence half-angle on specific impulse and first-stage mass fraction are shown in Figures 3-5 and 3-6, respectively. The resultant effect of these two variables on total growth factor

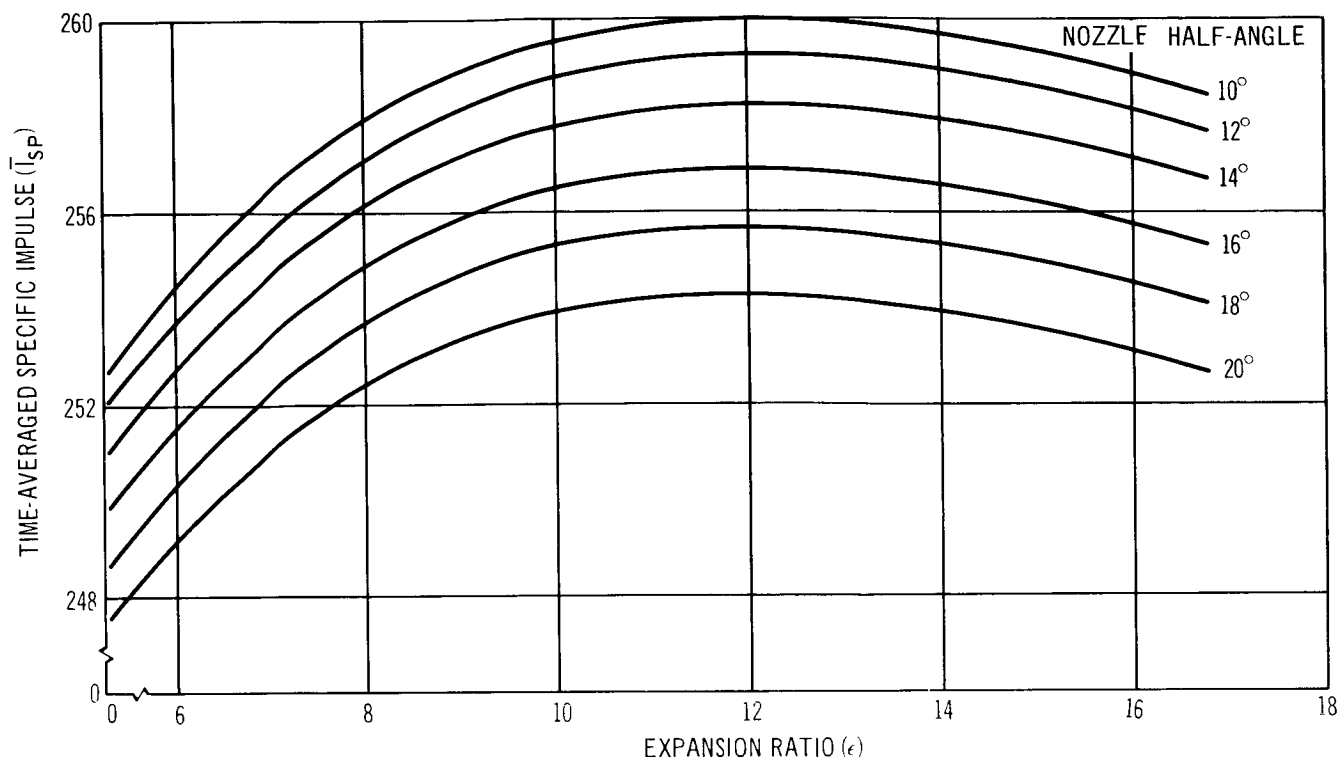


Figure 3-5. First-Stage Nozzle Optimization Effect on Specific Impulse

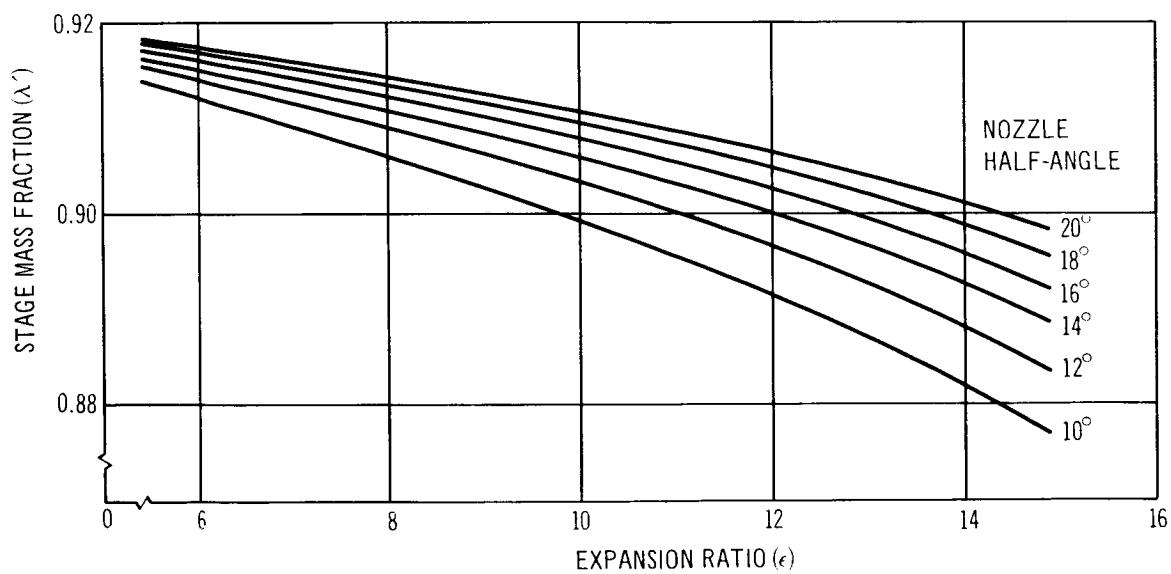


Figure 3-6. First-Stage Nozzle Optimization Effect on Mass Fraction

is shown in Figures 3-7 and 3-8. As can be seen, the optimum expansion ratio is 8.3:1 and the optimum divergence half-angle is  $13^\circ$ . Although the optimization study was performed for the Phase I HES-2G vehicle and trajectory characteristics, the optimized parameters were used throughout the study with the exception of those vehicles in which the resultant first-stage nozzle exit diameter was less than the stage diameter of 260 in. Those nozzles were expanded to that point where the exit diameter approximately equaled the stage diameter. In no case did this result in separated flow occurring in the nozzle at sea-level conditions. For the reference propellant and chamber pressure, separated flow would occur at sea level conditions at an expansion ratio of approximately 18.5:1 based on empirical data.

Because the interstage skirt between the first and second stages limited the expansion ratio to approximately 20:1 and this stage operates entirely at near vacuum conditions, no optimization of the second-stage nozzle expansion ratio was attempted. A contoured nozzle was used for the second stage to decrease nozzle and interstage length with an attendant decrease in inert weight. The contoured nozzle length is approximately 75% of the length of a  $15^\circ$  conical nozzle.

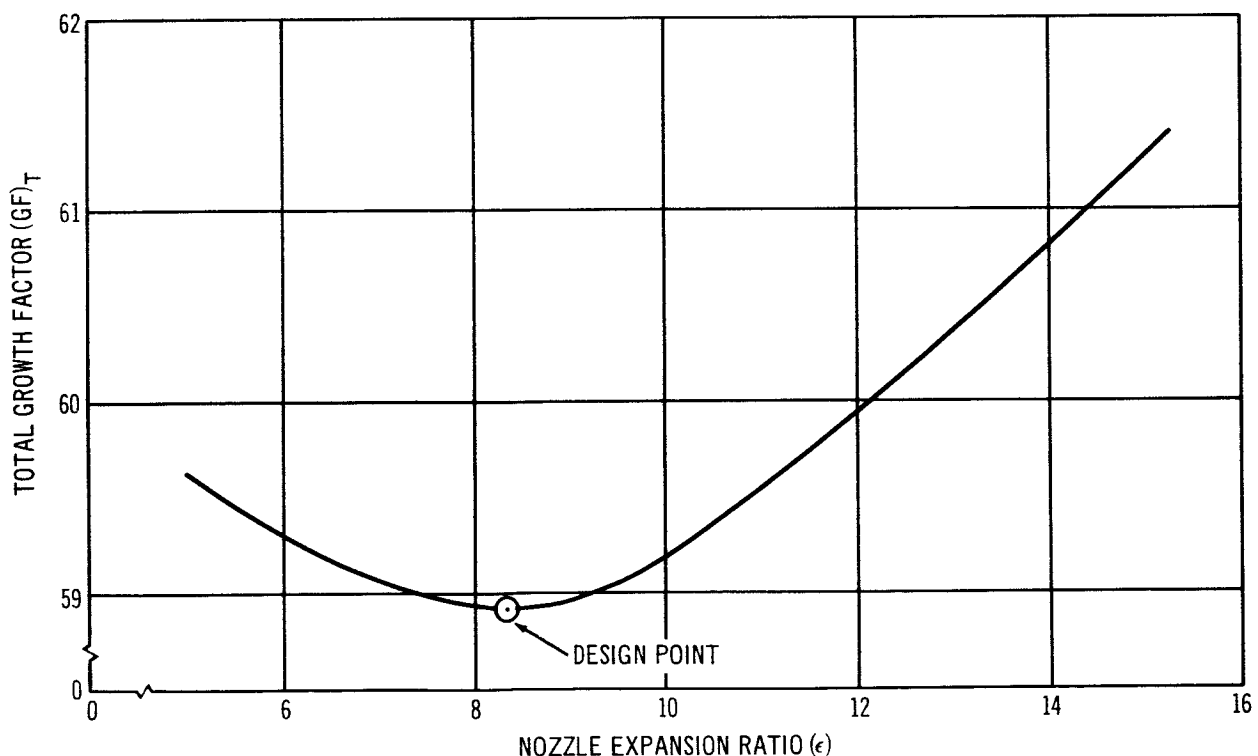


Figure 3-7. First-Stage Nozzle Optimization Effect of Expansion Ratio



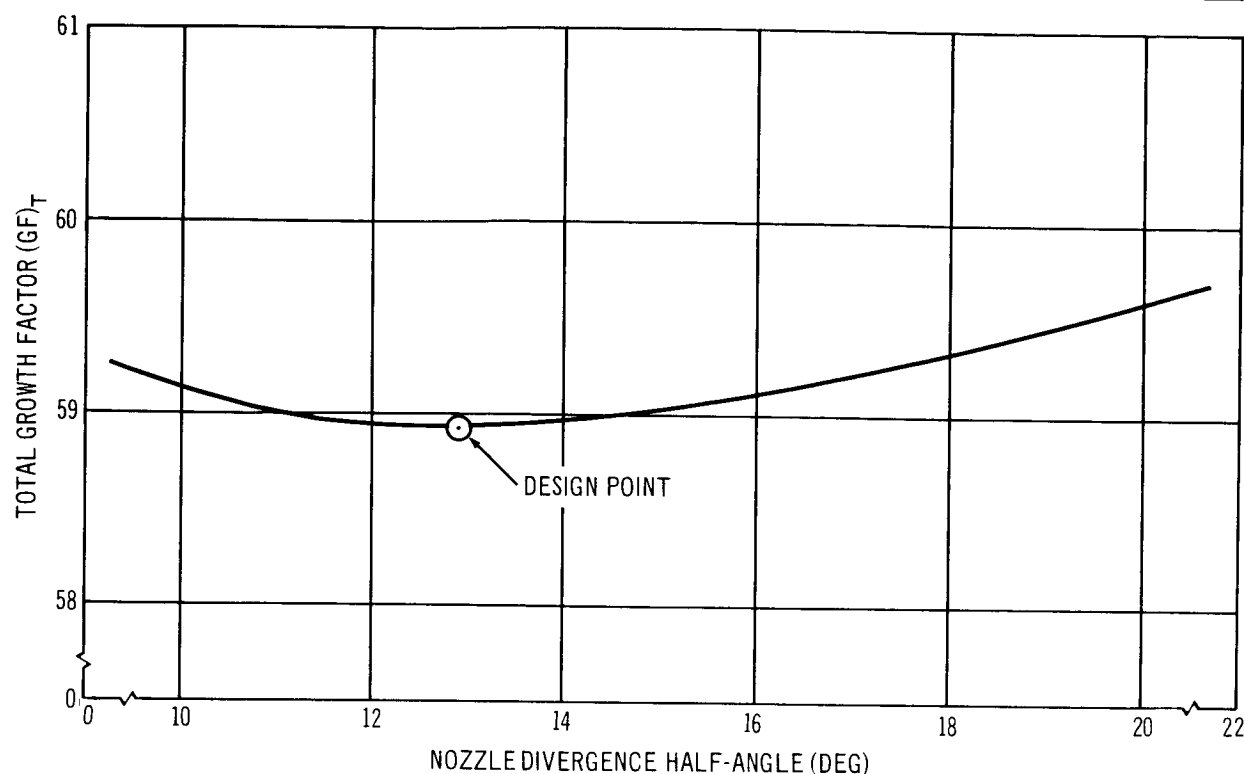


Figure 3-8. First-Stage Nozzle Optimization Effect of Nozzle Divergence

A third-stage nozzle optimization study was performed with expansion ratios ranging from 25:1 to 45:1. Contoured nozzles were used with a contoured length to 15° cone-length ratio of approximately 0.75:1. As for the first stage, the effect of expansion ratio on total growth factor was determined taking into account delivered vacuum specific impulse, nozzle weight, and inert interstage weight. Optimization was performed initially for the Phase I third-stage propellant loading of 526,000 lb. The effect of expansion ratio on specific impulse and stage mass fraction for this propellant loading is shown in Figure 3-9. The resultant effect on total growth factor is shown in Figure 3-10 with the optimum expansion ratio occurring at 32.5:1. Concurrent investigation of the effect of redistribution of stage velocity indicated potential benefits from a third-stage propellant loading of 250,000 lb and an optimization study was performed for this loading. The effect of nozzle expansion ratio on vacuum specific impulse and stage mass fraction for this propellant loading is shown in Figure 3-11 and the resultant effect on total growth factor is shown in Figure 3-12. The optimum nozzle expansion ratio of 40:1 was used throughout the study for the 156-in. diam motors for third-stage as well as second-stage applications.

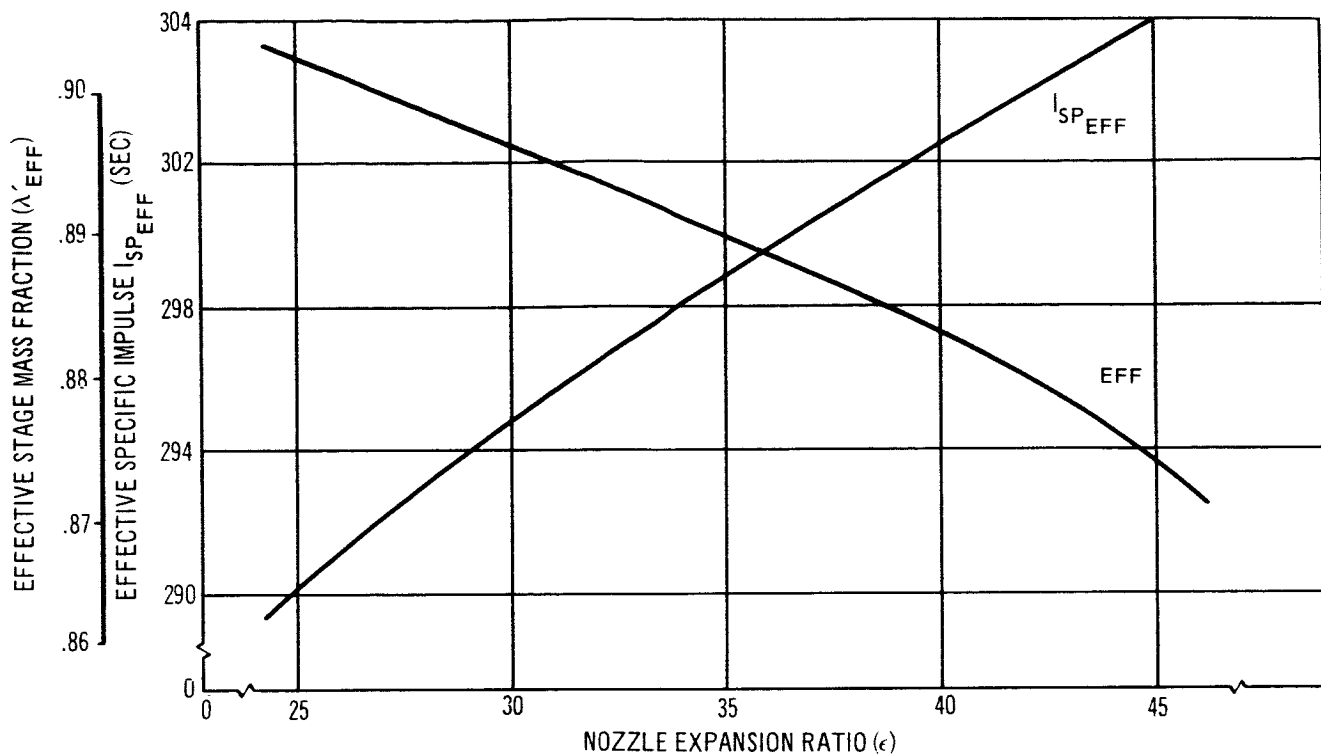


Figure 3-9. Third-Stage Characteristics ( $W_{P_3} = 526,100$  lb)

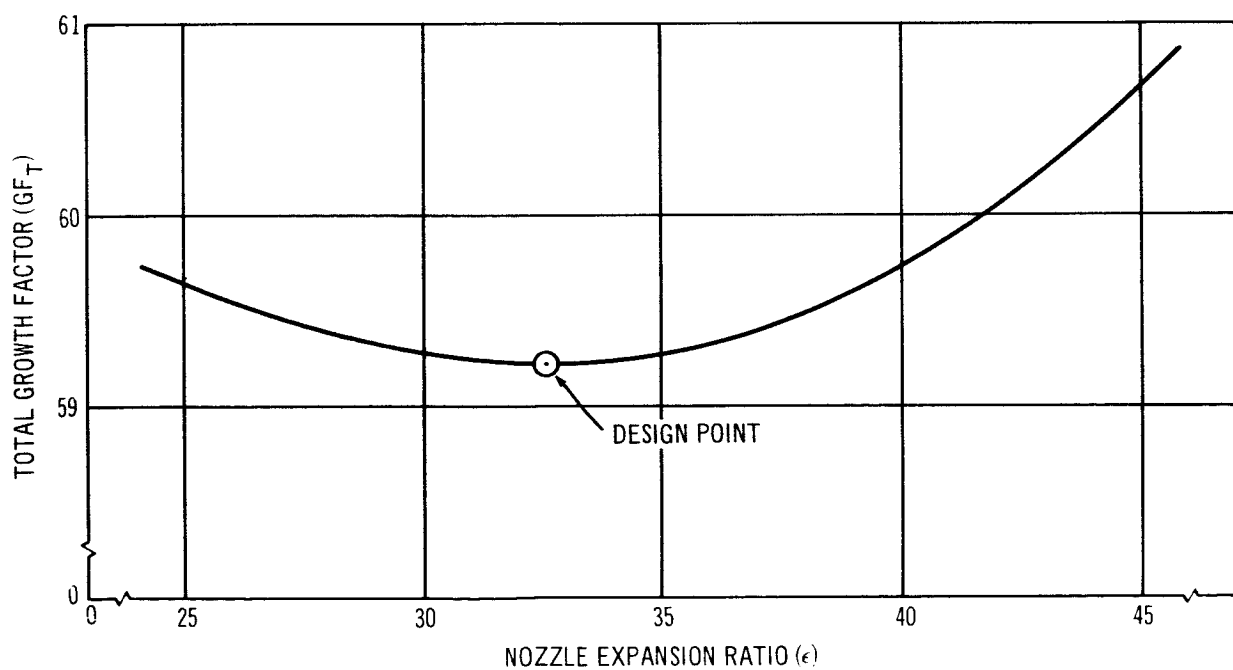


Figure 3-10. Third-Stage Nozzle Optimization ( $W_{P_3} = 526,100$  lb)

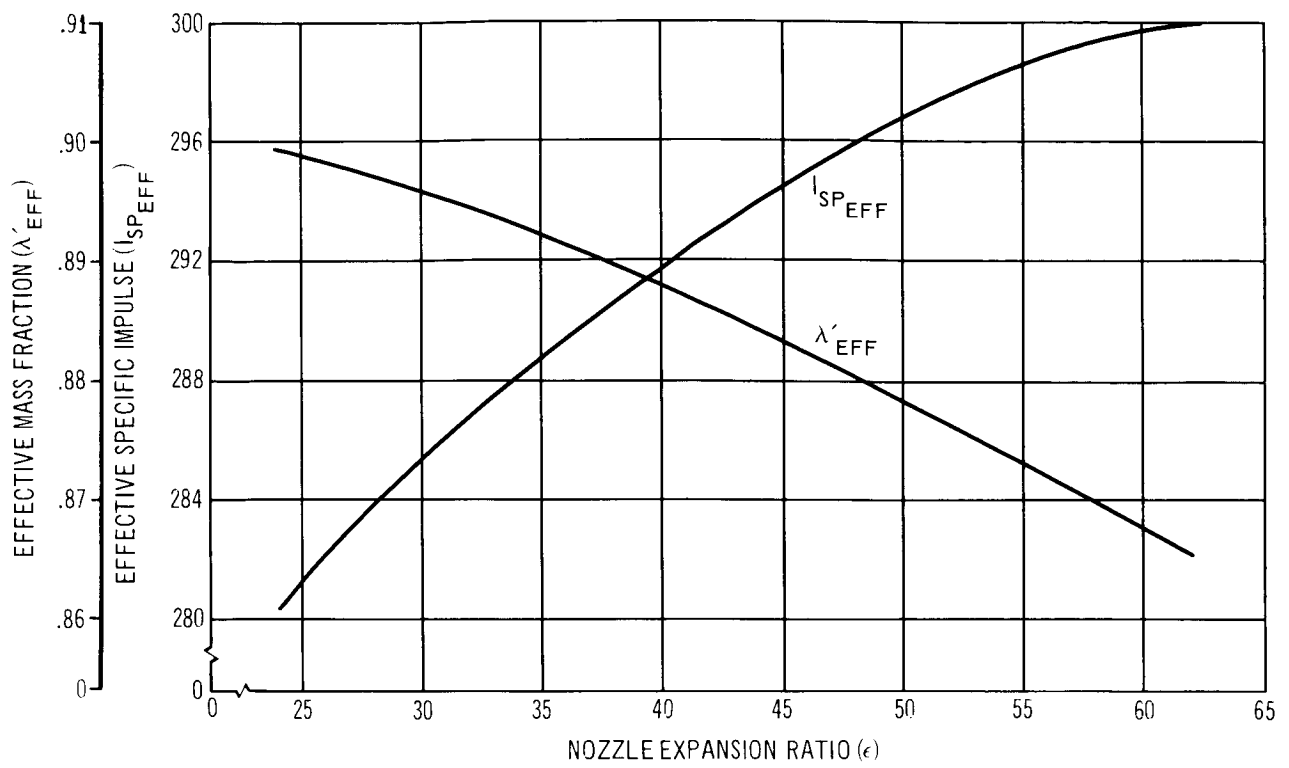


Figure 3-11. Third-Stage Characteristics ( $W_{P3} = 250,000$  lb)

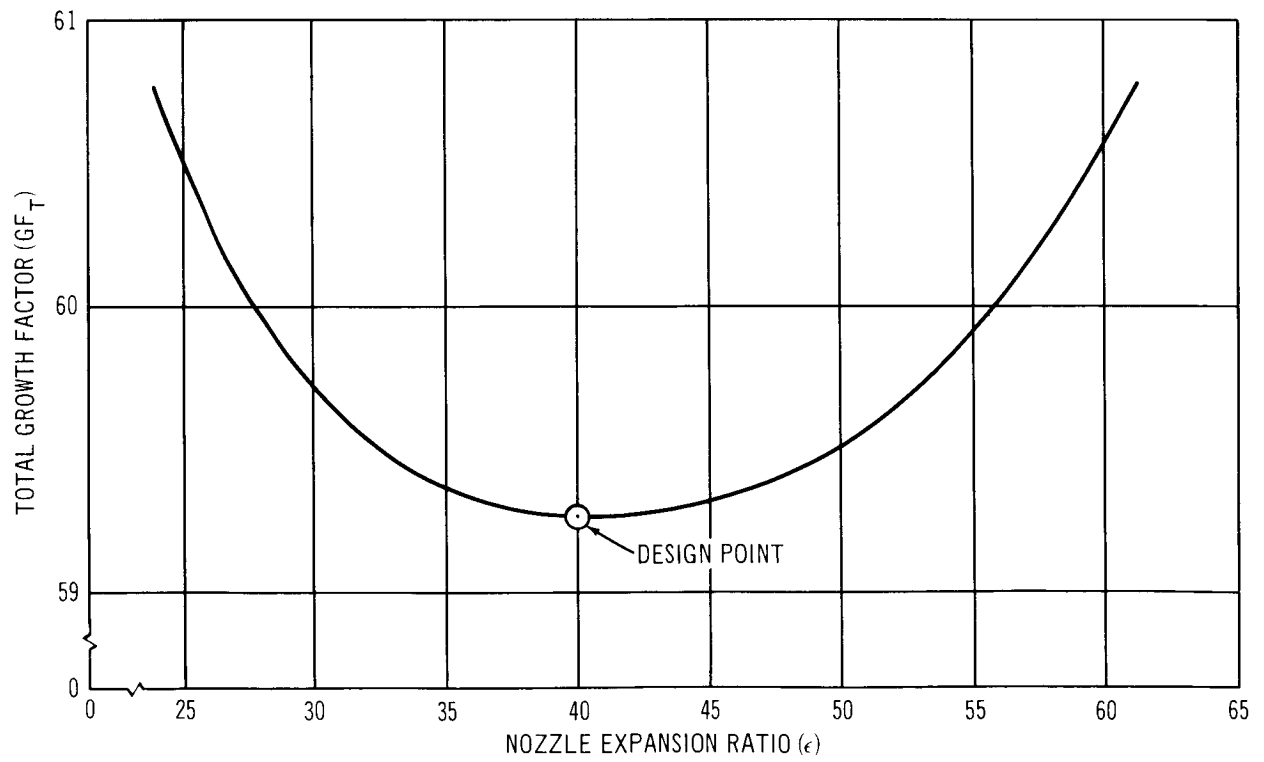


Figure 3-12. Third-Stage Nozzle Optimization ( $W_{P3} = 250,000$  lb)

### 3.1.2.2 Stage Velocity Distribution

Results of the Phase I Study indicated that a decrease in third-stage velocity would decrease the total vehicle growth factor. This preliminary analysis did not take into account, however, the side effects of decreased third-stage propellant weight on steering requirements. A characteristic of head-end steering vehicles is that as third-stage weight decreases for a given payload weight, the CG moves forward and decreases the control moment arm, possibly resulting in control reversal as booster propellant is expended. Control reversal occurs when the CG moves forward of a line connecting the two steering engines, that is, at approximately the trailing edge of the spacecraft. Required control thrust in pitch would become infinite in magnitude and, if the forward movement of the CG continued, would result in control moments opposite in sign to those required. This condition was prevented in this study by controlling the minimum size for the third stage. The increase in steering thrust requirements that occurs with decreased propellant weight above this limit results in an increase in steering engine size, steering propellant required, and inert payload weight with a consequent increase in booster size for a given impulsive velocity. This tradeoff necessitated a study to determine the limits on decrease in third-stage velocity.

Study-time limitations prevented an exhaustive optimization study; however, the effect of third-stage propellant weight on steering requirements was investigated for the HES-2G vehicle and is shown in Figure 3-13. As can be seen, the required control thrust increases rapidly as propellant weight decreases below about 350,000 lb. Impulsive sizing of the vehicle, based on minimizing the growth factor, indicated that a lower third-stage propellant weight (on the order of 200,000 pounds) would be desirable. This analysis, however, did not take into account the full effect of third-stage size on steering requirements. A compromise propellant weight of approximately 250,000 lb was selected with the knowledge that tailoring the thrust-time curve would further reduce maximum control thrust requirements. This is discussed further in the following section. The ratio of second-stage velocity to first-stage velocity was optimized at 1.03 to provide a vehicle with a minimum total growth factor (maximum payload mass fraction).

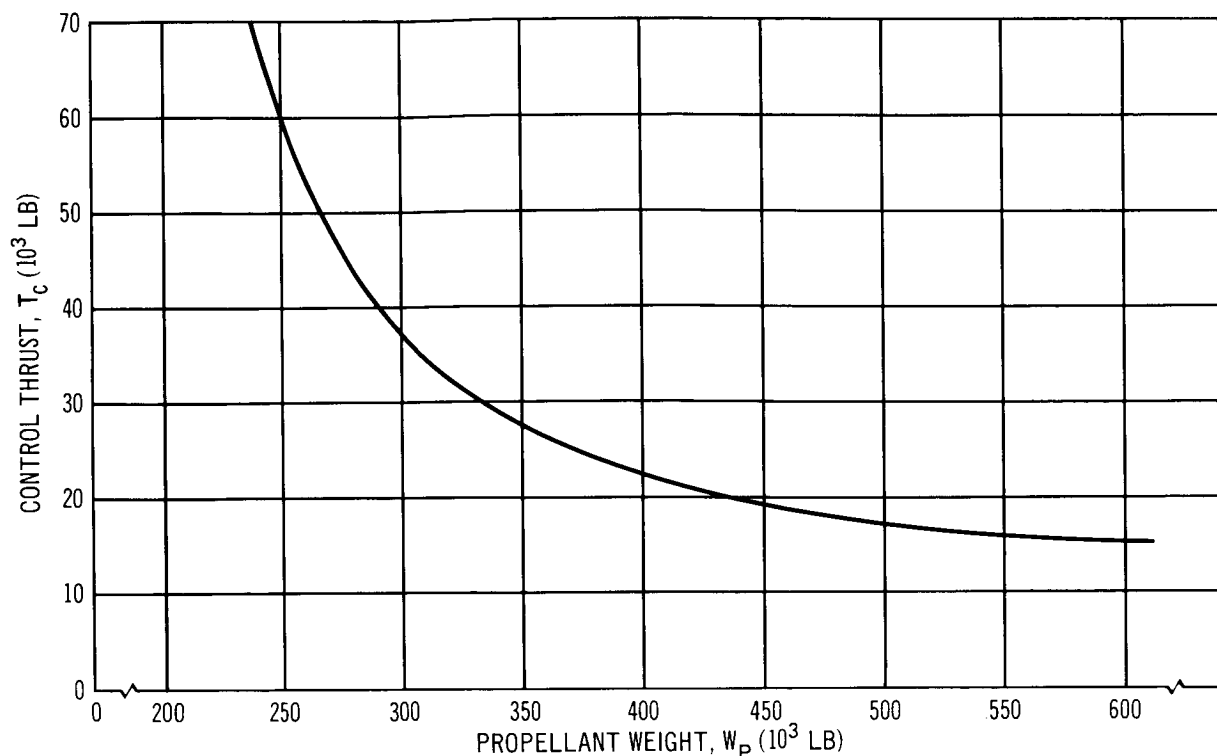


Figure 3-13. Effect of Third-Stage Propellant Weight on Maximum Control Thrust (Neutral Thrust-Time History)

#### Cost Sensitivity to Propellant Distribution

The Configuration I vehicle was sized to provide a minimum-size booster, that is, the smallest lift-off gross weight within certain constraints imposed by the steering system. Optimum performance, corresponding to minimum size, does not, however, always result in minimum cost.

The vehicle design sensitivities were used to establish the cost trends resulting from off-designing the size-optimum propellant distributions. These trends are shown in Figure 3-14. A reduction in third-stage velocity through a reduction of third-stage propellant would clearly lower the total cost of the three solid propellant motors. The trade-off here is approximately a 3% reduction in total motor cost for a 1,000 fps reduction in third-stage impulsive velocity.

A corresponding decrease in motor costs may be made by increasing the second- to first-stage velocity ratio. This reduction is, however, quite small.

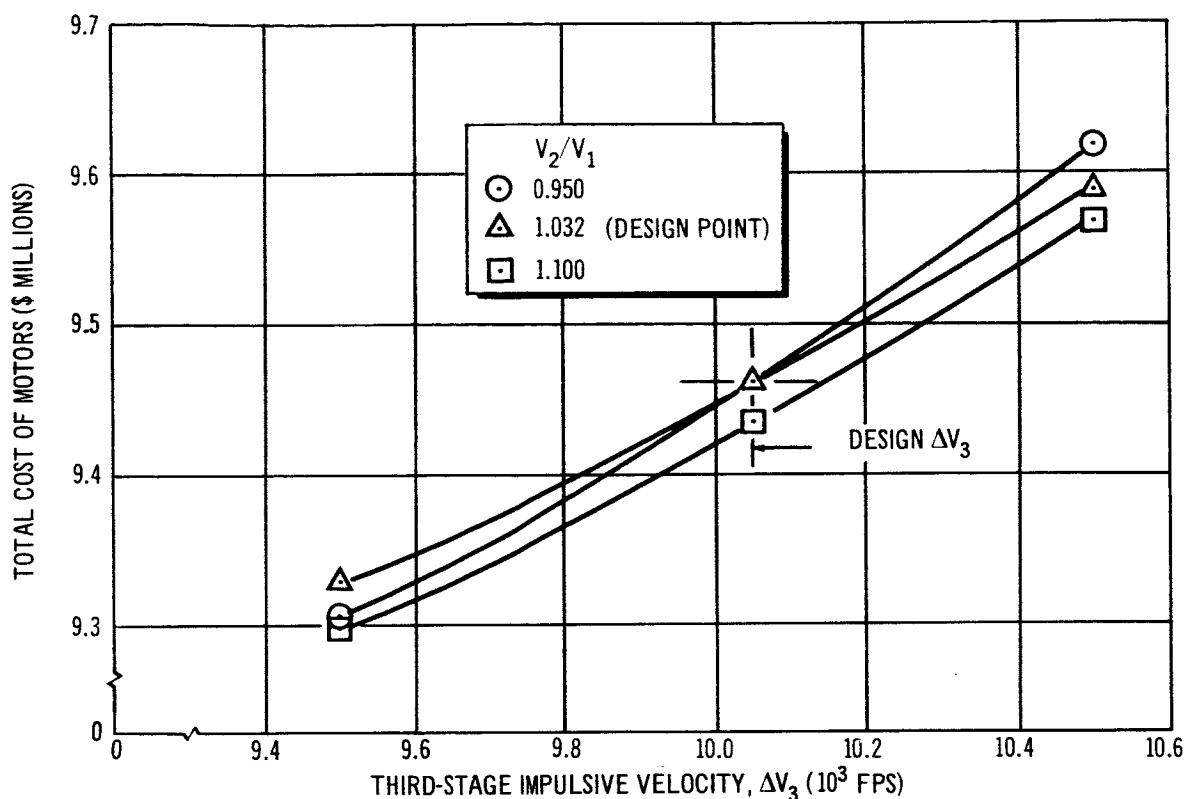


Figure 3-14. Effect of Stage Velocity Distribution on Total Motor Cost

The Configuration I vehicle is non-optimum from the standpoint of achieving a third-stage velocity which would give minimum size. This is because the steering system capabilities establish a minimum size of third-stage motor which is some 50,000 lb larger than that indicated for minimum total vehicle size. Thus, it is not possible to further reduce total costs without increasing the complexity of the steering system.

#### Cost Sensitivity to First-Stage Propellant Type

The three stages of the Configuration I launch vehicle use an HC type of propellant formulation. The selection was made on the basis of performance of the propellant. The additional cost involved over and above the use of a PBAN type is estimated to be about \$150,000 or about 3% for the case of the first stage only. No attempt was made, therefore, in the comparative studies to incorporate the more cost-optimum propellant.

#### 3.1.2.3 Thrust-Time Shaping - Third Stage

As discussed in the preceding section, the decreasing control moment arm which occurs as propellant is expended results in an increase in required control thrust. This is especially true of a stage which has a constant, or neutral, thrust-time history. This effect is shown in Figure 3-15 for the HES-2G third stage with neutral and with regressive burning. In the absence of aerodynamic disturbances, as during second- and third-stage burning, the primary disturbing influences are thrust misalignment and eccentricity. Consequently, by tailoring the solid propellant grain to decrease thrust as burning progresses, thereby providing a regressive thrust-time curve, this problem of rapidly increasing control-thrust requirement can be alleviated as shown in Figure 3-15. Figure 3-16 shows the control thrust required at the beginning of third-stage burning and at web burn out as a function of degree of regressivity. In order to obtain a flat control thrust-time history, which would serve to minimize control propellant, a regressivity ratio (ratio of initial to final thrust) of approximately 22:1 would be required. Preliminary investigation of grain design for a 156-in. diam motor with 250,000 pounds of propellant indicated that a regressivity ratio of approximately 3.2:1 was easily attainable without degrading motor volumetric loading or increasing propellant sliver fraction to a large extent. Further grain design investigation, along with its effect on control thrust requirements, should reveal additional potential decreases in control thrust, steering propellant, and payload weight.

Preliminary investigation of the effect of regressivity on second-stage control thrust requirements showed relatively low potential for savings. Consequently, this aspect was not pursued. Further investigation would, however, provide additional savings in payload weight at no penalty to operational costs of the vehicle.

#### 3.1.2.4 Trajectory Reshaping

The Phase I vehicle sizing studies were accomplished using ballistic trajectories which do not necessarily result in minimum energy trajectories. A brief study was conducted to evaluate the potential benefit of a reshaped trajectory. The scope of this study was limited to that necessary to determine a rough order of magnitude estimate of the potential gain.

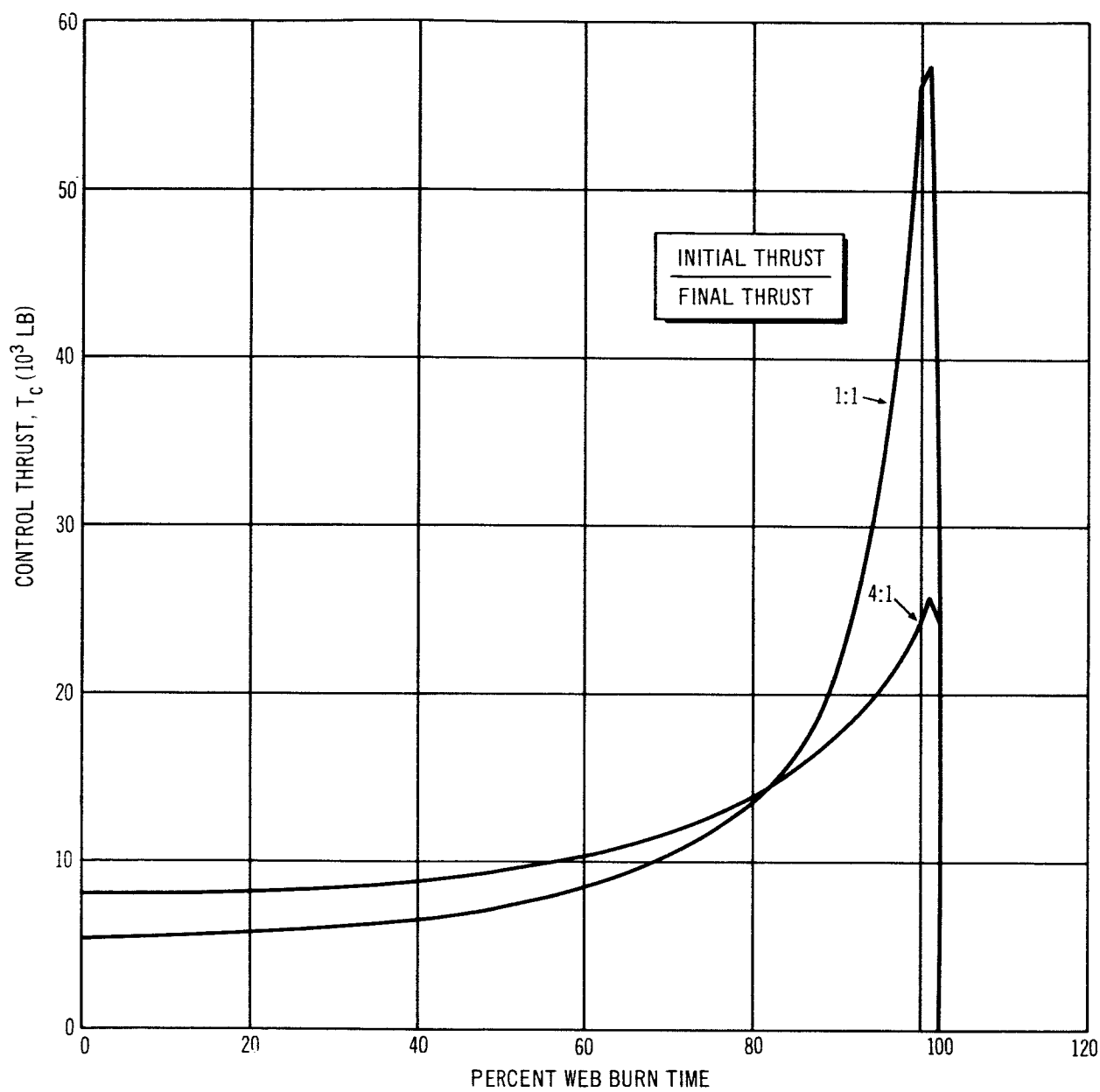


Figure 3-15. Typical Third-Stage Control Thrust Histories



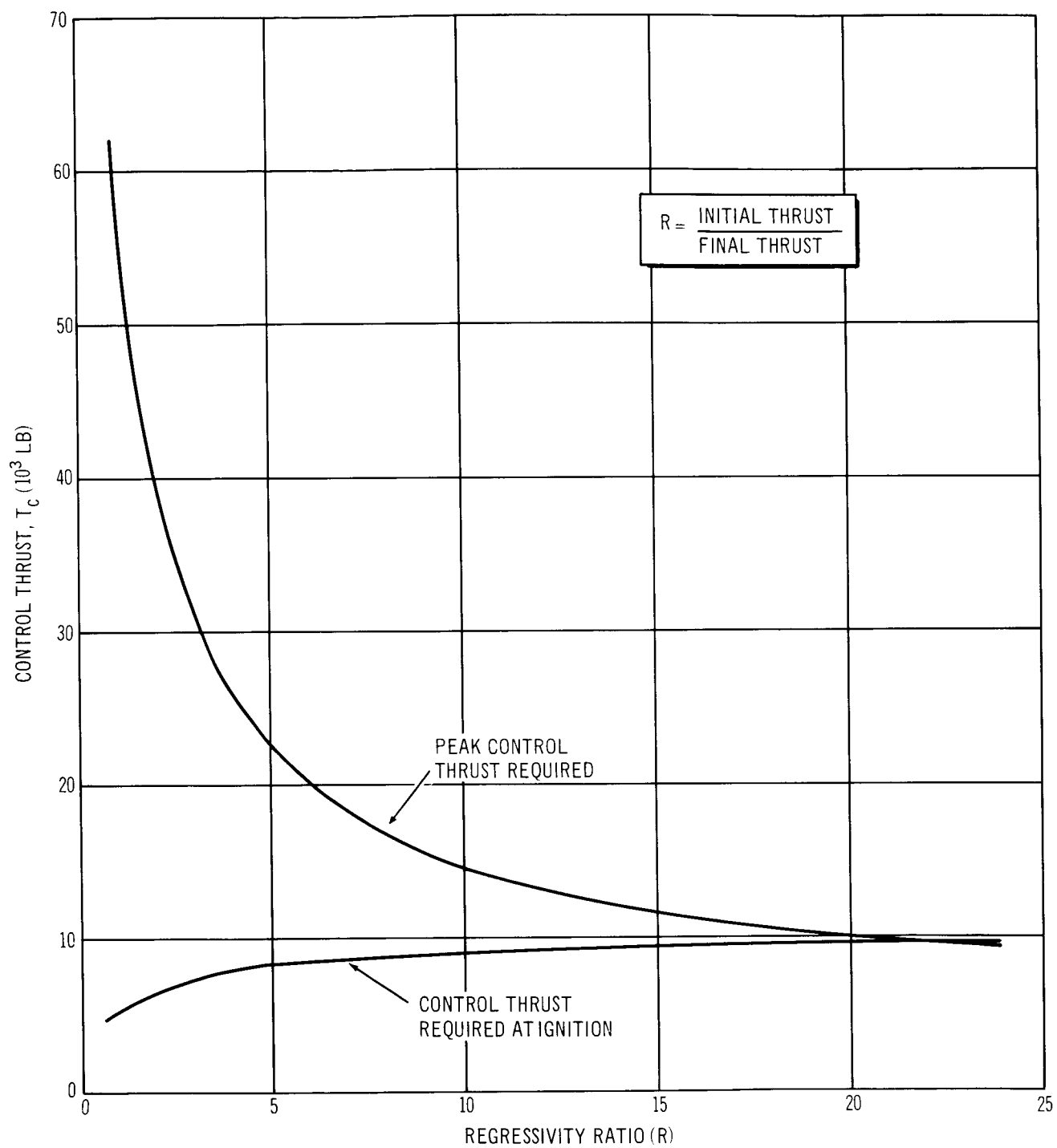


Figure 3-16. Effect of Regressivity on Control Requirements

Three approaches could be used to accomplish this evaluation using the variables of payload weight, launch vehicle size, or apogee conditions as parameters for optimization. To minimize the effort required to achieve the study objective, the approach of holding apogee conditions and launch vehicle characteristics constant and maximizing payload weight was used. Because of the interaction of launch vehicle characteristics, steering system characteristics, payload weight in the head-end-steering-type vehicles, and the number of independently variable launch vehicle characteristics, the most desirable approach consisting of determining the minimum-size launch vehicle for a given usable payload and set of apogee conditions, was not tractable for this study effort.

The conditions of a 300-nmi apogee altitude, a zero-degree flight-path angle and an apogee velocity of 24,447 fps was selected from a revised HES-2G vehicle ballistic trajectory as the desired reference apogee condition. The Configuration I launch vehicle used in this trajectory was used throughout this study effort. The solid-propellant motors making up this vehicle all utilized neutral thrust-time curves. An IBM calculus of variations, two-dimensional optimization program was utilized to determine payload-carrying capability as a function of burnout altitude, flight-path angle, and velocity for the various stages as well as pitch rate.

The results obtained from this study indicated a potential increase in payload weight of 4000 lb, approximately a 4% increase, through trajectory reshaping. Using the final Configuration I vehicle as a model, this would imply an approximate 200,000-lb decrease in launch-vehicle weight for the required payload.

### 3.1.3 Steering System Optimization

#### 3.1.3.1 Guidelines and Assumptions

The guidelines and assumptions used in the Phase II study steering analysis were the same as those used in the Phase I study (Reference 1). A list of the guidelines and assumptions used in all steering analyses are as follows:

1. Adequate control was required to maintain constant attitude flight through the specified wind-profile envelope.
2. The specified wind-profile envelope was a 95% ETR envelope with standard gust velocities superimposed.
3. Control capability was required for both full headwinds and full sidewinds considered acting separately.
4. Steering response capabilities correspond to a second order system, with a natural frequency of 0.15 rad/sec and 0.7 damping ratio.
5. Maneuvering moment requirements provide the capability of proportionally following step changes in attitude rate commands of  $0.35^\circ/\text{sec}$  in pitch and  $0.1^\circ/\text{sec}$  in yaw.
6. The sources of disturbing moments and their uncertainty levels are as follows:
  - A. Aerodynamic coefficients known to  $\pm 5\%$ .
  - B. Booster stabilizing fins aligned to the design position within  $\pm 6$  min. of arc.
  - C. Misalignment of stages with respect to a reference centerline within  $\pm 0.3^\circ$ .
  - D. Misalignment of solid-motor thrust of  $\pm 6$  min. of arc.
  - E. Eccentricity of solid-motor thrust of  $\pm 0.88$  in.
  - F. Lateral CG location from geometric centerline of  $\pm 1.0$  in.

#### 3.1.3.2 Steering Control Systems

The steering control used for Configuration I incorporates two engines, one mounted near each trailing edge tip of the HL-10. In their neutral positions during the ascent trajectory, the engine thrust vectors are directed  $30^\circ$  out from the vehicle's centerline in yaw to reduce plume-impingement heating problems on the aft adapter. In pitch, the thrust vectors lie in the pitch plane in their neutral position. For control in pitch, the engines are deflected simultaneously up or down from the pitch plane. For roll control, they are deflected in opposite

directions from the commanded pitch position. For yaw control, one engine is deflected outboard and the other engine is deflected inboard from the neutral yaw position.

To eliminate yaw coupling into pitch and roll, the engine's outer gimbal is rotated for yaw and the engine's inner gimbal for pitch. There is cross-coupling from pitch and roll into yaw and between pitch and roll themselves, but this is insignificant unless large pitch and roll commands occur simultaneously. The steering analysis has shown that such a condition will not occur.

Normally, both pitch and yaw gimbal deflections are limited to  $\pm 30^\circ$  from the neutral positions. Maximum-moment effectiveness in pitch will always occur with the engines fully deflected. In yaw, this is not always true. For maximum effectiveness, it is obvious that the inwardly deflected engine should be against the inboard stop, thus making it parallel to the vehicle centerline. It cannot be deflected further because of plume-impingement heating of the aft adaptor. For rearward CG locations, the outward directed engine should be against its outboard stop, or  $60^\circ$  out from the centerline. As the CG moves forward, however, full outboard engine deflection is no longer the most effective condition. As shown in Figure 3-17, the maximum effectiveness of the outboard directed engine occurs when the thrust vector is normal to a line connecting the CG and the engine gimbal point. Thus, it is assumed that control system logic continuously reduces the  $60^\circ$  outward limit to the most effective value for that limit when its value has become less than  $60^\circ$ .

#### 3.1.3.3 Steering-Engine Throttling

The steering analysis determined the control engine thrust level required for control during each second of flight, assuming maximum effective engine deflection. It was then assumed that the control engines would be throttled in finite steps to approximate the required control thrust curve to minimize the quantity of control propellant required. Thus, during a given time period, the engine thrust would be set equal to the maximum thrust required during that time period and actual control achieved by control engine deflections. In the Phase I study, the time periods during which a constant throttling ratio was used corresponded to the stage flight times. During the Phase II study, intermediate

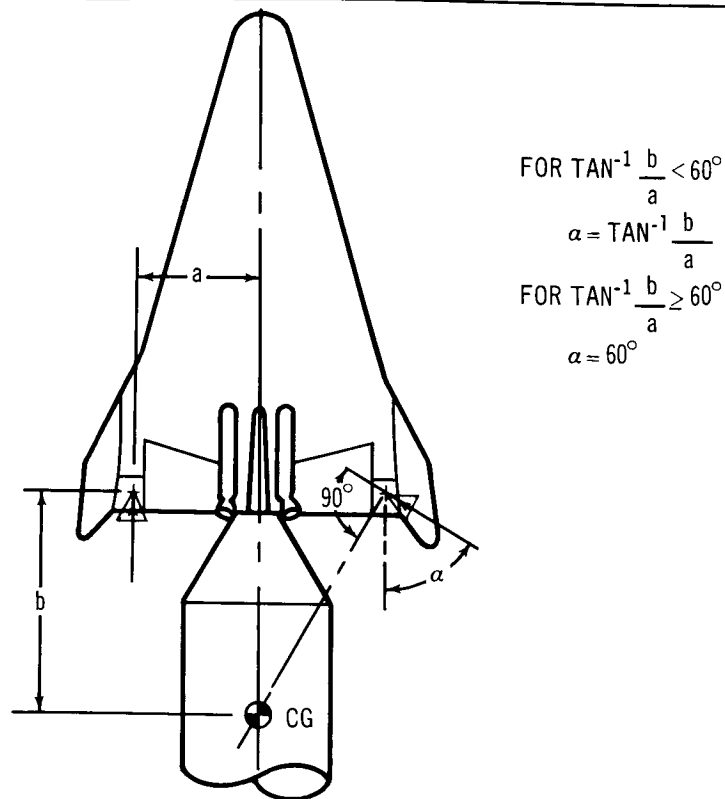


Figure 3-17. Control Engine Geometry for Maximum Yaw Steering Moment – Configuration I

throttling ratio changes were made to approximate the required thrust curve to further reduce control propellant requirements. Figure 3-18 illustrates this concept of step throttling.

It will be noted in Figure 3-18 that there is a large increase in thrust required near the end of the third stage and a smaller increase of thrust required at the end of second stage. This increase is primarily needed because of the forward movement of the CG, which shortens the effective control moment arm. This is particularly true for the yaw axis (Figure 3-17) because of the availability of both engines for control on the pitch axis; while in yaw, one engine is always providing an opposing moment. Thus, as the CG moves forward and the yaw-moment arms of the two engines become equal, the ratio of yaw-moment effectiveness to pitch-moment effectiveness decreases very rapidly. During exoatmospheric phases of flight, pitch and yaw disturbing moments are essentially equal; thus, for optimum control, the yaw/pitch effectiveness ratio should be equal to one. Since yaw effectiveness is limited, the control-thrust requirements become primarily dependent upon the yaw control available; thus, yaw-control moment capability becomes a dominant factor in the determination of steering propellant requirements.

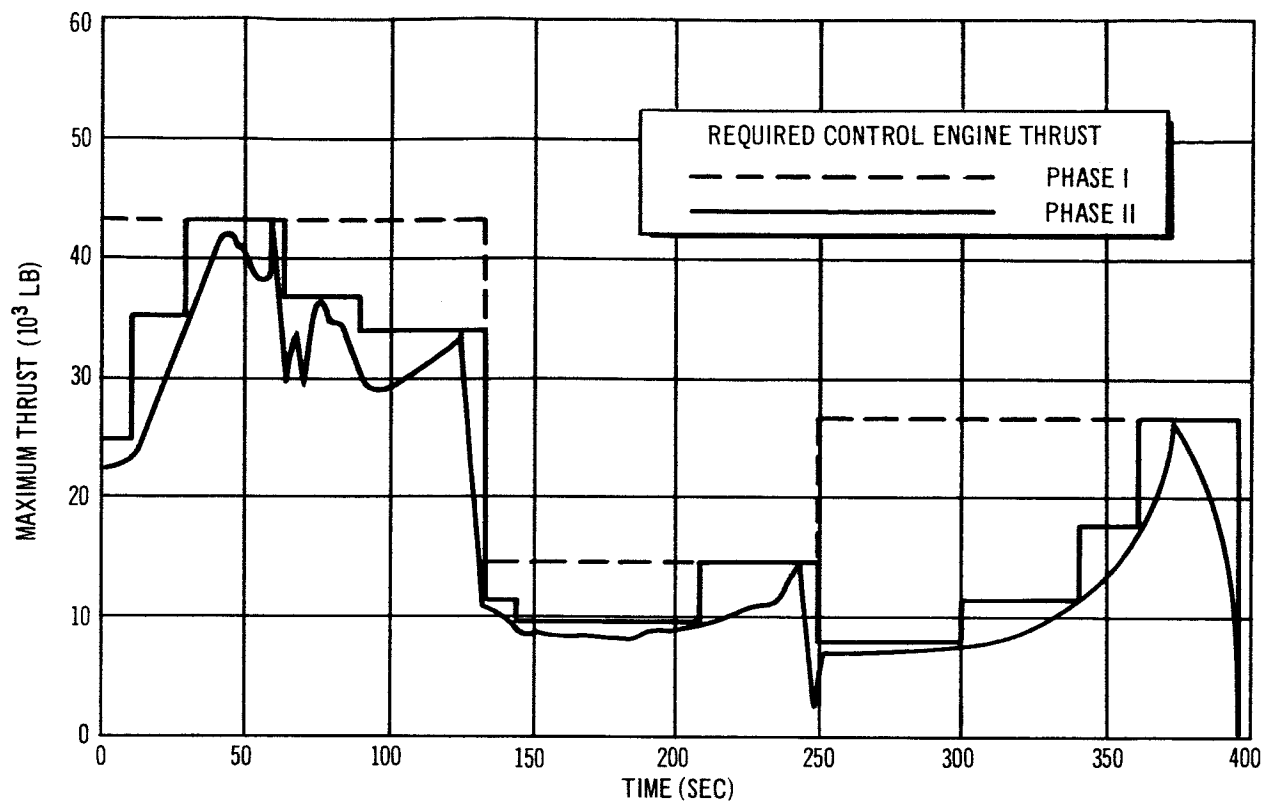


Figure 3-18. | Steering Engine Step Throttling

One means of increasing the yaw control available would be to differentially throttle the engines in addition to gimbaling them, that is, decrease the thrust of the opposing engine below the nominal thrust level while increasing the thrust of the other engine a like amount above the nominal level. Figure 3-19 shows the effect of differential throttling, assuming the pitch gimbal angle to be zero. As would be expected from the previous discussion, the benefits of this method of control occur primarily during the final stage, when the CG is far forward. Also, during the major part of first-stage flight, yaw-moment requirements are smaller than pitch-moment requirements and the yaw-pitch-effectiveness ratio is near a value of one, thus more yaw-moment effectiveness is available than is needed. Further study of differential throttling was limited to the second and third stages of Configuration I.

In the presence of a pitch gimbal angle, differential throttling will induce roll moments which must be balanced by differentially gimbaling the engines in the pitch plane. Also, the amount of throttling possible is limited by the fact that

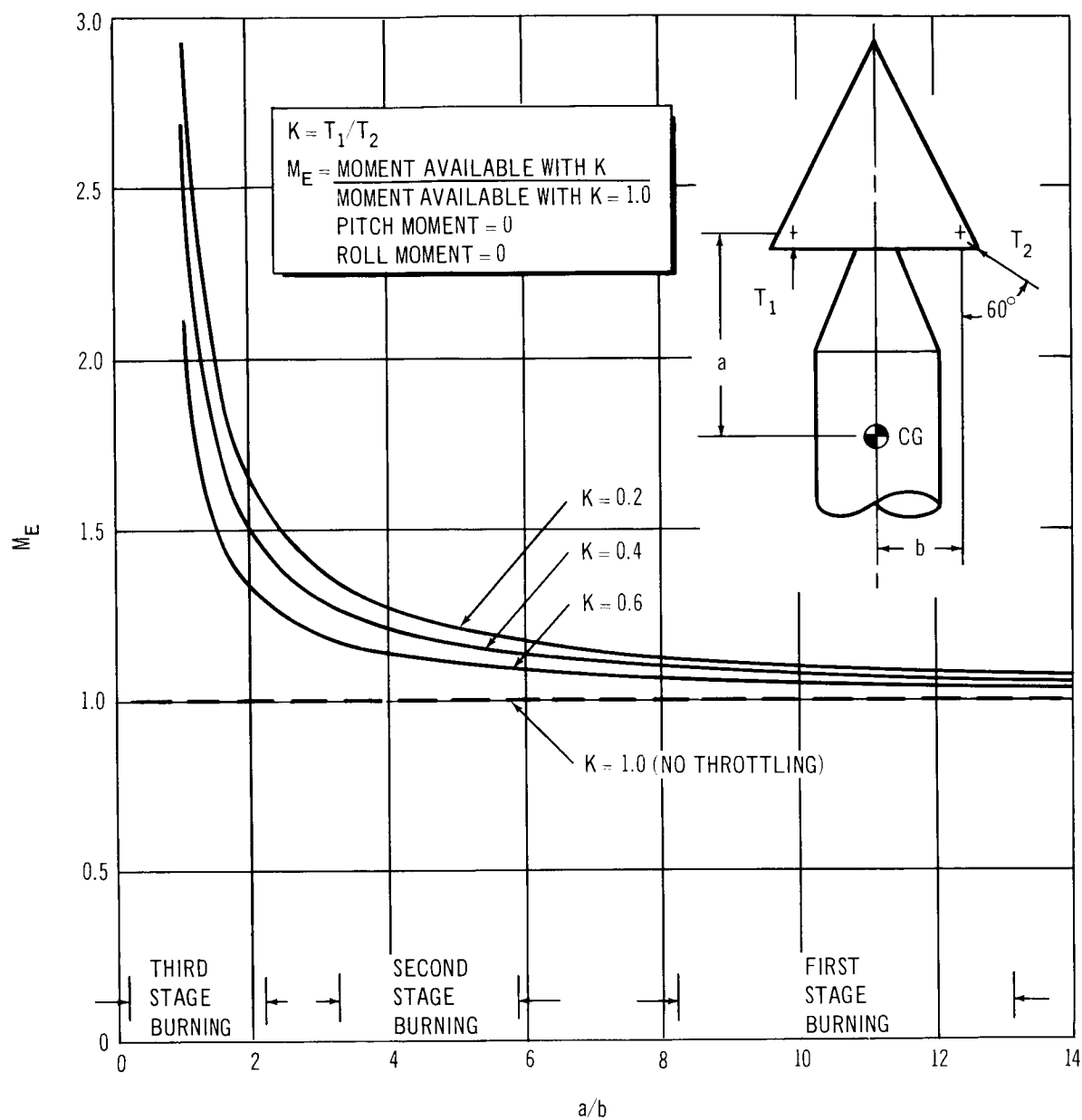


Figure 3-19. Yaw-Control Moment Effectiveness-Differential Throttling

it is the throttled down engine that must oppose the induced roll. Taking these effects into account, two time points in the third stage and one in the second stage were investigated for the differential throttling system. The resulting control thrust-levels required, along with the requirements without differential throttling, are presented in Figure 3-20.

In addition, a somewhat simplified differential throttling system was considered. Since it would require rather sophisticated control logic to simultaneously differentially throttle and gimbal the engines for yaw control, it was assumed that the yaw gimbals would be locked in their neutral position. Yaw control would then be by means of differential throttling only. Two time points in the third stage were investigated using this technique (Figure 3-20).

It can be seen that the two systems require essentially the same nominal thrust level near the end of third-stage burn. The system with the locked yaw gimbals requires an essentially constant nominal thrust level throughout third stage, while the other system requires slightly less thrust initially. This slight increase in the nominal thrust level during third stage would hardly justify symmetrical throttling of the engines to maintain the nominal thrust level shown. Thus, a constant nominal thrust would be used and would correspond to the thrust level required by the locked yaw gimbal system. The thrust requirements of the two systems are basically the same.

By incorporating such a system, weight savings of the control propellant for the third stage of the Configuration I vehicle would be approximately 6,200 lb. This would correspond to a payload increase of about 700 lb. Savings on the second stage would be considerably less, while on the first stage they would be negligible.

A system of this type would be considerably more complex than the gimbaling system alone, thus the cost and weight would be greater and the reliability less. Since much more study would be required to see if the use of such a system could be justified, no further consideration was given to it in this study.



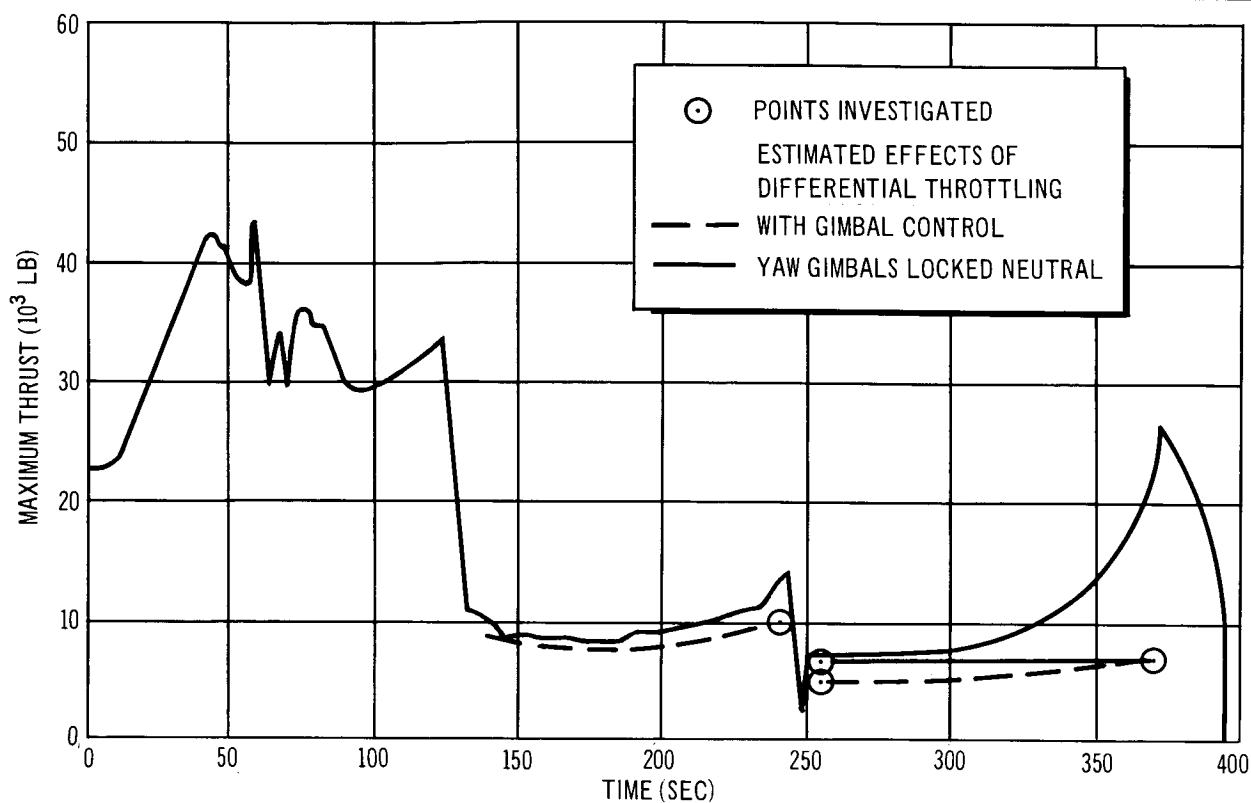


Figure 3-20. Effects of Differential Throttling

#### 3.1.3.4 Steering Simulation Program

The Fortran steering simulation program used for the Phase I study was extensively revised in two areas for the Phase II study. The first of these revisions was the incorporation of capability for evaluating a tailend steering system in addition to the HL-10 mounted two-engine system and the adapter mounted four-engine system. The second change was a complete revision of the aerodynamic representation of the vehicle. This is discussed in detail in the following section.

The program computes all trajectory parameters as a function of time and all aerodynamic coefficients as a function of Mach number. These variables are put in the program in the form of a series of straight-line approximations to the actual curves. The standard wind-profile envelope is entered in a like manner as a function of altitude. The gust profile is superimposed on the wind envelope at its maximum value and shifted to center at the altitude where peak dynamic pressure occurs. Dynamic pressure is then adjusted to account for relative

wind for both head and sidewind conditions. For the headwind case, angle of attack is computed, and for the sidewind case, sideslip angle is computed. From this data, the nominal pitch and yaw moments are computed for headwind and sidewind cases, respectively. Since only gravity turn trajectories were considered, these are the only nominal aerodynamic moments present.

The various uncertainties then computed are (1) 5% uncertainty of nominal moments; (2) pitch, yaw, and roll moments caused by fin misalignments; (3) roll moments caused by fin dihedral effect, assuming  $1^\circ$  sideslip for the headwind case and  $1^\circ$  angle of attack for the sidewind case; and (4) pitch, yaw, and roll moments caused by thrust and body eccentricities and misalignments. The uncertainty moments applicable to each particular case are then root-sum-squared (RSS). The RSS values are added to and subtracted from the nominal moment values for use in computing required thrust. The four resulting conditions are as follows:

1. Headwind Case--Nominal aerodynamic pitch moment plus uncertainties, yaw moment attributable to uncertainties, and roll moment attributable to uncertainties.
2. Headwind Case--Nominal aerodynamic pitch moment minus uncertainties, yaw moment attributable to uncertainties, and roll moment attributable to uncertainties.
3. Sidewind Case--Pitch moment attributable to uncertainties, nominal aerodynamic yaw moment plus uncertainties, and roll moment attributable to uncertainties.
4. Sidewind Case--Pitch moment attributable to uncertainties, nominal aerodynamic yaw moment minus uncertainties, and roll moment attributable to uncertainties.

The moments listed above may be either positive or negative; however, the sign of the moment only determines the direction in which the control engines are gimbaled. The equations derived for determining the required control thrust make the assumption that all applied moments are positive in sign. Thus, only the absolute values of the moments are used in the following discussion.

In each case, additional maneuvering control-moment requirements are added to the absolute values of the pitch- and yaw-moment requirements. These amount to sufficient control for  $0.148^\circ/\text{sec}^2$  acceleration in pitch and  $0.043^\circ/\text{sec}^2$

acceleration in yaw. These values were derived for the Phase I study (Reference 1). No roll maneuver requirements were analyzed.

Once the total pitch, yaw, and roll moments are determined, the control thrust is separately computed for each of the four cases. A moment equation may be written for each of the three vehicle axes: pitch, yaw, and roll. This results in three equations in four unknowns. In the case of the HL-10 mounted engines, the unknowns are (1) left-hand engine pitch gimbal angle, (2) right-hand engine pitch gimbal angle, (3) yaw gimbal angle, and (4) engine thrust. It is then assumed that the yaw gimbals are in their most effective position, thus eliminating the yaw gimbal angle as an unknown and making it possible to solve for the other three. The maximum deflection of the pitch gimbal is then the gimbal deflection of the control engine opposing the applied roll moment. If this value is less than  $30^{\circ}$ , all conditions are satisfied and the solution is stored for later print out. However, if the maximum pitch gimbal deflection exceeds  $30^{\circ}$ , it is necessary to recompute the thrust and gimbal angles. This is done by starting with the assumption that the engine opposing the applied roll moment is at its maximum position of  $30^{\circ}$ . The resulting solution then provides the required control thrust and the corresponding gimbal angles. In this case, the yaw gimbal angle will always be less than its maximum capability. The method of computing control thrust for the adapter mounted engine configuration is essentially the same.

For the tailend steering configurations examined in the comparative studies, it is assumed that the booster engine nozzle is effectively gimballed in pitch and yaw. The required effective gimbal angles are computed and stored for printout. In this case, thrust misalignment is expressed as a resultant gimbal angle. Thus, the additional roll moment caused by this angle, the moment arm caused by the eccentricity of the thrust vector, and the CG mislocation are computed and added to the other roll moments. The total roll moment is then stored for later printout. These data are then readily converted to fluid-injection system requirements for pitch-control and yaw-control and reaction-control requirements for roll control.

### 3.1.3.5 Aerodynamic Representation

It was felt that the Phase I study was rather conservative in assuming constant aerodynamic coefficients equal to the transonic values. For this reason, a more realistic approach was taken to the vehicle aerodynamic representation. The Mach number is computed for each second of flight, and all aerodynamic coefficients are then computed as a function of the Mach number. In addition, pitch and yaw stabilizing fin characteristics are a function of their respective spans and aspect ratios as well as Mach number. The equations used are listed below. Table 3-2 shows the nomenclature used. Nominal pitch and yaw equations are of the same form, thus the yaw equations are not listed here.

Nominal body moments

$$C_{M_{0B}} = (C_{M_{\alpha B}} + C_{M_{\alpha^2 B}} |\alpha|) \alpha$$

$$C_{N_B} = (C_{N_{\alpha B}} + C_{N_{\alpha^2 B}} |\alpha|) \alpha$$

$$T_B = \left( C_{M_{0B}} + \frac{L_{CG} - L_{REF}}{D_{REF}} C_{N_B} \right) A_{REF} \cdot D_{REF} \cdot Q_T$$

Nominal fin moments

$$C_{N_{\alpha F}} = \left( \frac{A_{FIN}}{A_{REF}} \cdot \frac{(b + 2R)^2}{(b + R)^2} \right) C'$$

$$C_{N_{\alpha^2 F}} = \frac{2 A_{FIN}}{A_{REF}} \cdot \frac{0.95 + 1.05R}{b + R}$$

$$L_{FIN} = L_{Body} - \frac{16 b}{AR}$$

$$T_F = (L_{CG} - L_{FIN}) \cdot \left( C_{N_{\alpha F}} + C_{N_{\alpha^2 F}} |\alpha| \right) \alpha \cdot A_{REF} \cdot Q_T$$

Total nominal moment

$$T_T = T_B + T_F$$

Table 3-2 (Page 1 of 2)  
AERODYNAMIC NOMENCLATURE

---

$A_{FIN}$	Fin area
$A_{REF}$	Reference area
AR	Fin aspect ratio
$\alpha$	Angle of attack
b	Fin exposed semispan
$C'$	Fin effectiveness coefficient
$C_{MoB}$	Total aerodynamic pitching moment coefficient of body*
$C_{M\alpha B}$	Linear aerodynamic pitching moment coefficient of body
$C_{M\alpha^2 B}$	Nonlinear aerodynamic pitching moment coefficient of body
$C_{NB}$	Total aerodynamic normal force coefficient of body
$C_{N\alpha B}$	Linear aerodynamic normal force coefficient of body
$C_{N\alpha^2 B}$	Nonlinear aerodynamic normal force coefficient of body
$C_{N\alpha F}$	Linear aerodynamic normal force coefficient of pitch fins
$C_{N\alpha^2 F}$	Nonlinear aerodynamic normal force coefficient of pitch fins
$C_{N\beta F}$	Linear aerodynamic normal force coefficient of yaw fins
$D_{REF}$	Reference diameter
$\alpha_p$	Pitch fin sweepback angle
$\alpha_\gamma$	Yaw fin sweepback angle
i	Fin misalignment angle
$L_{Body}$	Vehicle overall length
$L_{CG}$	Distance from vehicle nose to CG
$L_{FIN}$	Distance from vehicle nose fin center of pressure
$L_{REF}$	Reference length
M	Mach number

---

\*"Body" refers to Configuration I vehicle without fins.

---

Table 3-2 (Page 2 of 2)

---

$Q_T$	Total dynamic pressure
$R$	Distance from fin center of pressure to vehicle centerline
$T_B$	Body torque about CG
$T_F$	Fin torque about CG
$T_i$	Torque about CG caused by fin misalignment
$T_{RD}$	Rolling torque caused by dihedral effect
$T_{Ri}$	Rolling torque caused by fin misalignment
$T_T$	Total torque about CG

---

Fin misalignment moments

$$T_i = (L_{FIN} - L_{CG}) \frac{2A_{FIN}}{A_{REF}} \cdot \frac{R}{b + R} \cdot C' \cdot i \cdot A_{REF} \cdot Q_T$$

$$T_{Ri} = \frac{2A_{FIN}}{A_{REF}} \cdot \frac{R^2}{b + R} \cdot i \cdot A_{REF} \cdot Q_T$$

Dihedral effect moments (assuming 1° sideslip angle)

$$T_{RD} = \frac{R}{2} \left\{ \left[ \cot \left( \gamma_P - \frac{1.0}{57.3} \right) - \cot \left( \gamma_P + \frac{1.0}{57.3} \right) \right] C_{N\alpha F} \cdot \alpha \right. \\ \left. - \left[ \cot (\gamma_Y - \alpha) - \cot (\gamma_Y + \alpha) \right] C_{N\beta F} \cdot \frac{1.0}{57.3} \right\} A_{REF} \cdot Q_T$$

Fin Coefficient  $C'$

If  $M \leq 1.0$

$$C' = \frac{2\pi AR}{2.0 + \sqrt{8.0 + AR^2 (1 - M^2)}}$$

If  $M > 1.0$ ;  $AR \sqrt{M^2 - 1} < 4.0$

$$C' = \left[ \frac{\pi}{2.414} - \left( \frac{\pi}{2.414} - 1 \right) \cdot \frac{AR \sqrt{M^2 - 1}}{4} \right] AR$$

If  $M \leq 1.0$ ;  $AR \sqrt{M^2 - 1} \geq 4.0$

$$C' = \frac{4.0}{\sqrt{M^2 - 1}}$$

The simplified aerodynamics of the Phase I study allowed a convenient method of fin optimization. Since the aerodynamic coefficients were constant, body and fin moments varied in the same manner and the center of pressure remained at a constant location. Thus, vehicle neutral stability could occur at one, and only one, time: when the CG coincided with the center of pressure. Accordingly, it was possible to have the steering simulation program compute a fin size to give neutral stability at any given time merely by determining the fin size required to make the center of pressure coincident with the CG at that given time (Figure 3-21). Optimization of the neutral stability time then allowed minimization of control thrust requirements.

With the incorporation of Mach number dependent aerodynamics, this method was no longer practical. The center of pressure now varies with Mach number, so there may be several times of neutral stability (Figures 3-22 and 3-23). In addition, because of the nonsymmetry of the HL-10 in pitch and yaw planes, optimization requires different sized pitch and yaw fins. The steering program was modified to provide for the input of pitch and yaw fin spans and aspect ratios.

### 3.1.3.6 Effect of Fin Configuration on Control Thrust Requirements

In the idealistic case, control thrust requirements would be at an absolute minimum if the vehicle being controlled were neutrally stable at all times. This would eliminate all aerodynamic disturbing moments. Obviously, this is impractical because of changing the aerodynamic characteristics and the vehicle CG movement with the consumption of propellant and control fuel. However, it

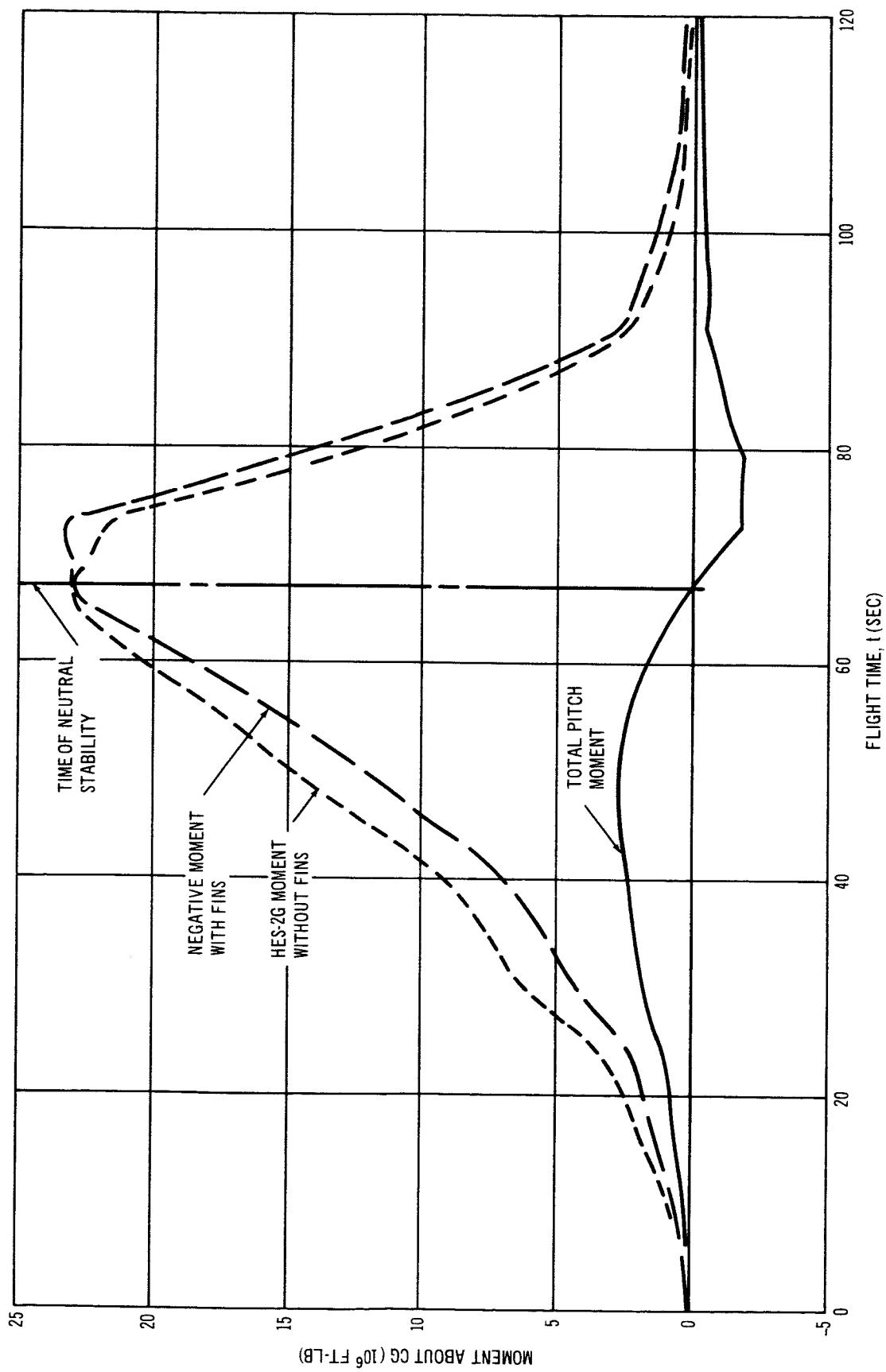


Figure 3-21. Aerodynamic Pitch Moment – Phase I, HES-2G



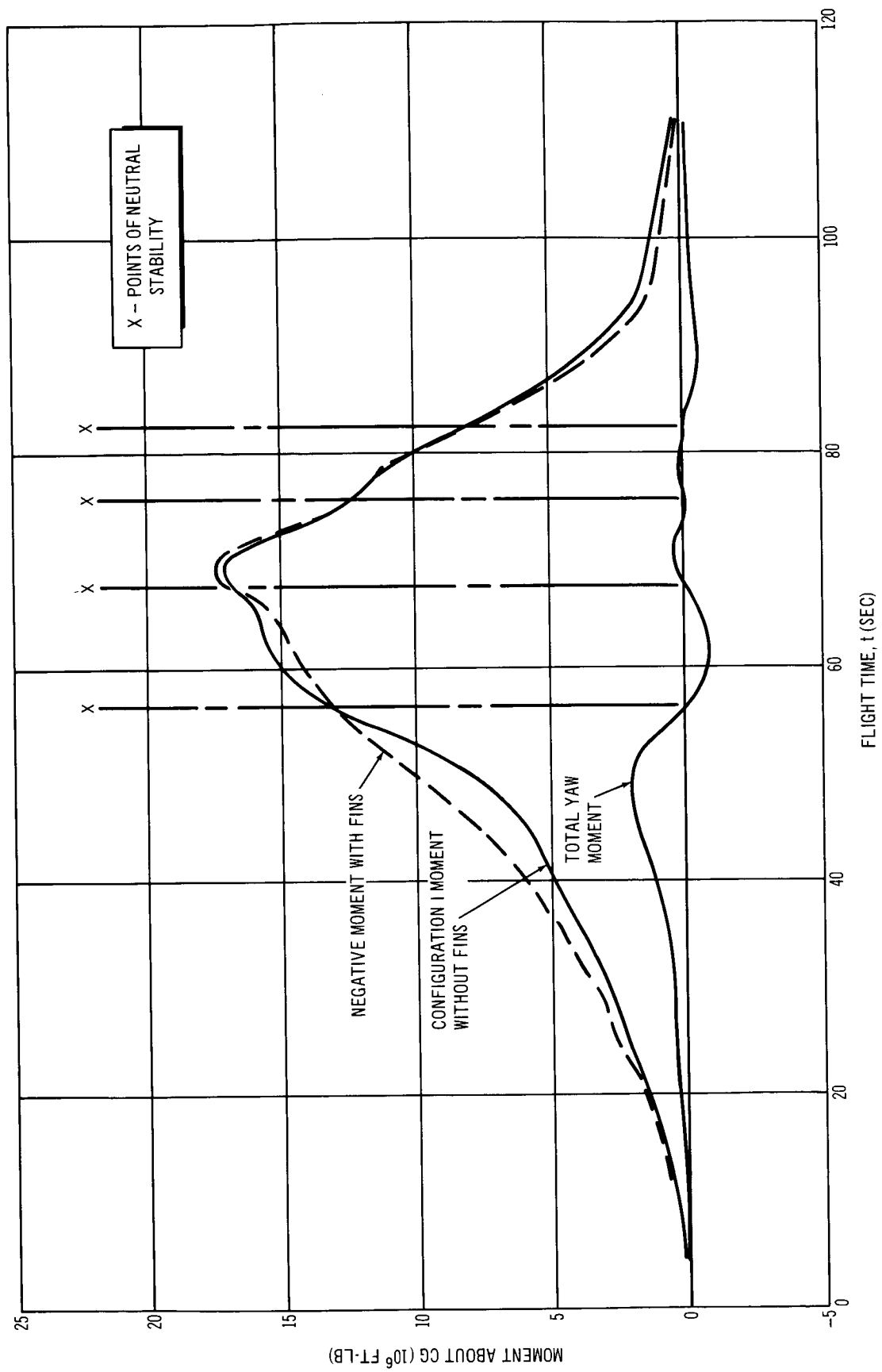


Figure 3-22. Aerodynamic Yaw Moments - Phase II Configuration I - Total Yaw Moment

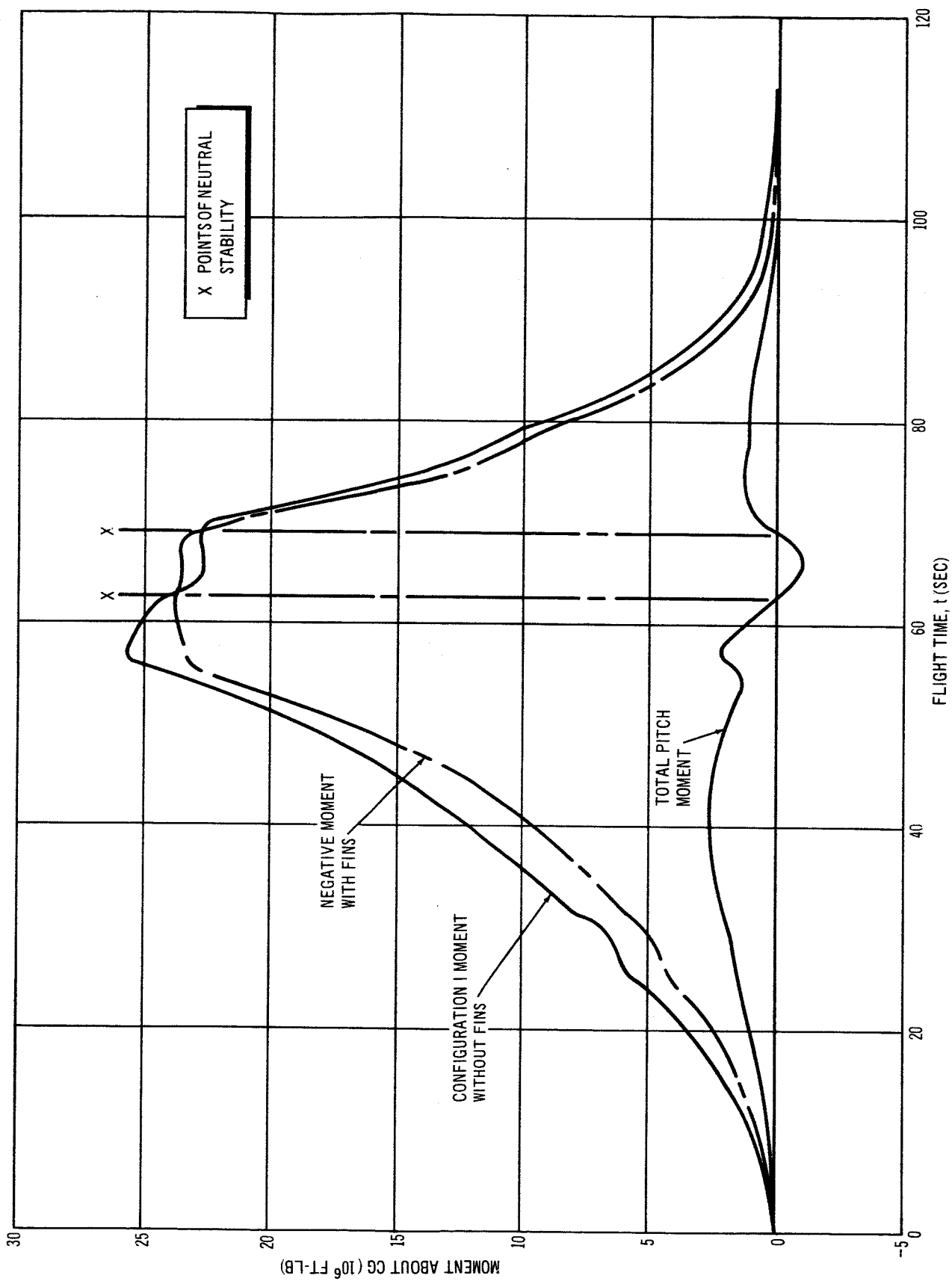


Figure 3-23. Aerodynamic Pitch Moments - Phase II, Configuration I - Total Pitch Moment

is possible to minimize the degree of vehicle stability or instability by judicious shaping and sizing of the stabilizing fins. Figure 3-23 illustrates the aerodynamic pitch-moment characteristics of Configuration I with the optimum pitch fin configuration. Figure 3-24 shows the effect of off-optimum fin configurations. It is seen that the effect of fin span changes is to raise or lower the moment curve, while maintaining the same approximate shape. Aspect ratio changes primarily affect the shape of the curve peak, as well as some general effect on the magnitudes.

Obviously, it is necessary to vary fin configurations to minimize control thrust requirements. In the case of unsymmetrical configurations, such as Configuration I, the pitch and yaw stabilizing fins will not necessarily be of the same size or shape. The steering program was modified to accept pitch-fin aspect ratio and span and yaw-fin aspect ratio and span as input data. Various combinations of these were then evaluated to arrive at an optimum configuration. Figures 3-25 and 3-26 illustrate the effect of these parameters on the maximum control thrust required at any time point during first-stage operation.

It will be noted that in Figure 3-25 there is a very sharply defined optimum point on the fin span curve. This may be explained by consideration of Figure 3-27. Part A of this figure represents the basic body pitch moment (without fins) and the negative fin moment for three different fin spans. The maximum control thrust requirement is a function of the maximum net vehicle moment, that is, the maximum difference between the body moment and the negative fin moment curves. In the case of fin span  $b_1$ , the control thrust requirement is proportional to  $x_1$ , and for fin span  $b_3$ , it is proportional to  $y_3$ .

The HL-10 pitch characteristics cause two distinct moment levels in the body moment curve in the critical transonic area, while the fin curves are essentially flat. Accordingly,  $x$  is then defined as the difference between the fin moment curve and the higher peak of the body moment curve and  $y$  is defined as the difference between the fin moment curve and the lower peak of the body moment curve. Since fin moment variation with fin span is essentially linear, plots of the absolute value of  $x$  and  $y$  versus fin span appear as shown on Figure 3-27. The resultant curve is  $xoy$  and corresponds to Figure 3-25. It is apparent

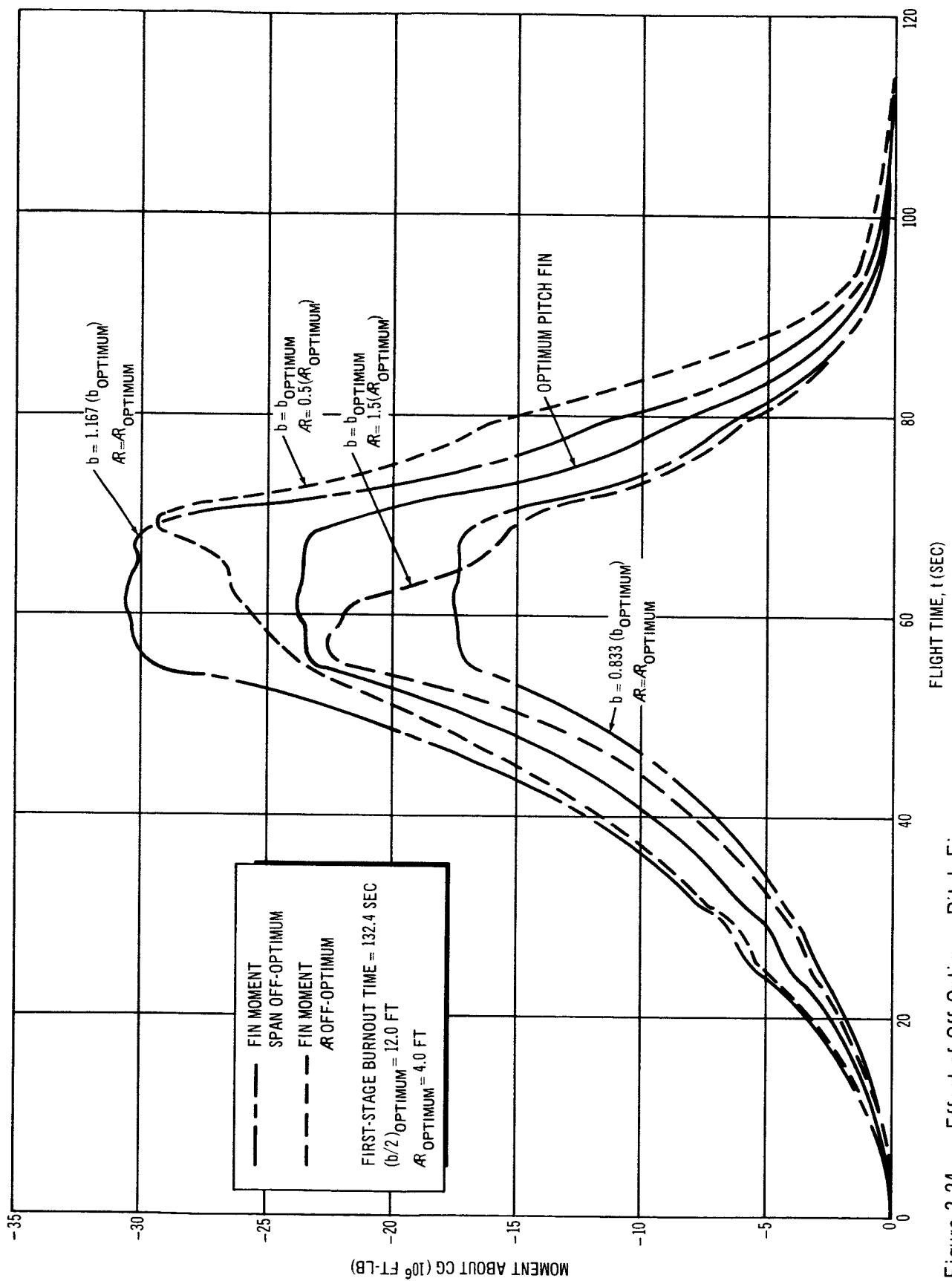


Figure 3-24. Effect of Off-Optimum Pitch Fins

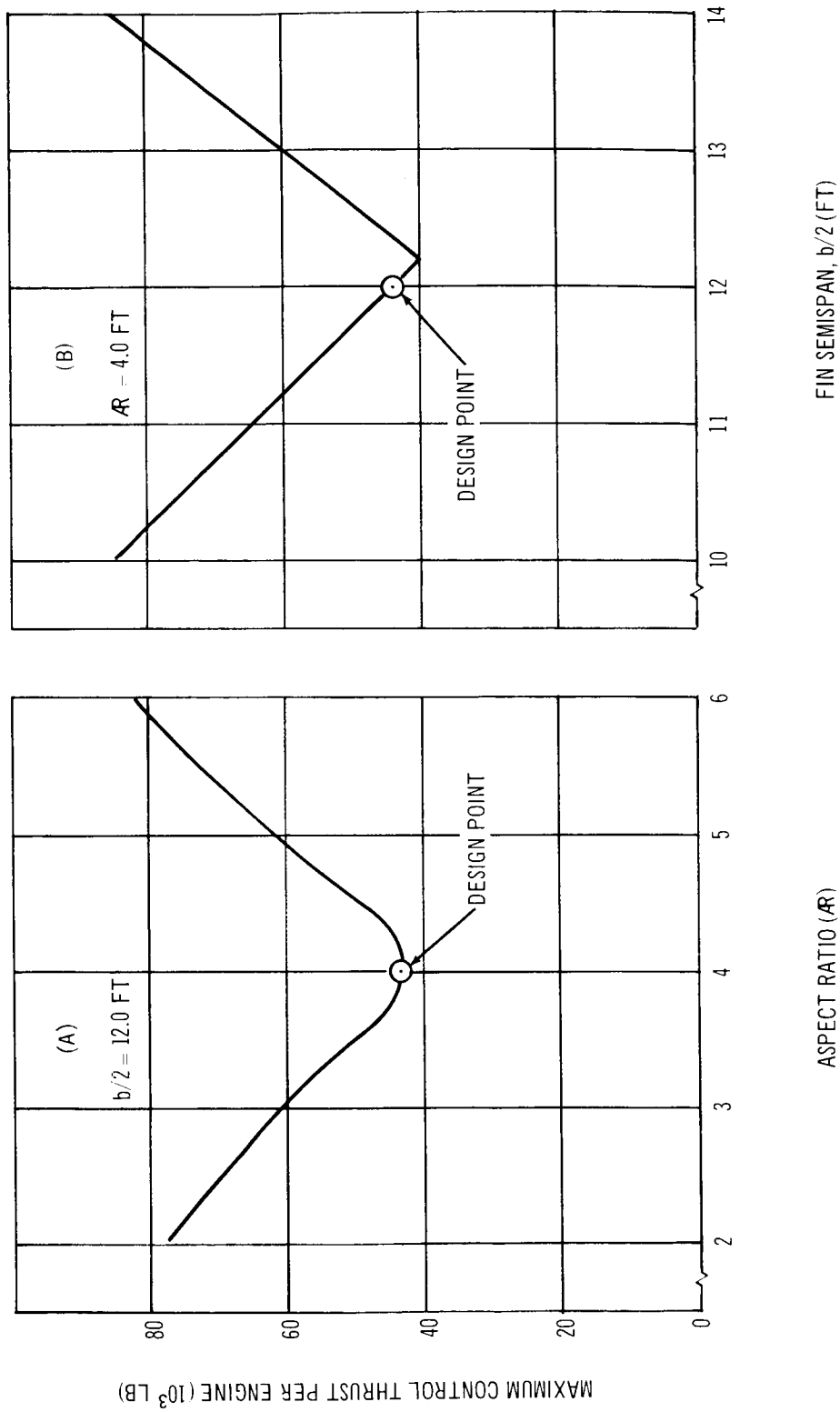


Figure 3-25. Effect of Pitch Fin Planform Shape-Yaw Fin -  $AR = 2.0$ ,  $b/2 = 8.0$  ft

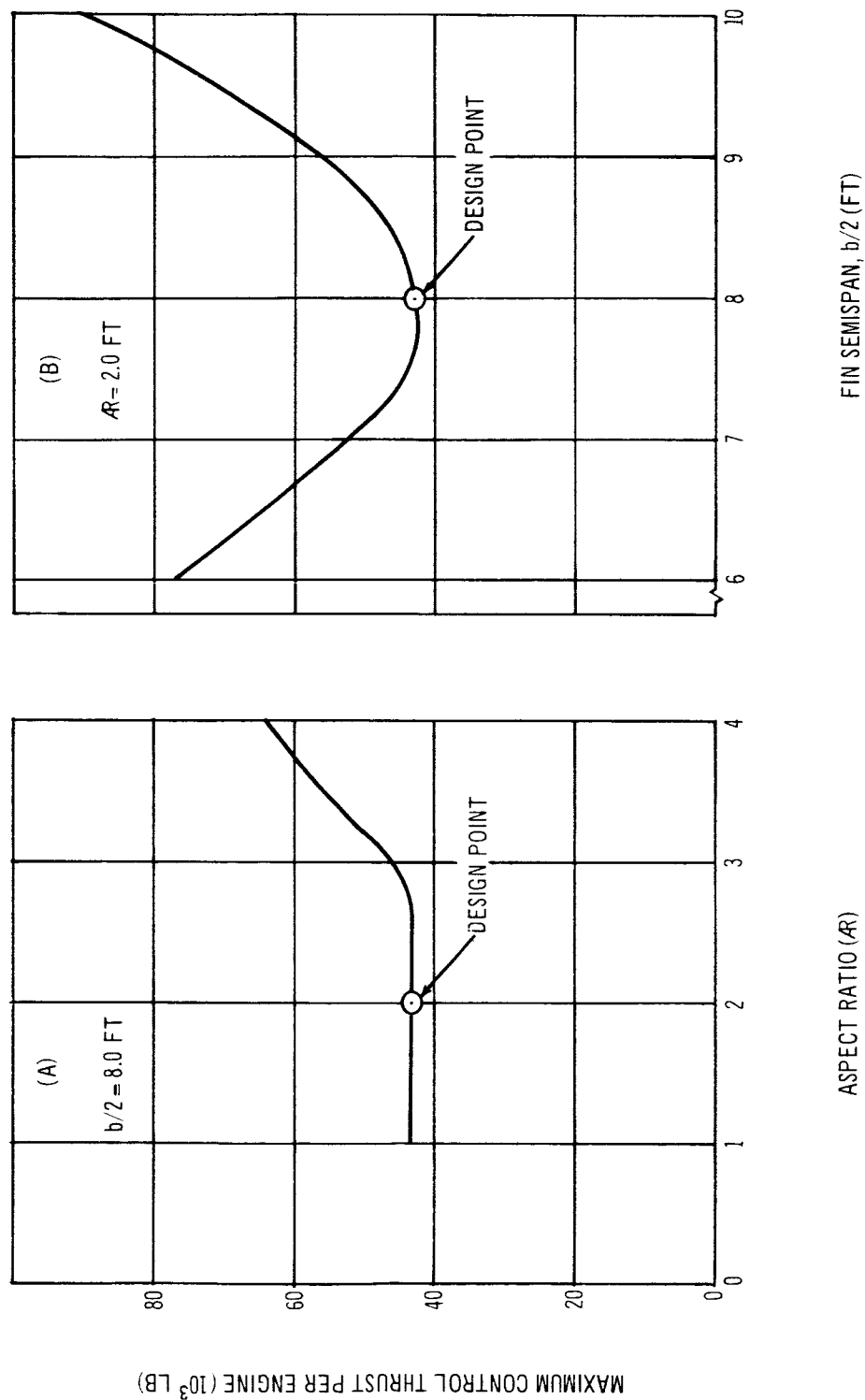


Figure 3-26. Effect of Yaw Fin Platform Shape-Pitch Fins —  $AR = 4.0$ ,  $b/2 = 12$  ft

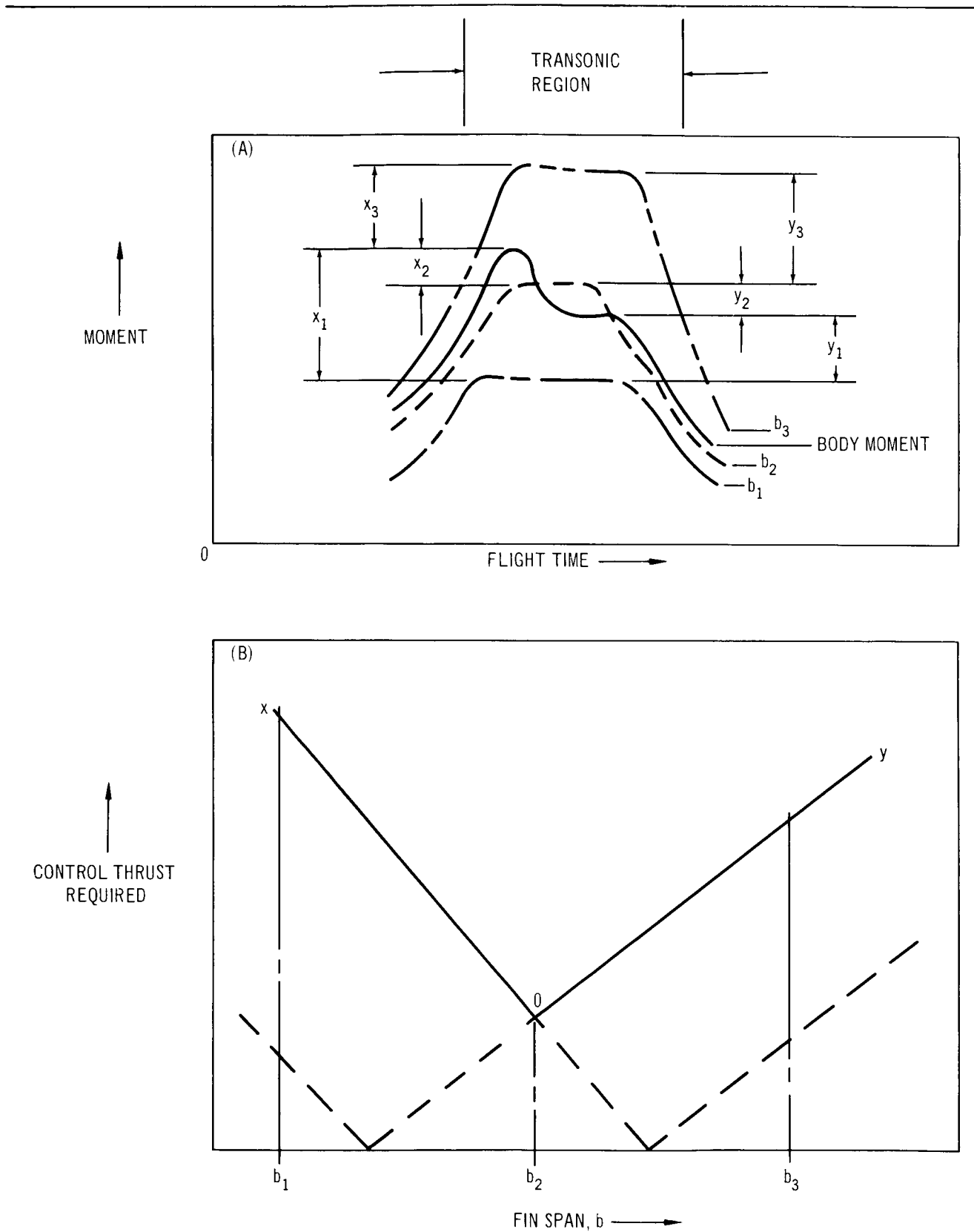


Figure 3-27. Effect of Aerodynamic Phenomena on Optimum Fin-Span Selection

that the optimum condition occurs when  $x = y$ . The absence of a sharp optimum point in Figure 3-25 is caused by the fact that fin aspect ratio variation causes a change in the shape as well as the magnitude of the fin moment curve.

The HL-10 characteristics are such that the wide moment variations evident in pitch in the transonic region are not as severe in yaw; therefore, the sharp optimum point is not present in the yaw fin optimization curves of Figure 3-26.

### 3.1.3.7 Control Thrust Requirements

Figure 3-28 represents a composite picture of the Configuration I control thrust requirements during first stage for each of the four cases studied. The resultant required control thrust curve (Figure 3-18) comprises the envelope of the maximum points of the composite curve.

It will be noted that the headwind case provides the critical control requirements during the first 90 sec of flight time. This is primarily caused by the fact that the horizontal component of vehicle velocity adds to the wind in the headwind case. Although this provides an angle of attack which is smaller than the sideslip angle produced in the sidewind case, the dynamic pressure in the headwind case is much greater. Also, the transonic pitching characteristics of the HL-10 produce large moments, as evidenced by the peak in control thrust at Mach 1 which occurs at 57 sec. After 90 sec the sidewind case produces the critical control thrust requirements. This is caused by the fact that the total aerodynamic pitch moment approaches zero at this time, while the yaw moment, although becoming smaller, maintains an appreciable value (Figures 3-22 and 3-23).

It is seen that the yaw moment, plus uncertainties, and yaw moment, minus uncertainties, essentially coincide between 0 and 25 sec and again between 70 and 85 sec. This is also true of the pitch moment curves beyond 105 sec. This occurs whenever the associated aerodynamic moment approaches zero and is caused by the fact that the absolute values of the disturbing moments are used (Section 3.1.5.4); thus,  $|0.0 + \text{uncertainties}| \approx |0.0 - \text{uncertainties}|$ .

During second and third stages, there are essentially no aerodynamic moments since the vehicle is beyond the sensible atmosphere. Also, headwinds and sidewinds lose significance; accordingly, pitch and yaw disturbing moments are



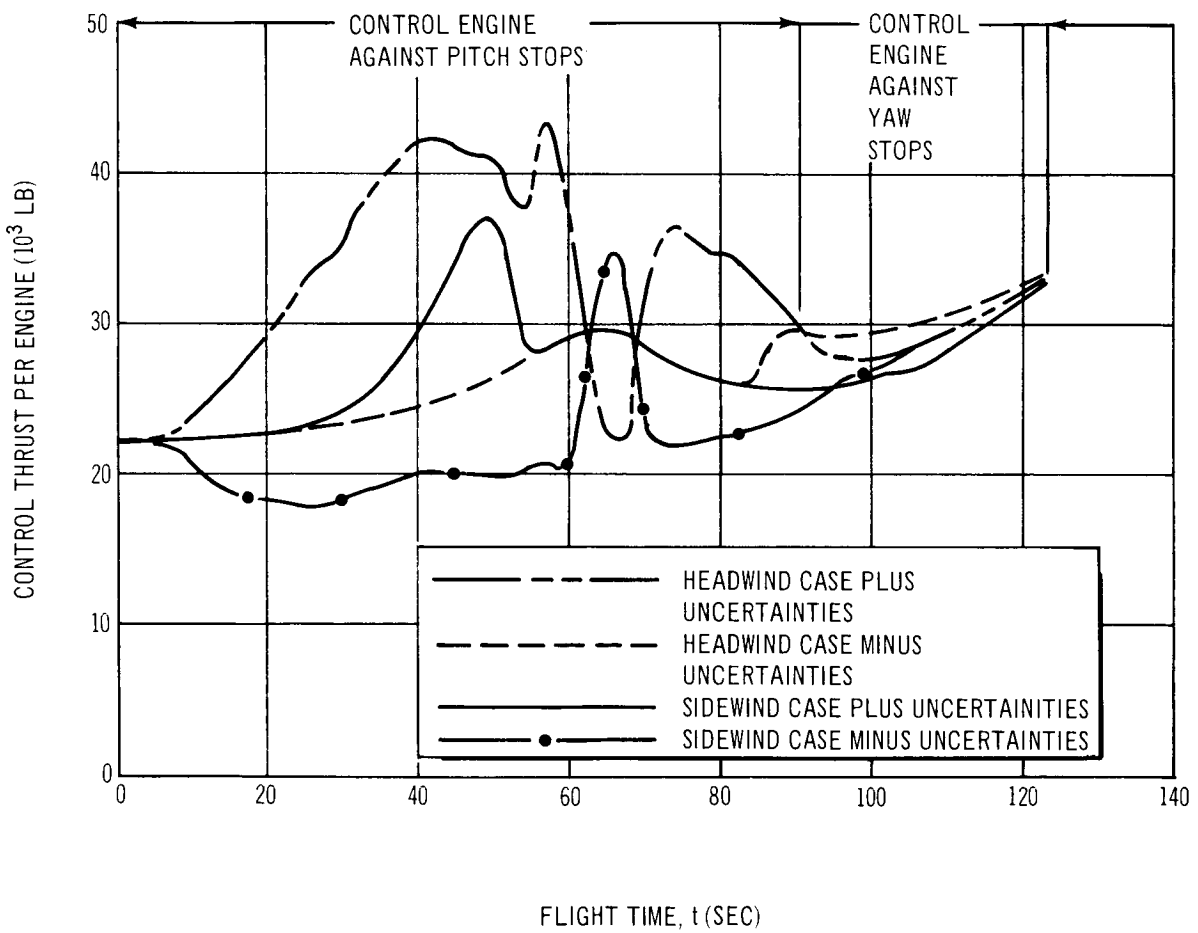


Figure 3-28. First-Stage Composite Control-Thrust Requirements – Configuration I

equal. The four cases of the first stage reduce to only one case; namely, pitch moment caused by thrust misalignment and eccentricity, plus pitch maneuvering requirement; yaw moment caused by thrust misalignment and eccentricity, plus yaw maneuvering requirements; and roll moment caused by thrust misalignment and eccentricity.

Since only this single case exists, the control requirements during second- and third-stage operations are not shown on Figure 3-28. The increasing thrust requirement during second and third stages (Figure 3-18) is caused by forward motion of the CG (Section 3.1.3.3).

#### 3.1.4 Abort Studies

The purpose of the studies discussed in the following paragraphs was to identify uniquely different characteristics and requirements inherent to the head-end steering system concept as they pertain to mission abort. The features of this system which were studied from this standpoint were the all-solid motor launch vehicle propulsion system, the steering system, and the lifting body spacecraft.

It was found helpful to begin with a brief failure mode analysis which was used primarily as a guide in determining abort propulsion-system sizing guidelines and constraints. Inclusion of detailed reliability analyses was not an objective of this study. The failure mode analysis was confined to failures of the all-solid propellant motors and steering systems. Only single failures were considered. Failures of other systems, which may or may not result in an aborted mission, have been examined in detail in current systems; remedial action required for this particular system concept is a more fitting subject for a program definition phase of development.

Failure modes were defined on the basis of inherent risks to the crew and passengers and are as follows:

1. Catastrophic Mode--This is a failure of the all-solid motor system or the steering system which requires a warning and immediate escape initiation prior to the actual failure. Three types of failures of the motor may cause explosive decompression of the motor case which will require speedy reaction from the abort system. These failures are overpressurization of the case, burn-through of the case, and structural failures.
2. Generative Mode--These are failure modes requiring abort but are relatively slow in developing a hazardous situation. Abort procedures may be initiated after the generative failure has occurred. An example of this type of failure is a main nozzle burn-through.
3. Minor Mode--These are failure modes resulting in some degradation in performance but not requiring an aborted mission.

Failure modes were examined through flight and the results are shown in Table 3-3. Catastrophic failures of the motors resulting in incipient high-order explosions require remedial action dictated by the necessity of escaping serious overpressure effects of the blast waves. Other catastrophic failures in the atmosphere, such as a hard-over steering control failure just after liftoff, require immediate abort initiation but do not require as severe an acceleration

Table 3-3  
FAILURE MODE CLASSIFICATIONS

Ignition	Main stage motor	Generative
Explosive decompression	Main stage motor	Catastrophic
Nozzle failure	Main stage motor	Generative
Thrust termination	Main stage motor	(see Separation System)
Separation system	Main stage motor and/or spacecraft	Generative
Steering system		
Tank leakage	Third stage	Generative
Overpressure	Third stage	Minor*
Pressure loss	Third stage	Minor*
Thrust loss	Spacecraft	Generative
Throttling failure	Spacecraft	Generative
Gimbal failure	Spacecraft	Generative

\* Redundant design provided for in Configuration I. Hence, no performance degradation results for single-failure situations.

environment. Catastrophic motor failures that occur outside of the sensible atmosphere do not require escape kinetics as severe as in the atmosphere but do require some separation distance to preclude damage from projectilized fragments.

For generative types of failures, the failure may occur and then the separation may be effected. Separation distances are those necessary to provide minimum hazard to the spacecraft when the failed stage is destructed. No escape provisions are provided for the minor failure category.

Those failure conditions noted in Table 3-3 that may be classed as steering-propellant-tank pressurization failures are classed as generative only if a non-redundant design is used. However, a redundant pressurization system is provided for in the conceptual design discussed herein. Overpressure is handled by vent valves where redundancy is both easy and cheap.

Tank leakages are not considered catastrophic under the concept of single failures. They should, however, rate a generative failure classification since, if allowed to exist over a long period, they could produce an explosive situation.

Steering system failures are classified as a shutdown or loss of thrust, a loss of throttling control, and a loss of gimbal control. Any one of these failures would be generative since adequate time exists after the failure occurs to separate the crew module. This type of classification also applies to ignition, nozzle, and separation failures for the same reasons.

It has been customary to treat all-solid propellant motors as potentially high-order explosives in a situation which involves a catastrophic type of failure. This has been the case even for polybutadiene propellants (composite) which are extremely difficult to explode in a high-order sense outside of a laboratory environment. The traditional treatment of these propellants has been to assign an equivalent TNT energy content expressed as a percentage.

In the Phase I Study, an abort propulsion system for the spacecraft was defined on the basis of a 2% TNT equivalent. Blast-wave characteristics were then determined which were used to specify the spacecraft structural criteria and malfunction warning characteristics necessary for the determination of relative accelerations for escape. In view of the lack of general agreement on what TNT equivalence should be used for polybutadiene propellants, it is treated as a variable in this study; abort-system weight and the related effect on payload capability are thus presented as functions of this variable.

#### 3.1.4.1 Pad Abort Requirements

The study of pad abort requirements is divided into two parts. One, dealing with the escape system sizing, is primarily concerned with the requirements for propelling the spacecraft to a safe distance from a launch pad explosion. The other part was concerned with the requirements for bringing the spacecraft to a safe landing on the earth's surface. The principal concern of this latter study was to see if the spacecraft could be brought to a normal horizontal landing on an adjacent or nearby airfield.

### The Escape Problem

The problem of escape from an incipient launch vehicle explosion is described in Figure 3-29. The spacecraft, or escape module, is located on the launch vehicle at some distance,  $x_1$ , from the center of the incipient explosion. At a time designated as  $t_0$ , a warning is received that an explosive situation is developing. Escape rockets are fired and the spacecraft is separated from the launch vehicle. The acceleration required will be a function of the amount of warning time available,  $t_w$ , and the distance,  $x_2$ , that is desired at the time of the explosion. The distance,  $x_2$ , is determined by the peak overpressure that the spacecraft is capable of withstanding and the blast-wave kinetics of the explosive materials.

The peak overpressure is large near the source of explosion but decays exponentially with distance as the spherical blast wave moves outward from the source. Therefore, the time available for accelerating the spacecraft a distance  $x_2 - x_1$  is

$$t_a = t_w - t_R + t_{BW} = \text{burn time of escape rockets}$$

where

$t_a$  = acceleration time or the burn time of the rocket propulsion system

$t_w$  = warning time

$t_R$  = reaction time

$t_{BW}$  = time for blast wave to travel a distance of  $x_2$

There is very little data on the explosive energy of polybutadiene propellants. Generally, the explosive energy characteristics are expressed as some equivalent weight of TNT. Since the blast wave characteristics of TNT explosives are well established, it is then possible to predict the variation of peak overpressure with distance under ideal surroundings. For a pad escape situation, with the launch pad terrain essentially flat, the blast wave will reflect from this surface causing a magnification of the peak overpressures. Factors of from two to eight are possible in this magnification, but values of two are valid for an ideal flat surface. For explosions occurring some distance above the reflecting plane, a factor of two should be somewhat conservative. This is accounted for in this study by effectively doubling the TNT equivalent weight.

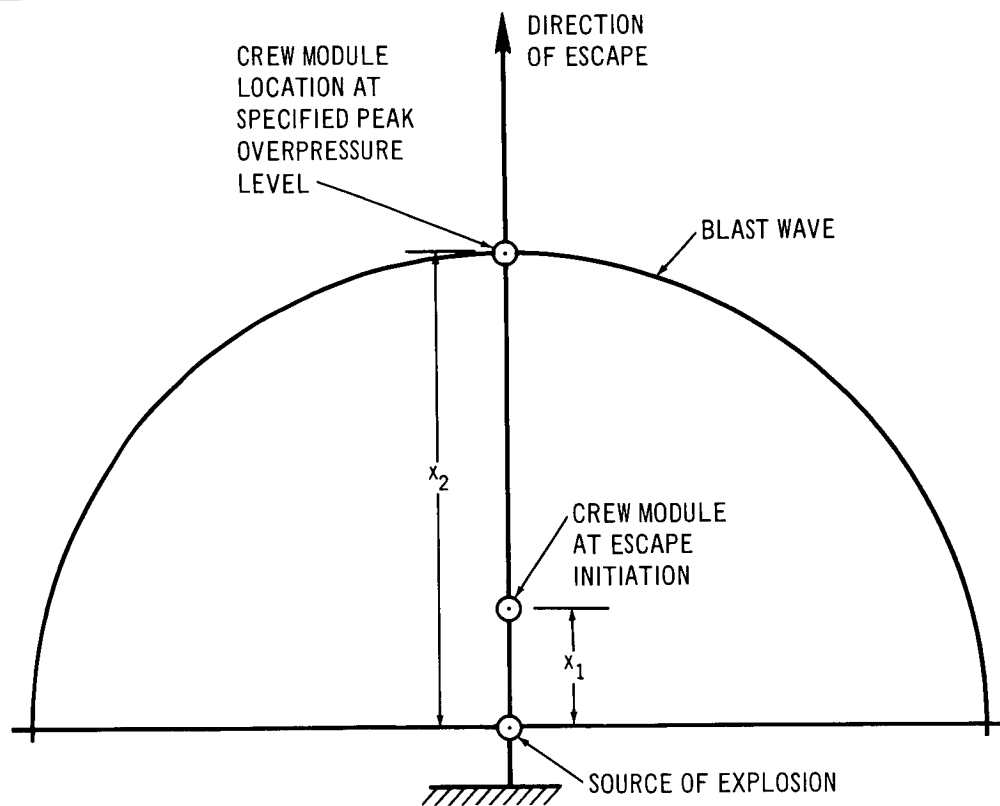


Figure 3-29. The Escape Problem

Figure 3-30 shows a chart containing the various factors necessary to size the escape system for the vehicle of this study, Configuration I. The chart is entered with the TNT equivalent weight which is obtained for Configuration I as shown in Table 3-4. For the purpose of introducing some conservatism in the sizing of the escape system, the distance  $x_1$  was assumed to be zero and the reaction time was assumed to equal the time the blast wave takes to reach the point  $x_2$ . Hence, the burn time of the escape rockets in this case equals the warning time requirement.

For the design escape requirements for the Configuration I vehicle, the TNT equivalent weight is based on 25% for the solid propellants and 10% for the storable liquids. Hence, the TNT equivalent is 1,254,125 lb plus 6,020 or 1,260,145 lb. Entering this curve at a peak overpressure of 10 psi results in a distance requirement of 1,010 feet. Ignoring the distance,  $x_1$ , the upper right hand part of the chart is read at 1,010 feet on the ordinate scale horizontally to the design warning time of 4 sec. At the intersection of the  $t_B = 4$  sec. curve, and dropping vertically down to the thrust-to-weight-ratio scale, a value of 3.62 is indicated. Continuing vertically downward into the lower right hand side

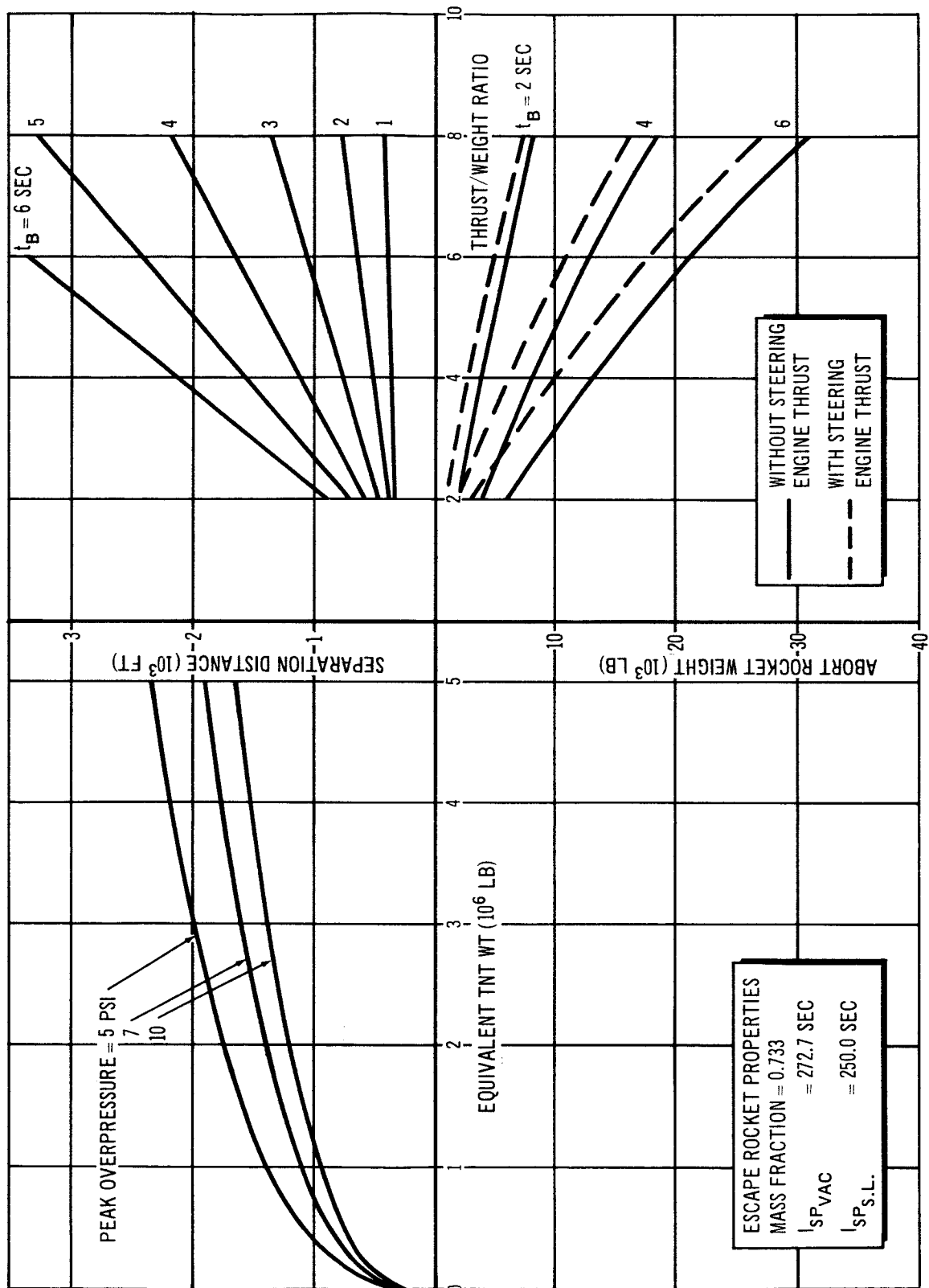


Figure 3-30. Escape Rocket Sizing Chart, Pad Abort



Table 3-4  
PROPELLANT WEIGHTS AT LIFTOFF

Location	Type	Weight (lb)
First Stage	All-Solid Composite	3,751,000
Second Stage	All-Solid Composite	1,013,000
Third Stage	All-Solid Composite	252,500
Steering Section	Storable Liquid	60,200
Total-Solid	Propellants	5,016,500
Total-Liquid	Propellants	60,200

of the chart at this value of thrust-to-weight ratio, two values of abort rocket weight may be determined based on whether the steering engines are operating or not. Thus, for the case of steering engines operating, the abort rocket weight is 5,500 lb. Without the steering engines, the weight is 7,500 lb. Since the escape motor unit sizes (900 lb each) of the Phase I study were used in the Phase II Study, the number of solid motor units would have to be seven to satisfy the steering motor operating case. This results in a total escape-motor weight of 6,300 lb.

It is felt that the steering-motor operating case is justified in selecting pad escape-motor sizes since the steering engines may be operated to full thrust- and gimbal-angle deflections prior to first-stage motor ignition.

The effect of the assumption of TNT equivalence may be seen in Figure 3-31. These data are based on varying the percent TNT equivalence from 2 to 50% and includes a constant 10% of the steering propellant.

The solid propellant motors are used in units weighing 900-lb each; this accounts for the broken line. Two of the units are carried throughout the ascent trajectory to provide for separation impulse in the event of the high-altitude abort situations discussed in Section 3.1.4.3.

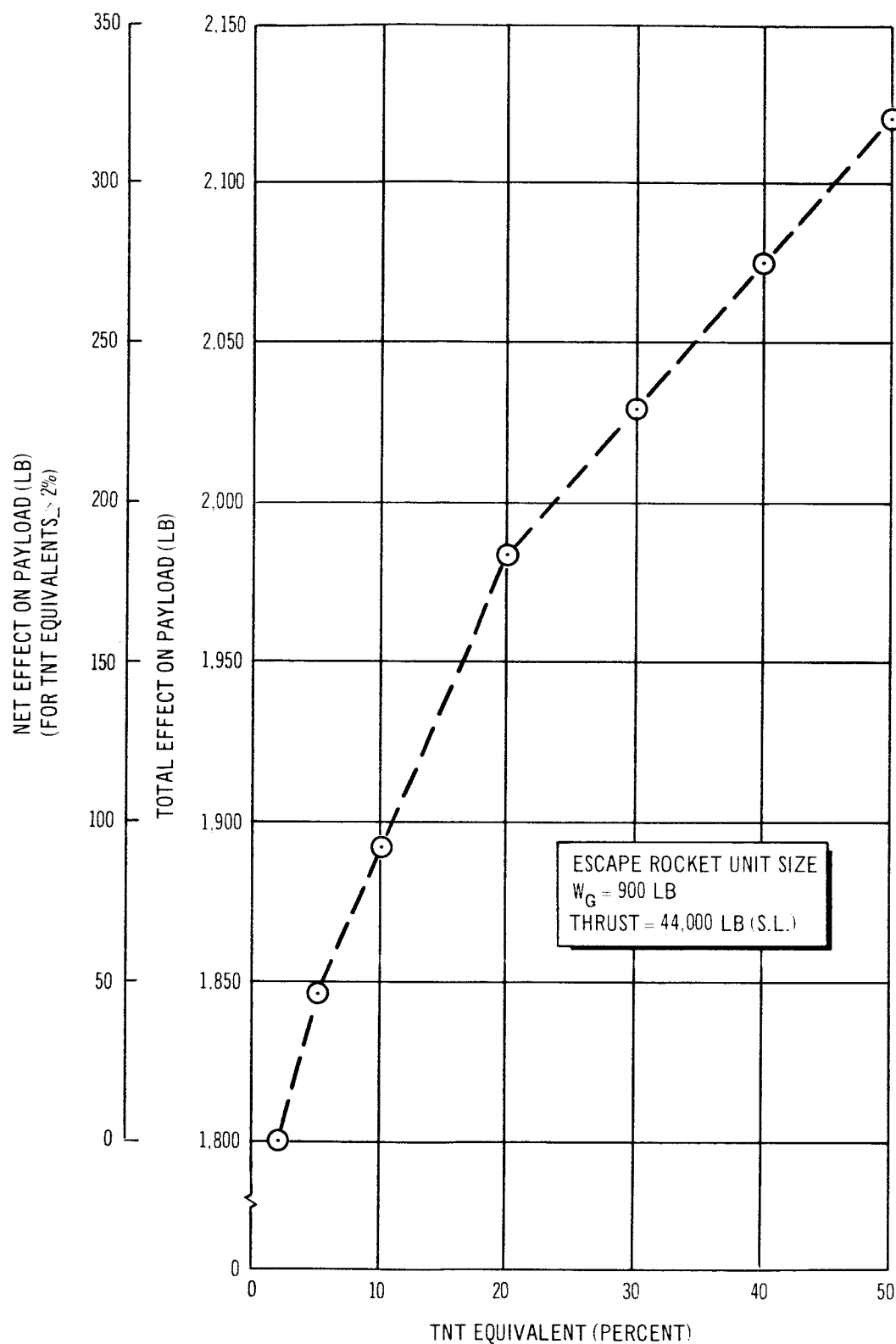


Figure 3-31. Effect of TNT Equivalence on Payload, Launch Pad Abort

As can be verified from Figure 3-31, very little effect on payload results from varying the TNT equivalence if part of the escape system must be carried throughout the ascent trajectory for separation purposes and if blast-wave effects out of the atmosphere are negligible.

#### Recovery From Pad Abort

The availability of propulsion on board the spacecraft suggested the possibility of recovering the spacecraft on an existing nearby airfield. A survey of existing airfields adjacent to Cape Kennedy revealed the relative locations and characteristics shown in Table 3-5.

Table 3-5  
AIRFIELDS ADJACENT TO LAUNCH SITE

Launch Site Location - 29° 34' N. Lat. 80° 42.5' W. Long.		
Airfield Name	Maximum Runway Length - Ft	Distance of Airfield from Launch Site - nmi
Daytona Municipal	5,700	33.6
J. F. Kennedy Memorial	11,200	37.2
Orlando Municipal	6,000	34.2
Patrick AFB*	9,000	32.3
Patrick AFB	9,000	28.8
McCoy AFB	12,000	36.6
Sanford NAS	8,000	27.7

\*Dog-leg flight to avoid overfly of Cape Kennedy and Cocoa Beach

The skid strip at Cape Kennedy was not considered since it is located in the midst of numerous launch complexes. In addition, the municipal airports of Table 3-5 were also ruled out from the standpoint of commercial air activities. While McCoy and Sanford are feasible recovery sites, Patrick AFB was selected as the primary site since transportation back to the launch site is relatively easy.

Flight profiles were investigated to establish whether the spacecraft was able to fly back to any of the feasible airfields. Basically, one type of profile was used and is described schematically in Figure 3-32.

The escape phase is vertical flight with propulsion provided by both the steering engines and the abort escape rockets described in Section 3.1.4.1. The steering engines are immediately gimbaled to a straight aft orientation, advanced to full thrust and the feed system is switched to the maneuvering propellants in the HL-10. At end of 4 seconds of burning, the abort rockets are jettisoned and the spacecraft is rolled to the proper azimuth for recovery at a preselected site. An inverted pull-over is initiated and continued until the vehicle reaches a flight-path angle of zero degrees. The spacecraft is then rolled into a normal upright orientation and the velocity is adjusted with the steering engines to that required for maximum  $(M) (\frac{L}{D})$ . Only those flight characteristics corresponding to constant altitude cruise were investigated.

The range attainable is a function of how the spacecraft is loaded, that is, the amount of maneuvering propellant that is carried. For cargo requirements above 5,000 pounds, the additional cargo is carried in the expendable cargo module and maneuvering propellants are off-loaded from the spacecraft. This results in a lighter spacecraft for launch-pad abort situations but also a smaller quantity of propellants for the cruise back to the airstrip.

The resulting range capability as a function of cargo loading is shown in Figure 3-33. The cruise-back altitude range is from 12,450 feet to 7,800 feet. Since these data are for constant altitude cruise, these altitudes correspond to the descent margins over the airfield.

The throttling requirements for the steering engines were investigated and found to vary between 12 and 18%.

Abort escape from the launch pad with a steering engine failure is considered to be very unlikely since it would require a double failure, that is, an additional failure of, say, the first-stage motor. For steering failures just off the launch pad, since no explosion of the launch vehicle is immediately likely, the abort escape rockets would provide the separation distance required for permitting the spacecraft to aerodynamically maneuver downrange and to an altitude where

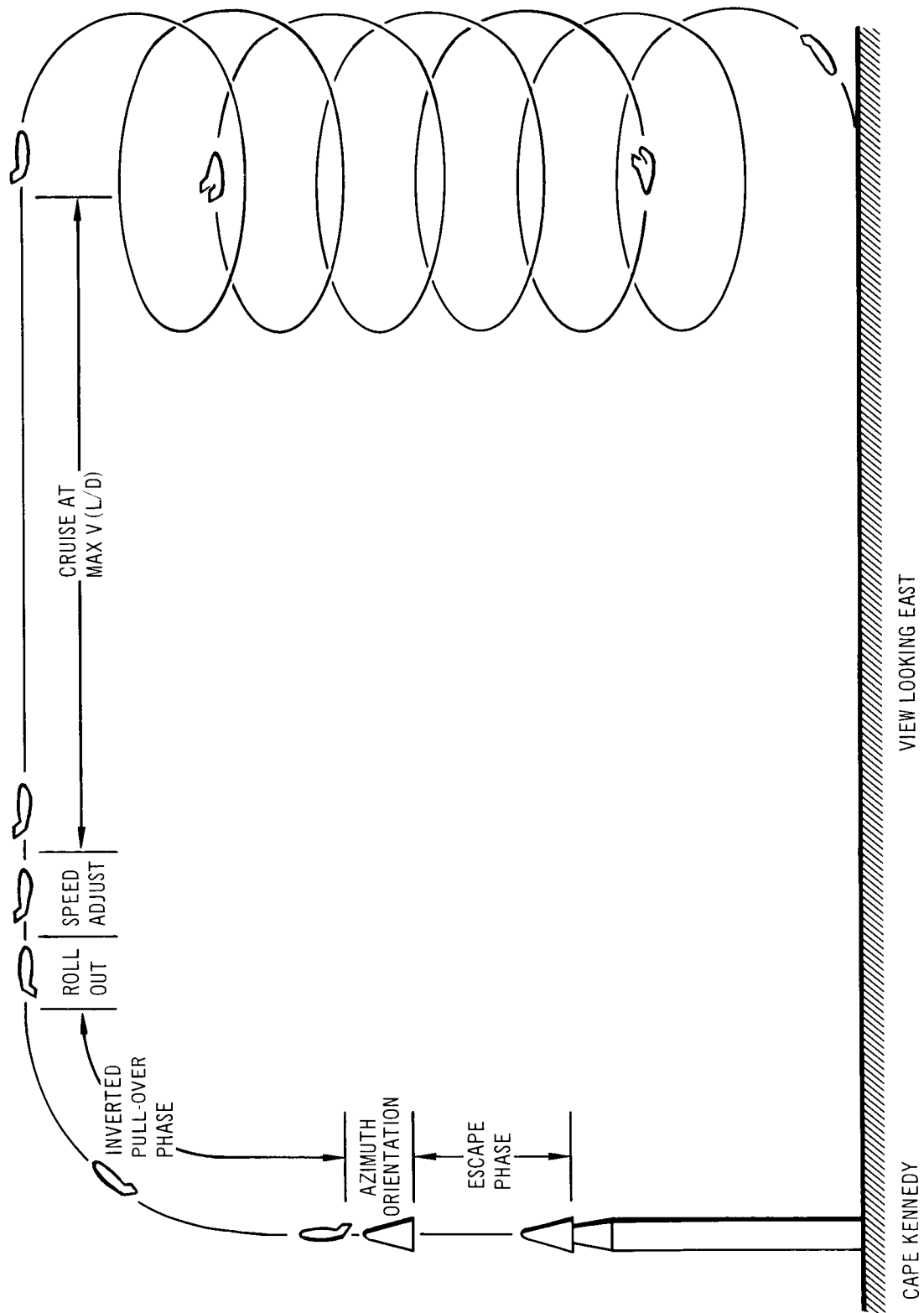


Figure 3-32. Pad Abort Recovery Profile

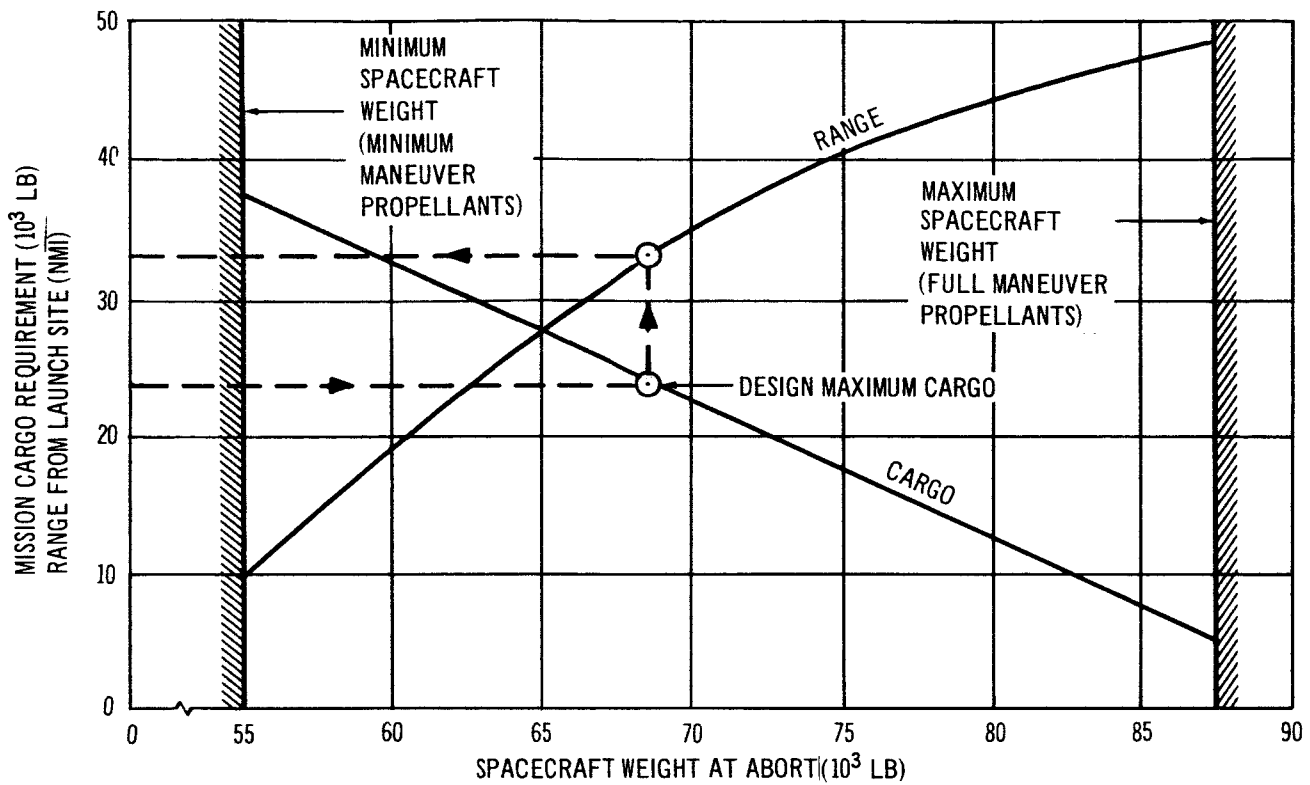


Figure 3-33. Spacecraft Range Capability, Pad Abort

parachutes could be deployed for a vertical landing in the water. The system concept provides for such a parachute system but a propellant dump system is recommended to reduce the fire hazards on landing and to minimize the parachute system weight.

#### 3.1.4.2 Abort at Maximum Dynamic Pressure

Abort at maximum dynamic pressure is important for two reasons. This condition in the ascent trajectory places the highest bending loads on the vehicle and, hence, presents a critical structural design point. Separation requirements at these conditions can be more severe than elsewhere in the flight because of the higher aerodynamic drag forces on the spacecraft. The flight conditions are presented in Table 3-6.

Table 3-6  
FLIGHT CONDITIONS AT MAXIMUM  
DYNAMIC PRESSURE

Time of Flight, sec	70
Maximum Dynamic Pressure, $q_{\max}$ lb/ft <sup>2</sup>	801
Flight Path Angle, deg	54.6
Distance from Launch Site, nmi	2.20
Mach Number	1.51
Altitude, ft.	34,987

#### 3.1.4.3 Abort Escape Propulsion Requirements

For the case of an incipient failure of the first-stage motor, that is, one resulting in a catastrophic situation requiring rapid separation of the spacecraft, several conditions are different from those encountered in escape from a launch-pad failure. Maximum dynamic pressure occurs at 70 sec in the flight of the Configuration I vehicle. There is, of course, less propellant on board at this time. The TNT equivalent weight is summarized in Table 3-7.

Table 3-7  
TNT EQUIVALENT WEIGHT AT MAXIMUM DYNAMIC PRESSURE

First-Stage Propellant, lb	1,696,358
Second-Stage Propellant, lb	1,013,000
Third-Stage Propellant, lb	252,000
TNT Equivalent at 25% of Total Propellant, lb	740,340
Steering Propellant, lb	40,305
TNT Equivalent at 10%, lb	4,031
Total TNT Equivalent, lb	744,371

At an altitude of 35,000 feet, there would be no blast-wave reflection of the peak overpressures due to ground effects. The effect of aerodynamic drag on the spacecraft is, however, sizable since the vehicle is traveling at a Mach number of 1.5. Since drag is important, accurate relative separation characteristics are dependent on a rather thorough drag analysis of both booster and spacecraft. It was felt that the conservative simplifying assumptions were thus justified for

this study. These assumptions were (1) full spacecraft drag, and (2) zero launch-vehicle drag. Two analyses were made, with and without steering engines operating. These data are plotted in Figure 3-34 and indicate that satisfactory separation distances are achieved even without steering engines operating and for the conservative assumption of no drag on the launch vehicle.

#### 3.1.4.4 Recovery From Abort Escape

Because of the relatively high energy of the spacecraft when abort escape has been accomplished at the maximum dynamic pressure condition and because of the small surface-range distance from Cape Kennedy, the recovery of the spacecraft on land at Patrick AFB was investigated and found to be feasible. This is the case for either steering engines operating or not operating.

Figure 3-35 presents the ground trace of the spacecraft when the steering engines are operating. After the escape-acceleration phase, a 60° bank to the right is initiated and held till a heading is achieved which corresponds to Patrick AFB. This heading is achieved at approximately 36 sec after abort escape initiation or at a total flight time of 106 sec. Figure 3-36 presents the velocity-altitude-time history of the escape and turn maneuvers.

The conditions existing at the end of the turn maneuver are summarized in Table 3-8.

Table 3-8  
CONDITIONS AT END OF TURN MANEUVER

Velocity, ft/sec	1224
Mach Number	1.26
Altitude, ft	73,243
Spacecraft Weight, lb	75,109
Distance to Patrick AFB, nmi	25.5

It is clear from the range studies previously presented that if the spacecraft thrust were terminated at this point and a glide was initiated to 12,000 feet where thrust was again initiated, the spacecraft range capability would be 40 nmi. This is more than adequate to reach Patrick AFB.



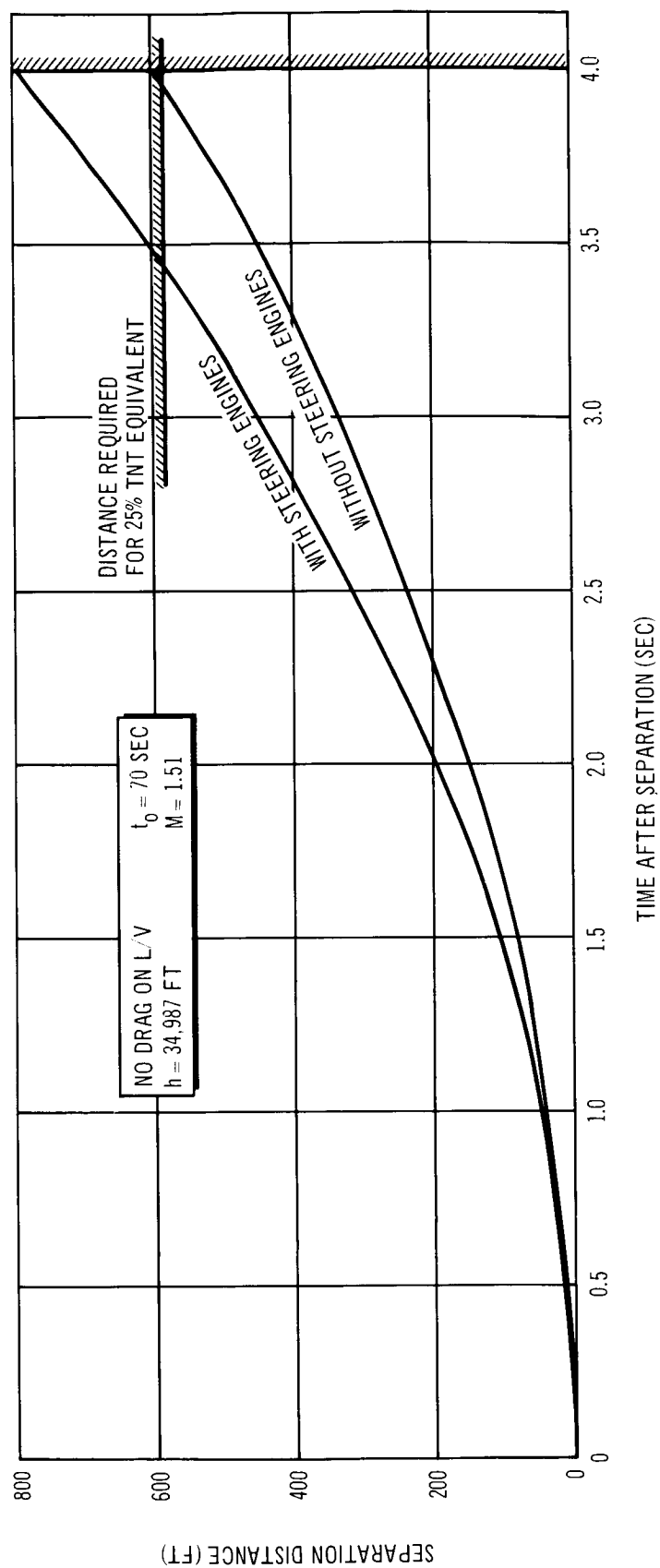


Figure 3-34. Relative Separation Distance, Abort Escape at Maximum Dynamic Pressure

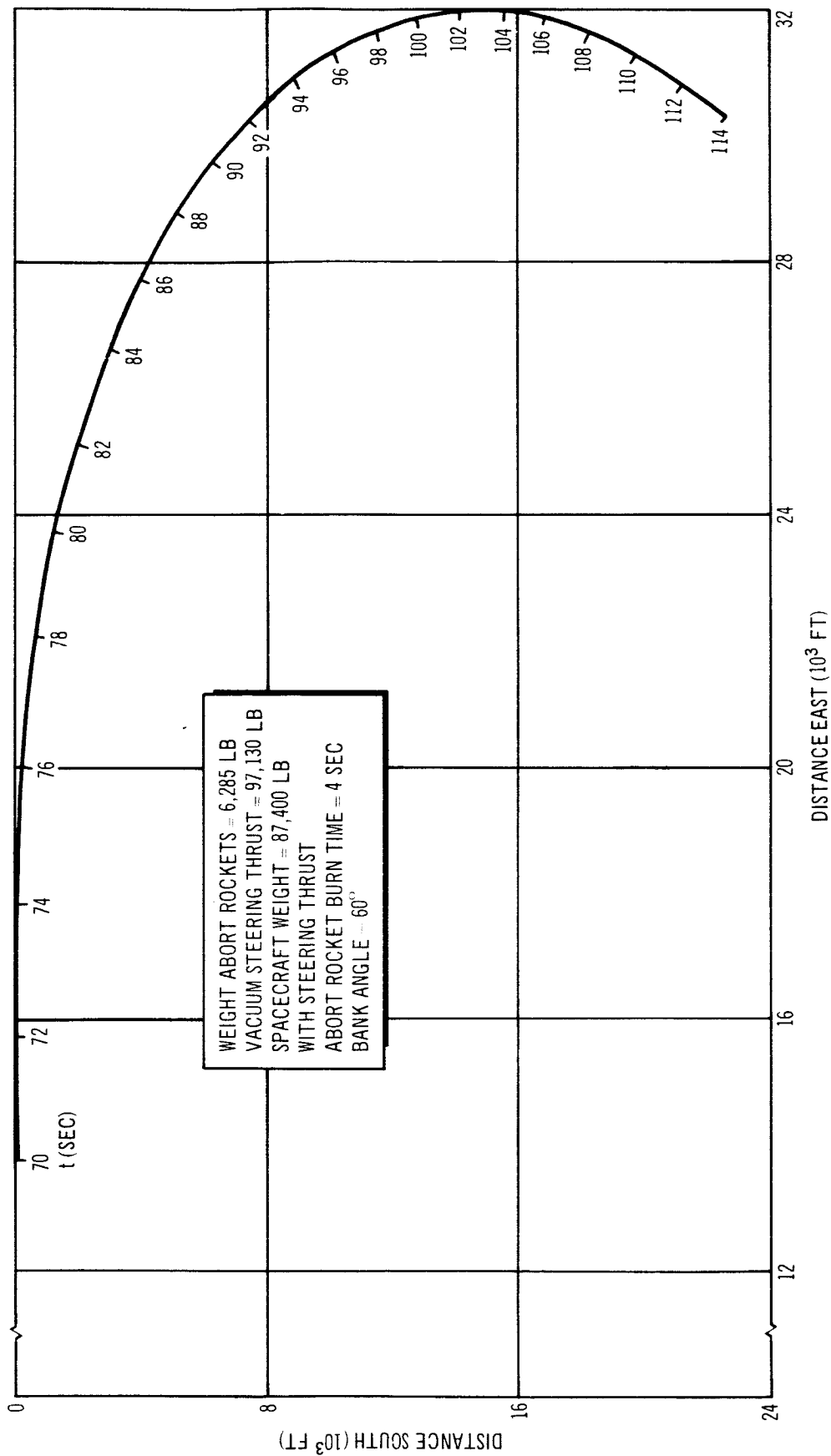


Figure 3-35. Ground Trace of Flight Path, Maximum Dynamic Pressure Abort

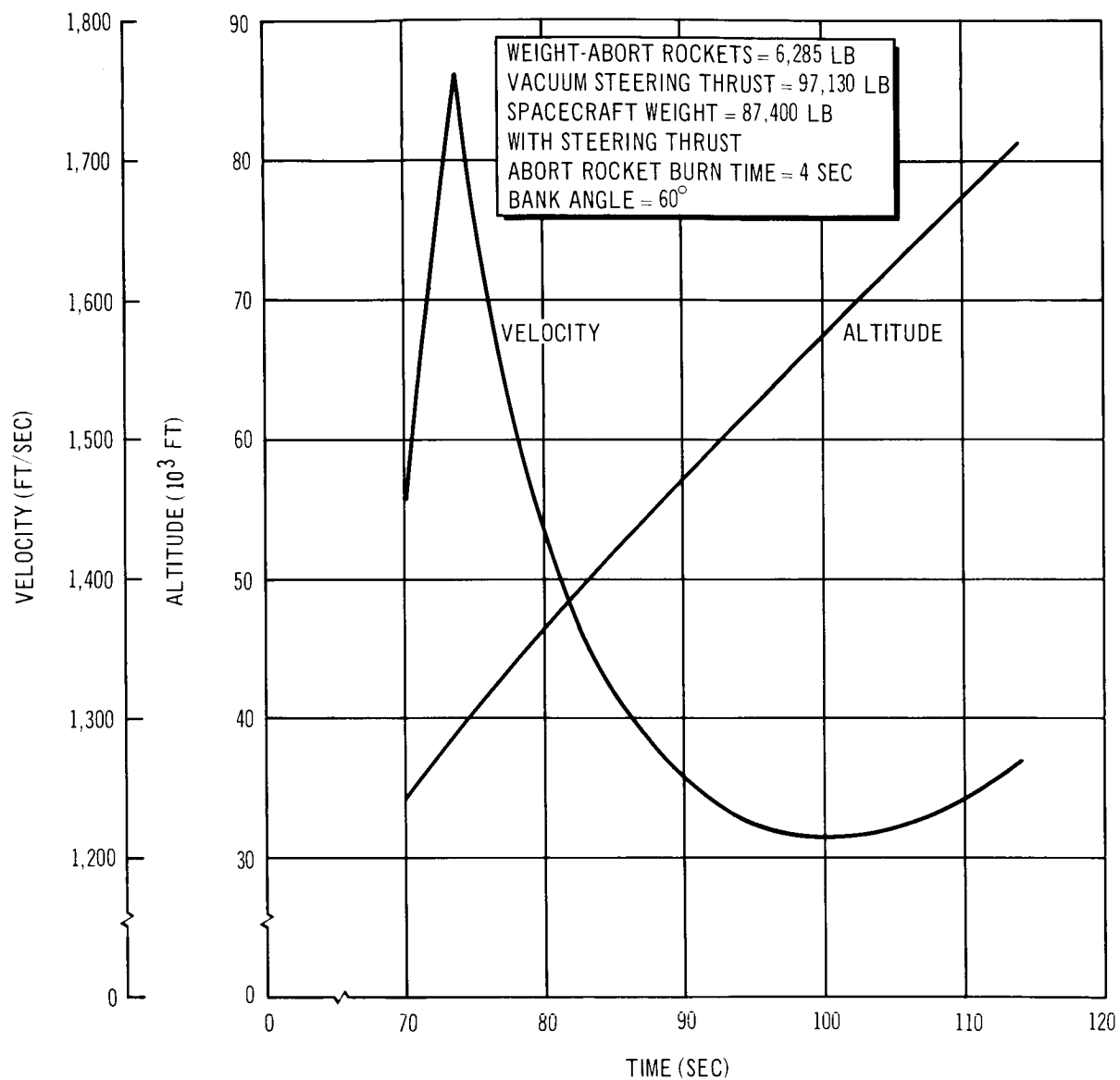


Figure 3-36. Flight Conditions – Escape and Turn Phase, Maximum Dynamic Pressure Abort

The recovery of the spacecraft in the maximum dynamic pressure regime when a steering failure occurs is somewhat more challenging though entirely feasible. While there is no requirement in this case to escape a blast wave overpressure condition, it was found desirable to utilize the escape rockets for providing good separation and for providing as high a level of energy as possible for the spacecraft.

The same maneuver is followed as for the case in which steering engines are operating. After the escape acceleration phase and the jettisoning of the escape rocket cases, a 60° bank is initiated to the right until a heading for Patrick AFB is achieved. The bank and turn, in this case, are controlled by the spacecraft reaction control system. Upon completion of the turn, the onboard maneuvering propellants are dumped and a glide phase initiated. The heading for Patrick AFB is achieved at 76 sec, after abort escape initiation, or at 146 sec after liftoff. The ground trace of the flight profile is shown in Figure 3-37. When the proper heading is obtained, the spacecraft will be 7.4 nmi east of the launch pad and 4.8 nmi south. The surface range from Patrick AFB is 23.6 nmi. Flight conditions through escape and the turn maneuver are shown in Figure 3-38. The velocity at the initiation of the glide phase is relatively high, 1,007 fps.

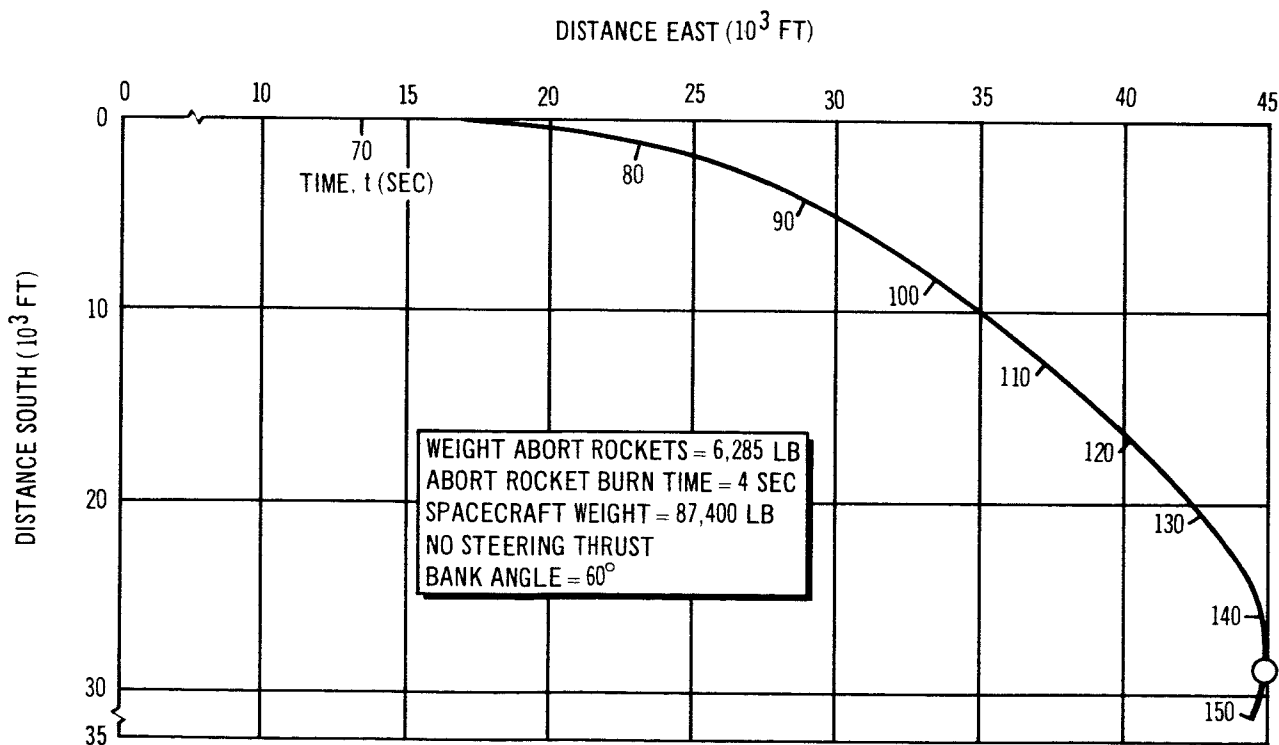


Figure 3-37. Ground Trace of Flight Profile, Maximum Dynamic Pressure Abort

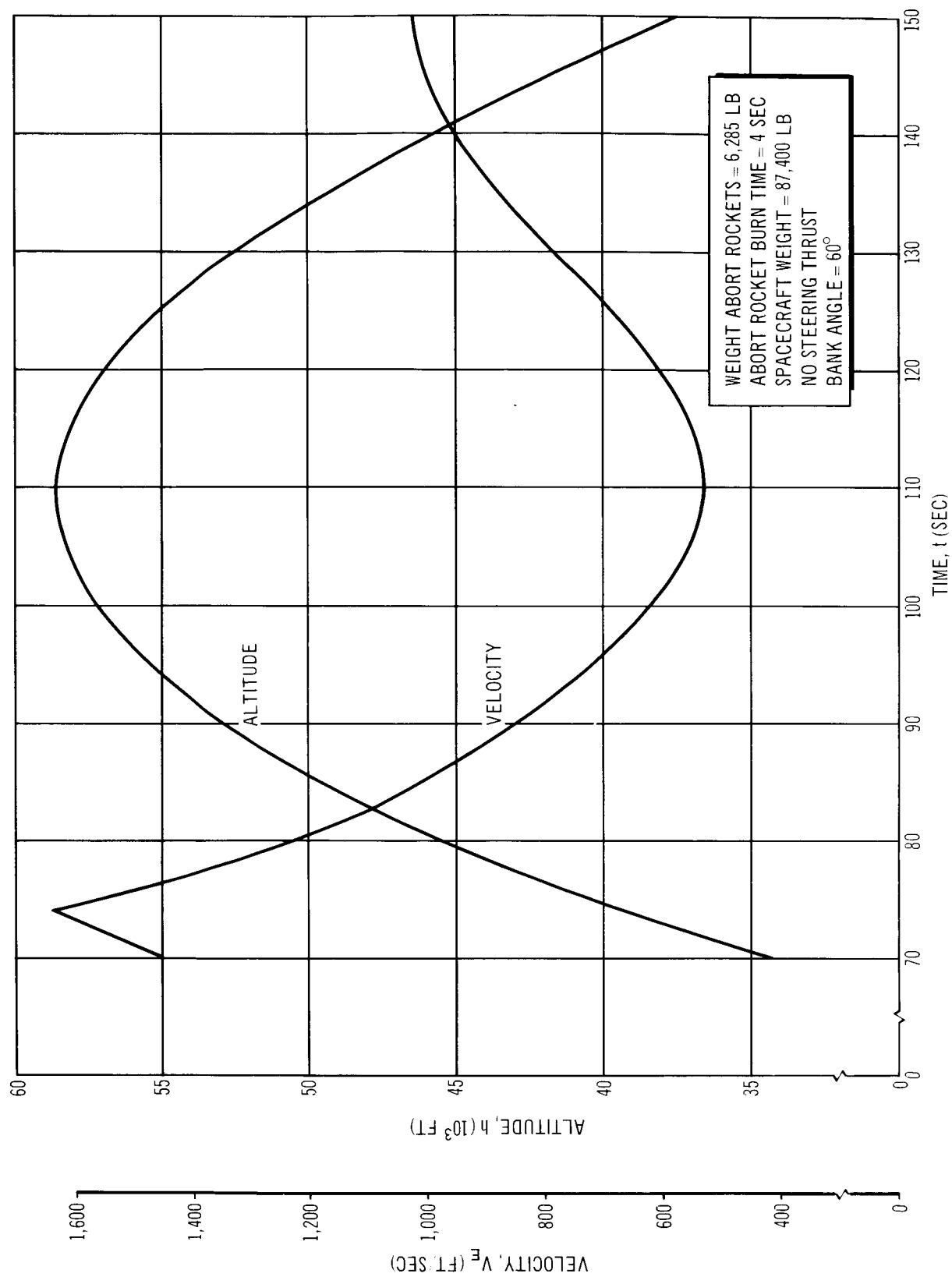


Figure 3-38. Flight Conditions, Maximum Dynamic Pressure Abort

An adjustment of altitude may be desirable to establish a better initial glide velocity. In any event, a lift-to-drag ratio of 4.0 would place the spacecraft over Patrick AFB at an altitude of 5,000 ft. Such a lift-to-drag ratio is within the capability of the HL-10 vehicle in the gear-up clean configuration.

In Section 3.1.7 consideration is given to the addition of separate in-orbit maneuvering engines and the potential reduction in spacecraft size is discussed. Such a modification would also improve the abort recovery characteristics in the event of a steering system failure.

#### 3.1.4.5 Abort at High Altitude

A high-altitude abort situation as discussed in this document is any abort which requires reentry into the sensible atmosphere. As with the other abort environments discussed in preceding sections, the availability of the steering engines for thrust and control affects the procedures used.

With a steering system failure, the principal factors in an abort recovery are reentry heating, dynamic pressure levels, and accelerations. These factors are directly related to the flight conditions along the design ascent trajectory. Flight path angle, velocity, and altitude determine the abort apogee conditions which, in turn, determine the reentry heating, dynamic pressures, and normal accelerations encountered in the atmosphere during the recovery phase. The objective in this part of the abort studies was to determine first whether the normal mission trajectories resulted in unacceptably high-recovery flight conditions.

Figure 3-39 shows in the lower of the two curves the locus of abort escape apogee altitudes for the case of a steering system failure requiring engine shutdown. The upper curve is the altitude-velocity limit curve determined by entry conditions selected so as not to exceed a maximum normal acceleration of 6 g's and a maximum dynamic pressure of 1,200 psf for a vehicle having a wing loading of 60 psf. It is felt that these conditions are entirely reasonable structural design criteria for the spacecraft. Since the nominal design trajectory does not impose entry conditions in excess of reasonable structural design criteria, no modification of the trajectory was required. In order to meet the wing loading requirement, all in-orbit maneuver propellants would have to be dumped prior to reentry into the sensible atmosphere.

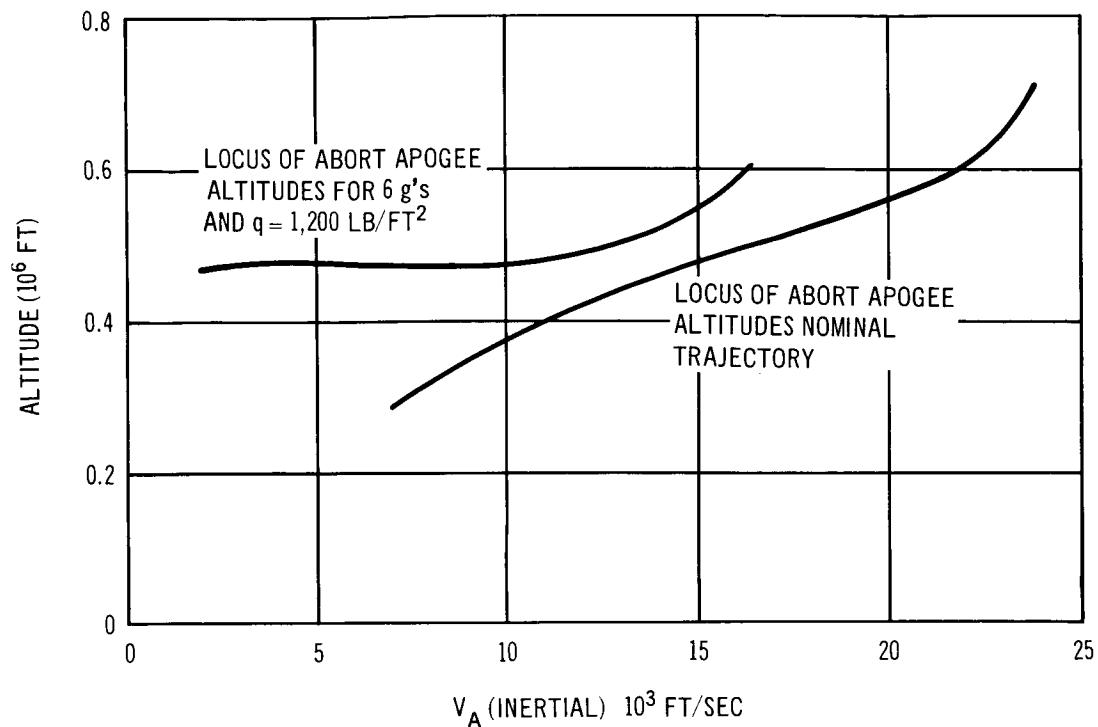


Figure 3-39. Steering-Failure Mode, Abort at High Altitude

For the case of a launch vehicle failure requiring an abort, and with steering engines operating on spacecraft maneuvering propellants, the locus of abort apogees can be adjusted through the application of velocity vector changes accomplished with the steering system. Thus, re-entry flight conditions may be controlled to less than those encountered with the steering failure case.

### 3.1.5 Spacecraft/Booster Compatibility

#### 3.1.5.1 Jet Interference Effects

Two types of steering engine jet interference with the freestream flow about the launch vehicle were considered. The first of these was the inviscid blockage effect, in which the jet plume is assumed to act as a nearly solid cylinder in close proximity with the vehicle; the second was the momentum spreading effect, in which the jet momentum was considered as added to a portion of the momentum in the freestream, thus creating an effective change in the flow direction near the vehicle.

The inviscid plume was analyzed and found to impinge on the vehicle some 13-plume diam downstream of the jet exit. In the most unfavorable case, one steering engine deflected  $30^\circ$  from its normal position. An analysis of the steering signals for either an aerodynamically stable or unstable vehicle showed that the plume effect is negligible for positive aerodynamic stability, and slightly favorable with respect to steering requirements for negative aerodynamic stability. It was concluded that steering requirements are conservatively estimated when plume blockage effects are ignored. The plume analysis included the effects of entrained freestream flow by the jet; it was found that the entrainment was complete in only 3 or 4 diam of the nozzle area, and that the effective plume diameter was less than 2-nozzle diam.

Viscous spreading of the jet was assumed to occur at some rate less than the local freestream speed of sound, and the jet momentum was compared to the freestream momentum with which it was mixed at the first-stage stabilizing fins. Since this was some 250 ft downstream of the jet, the spreading took place over a relatively large area, with the result that at maximum,  $q\alpha$ , and assuming a jet spreading rate only  $1/10$  the speed of sound, the momentum ratio was  $2 \times 10^{-14}$ , an entirely negligible quantity. At a higher speed, near the time for first-stage burnout, the momentum ratio increased to  $3.7 \times 10^{-3}$ , which is still considered negligible.

It is reasoned that since the greatest effect of the added momentum occurs when the steering engine exhausts parallel to the vehicle, the added momentum effectively decreases the local flow angle. Because of the spreading, the decrease in flow angle is greatest near the forward part of the vehicle, resulting in a



rearward shift of the instantaneous center of pressure. Since the center of pressure is ahead of the CG during the critical portions of the first-stage trajectory, this is a torque-relieving effect and would reduce the requirement for steering torque. It is concluded that the steering thrust requirements are conservatively estimated when jet interaction effects are ignored.

### 3.1.5.2 Rigid and Flexible Body Control Analysis

#### Approach

The relatively large size and slenderness of the Configuration I baseline vehicle suggests the importance of an analysis of flexible body influences on the control system. This section describes the approach taken relating to the influence of the structure on the complexity of the control system of this vehicle.

The control problem was attacked by initially establishing a set of system gains, based on rigid body considerations only, which satisfied the requirements for natural frequency, damping, gain, and phase margin. These requirements were, respectively, 0.15 cps, 0.7, 6 dB, and 20°. The initial two values are specified to allow the vehicle to follow trajectories typical of the type to be flown, whereas indicated stability margins are necessary to allow for tolerance buildup in the hardware components used to mechanize the system.

Following the establishment of acceptable rigid body control system characteristics, the influences of three vehicle bending modes were superimposed, and necessary adjustments of controller parameters were performed to again meet performance requirements demanded of the system.

Inasmuch as bending influences are most severe during the first stage of booster operation, it was deemed sufficient to show a satisfactory level of compatibility of these effects with control system operation at two flight times during this period which normally characterize the periods of major difficulty. These are, respectively, liftoff when bending frequencies are at a low level and the time of maximum dynamic pressure when aerodynamic loads are at or very close to their maximum. Therefore, stability analysis work was restricted to the two flight times of zero and 70 seconds corresponding to the two events mentioned above.

#### Study Results

To properly follow the development described below, Table 3-9 is included to indicate definitions and units of all major parameters.

Table 3-9  
TABLE OF SYMBOLS FOR FLEXIBLE VEHICLE  
CONTROL SYSTEM ANALYSIS

Parameter		Units
$t$	Time of flight	seconds
$K_\theta$	Attitude loop gain	volts/deg
$K_R$	Rate loop gain	volts/deg/sec
$K_M$	Actuator gain	deg/sec/volts
$K_{D\delta}$	Actuator position gain	volts/deg
$M_\delta$	Control moment derivative	deg/sec <sup>2</sup> /deg
$M_{\alpha t}$	Tail aerodynamics moment derivative	deg/sec <sup>2</sup> /deg
$M_{\alpha B}$	Body aerodynamics moment derivative	deg/sec <sup>2</sup> /deg
$\phi_i(x)$	Relative deflection of $i^{\text{th}}$ bending mode at station $x$	N. U.
$\phi'_i(x)$	$\partial\phi_i/\partial x$ , relative deflection of $i^{\text{th}}$ bending mode per unit of station length at station $x$	inches <sup>-1</sup>
$M_i$	Modal mass of $i^{\text{th}}$ bending mode	slugs
$\xi_i$	Damping of $i^{\text{th}}$ bending mode	N. U.
$\omega_i$	Frequency of $i^{\text{th}}$ bending mode	rad/sec
$\xi$	Laplace operator	
$K_{Bi}$ $K_{ti}$	{ Conversion constants between aerodynamics-caused angular acceleration and aerodynamics force at tail and body for $i^{\text{th}}$ bending mode	lb/deg/sec <sup>2</sup>
$K_{\delta i}$	Conversion constant between control angular acceleration and control force for $i^{\text{th}}$ bending mode	lb/deg/sec <sup>2</sup>
CN(1)	Compensation network in actuator forward path	volts/volt
CN(2)	Compensation network in actuator position feedback path	volts/volt
$\alpha$	Angle of attack	degrees
$\theta$	Vehicle attitude	degrees
$\theta_c$	Commanded vehicle attitude	degrees
$\delta$	Control engine actuator position	degrees
$\dot{\theta}$	Rigid body vehicle angular rate	deg/sec
$\dot{\theta}_{Bi}$	Vehicle angular rate due to $i^{\text{th}}$ mode bending and measured by the rate gyro	deg/sec
$E$	Modulus of elasticity	lb/in. <sup>2</sup>
$I$	Section moment of inertia	in. <sup>4</sup>

The assessment of vehicle bending influences on control requires an analysis of structural characteristics to determine stiffness or EI profiles, and internal loading arrangements. Figure 3-40 shows the stiffness profile of the baseline vehicles at both the liftoff and 70-second points. The two profiles are identical in that the modulus of elasticity for the solid propellant was considered negligible relative to the primary structure. Stiffness and mass distribution data were used to arrive at bending mode shapes along with modal frequencies and masses through use of a Douglas version of a Myklestad digital computing program. This information is shown on Figures 3-41 and 3-42. It is seen that mode shape curves terminate at vehicle station 528, and trailing-edge station of the HL-10 spacecraft. This is due to the assumption made that the lifting body payload was infinitely stiff and was cantilevered from the structural adaptor. This assumption will not materially affect the validity of the study results.

The control system model used for both the rigid body and flexible body stability analysis is shown in Figure 3-43. The area shown within the dashed line depicts the modal method used to describe bending effects.

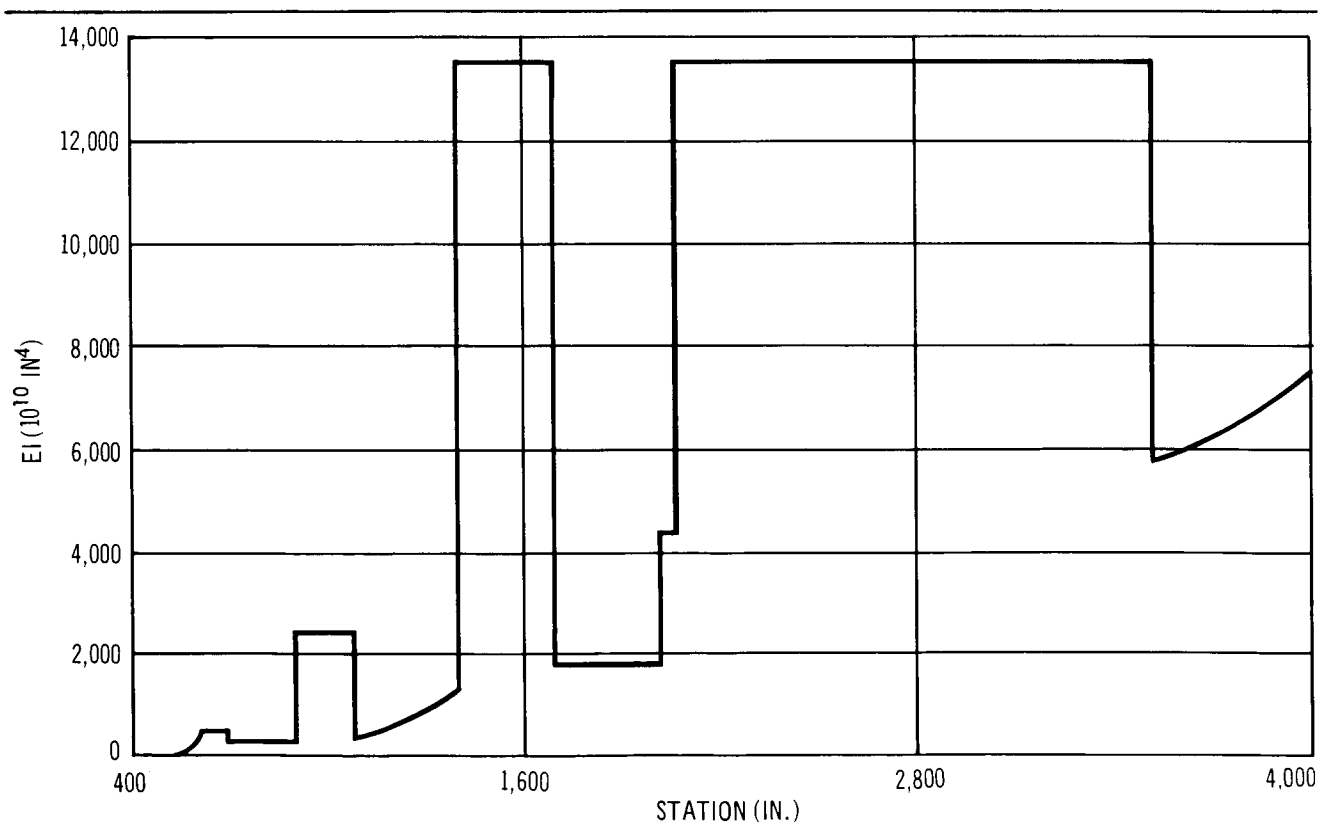


Figure 3-40. EI Distribution-Configuration I

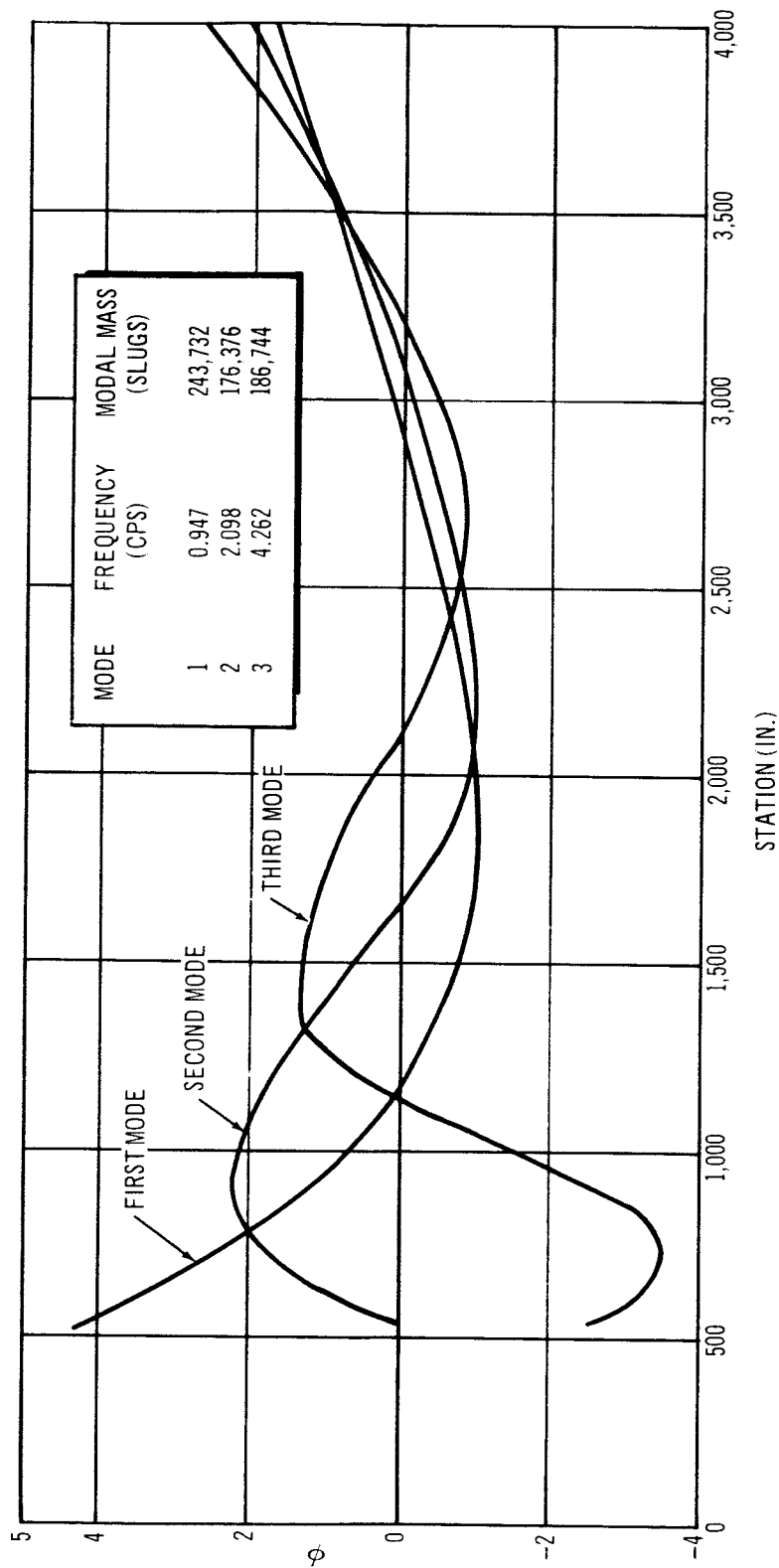
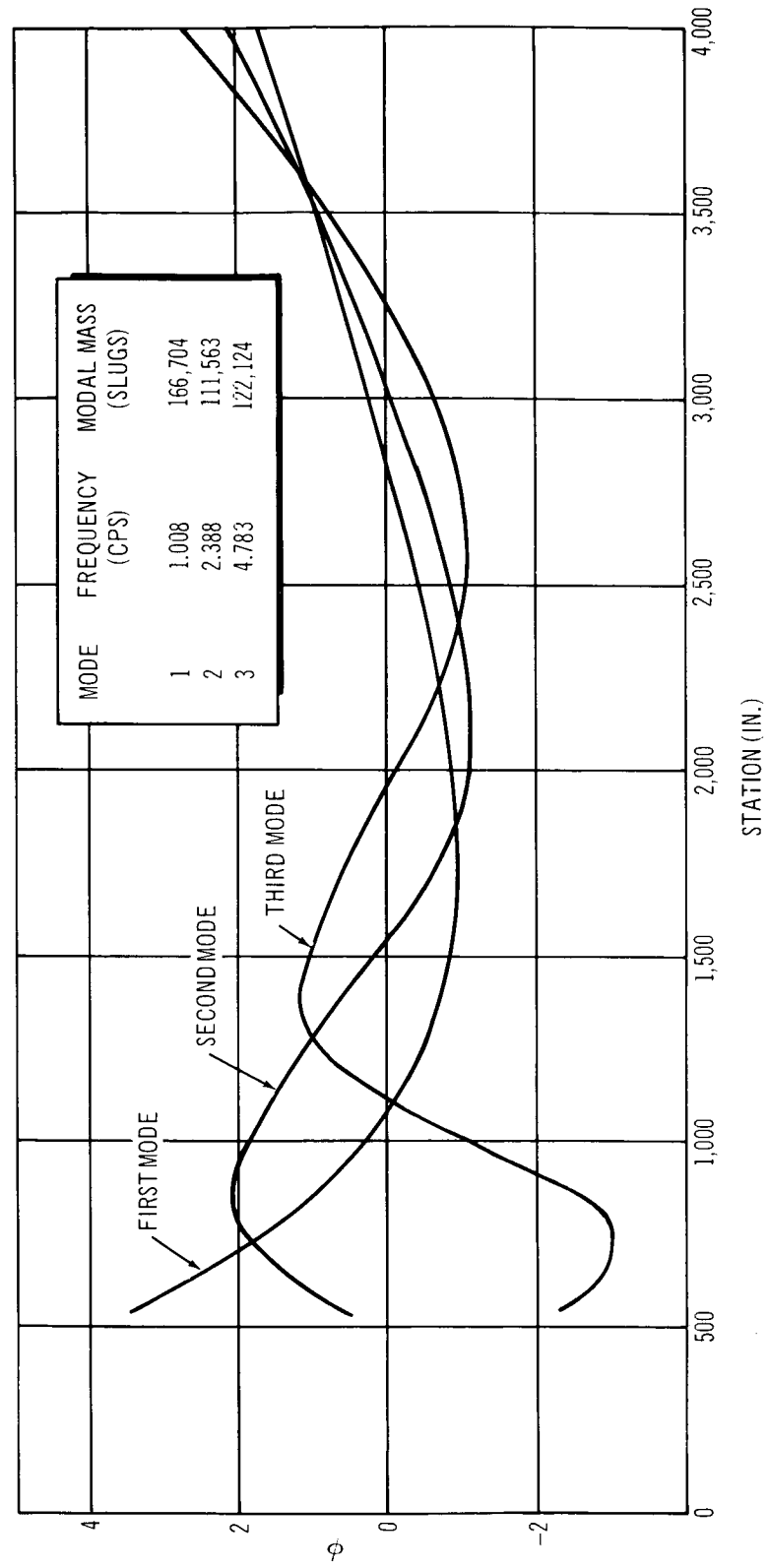


Figure 3-41. Bending Mode Shapes Configuration I,  $t = 0$

Figure 3-42. Bending Mode Shapes Configuration I,  $t = 70$  sec

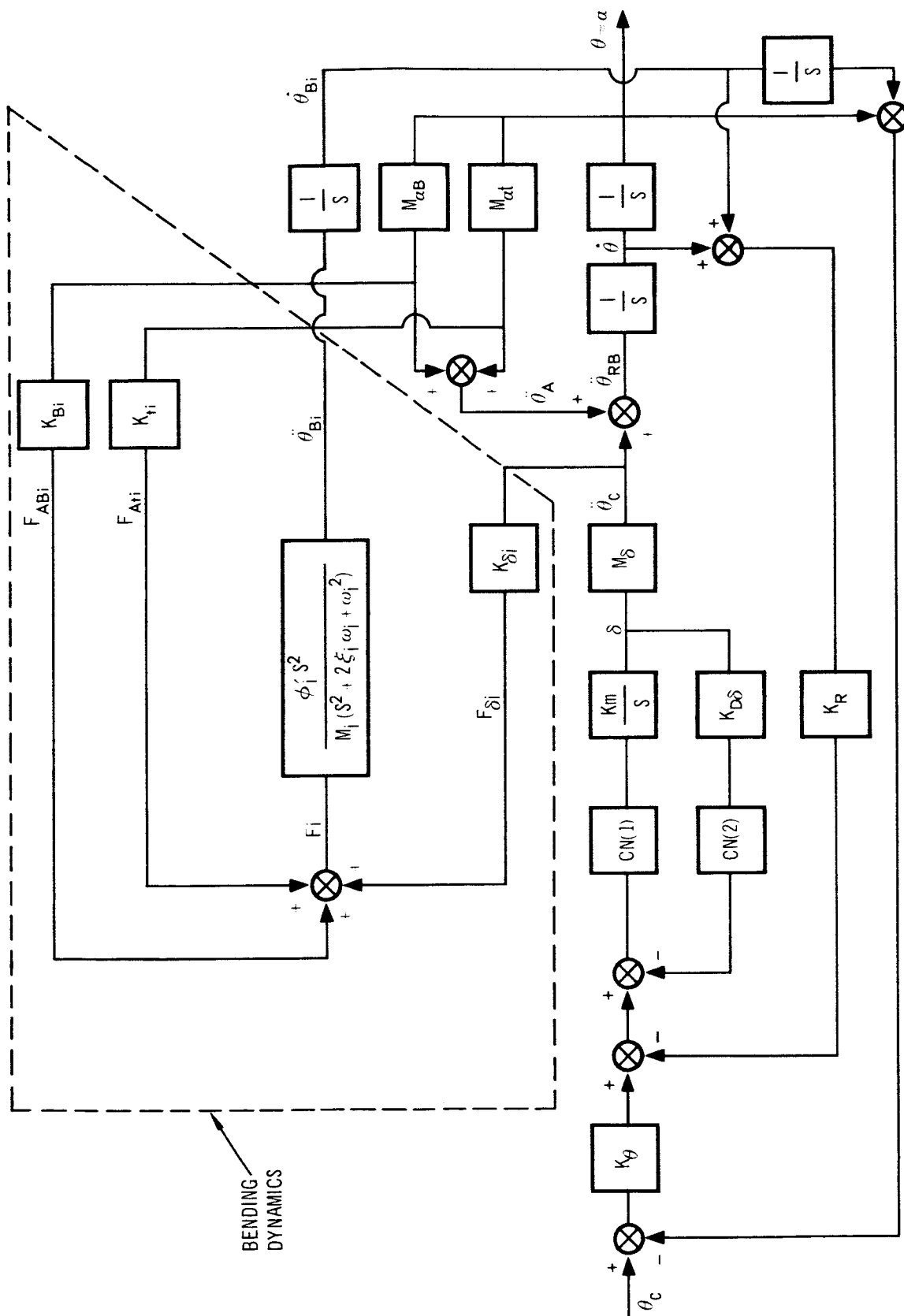


Figure 3-43. Flexible Vehicle Control System Model

Inertial coupling of the control engines to the vehicle (a form of tail-wags-dog with the tail displaced) was neglected in this study in view of the small engine size employed. A vehicle pitch-plane analysis was assumed sufficient to illustrate the feasibility of controlling the flexible vehicle. Table 3-10 shows the control system parameter values derived for both rigid and flexible vehicle and represents an acceptable performance condition for all conditions shown. That is to say, compensation and/or gain changes necessary to control the flexible airframe relative to the rigid body vehicle in such a way as to maintain acceptable transient characteristics and stability margins are indicated.

Note also on Table 3-10 that both aerodynamic and control engine derivatives are shown. Two values of aerodynamic stability derivatives for each flight time point are necessary to describe the model employed. These data were based on a two-point loading condition wherein aerodynamic torques and forces were concentrated at two body locations: one at the center of pressure of the stabilizing fins and the other judiciously placed at station 330 or approximately 63% of the HL-10 body length measured aft from the nose.

Table 3-10  
CONTROL SYSTEM PARAMETER VALUES

Condition	T	$K_\theta$	$K_R$	$K_M$	$K_{D\delta}$	CN(1)	CN(2)
No bending	0	16.10	17.90	-18.0	-0.1	1.0	1.0
	70	9.17	10.20	-18.0	-0.1	1.0	1.0
Bending/rate gyro at station 528	0	16.10	22.40	-18.0	-0.1	$\frac{s^2 + 6.45s + 115.5}{s^2 + 4.3s + 115.5}$	$\frac{100s + 314}{3.14s + 314}$
	70	9.17	12.75	-18.0	-0.1		
Bending/rate gyro at station 1000	0	16.10	17.90	-18.0	-0.1	1.0	$\frac{30s + 378}{12.6s + 378}$
	70	9.17	10.20	-18.0	-0.1	1.0	

NOTE:

Liftoff Condition

70-Second Conditions

$\omega_1 = 5.95$	$\xi_1 = 0.007$	$\omega_1 = 6.29$	$\xi_1 = 0.007$
$\omega_2 = 13.2$	$\xi_2 = 0.01$	$\omega_2 = 15.02$	$\xi_2 = 0.01$
$\omega_3 = 26.8$	$\xi_3 = 0.01$	$\omega_3 = 30.0$	$\xi_3 = 0.01$
$M_\delta = -0.00985$		$M_\delta = -0.173$	
$M_{\alpha t} = 0.0$		$M_{\alpha t} = -0.238$	
$M_{\alpha B} = 0.0$		$M_{\alpha B} = 0.252$	

- Two rate gyro locations were examined in the flexible vehicle study. A location was selected in the spacecraft at station 528 consistent with the study objective of simplification of the launch vehicle. The other location was selected upon examination of the data of Figures 3-41 and 3-42 on the basis of selecting an optimal location for maximizing the stability margins. This second location was chosen at station 1000.

An important factor which must be considered relative to gyro placement is transient response, that is, the time to reach 80% of the commanded rate. Of course transient overshoots are assumed in restricting the discussion to use time only. The transient response characteristics are shown in Figures 3-44 and 3-45. These data indicate that overshoots were held to between 20 and 25% regardless of gyro placement. A slowdown in response time of between 0.15 and 0.25 second results from locating the gyros in the payload compared to the location at station 1000. These differences in response time are not considered significant for two reasons: (1) the guidance system could be designed to accept them, and (2) control system gains were not optimized in this study. In view of the potential optimization, some improvement in transient time could undoubtedly be achieved.

The response time characteristics and the stability margins for Configuration I are summarized in Table 3-11. The results are shown for the two gyro locations, for the two flight times, and for both rigid body and flexible body cases. These data reveal that there is infinite gain margin for the gyros located at station 1000. Compensation is required, however, to produce the margins shown in Table 3-11. This compensation consisted of a relatively simple gain schedule and completely passive shaping networks. With compensation, rate gyros could be located in the spacecraft and provide completely adequate gain and phase margins.

Nyquist plots are included as Figures 3-46 through 3-55. The rigid body data for no bending and no compensation are shown in Figures 3-46 and 3-47. The uncompensated cases for the gyros located in station 1000 are shown in Figures 3-48 and 3-49 while the uncompensated data for station 528 (payload location) are shown in Figures 3-50 and 3-51. The use of simple gain schedules and completely passive shaping networks resulted in compensated stability margins as shown in Figures 3-52 and 3-53 for the station 1000 location and in Figures 3-54 and 3-55 for the physical location.



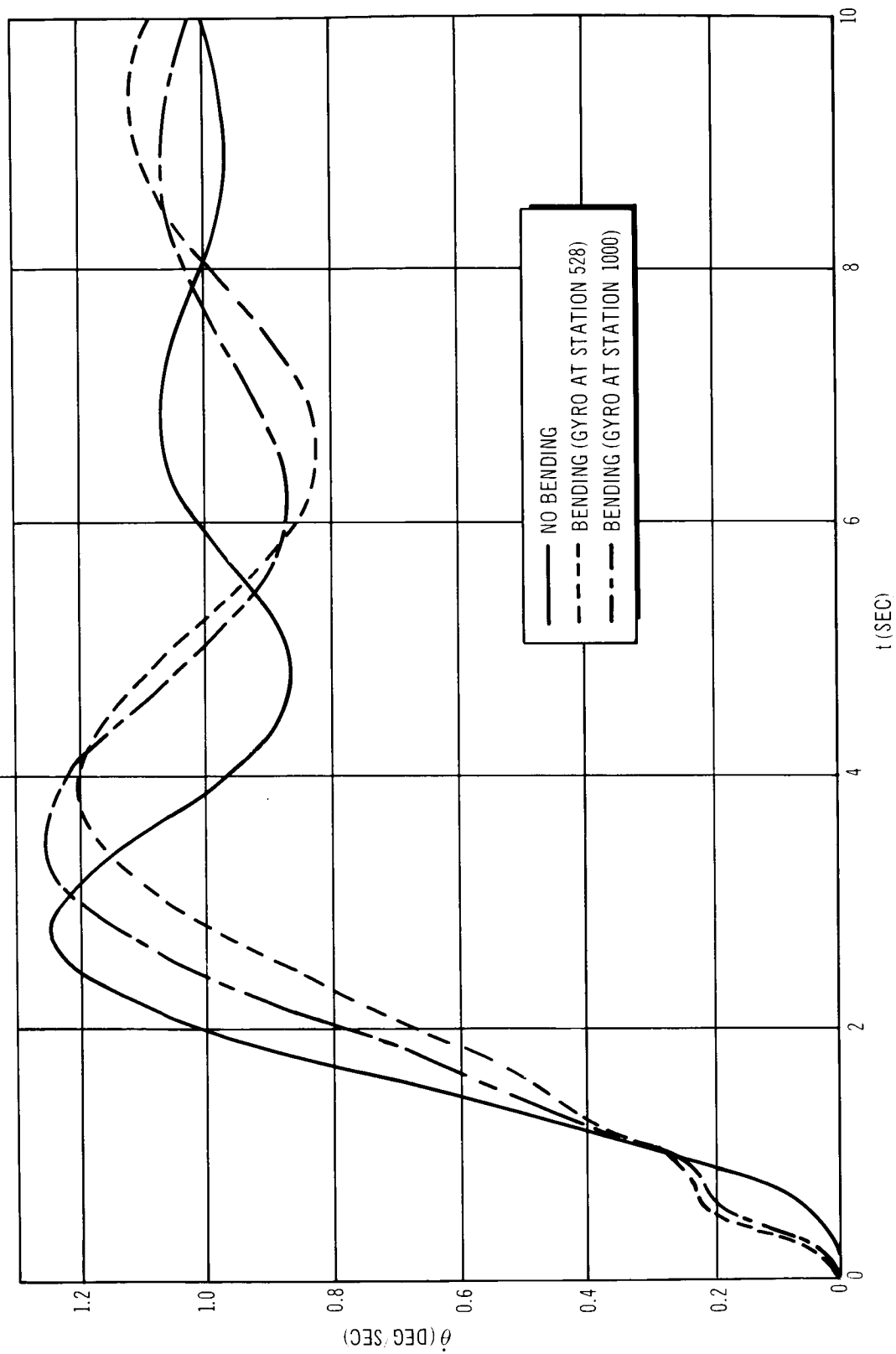


Figure 3-44. Vehicle Time Response to Unit Step Command Configuration I,  $t = 0$

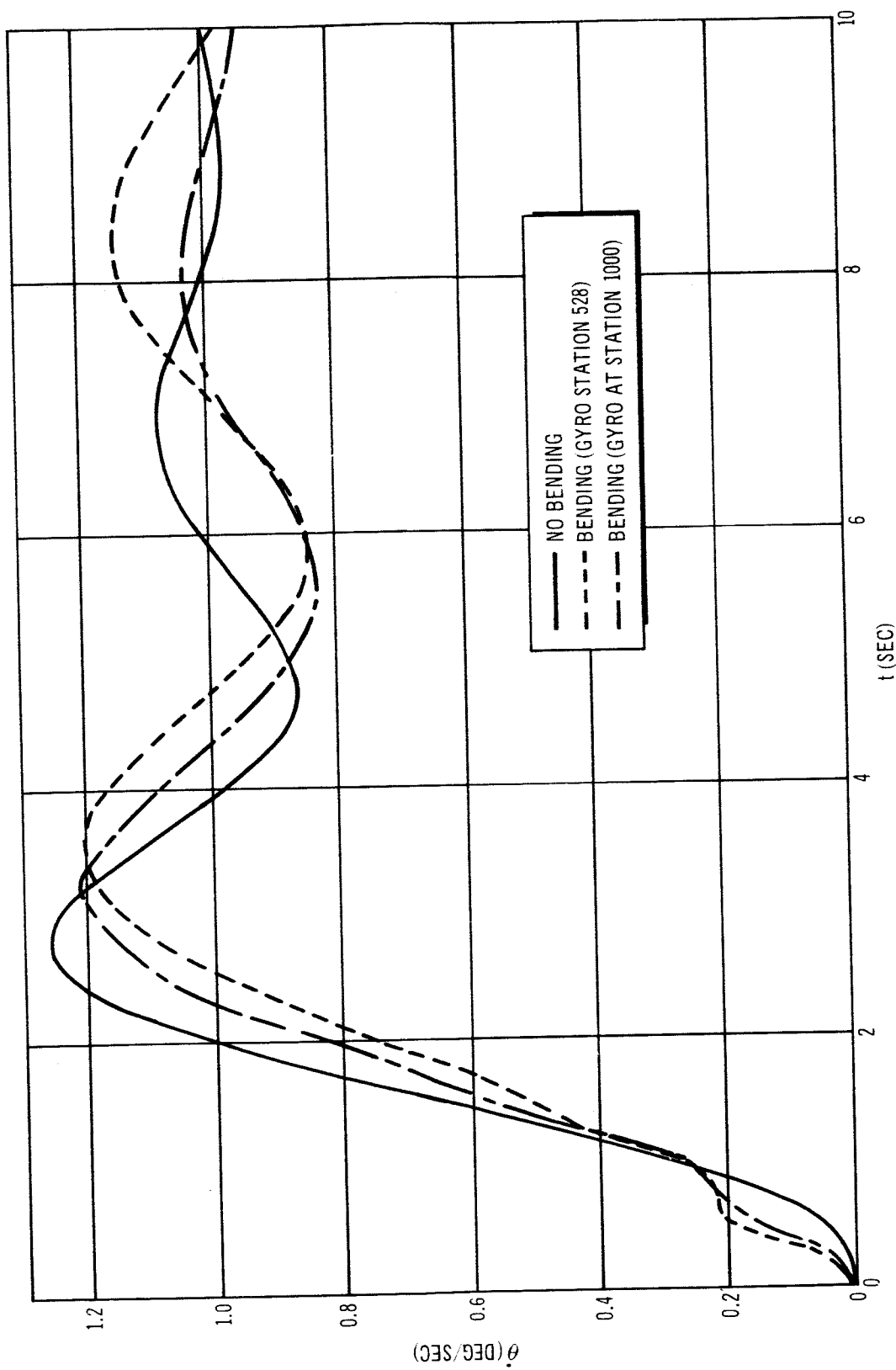


Figure 3-45. Vehicle Time Response to Unit  $\dot{\theta}$  Step Command-Configuration I,  $t = 70$  sec

Table 3-11  
HES BASELINE STABILITY CHARACTERISTICS

	t (sec)	Response Time (sec)	Gain Margin (db)				Phase Margin (Deg)			
			R.B.	F <sub>1</sub>	F <sub>2</sub>	F <sub>3</sub>	R.B.	F <sub>1</sub>	F <sub>2</sub>	F <sub>3</sub>
No bending	0	1.7	6.0	NA	NA	NA	30	NA	NA	NA
	70	1.7	6.0	NA	NA	NA	33	NA	NA	NA
Bending/rate gyro at Station 528	0	2.3	5.6	∞	∞	14.9	48	23	∞	45
	70	2.1	6.0	∞	12.0	40.0	35	22	55	62
Bending/rate gyro at Station 1000	0	2.05	8.3	∞	∞	∞	100	21	∞	45
	70	1.95	7.6	∞	∞	∞	70	20	∞	45

NOTES:

NA = not applicable

R.B. = rigid body

F<sub>1</sub> = first bending mode resonance

F<sub>2</sub> = second bending mode resonance

F<sub>3</sub> = third bending mode resonance

Response Time = time for vehicle to reach 80% of command rate

### Conclusions

The Configuration I baseline vehicle can be controlled as a flexible body using state-of-the-art techniques. Its bending characteristics are similar to those of the Saturn C-5 vehicle during the first stage of boost. A relatively simple gain schedule and completely passive shaping networks should suffice for compensation over first-stage operation. Response times of approximately 2 seconds are maintainable through employment of this simple compensation.

Selection of final controller networks should be preceded by a more sophisticated bending analysis, that is, one which includes the cross-coupling effects of longitudinal and transverse vibrations. Shear stiffness should also be accounted for because it has a tendency to lower slightly the bending mode resonant frequencies.

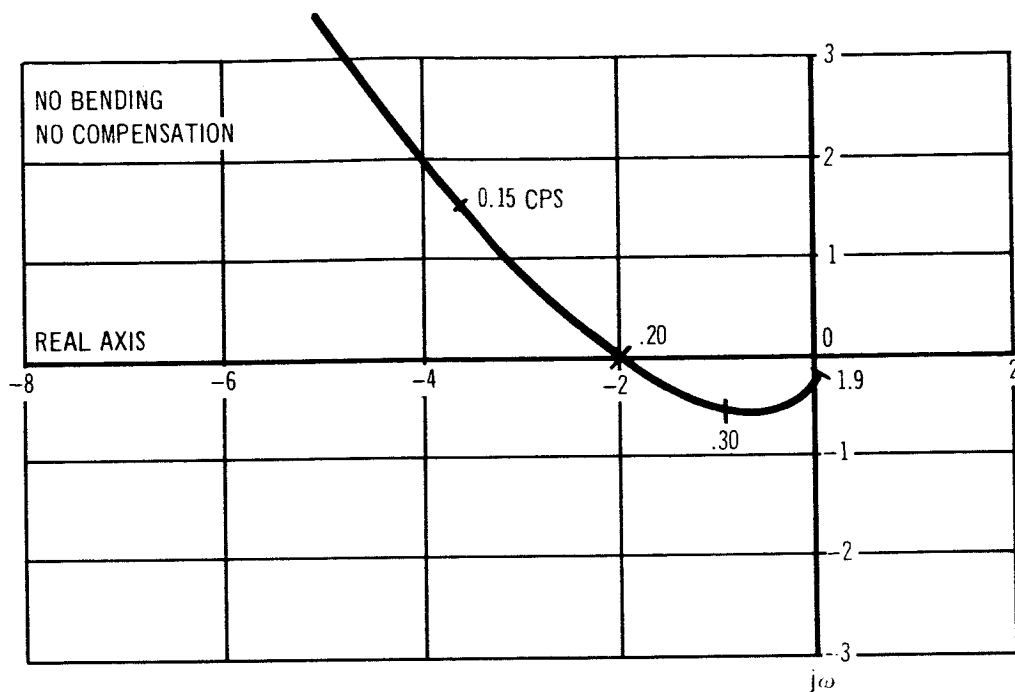


Figure 3-46. Nyquist Diagram – Configuration I,  $t = 0$

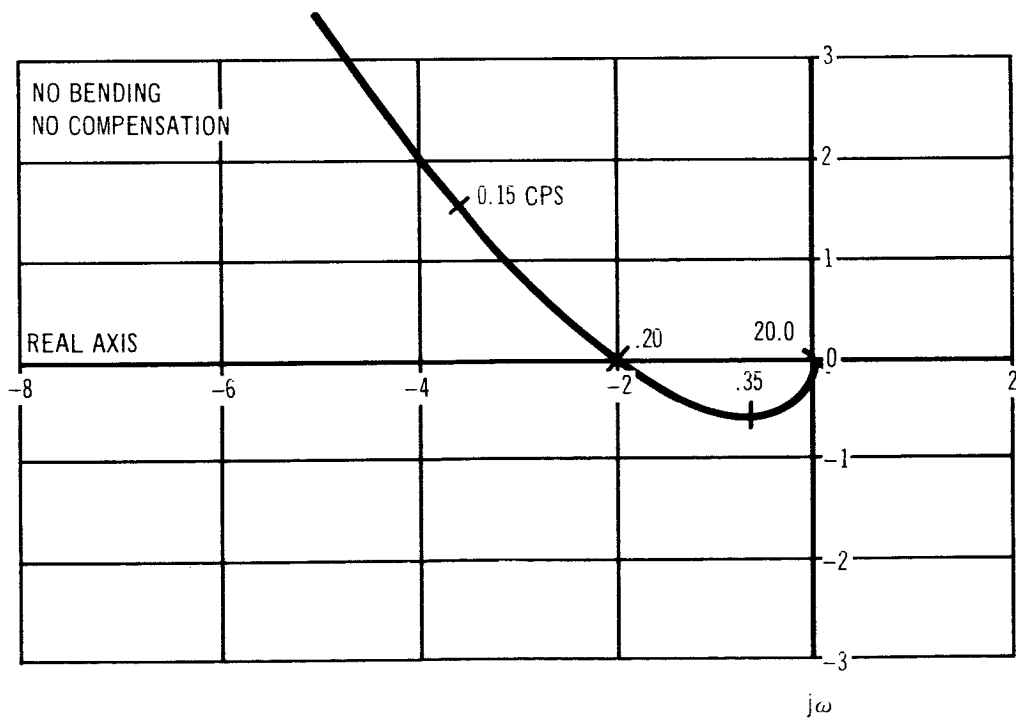
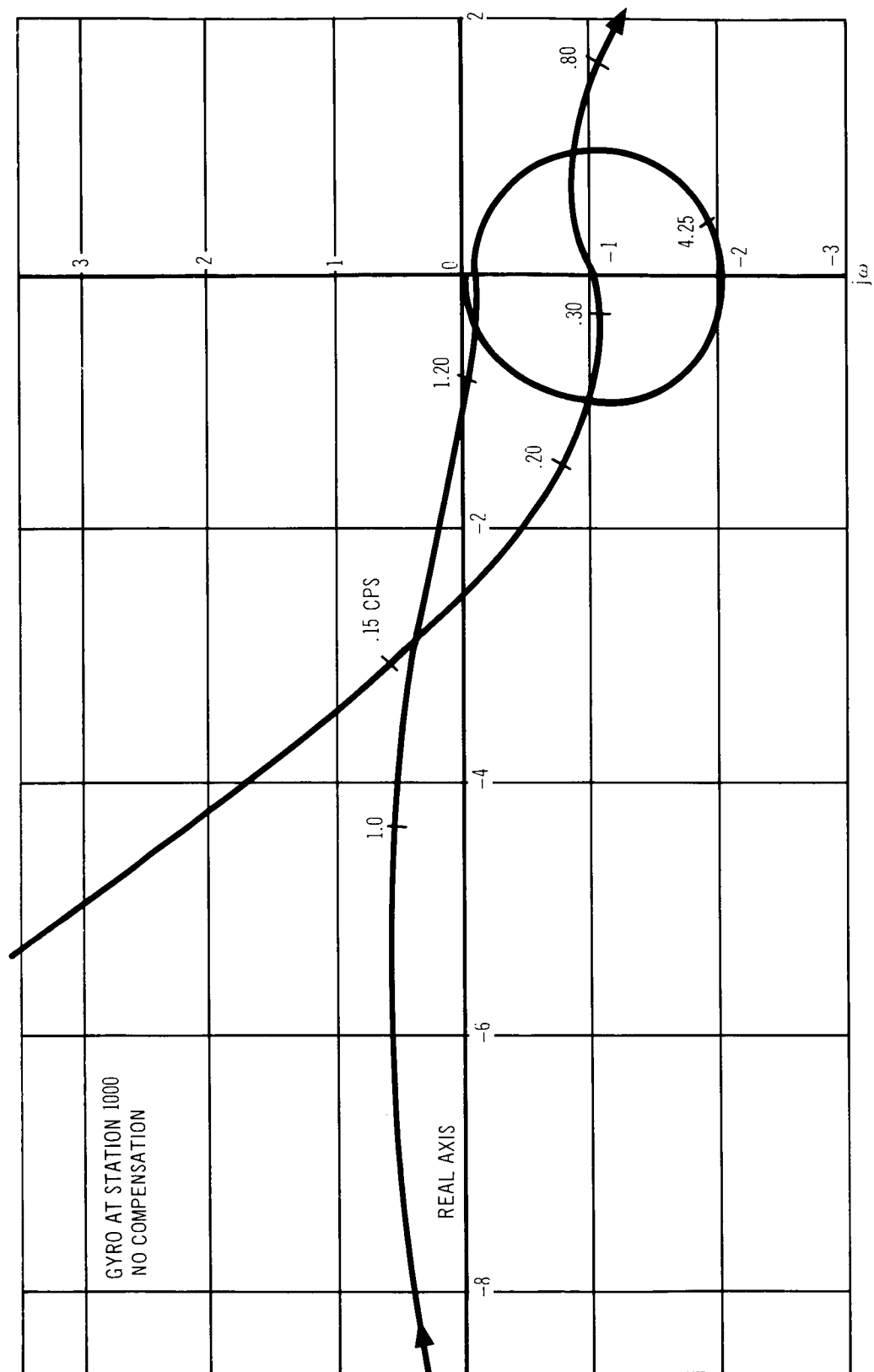


Figure 3-47. Nyquist Diagram – Configuration I,  $t = 70$  sec

Figure 3-48. Nyquist Diagram-Configuration 1,  $t = 0$

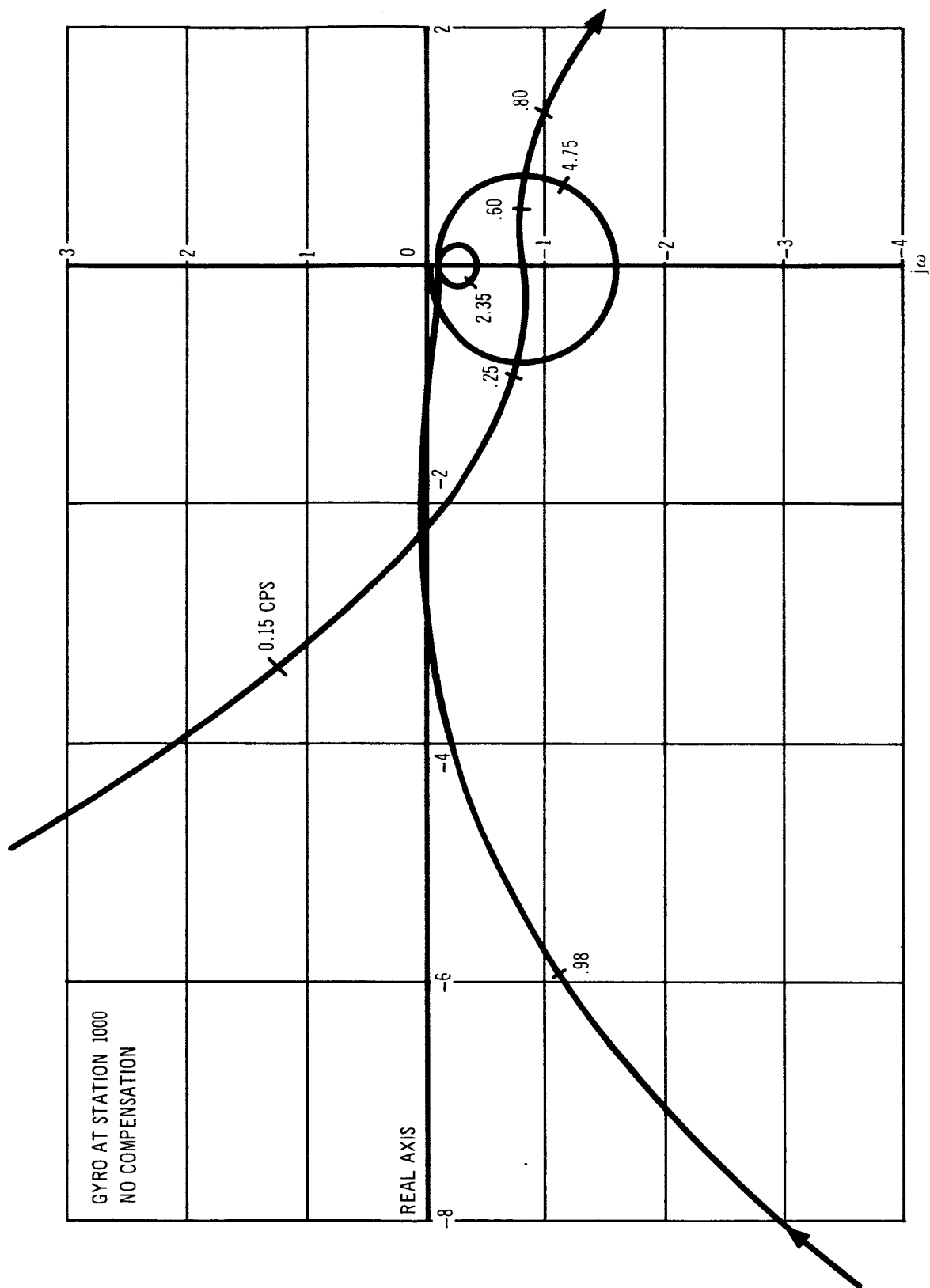


Figure 3-49. Nyquist Diagram-Configuration I,  $t = 70$  sec

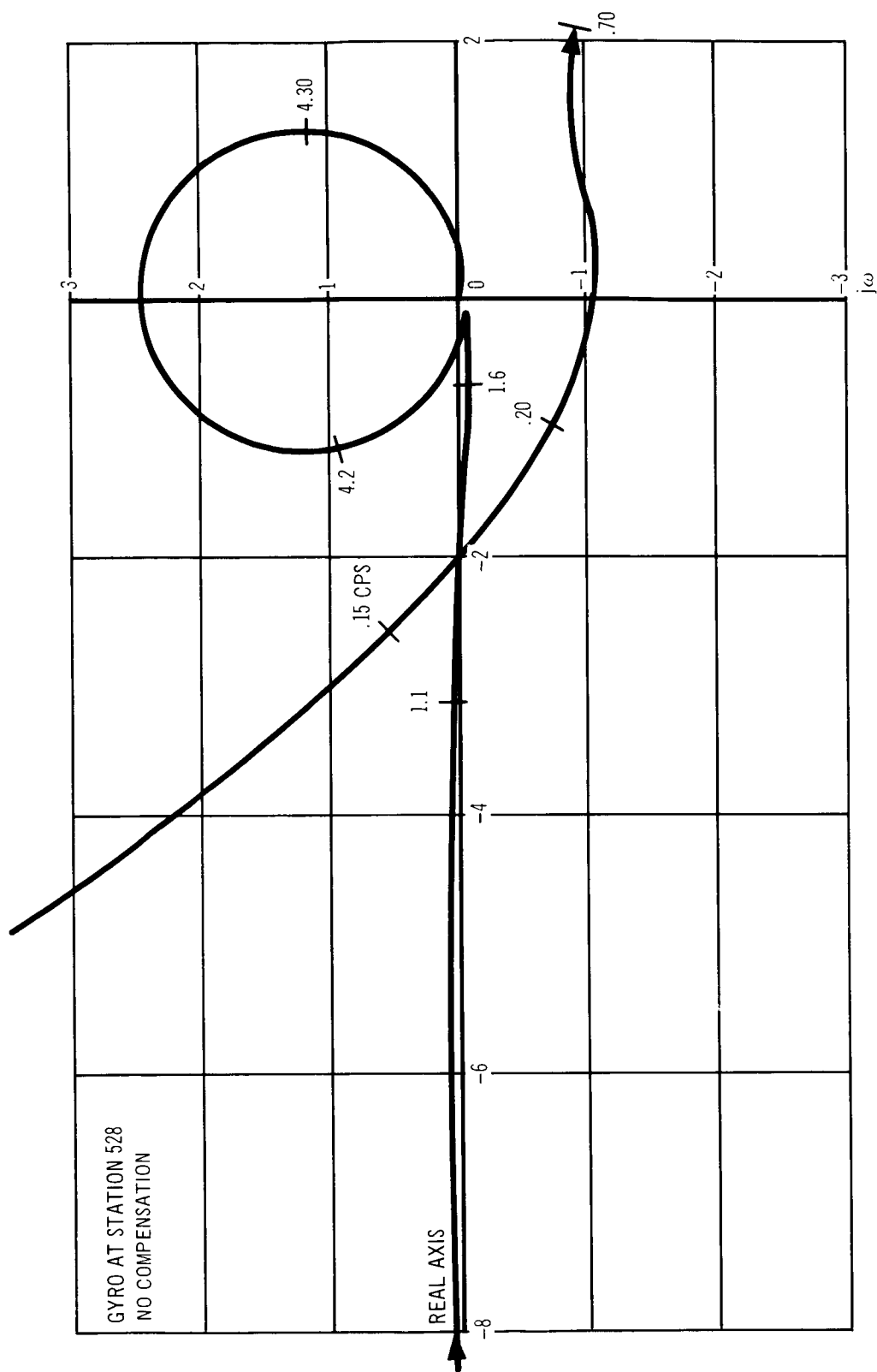


Figure 3-50. Nyquist Diagram Configuration I,  $t = 0$

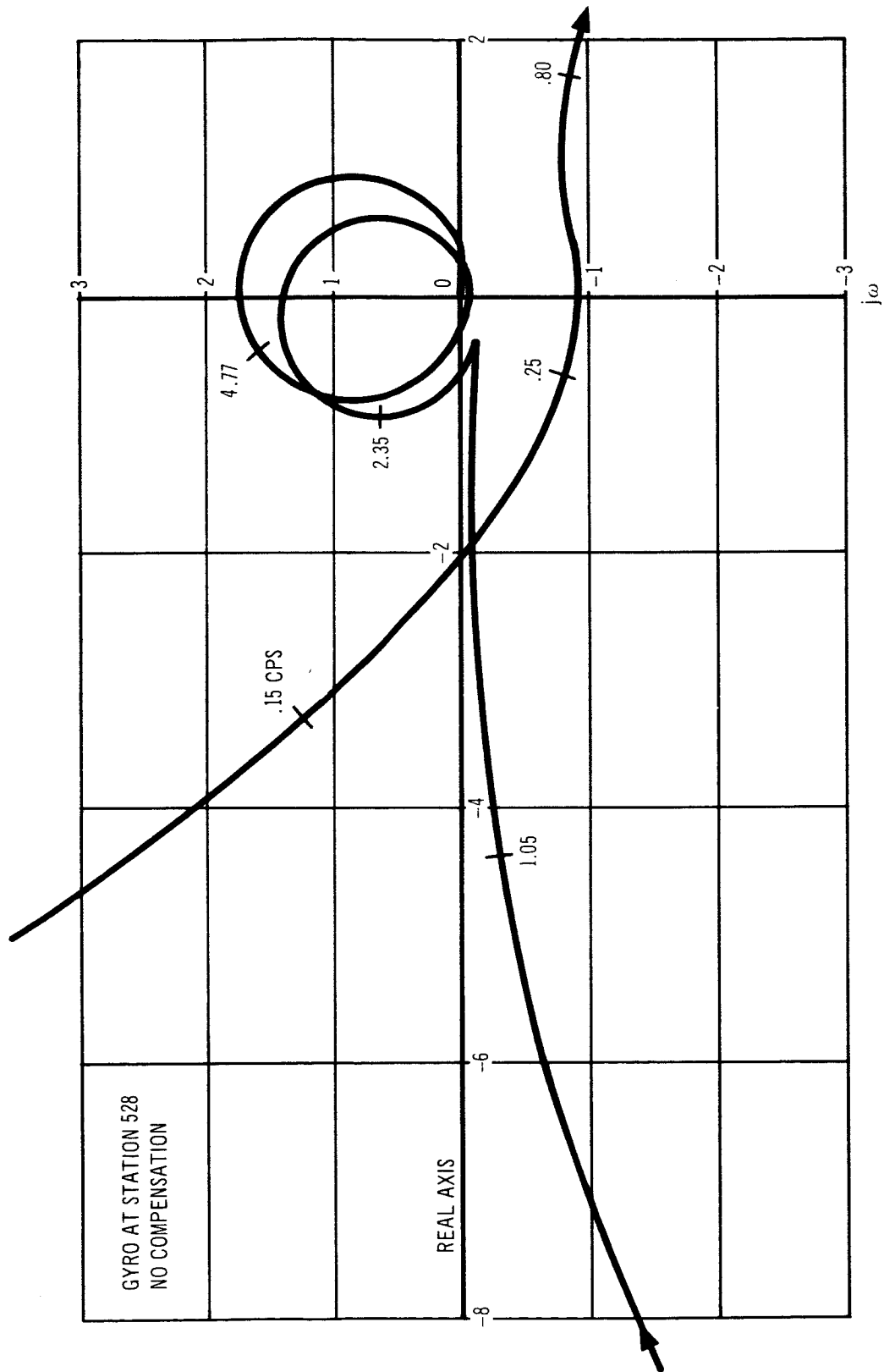
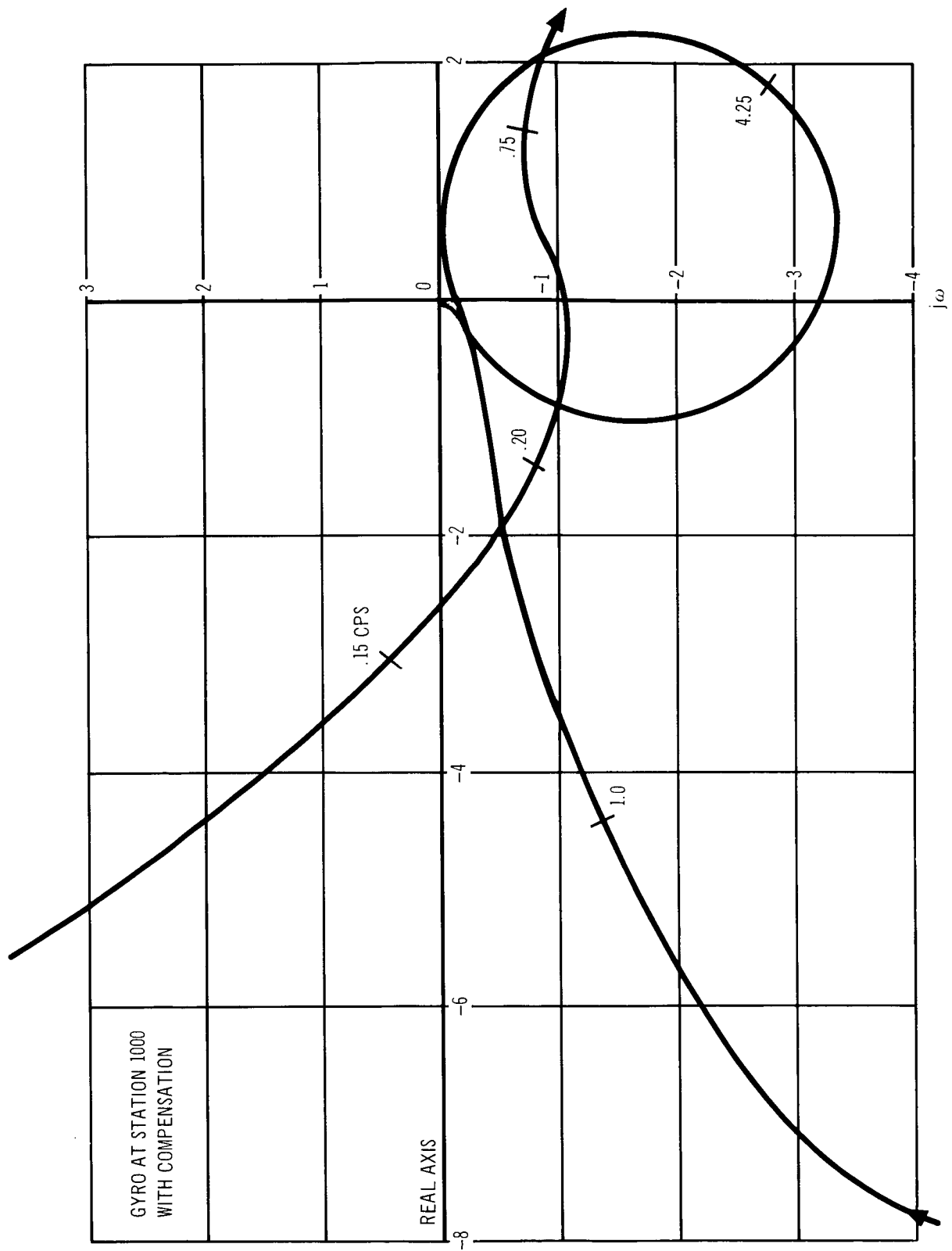


Figure 3-51. Nyquist Diagram – Configuration I,  $T = 70$  sec



Figure 3-52. Nyquist Diagram - Configuration I,  $T = 0$  sec

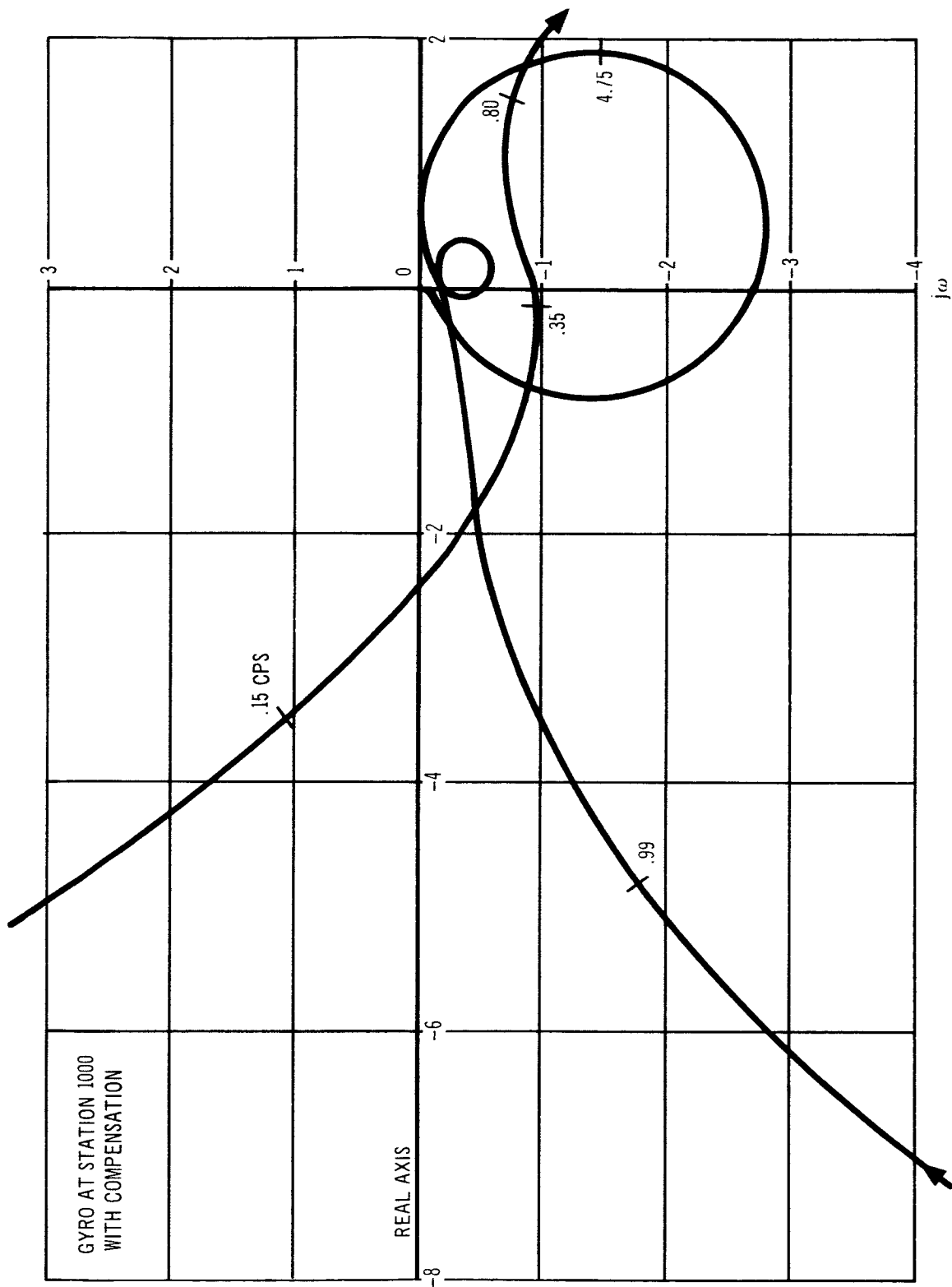


Figure 3-53. Nyquist Diagram - Configuration I,  $T = 70$  sec



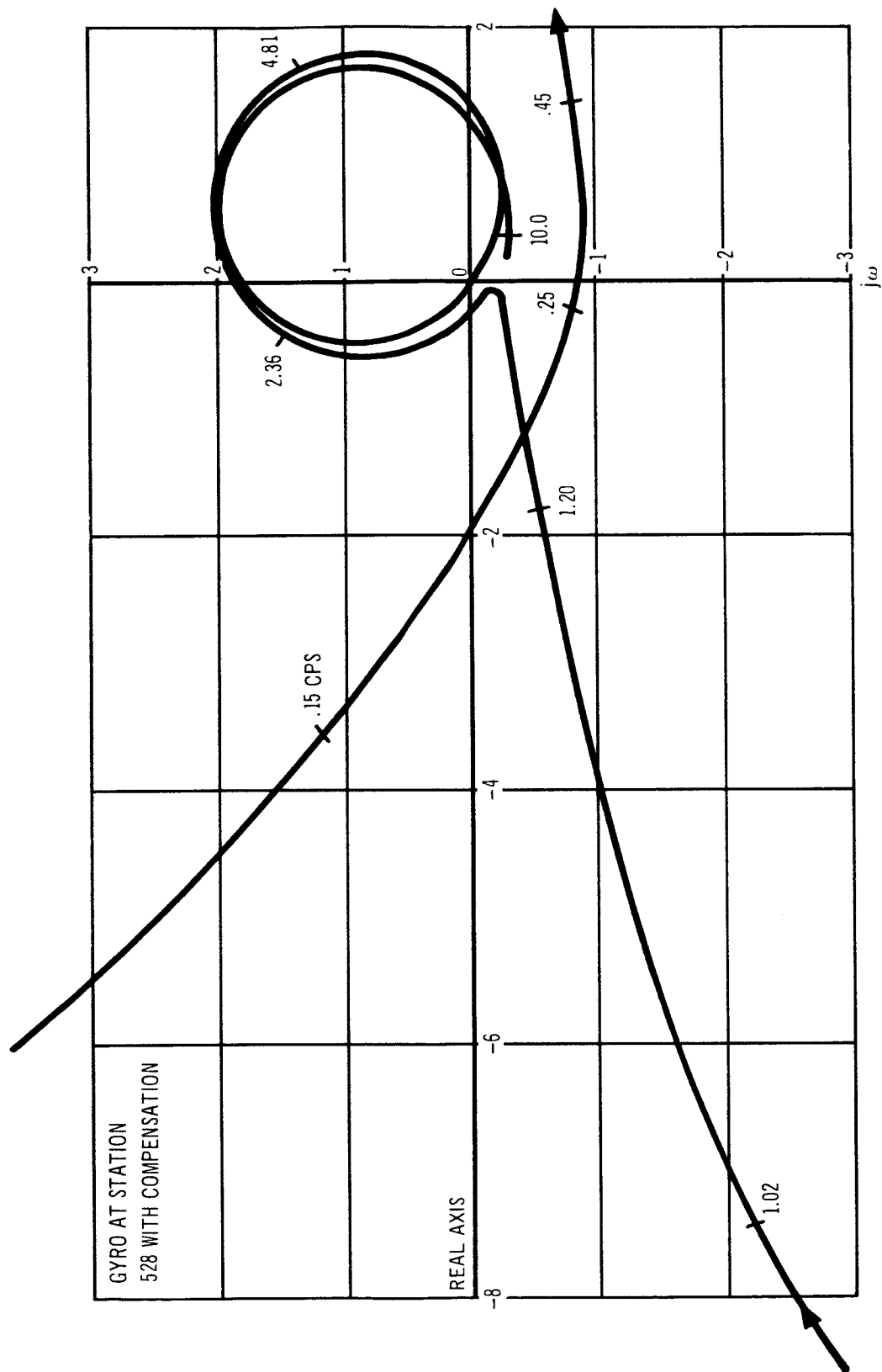


Figure 3-55. Nyquist Diagram - Configuration I,  $t = 70$  sec

### 3.1.6 Summary

As discussed in the preceding sections, the objective of the vehicle refinement and optimization studies was to investigate those technical areas which were made apparent at the end of the Phase I studies as either requiring additional refinement or offering a high potential for reduction in vehicle size. Those areas selected for optimization included booster nozzle characteristics, stage velocity distribution, booster motor thrust-time shaping, trajectory shaping, and the control requirements and related steering system characteristics.

The approach used and study results were presented in the preceding paragraphs.

The resultant change in the Configuration I, or HES-2G, vehicle from the Phase I to the Phase II study is shown in Table 3-12. The vehicle is approximately 925,000 lb lighter and 33 ft shorter at liftoff while the useful load in orbit and mission profile is identical. The change in velocity distribution and the net effect on growth factor is shown in Figure 3-56.

Table 3-12  
COMPARISON OF GROSS VEHICLE CHARACTERISTICS, PHASES I AND II

	Phase I	Phase II
Payload weight (lb)	107,000	108,100
Useful load (lb)	6,600	6,600
$\Delta V$ in 300 nmi orbit (fps)	5,690	5,820
Gross weight at liftoff (lb)	6,653,141	5,727,830
Total vehicle length (ft)	355	322
Steering system		
Total steering propellant (lb)	85,780	60,200
Maximum vacuum steering thrust per engine (lb)	50,000	46,350
Vehicle stage characteristics		
First stage propellant weight (lb)	4,000,000	3,751,000
Second stage propellant weight (lb)	1,350,000	1,013,000
Third stage propellant weight (lb)	526,100	252,500
Trajectory characteristics		
Maximum axial acceleration (g's)	7.18	4.51
Maximum dynamic pressure (psf)	721	801

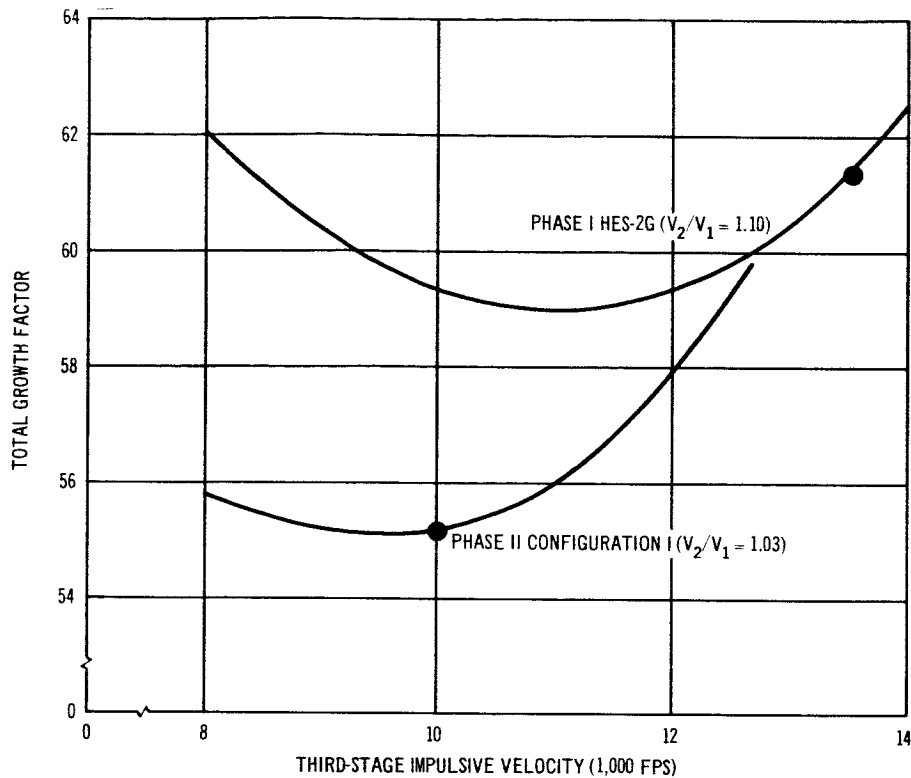


Figure 3-56. Stage Velocity Optimization

Although other approaches were considered, the steering system technique of preprogrammed step throttling of both engines with differential gimbaling was retained as the most effective approach. Based on the studies accomplished, the potential increase in payload gained by using differential throttling did not offset the added complexity required. A comparison of the Phase I and Phase II programmed thrust history is shown in Figure 3-57. The requirements imposed on the steering system, including gimbaling, throttling, restart, and the other characteristics assumed, were discussed with engine manufacturers relative to potential problem areas. No problem areas requiring solution outside of present techniques were felt to exist. Sufficient criteria for evaluation of gimbal rate or throttling response requirements were not available, however.

Aerodynamic fin size, planform shape, and the consequent vehicle neutral stability times were found to have a large effect on control requirements. These fins were sized to minimize steering system propellant requirements.

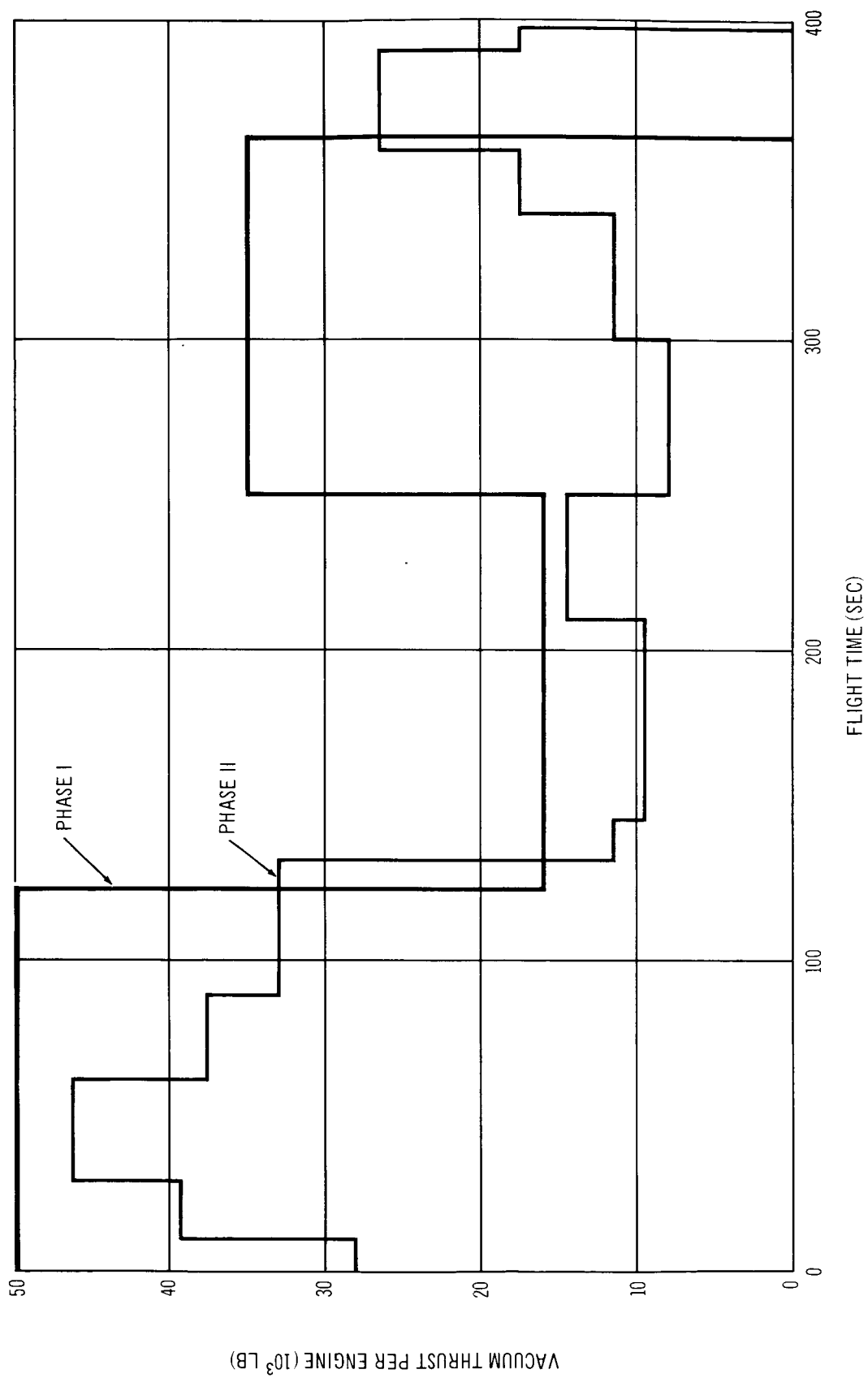


Figure 3-57. Control Thrust History, Phases I and II

Failure modes were investigated in this study to determine the general requirements for safe escape and recovery when a mission abort is required on the launch pad, at flight conditions corresponding to maximum dynamic pressure, and at high altitude. An abort escape system was sized for a TNT equivalence of 25% of the booster propellant weight and for the launch-pad abort situation.

The abort requirements for escape from catastrophic failures of the solid propellant booster motors and from generative failures of either the booster motors or the steering system were investigated. These requirements were met by an abort system utilizing seven solid-propellant abort motors weighing 6,300 lb in combination with the steering engines drawing propellant from the tankage on board the spacecraft. This system provides a maximum abort acceleration of 3.6 g's when the steering engines are used and provides for a normal landing from pad abort on such existing airfields as Patrick AFB.

Safe escape may be accomplished from catastrophic failures of the booster motors at the maximum dynamic pressure condition in the ascent profile. Normal horizontal landings may be made for these conditions at airfields located in the vicinity of Cape Kennedy such as Patrick AFB. Escape from generative failures of the steering system may also be safely conducted with a return to land.

Abort escape-system sizing resulted in the conclusion that the level of TNT equivalence specified for the booster propellants had little effect on the payload of the vehicle since separation requirements in second- and third-stage flight for generative failure modes will probably design the size of the system.

Recovery from abort situations at high altitudes can be accomplished from nominal design trajectories without exceeding 1,200 psf dynamic pressure and 6 g's of normal acceleration.

The influence of the spacecraft/booster configuration on control-system complexity was investigated by means of both a rigid and a flexible body analysis at two flight conditions: liftoff and maximum dynamic pressure. The results of this analysis indicate a first-mode bending frequency of 0.947 cps, or approximately the same as that for Saturn V. The location of bending-rate gyros in the spacecraft is technically feasible and would result in a control-system design possessing adequate gain and phase margins. The design could



be accomplished with a simple gain schedule and a completely passive shaping networks during first-stage operation.

### 3.1.7 Recommendations for Further Study

As a consequence of Phase II investigations, additional study areas were made apparent as offering potential improvement in the vehicle design and the system concept, making them more operationally and economically attractive. These areas of investigation are discussed in this section as recommendations for additional study.

The potential advantage of incorporating either of two different approaches to satisfying steering and maneuver propulsive requirements were investigated. These approaches were: (1) using a pressure-fed, low thrust, storable-propellant propulsion system for maneuver requirements and a separate pump-fed, storable-propellant propulsion system for steering requirements; and (2) using a pressure-fed, low thrust, storable-propellant maneuver propulsion system and a pump-fed, cryogenic-propellant steering system. The brief study performed indicated potential vehicle-size reduction for both of these approaches as indicated in Table 3-13. Configuration I is the Phase II, Configuration I, vehicle. Configuration IA utilizes the Configuration II spacecraft described in Section 3.3.3, with two 4,000-lb thrust, pressure-fed, storable, propellant ( $N_2O_4$  - MMH) maneuver engines with the Configuration I, gimbaled, pump-fed steering engines added. The Configuration I steering-propellant module is also used on Configuration IA. Configuration IB has the Configuration IA spacecraft with two gimbaled, pump-fed cryogenic-propellant ( $O_2-H_2$ ), high-pressure steering engines. The required liquid oxygen and hydrogen would be carried in a redesigned steering propellant module. This investigation was too brief to be used for selecting an approach since operational and economic considerations were not taken into account. Additional study does appear to be warranted based on the indicated weight reductions, however, and should take into account these considerations.

Additional technical optimization is warranted in the areas of solid-motor performance characteristics. An investigation of launch-vehicle stage weights might lead to improved mass fractions with a consequent reduction in vehicle size. Cost optimization studies, taking into account solid-propellant type and

Table 3-13  
EFFECT OF SPACECRAFT PROPULSION TYPE

Configuration	I	I-A	I-B
Maneuver System	Pump-fed Storable $I_{spV} = 288.5$	Pressure-fed Storable $I_{spV} = 307.3$	Pressure-fed Storable $I_{spV} = 307.3$
Steering System	Pump-fed Storable $I_{spV} = 288.5$	Pump-fed Storable $I_{spV} = 288.5$	Pump-fed Cryogenic $I_{spV} = 424.0$
Gross Payload Weight	108,100	102,100	112,150
Spacecraft	87,400	81,800	81,800
Usable Propellant	43,000	37,860	37,860
Steering Module	70,700	70,700	58,760
Usable Propellant	60,200	60,200	38,200
Gross Weight at Liftoff	5,727,800	5,428,300	5,539,050
Payload	108,100	102,100	112,150
Third Stage	307,700	291,700	299,100
Second Stage	1,146,900	1,086,700	1,108,300
First Stage	4,165,100	3,947,800	4,019,500

stage-velocity distribution, would provide a more cost-effective vehicle. These studies, which were not possible within the scope limitations of the Phase II study, would provide an even more competitive logistics-vehicle concept.

A rather conservative approach was taken in both the Phase I and Phase II studies with respect to wind effects. Figure 3-58 illustrates the wind profile envelope used and several typical wind velocity profiles. Since any wind profile within the wind profile envelope could be encountered on any given flight, the steering system must be capable of meeting all conditions defined by the envelope. A vehicle may, however, fly through a region of wind velocity so high that control cannot be maintained, provided that it emerges from this region soon enough that the control system can regain control and correct for

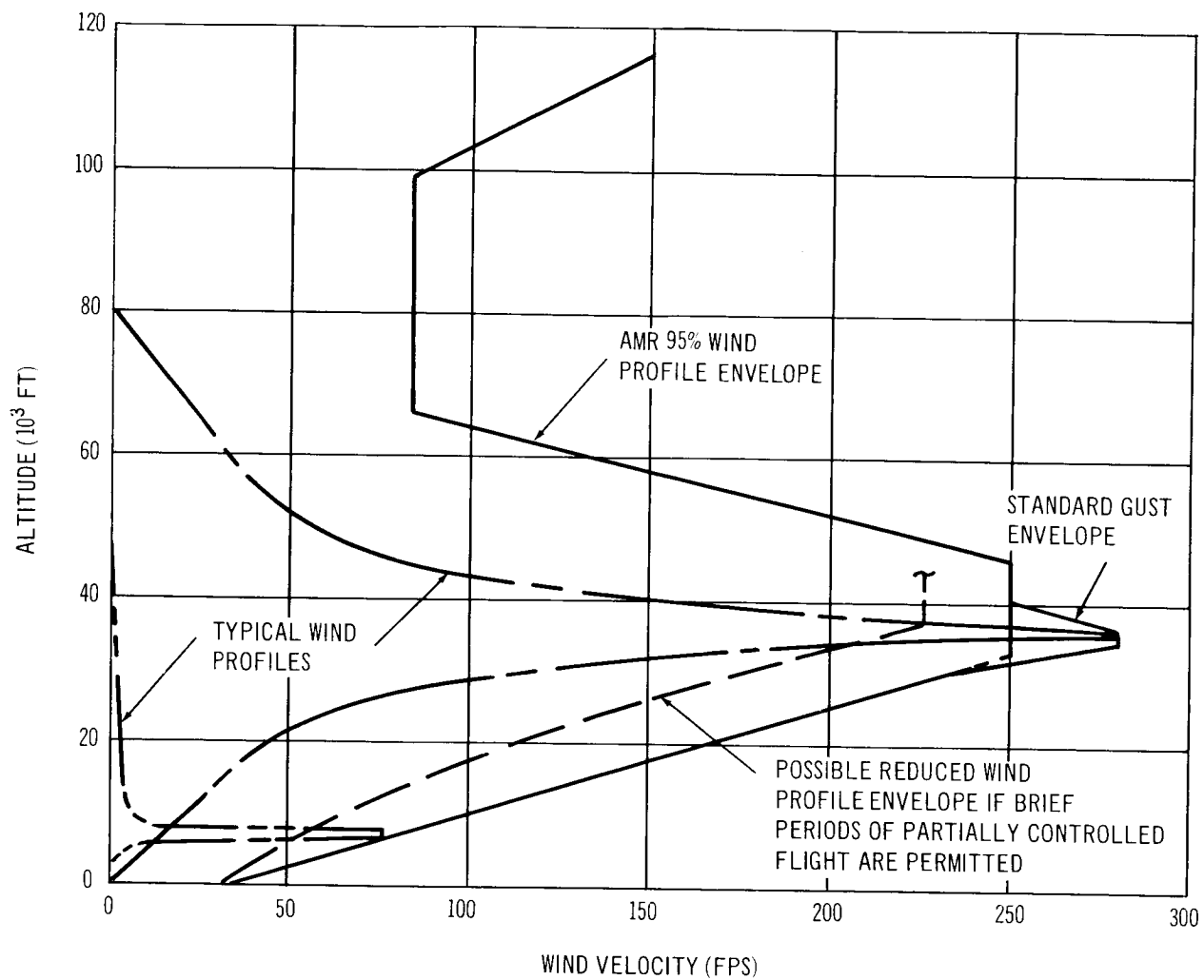


Figure 3-58. Relation of Wind Profiles and Wind Profile Envelopes

any errors brought about during the period of uncontrollability. More complete definition of a guidance and control system and a detailed performance analysis could result in the reduced wind profile envelope shown in Figure 3-58, thus providing a savings in control propellant.

The brief study of differential throttling performed during Phase II could not justify its use at that time; however, a more detailed study and system definition is necessary to determine whether the savings in control propellant could justify the added system complexity with its associated increase of weight, cost, and decrease in reliability.

Further investigation of the head-end steering concept should include an in-depth investigation of steering engine requirements and the consequent effects on the vehicle design, operational, and economic characteristics. This investigation would require a definition of steering-engine maximum gimbal capability, and gimbal and throttle rate and response characteristics. Optimization of engine operating characteristics such as chamber pressure, propellant mixture ratio, and nozzle expansion ratio would also be required.

The abort studies were accomplished assuming that a ported forward-dome thrust-reversal system would provide an adequate decrease in stage thrust to allow spacecraft separation. This thrust reversal system was also used for purposes of nominal trajectory stage separation. These studies did not investigate this system or its requirements in depth, however, and all ramifications to the vehicle system were not considered. A study should be performed investigating those thrust degradation techniques such as thrust reversal ports, auxiliary thrust reversal motors, water quench, and motor-case destruct systems which would provide spacecraft abort and stage separation capability with the least penalty to the vehicle system.

The determination of the effect of abort accelerations and trajectories on spacecraft stability and handling characteristics was not within the scope of this study. This area of investigation must be pursued before the feasibility of normal airfield landing after abort can be resolved.

## 3.2 SYSTEM DESCRIPTION

This section describes the total system aspects required to establish a planning type of estimate of mission cycle time and operations costs. Major subjects included in this discussion are (1) the major events in the operations cycle of the Configuration I vehicle with the man-hour and elapsed time requirements; (2) a brief discussion of the assumptions used to describe the ground support facilities; (3) a first-order type of analysis of refurbishment costs; and (4) some range safety criteria unique to the vehicle concept.

### 3.2.1 The System Operations Cycle

The significant events in the operations cycle are shown in Figure 3-59. The ensuing discussion will start with the logistics requirements for providing spacecraft and launch-vehicle hardware to Cape Kennedy. This is noted in Figure 3-59 as Vehicle Supply Logistics and consists of new launch-vehicle hardware including such items as the steering-propellant tank modules, cargo module adapters, main-stage solid-propellant motors, and associated nozzles, skirts, and other items required to assemble the launch-vehicle stages. The spacecraft logistics involve both new spacecraft from the manufacturer's site and the spacecraft recovered from a mission.

The next step in the cycle is the processing of the vehicle components in the various assembly and checkout buildings near the launch site. Such processing includes acceptance testing, refurbishment tasks for the used spacecraft, required assembly tasks, checkout, and, finally, the erection of the vehicle at the launch complex. The processing phase is considered ended with the mating of the spacecraft and cargo module adapter to the erected third stage.

The prelaunch and launch phases consist of the all-systems checks that are required and the final countdown leading to the actual liftoff.

The space operations phase of the vehicle-use cycle was not a subject for study in this report. Docking procedures at the space station were studied and discussed in the Phase I report and these procedures are used in this study. Ground support requirements for ascent and rendezvous are those of the Gemini system. Re-entry guidance and navigation requirements were assumed the same as used in Reference

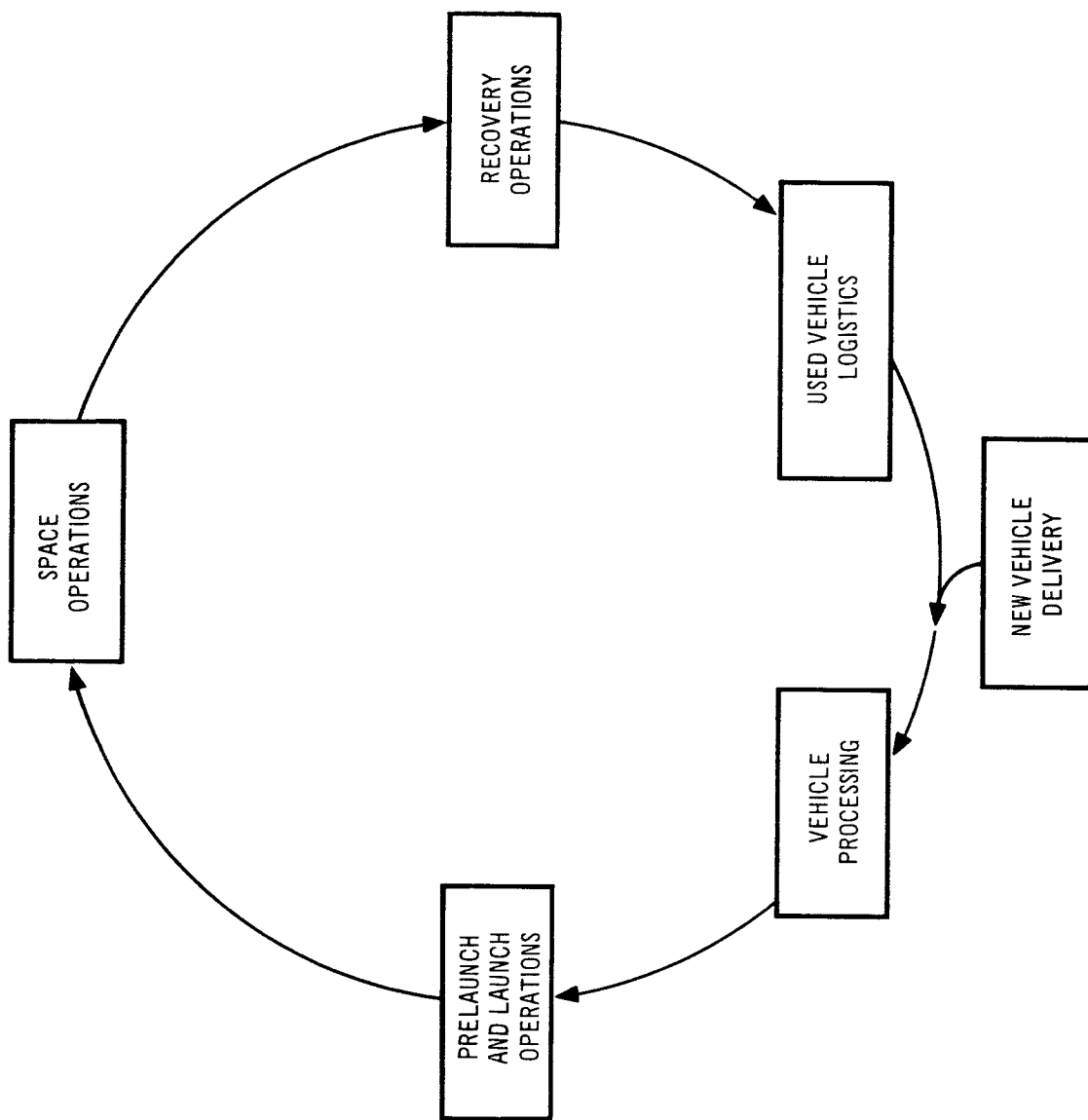


Figure 3-59. System Operations

The recovery phase is defined in this study as beginning with a normal landing at one of the planned recovery sites. The termination of this phase is at the point when the spacecraft leaves the recovery site on its way to the refurbishment site. At this time, the vehicle-supply logistics phase is entered and the cycle has been completed.

#### 3.2.1.1 Vehicle Supply Logistics

The vehicle-supply logistics consist of three elements: (1) the supply of launch vehicle hardware to Cape Kennedy; (2) the supply of new spacecraft to Cape Kennedy; and (3) the return of used spacecraft to Cape Kennedy.

##### Launch Vehicles

The launch-vehicle supply is assumed to include all expendable hardware. The detailed shipping requirements were not investigated in this study. A major problem area is the transportation of the solid-propellant booster motors.

The concept selected for use in this study was the one discussed in Reference 1. This concept consists of the shipment from one or both of the large solid-motor facilities in Brunswick, Georgia and Homestead, Florida. The configuration for shipment would be loaded motor cases without nozzles. Shipment would be in a shipping cradle which would also serve as part of the erection complex at Cape Kennedy. An important feature of this concept is that the first-stage motor is never removed from the cradle in the period from crating at the motor manufacturer's site until it is fully erected in the launch complex. This is discussed in more detail in Section 3.2.1.2. The transportation from the manufacturer's site is by barge up the inland waterway to transfer docks in the vicinity of Mosquito Lagoon.

Transportation costs for launch-vehicle components were not investigated in this study. Previous studies by Thiokol and Aerojet show these costs to be in the neighborhood of \$50,000 for a single 260-in. motor independent of propellant loading. This is a very small fraction of the total operations cost per flight and, hence, was ignored as a factor affecting the objectives of this study.

## Spacecraft

Transportation of the spacecraft by rail, air, and ship was studied from the standpoint of feasibility and first-order costs. The study results are discussed in terms of shipment to Cape Kennedy from the spacecraft manufacturers site and from the recovery site.

Shipment from the recovery site was determined to be a pivotal factor since the shipping time could significantly influence the cycle time for the spacecraft and, hence, the inventory required to meet a given flight frequency. Since runway length requirements for landing the spacecraft are compatible with the operation of the Super Guppy and C-5A transports, these craft were investigated on the basis of loading and shipping criteria. Rail and water shipping would involve an undue restriction on the location of the landing sites and would, in addition, require sizable amounts of shipping time.

Investigation of shipping clearances in the Super Guppy resulted in the requirement for a field joint which would permit the Configuration I spacecraft to be disassembled into two major sections as shown in Figure 3-60. This field joint is located at Station 306 just aft of the pressurized-cargo-compartment aft bulkhead and just forward of the aft propellant tankage. Only one pressurized region is affected, that of the crawl tube to the aft docking station. The aft main-gear main-structural attach points would be unaffected permitting the forward section to be supported on the main gear and nose gear. The folding fins would be rotated forward and the central fin removed.

Transporting by the C-5A would require the same disassembly features as described for the Super Guppy except that the outboard fins would be completely removed.

Investigation of shipping costs resulted in first order costs of from \$8 to \$10 per air mile for a weight equivalent to the Configuration I spacecraft. For planning purposes, this would be about \$25,000 to \$35,000/shipment. Current cost estimates for barge shipments are projected at from \$60,000 to \$70,000/trip.



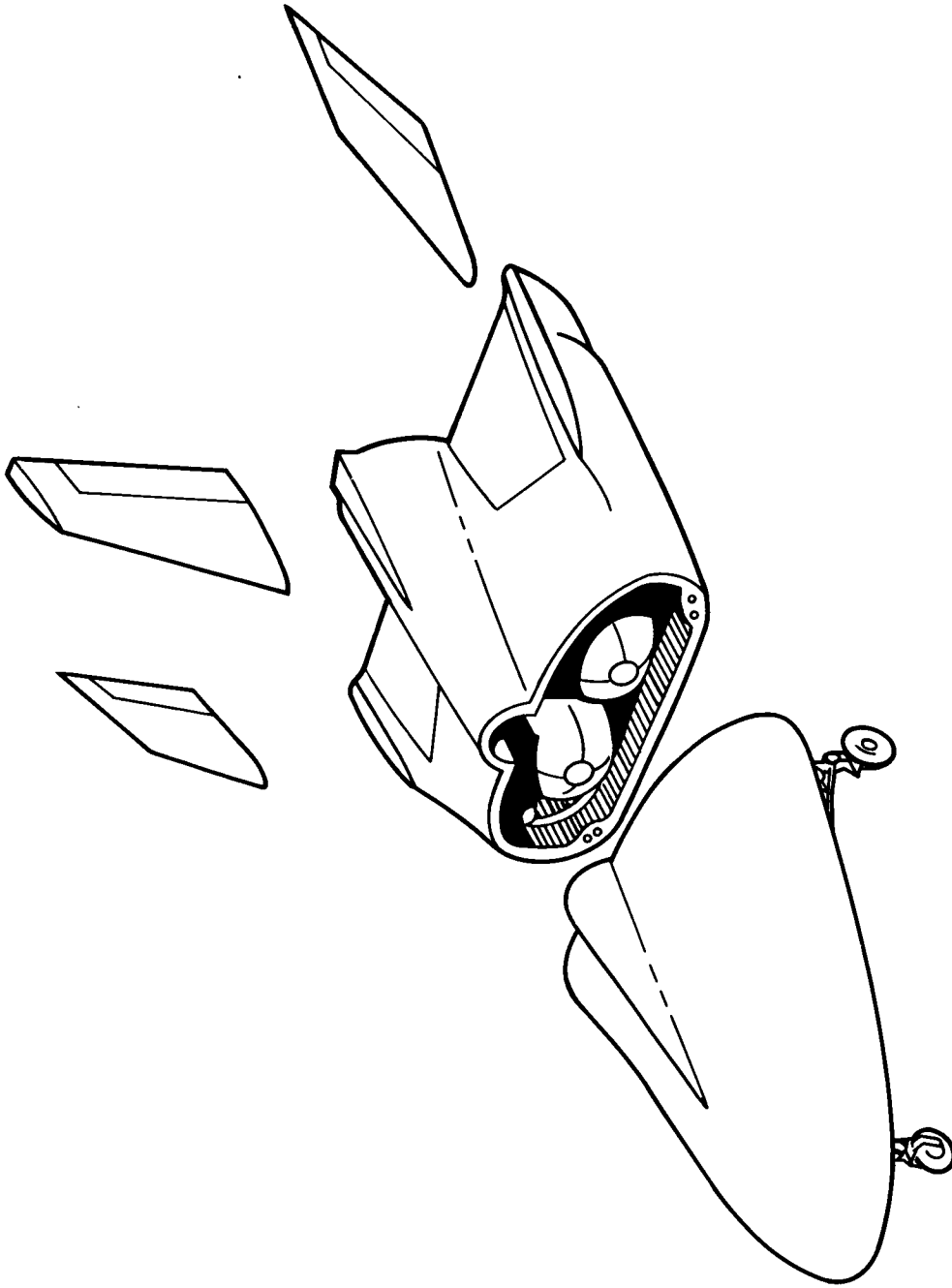


Figure 3-60. Spacecraft Disassembled for Shipment in C-5A

Consideration of the above cost and compatibility factors resulted in the selection of air transportation as the principal mode of shipping from the recovery site to the refurbishment site. This selection was felt to be justified also for shipment between the manufacturer's site and the launch site. Although the time factor may not be so important for the new vehicle delivery, short delivery times are advantageous. Cost factors alone are strong elements in favor of air shipment for new vehicle delivery.

#### 3.2.1.2 Vehicle Processing at the Launch Site

Upon receipt at the launch site, both spacecraft and launch vehicle components are processed in a series of time-phased events as shown in the master flow chart, Figure 3-61. For reasons presented later in this section, the refurbishment tasks for the spacecraft are accomplished at the launch site location.

##### Launch Vehicle

The concept of handling the larger components of the total vehicle is described pictorially in Figure 3-62. The chain of events begins with the removal of the shipping cradle from the barge at Cape Kennedy. The movement is then either to the solid-motor building for processing as a stage or to the solid-motor storage buildings. Assembly of the nozzle to the motor, the interstage skirts, and installation of such subsystems as range safety, ignition, and electrical circuitry is accomplished at this point. The steering-propellant tankage section is checked out and mated to the third-stage motor at this same location. No ordnance devices are installed, however, until the launch vehicle has been erected and an all-systems check has been accomplished.

Assembly of stage components is accomplished without removal from the shipping cradle. Upon completion of stage checkout, the stage is transported to the launch complex as shown in Figure 3-62. The launch-complex concept chosen for this study is a modification and refinement of the concept used for the Phase I study, Reference 1. The complex consists of a reinforced-concrete underground silo and employs elevator-like platforms operated by a roll-ramp means of actuation. The upper part of the site is widened to permit rotation of the stage into an upright position. The shipping cradle is mounted in a transporter at the barge unloading step and is transported through assembly and

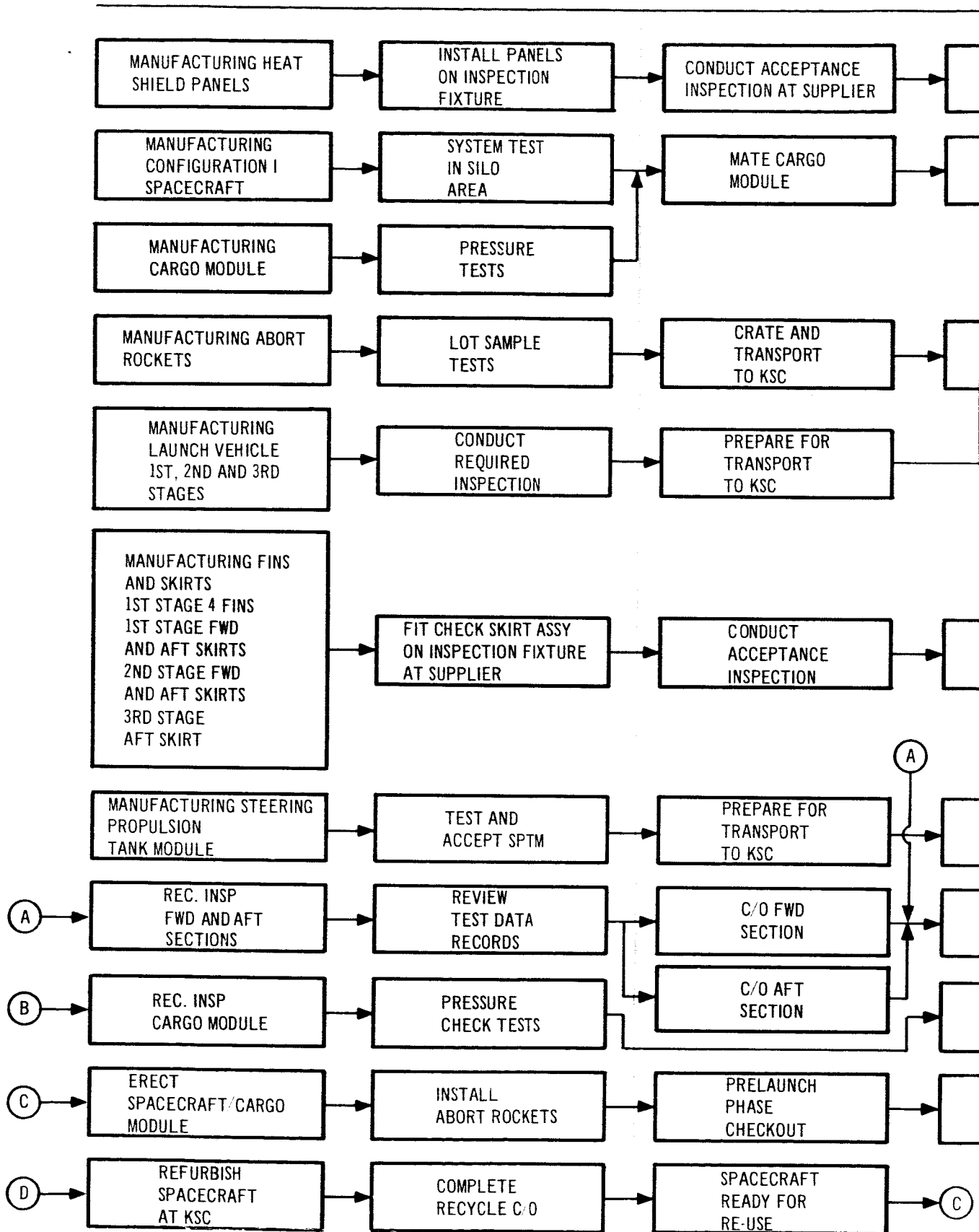
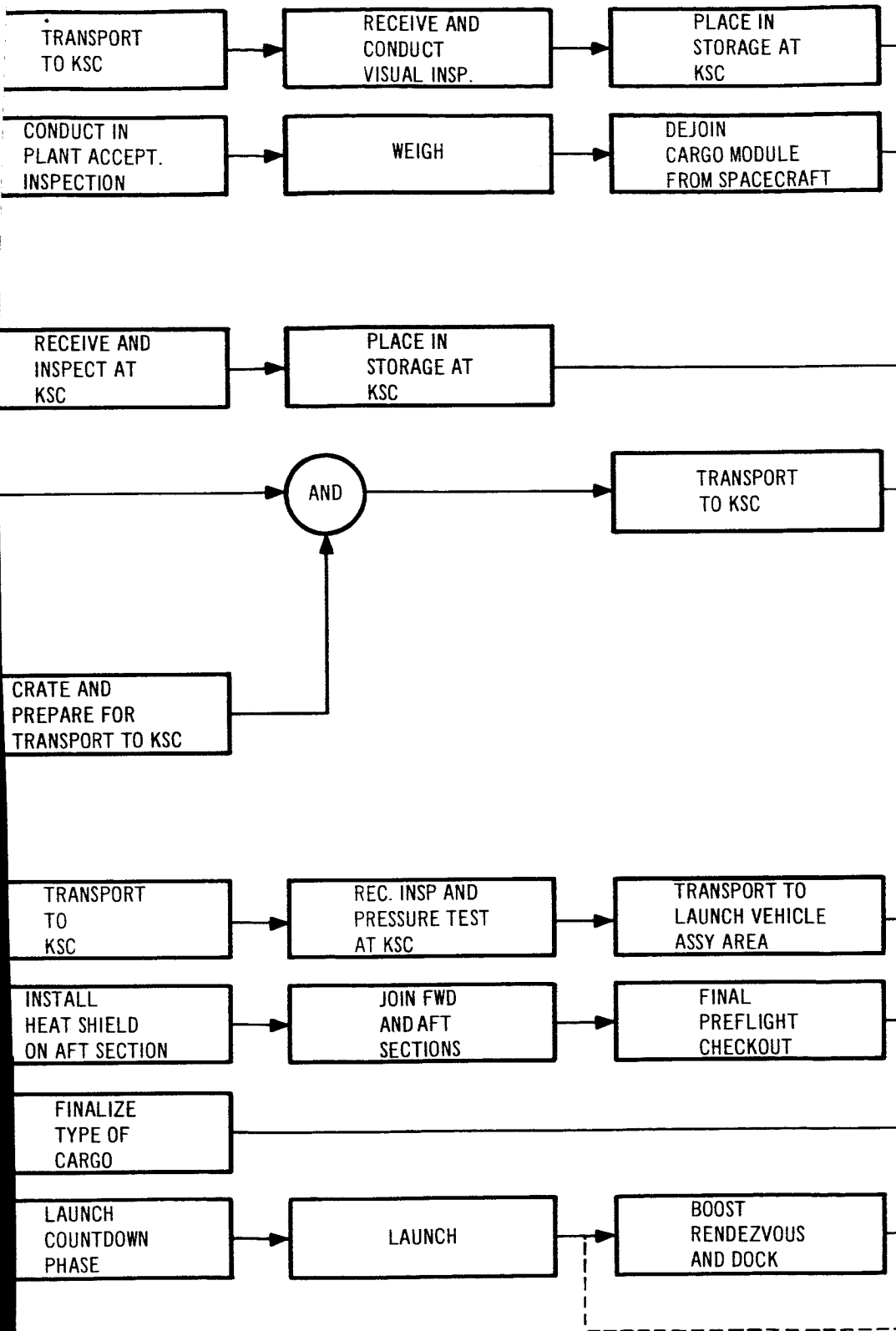
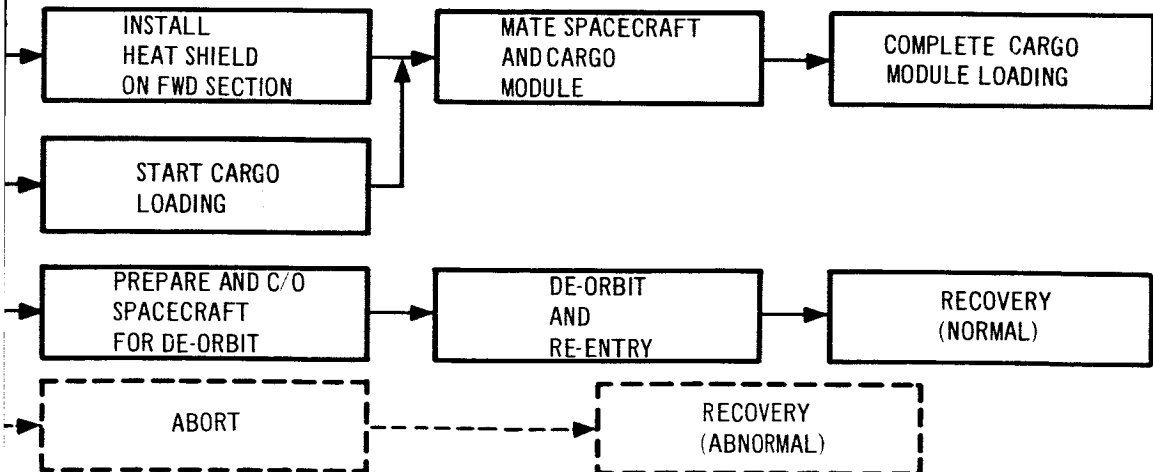
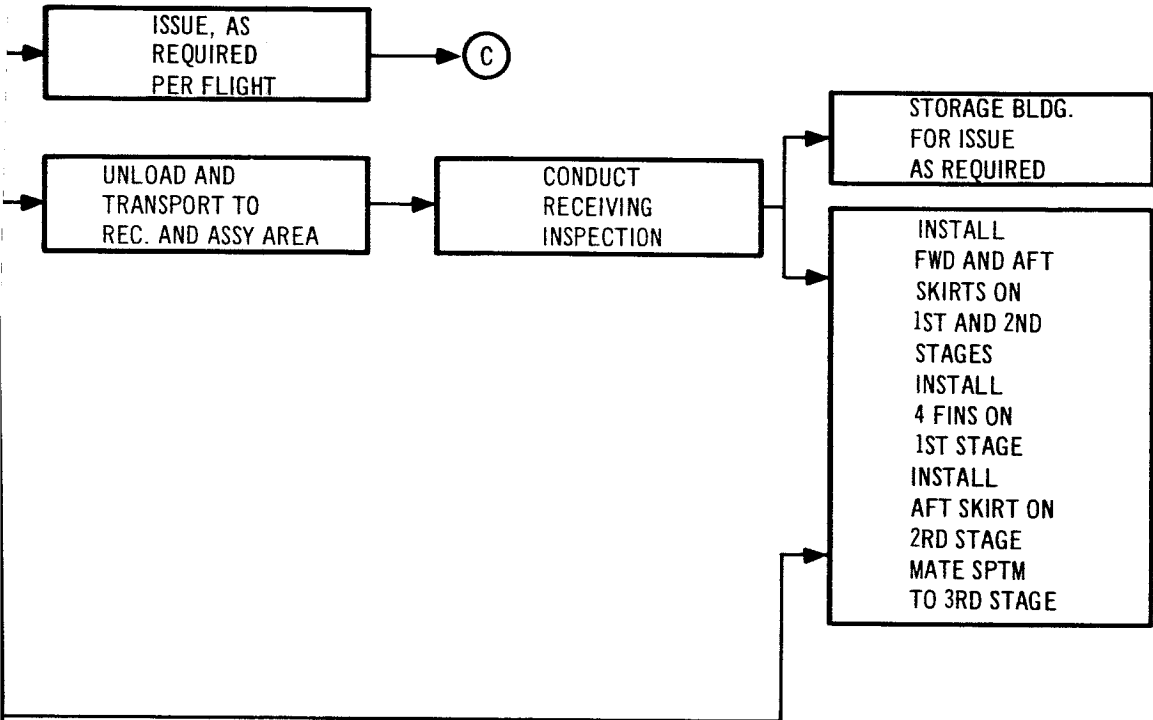
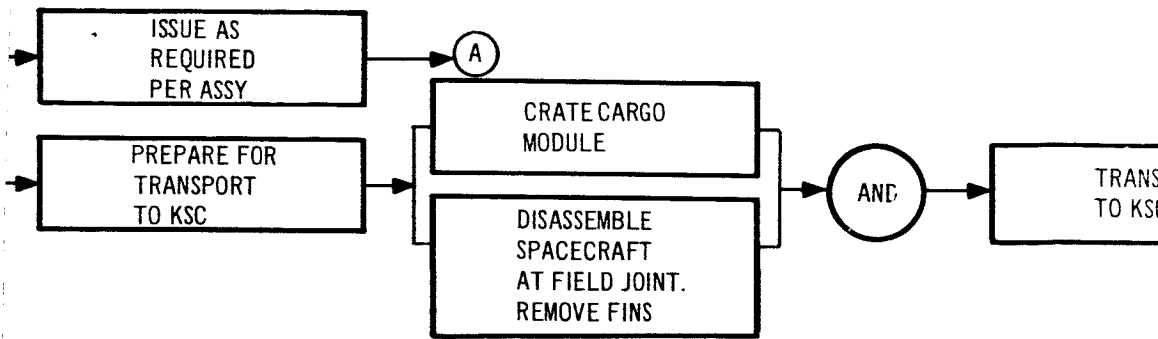
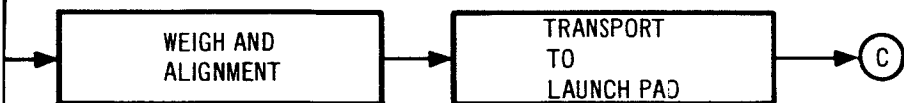
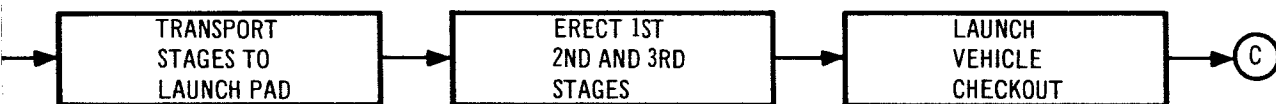


Figure 3-61. Configuration I Spacecraft/Adapter and Launch Vehicle Master Flow Chart







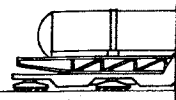
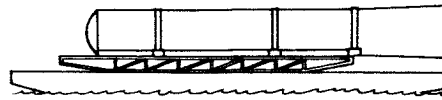
124-4

TYP ALL  
STAGES

BARGE

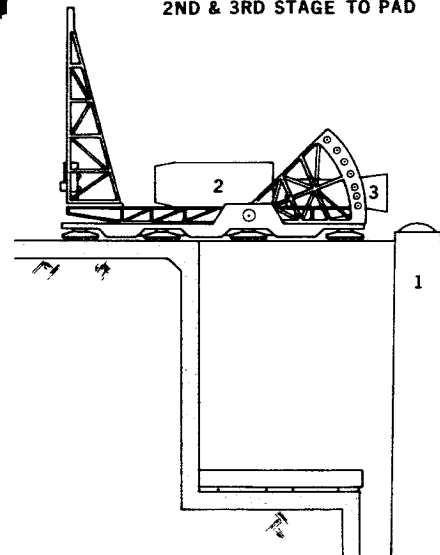
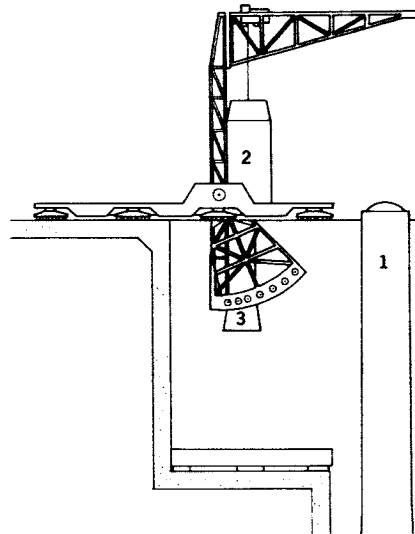
TR

SUPPLY



ERECTION

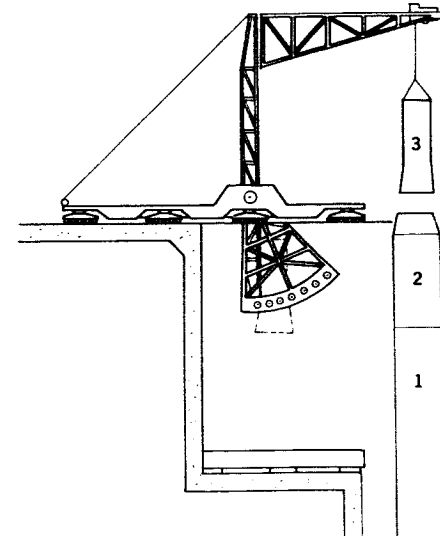
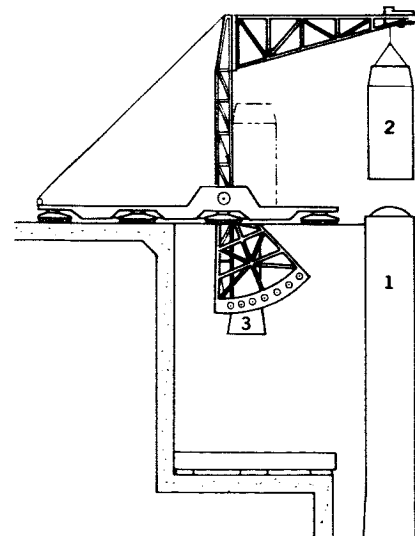
2ND & 3RD STAGE TO PAD



PAD  
OPERATIONS

2ND STAGE ASSEMBLY

3RD STAGE ASSEMBLY



TRANSPORTER

STORAGE

TRANSPORTER

ACTIVATION

POSITIONING

ERECTION

2ND AND  
3RD STAGE

SLOT TYPICAL  
ALL VIEWS

SPACECRAFT AND ADAPTOR

ERECTION

PAYLOAD  
AND  
ADAPTOR

3

2

1

3

2

1



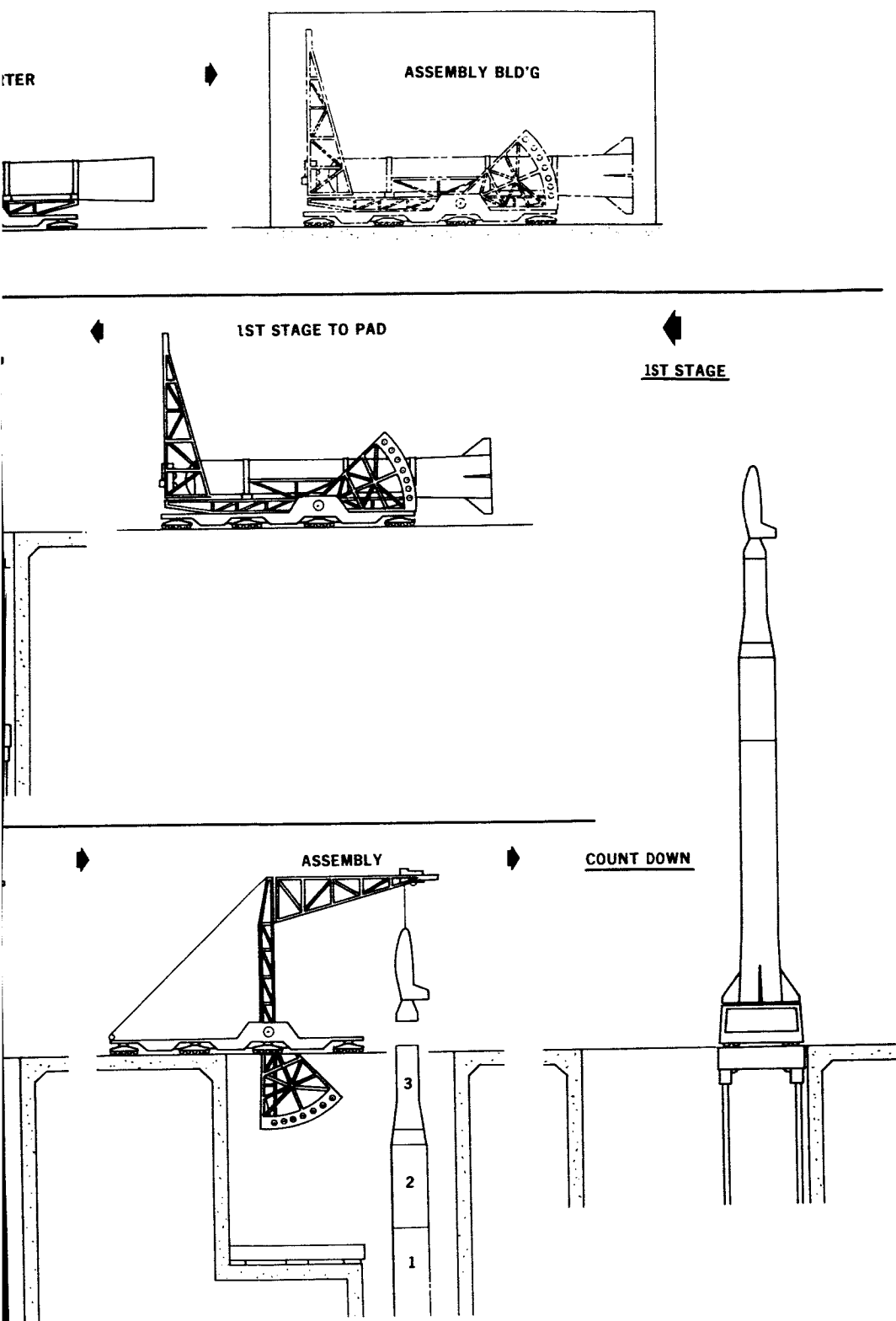


Figure 3-62. Conceptual Ground Handling Plan – Configuration I Space System

checkout to the launch complex. The transporter is fitted with a structural pivot bearing and the cradle with a pivot shaft. Upon alignment with the silo opening, the load bearing wheels on the end of the cradle are in position to drop into a slot which is cast into the side of the silo. Part of the load of the motor is then progressively transferred from the end of the cradle to the side of the silo as the cradle rotates the stage to an upright position.

When a vertical position is reached on the first-stage erection, a roll-ramp actuated platform is moved up to mate with the lower end of the aft skirt assembly. Mounted to this platform is the blast deflection pedestal which actually carries the vehicle load to the platform. The roll-ramp platform on the right hand side of the pit is then aligned with the left-hand platform and the stage is translated by rail to the right-hand platform after release from the shipping cradle. The cradle is then rotated back to the horizontal location and removed to the solid motor building via the transporter.

The same shipping cradle can transport both the second and third stages together utilizing a different set of mounting points. This is also shown in Figure 3-62. A boom-truss arrangement with a trolley hoist is attached to the cradle at this time. When alignment at the silo is accomplished, the two stages are rotated into a vertical position in the same manner as the first stage. The upper of the two stages, the second stage, is positioned over the first stage and mating operations are accomplished. Similarly, the third stage is hoisted and translated into a mating position with the second stage. At this point, the launch vehicle receives an intermediate checkout after which it is ready to receive the spacecraft and cargo module adapter.

The foregoing steps are time phased as shown in Figure 3-63. The projected pad occupancy time up to the mating of the spacecraft is 14 days. The time phasing of the second and third stages as shown in this figure would have to be adjusted to accept the transporting concept shown in Figure 3-62.

The projected man-hour requirements are presented in Table 3-14. They total 20,456 hours.

checkout to the launch complex. The transporter is fitted with a structural pivot bearing and the cradle with a pivot shaft. Upon alignment with the silo opening, the load bearing wheels on the end of the cradle are in position to drop into a slot which is cast into the side of the silo. Part of the load of the motor is then progressively transferred from the end of the cradle to the side of the silo as the cradle rotates the stage to an upright position.

When a vertical position is reached on the first-stage erection, a roll-ramp actuated platform is moved up to mate with the lower end of the aft skirt assembly. Mounted to this platform is the blast deflection pedestal which actually carries the vehicle load to the platform. The roll-ramp platform on the right hand side of the pit is then aligned with the left-hand platform and the stage is translated by rail to the right-hand platform after release from the shipping cradle. The cradle is then rotated back to the horizontal location and removed to the solid motor building via the transporter.

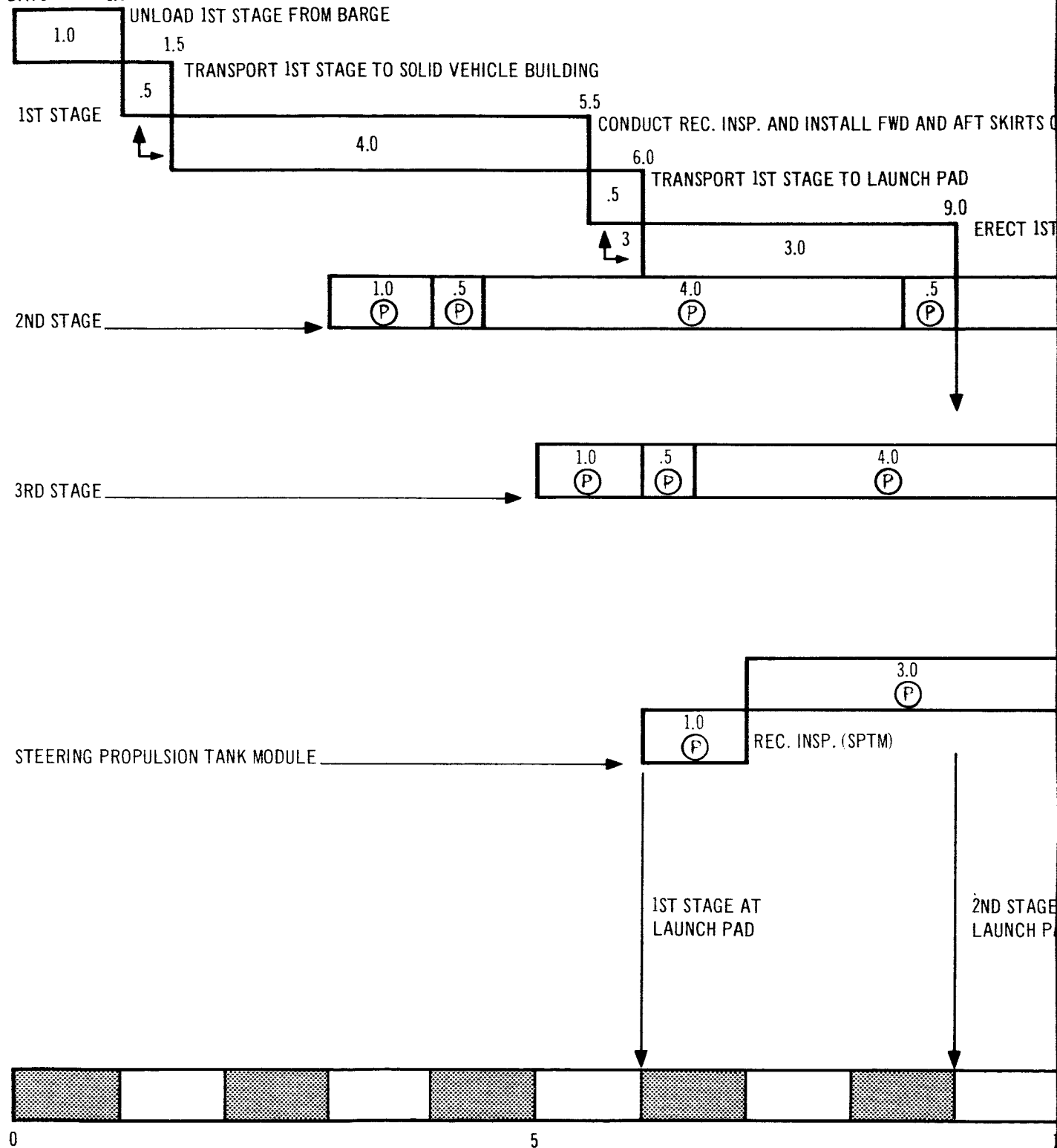
The same shipping cradle can transport both the second and third stages together utilizing a different set of mounting points. This is also shown in Figure 3-62. A boom-truss arrangement with a trolley hoist is attached to the cradle at this time. When alignment at the silo is accomplished, the two stages are rotated into a vertical position in the same manner as the first stage. The upper of the two stages, the second stage, is positioned over the first stage and mating operations are accomplished. Similarly, the third stage is hoisted and translated into a mating position with the second stage. At this point, the launch vehicle receives an intermediate checkout after which it is ready to receive the spacecraft and cargo module adapter.

The foregoing steps are time phased as shown in Figure 3-63. The projected pad occupancy time up to the mating of the spacecraft is 14 days. The time phasing of the second and third stages as shown in this figure would have to be adjusted to accept the transporting concept shown in Figure 3-62.

The projected man-hour requirements are presented in Table 3-14. They total 20,456 hours.

ACCUM.

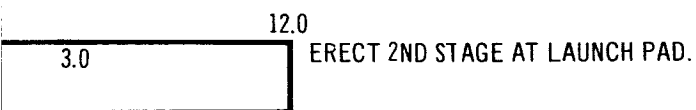
DAYS → 1.0



127-1

ON 1ST STAGE AND INSTALL (4) FINS ON AFT SKIRT

STAGE AT LAUNCH PAD.



12.0

NOTE:

TIME SHOWN AND EVENTS FOR  
1ST STAGE PREPARATION PRIOR TO  
ERECTING IS TYPICAL FOR  
2ND AND 3RD STAGES.

(P) = PARALLEL OPERATIONS

↑ = SCHEDULED 2 SHIFTS 8 HRS/DAY

↑3 = MAY REQUIRE UNSCHEDULED  
3RD SHIFT

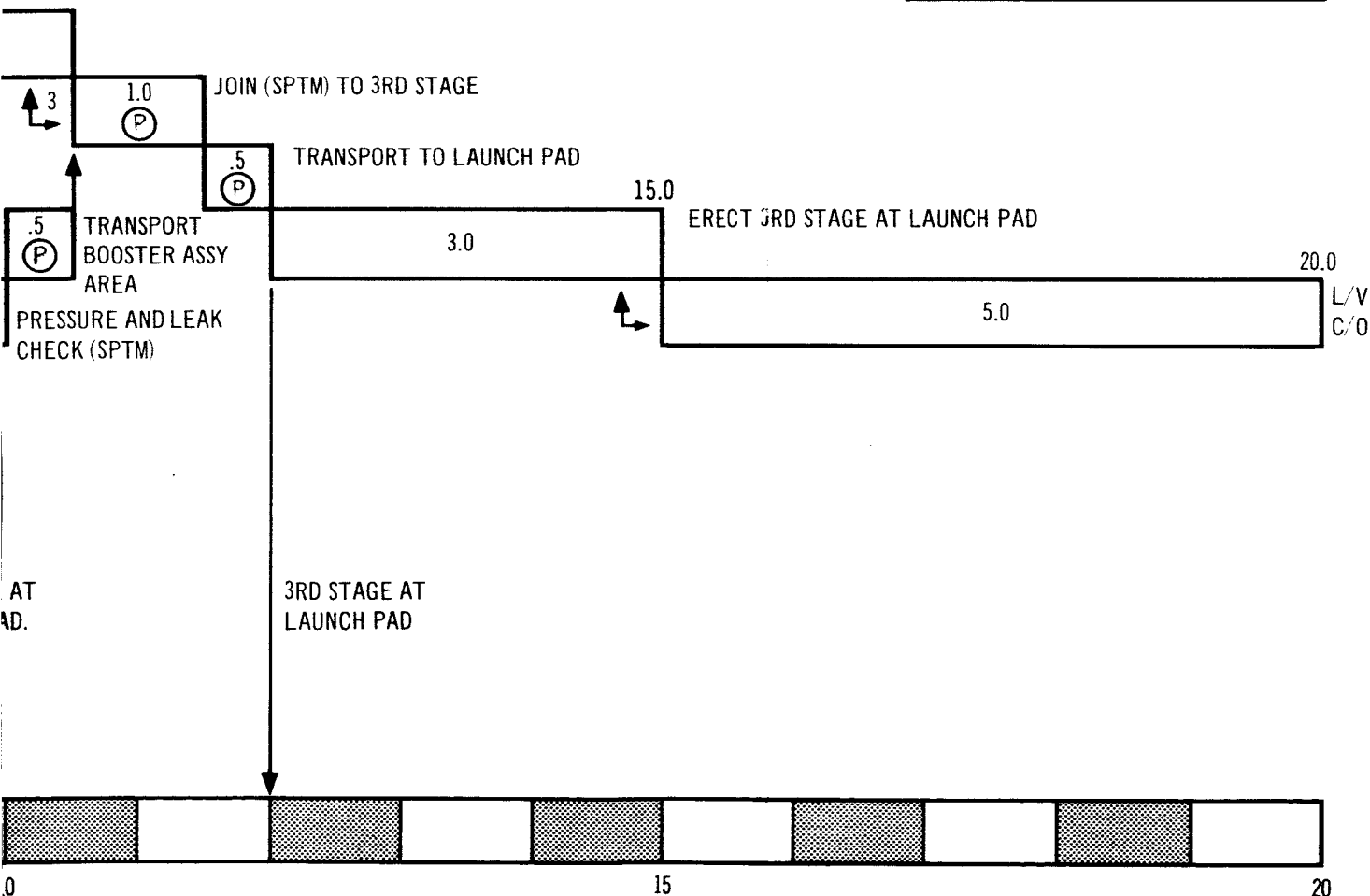


Figure 3-63. Launch Vehicle Processing Time (Days)

Table 3-14  
HOURS AND PERSONNEL REQUIRED FOR  
LAUNCH-VEHICLE PREPARATION

Event	Number of Men	Hour Per Operation	Subtotal Hours
Unloading 1st, 2nd and 3rd stages	50	800	2,400
Transport stages from barge to booster receiving and assembly area	30	120	360
Conduct receiving inspection and install forward and aft skirts on stages	30	1,920	5,760
Transport stages to launch pad	30	120	360
Erect 1st stage and attach (4) fins	50	2,896	2,896
Erect 2nd and 3rd stages	50	2,800	5,600
Receive inspect steering propulsion tank module (SPTM)	10	80	80
Test (SPTM)	10	240	240
Transport (SPTM) to booster assembly area	10	40	40
Join (SPTM) to 3rd stage	20	320	320
Complete booster checkout at launch pad	50	2,400	<u>2,400</u>
Total hours			20,456

### Spacecraft

The spacecraft is received at Cape Kennedy in two major sections. The conceptual configuration for shipment is also characterized by the absence of any of the heat shield panels on the new spacecraft. These are assembled after a particular status in field station checkout has been achieved and is discussed in more detail in the following sections.

New Spacecraft -- The sequence of events and elapsed time requirements for processing a new spacecraft are shown in Figure 3-64. These tasks include a full static-firing checkout of the engines which is accomplished at a time prior to joining the fore and aft sections.

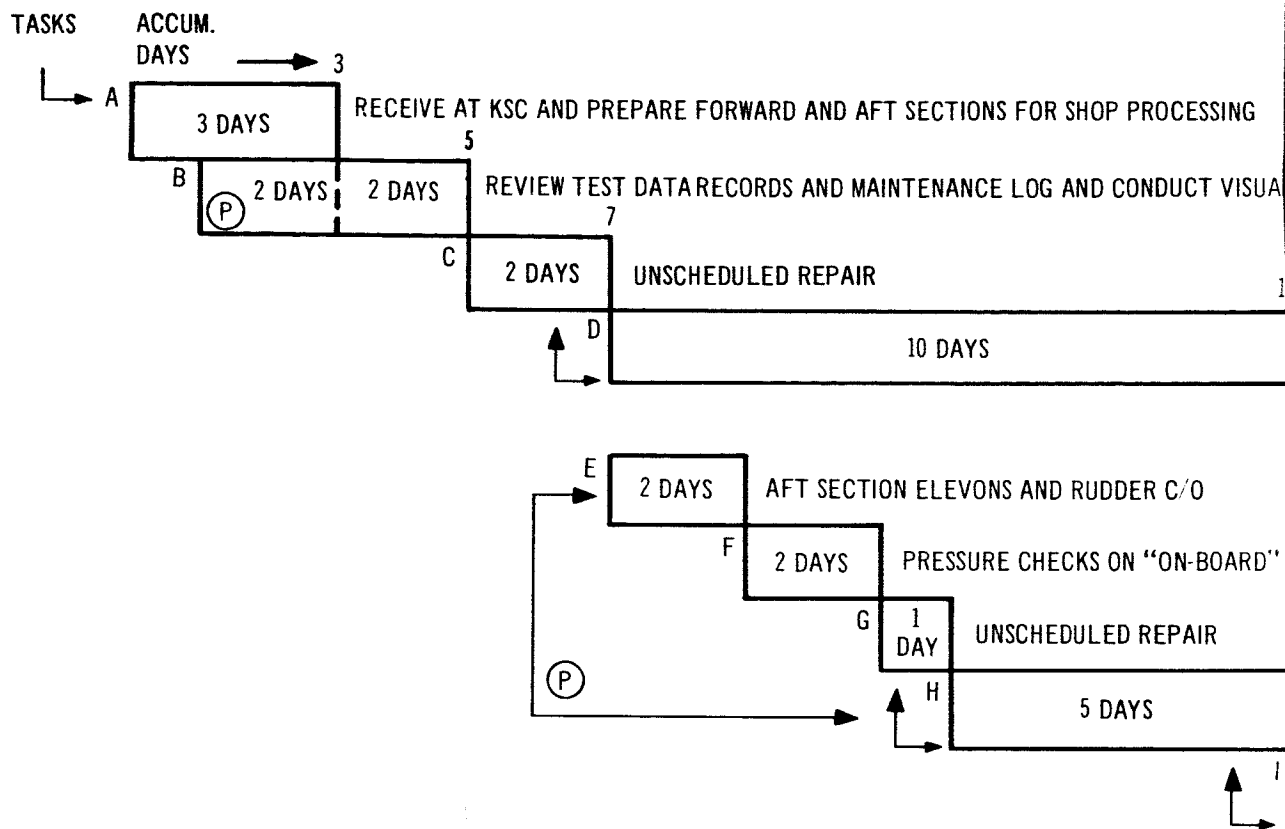
An examination of the time required for a procedure wherein the static firing of the engines is accomplished after joining the fore and aft sections showed that an additional two days would be required. There would be the advantage, however, of using the forward section propellant tanks and the full-feed system in this procedure.

Comparison of the elapsed-time requirements for the spacecraft with those of the launch vehicle clearly shows the spacecraft to be the pacing operation. The total time from receipt at Cape Kennedy to the point where the spacecraft is ready for mating to the launch vehicle is 39.5 days.

In this concept, the cargo module adapter carries the consumable supplies, that is, those demanded by the space station on a regular basis. These are loaded and the module is balanced before mating to the spacecraft. The cargo carried internally to the spacecraft is loaded according to a weight and balance schedule after the spacecraft is mounted on the launch vehicle. This has the advantage of keeping a certain fraction of the cargo flexible right up to the final countdown.

A summary of the man-hour requirements for each task is shown in Table 3-15. The total number of personnel for each task is also listed in this table.

Used Spacecraft -- The projected tasks associated with bringing a used spacecraft to a flight-readiness condition are shown in Figure 3-65. Many of these tasks it will be noted are the same as for a new spacecraft. The tasks which are uniquely refurbishment are called out as such in the figure. Because of scheduling advantages related to the integration of refurbishment tasks with the normal preflight processing tasks, the concept of a unified refurbishment site and launch-site physical location was adapted for this study. Another significant advantage of this concept is the shortened logistic path from recovery site to launch site thereby minimizing the receiving inspections and handling damage.



LEGEND:

(P) = PARALLEL TASK OPERATION.

↑ = SCHEDULED 2 SHIFTS (8 HRS/DAY)

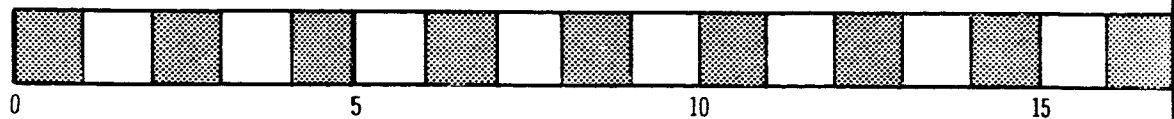


Figure 3-64. New Spacecraft Processing Time (Days)



L INSPECTION

FORWARD SECTION PREFLIGHT C/O  
END-TO-END SUB SYSTEM TESTING AND UNSCHEDULED REPAIR

PROPULSION SYSTEM

INSTALL ABLATIVE HEAT SHIELD PANELS, FINS AND ELEVONS  
ON AFT SECTION

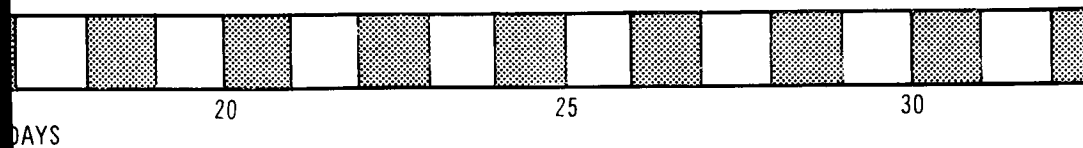
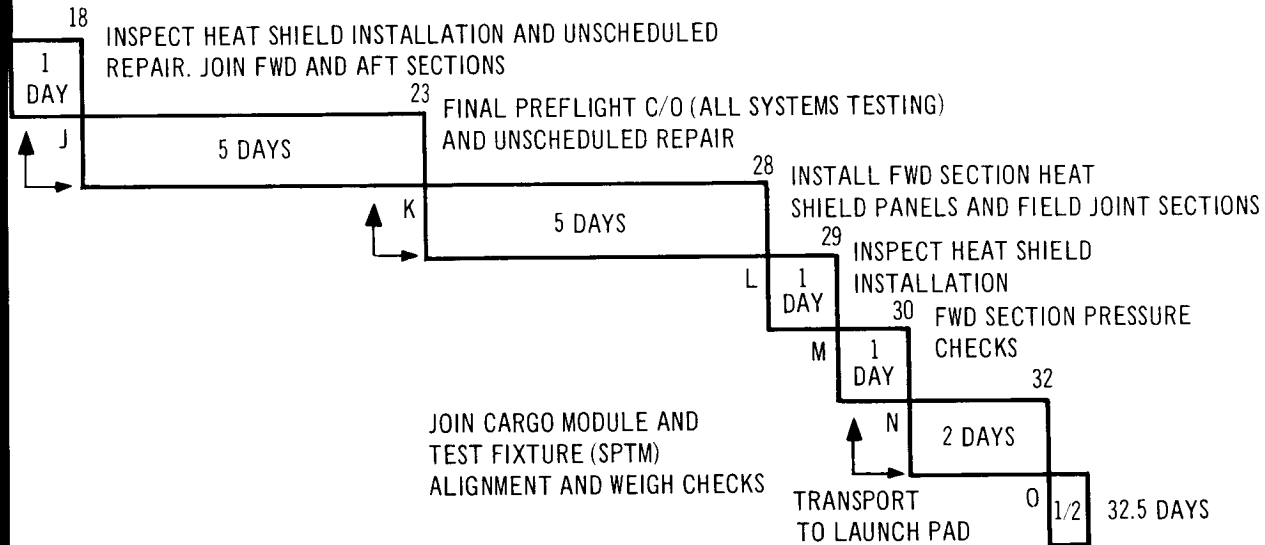
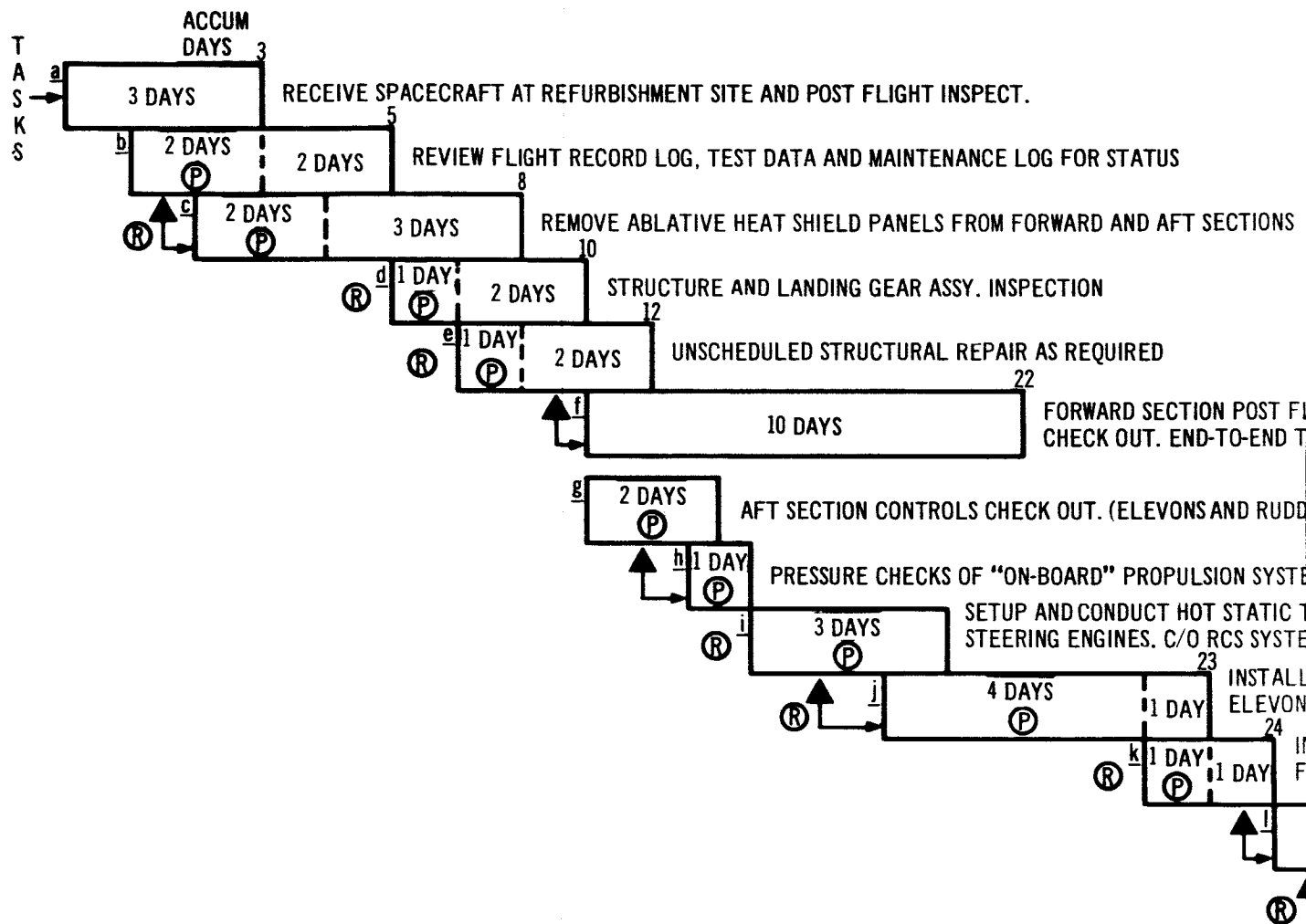


Table 3-15  
MAN-HOURS REQUIRED TO ACCOMPLISH NEW  
SPACECRAFT PROCESSING

Tasks*	Number of Men	Hours
A	30	720
B	30	960
C	10	160
D	120	9,600 (60 M/Shift) 2 shifts
E	15	240
F	10	160
G	10	80
H	35	2,800
I	10	160
J	60	2,400 (30 M/Shift)
K	35	2,800
L	6	48
M	10	80
N	40	640 (20 M/Shift)
O	30	120
Total Hours:		20,968

\*Refer to Figure 3-64 for task descriptions.

Additional data on refurbishment costs, as differentiated from costs which are common to the processing of new spacecraft, are discussed further in Section 3.2.2.



LEGEND:

Ⓟ = PARALLEL OPERATION.

Ⓡ = REFURBISHMENT TASKS

▲ = SCHEDULED TWO(2) SHIFTS/WORK DAY. (8 HR SHIFTS)

Figure 3-65 Used Spacecraft Processing Schedule

39 1/2 DAYS

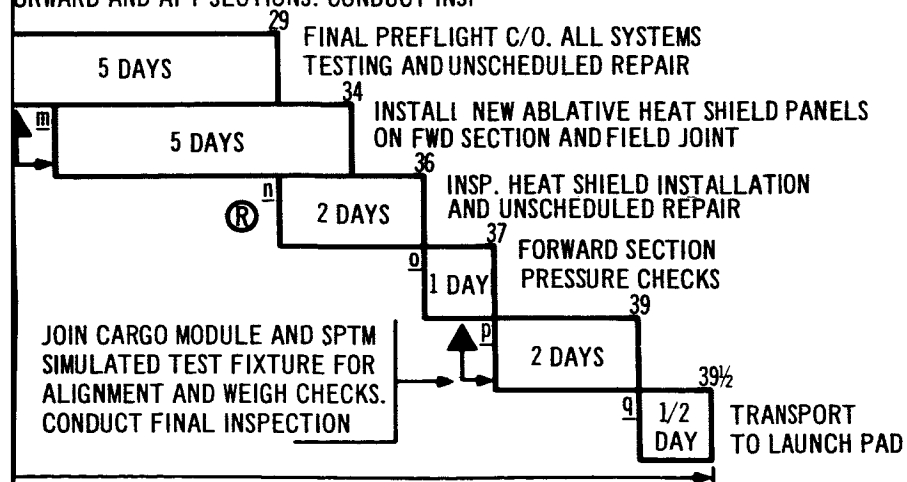
LIGHT SUB SYSTEMS  
TYPE TESTING

ER).

EM  
TEST FIRING OF AFT SECTION  
M

NEW ABLATIVE HEAT SHIELD PANELS AND  
AND RUDDER ASSY ON AFT SECTION

INSTALL NEW LANDING GEAR SKIDS AND JOIN  
FORWARD AND AFT SECTIONS. CONDUCT INSP



132-2

The time phasing of tasks shown in Figure 3-65 and the man-hour requirements presented in Section 3.2.2 both reflect a basic underlying design philosophy assumed in the conceptual procedures. This philosophy is very similar to, and benefits from, the experience that NASA has obtained with the X-15 aircraft. This philosophy is characterized by several basic precepts which are (1) design for long critical life in subsystem components; (2) design subsystems for self check capability requiring no removal; and (3) design for a scheduled maintenance plan that makes maximum use of (1) and (2) above.

#### 3.2.1.3 Prelaunch and Launch Phase

The prelaunch phase covers that period after mating of the spacecraft and cargo module-adaptor to the launch vehicle and includes the all-systems checks that are made to confirm the flight readiness of the vehicle. This schedule is shown in Figure 3-66. Installation of ordnance items is accomplished in this period. It is estimated that a total of 13 days is required for these procedures.

Also shown in Figure 3-66 are the scheduled steps required in the final countdown. Currently-known requirements indicate that a 14-hour period is sufficient to cover all necessary steps. The concept of checkout employed for the Configuration I vehicle provides for a checkout crew to be onboard the spacecraft performing many of the checks normally accomplished in the blockhouse for current systems. The flight crew enters the spacecraft at about T-5 hours and takes over the remaining checkout tasks.

The number of personnel and the man-hour requirements are summarized in Table 3-16 for both prelaunch and countdown phases. The total calendar days required for pad occupancy is 32, compared to a projected Saturn IB requirement of 48 days in the 1969 time period.

#### 3.2.1.4 Spacecraft Recovery

This aspect of the use-cycle of the Configuration I spacecraft was confined to an investigation of the number of recovery sites required and the cost of these sites. The number of recovery sites required is a function of the inclination of the orbit from which the spacecraft is recovered, the maximum permissible wait time in orbit before deorbit is required, the orbital altitude, and the cross-range capability of the re-entering spacecraft.

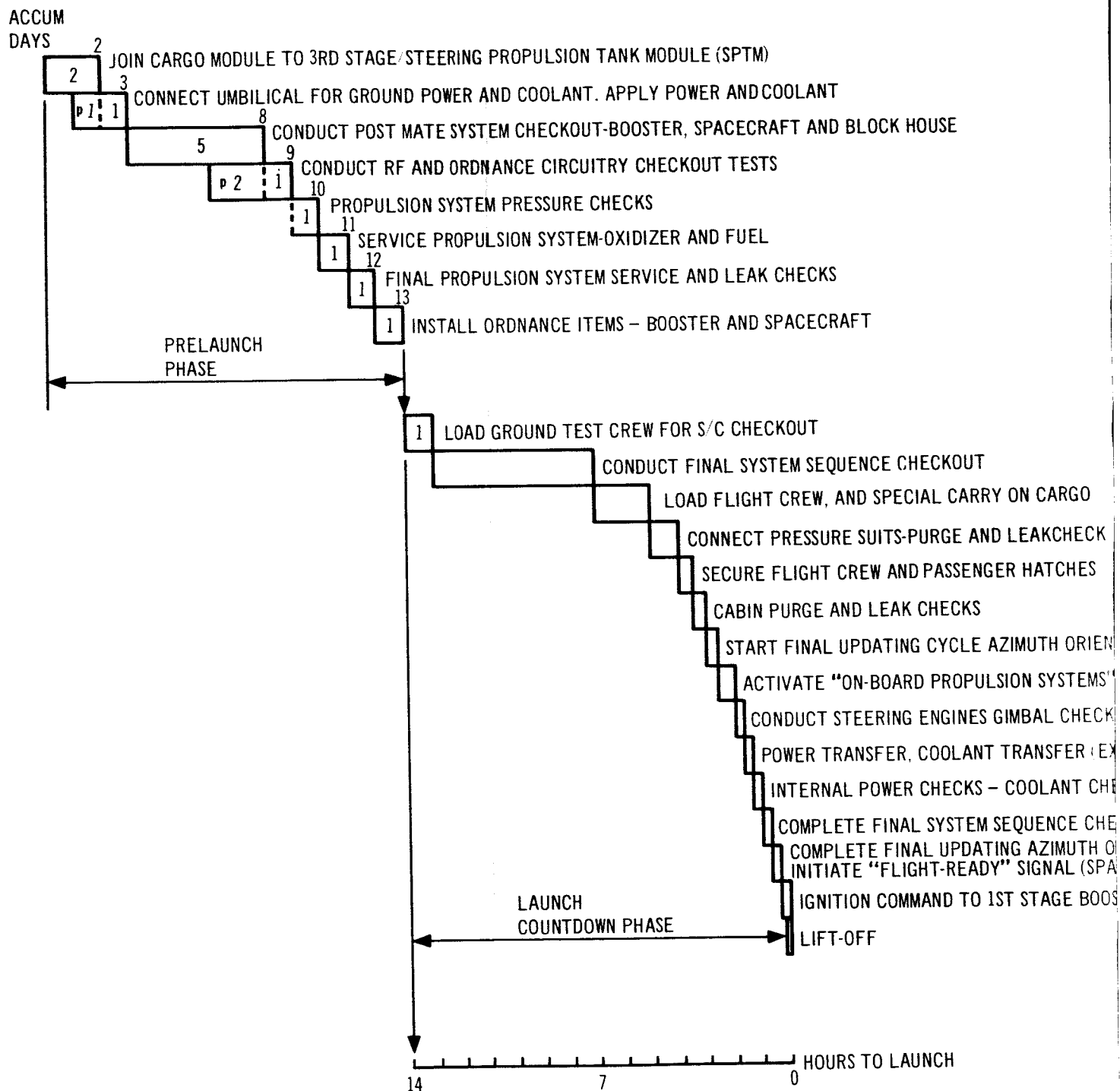


Figure 3-66. Configuration I - Prelaunch and Launch Countdown Phases

- 
- NOTES: 1. PRELAUNCH PHASE BEGINS  
WITH THE ARRIVAL OF THE  
SPACECRAFT AT THE LAUNCH  
PAD. BOOSTER IS IN PLACE,  
CHECKED OUT AND READY FOR  
SPACECRAFT JOINING.
2. LAUNCH COUNTDOWN PHASE  
BEGINS WHEN TEST CREW  
ENTERS SPACECRAFT.
3. PRELAUNCH PHASE ELAPSED  
TIME IS SHOWN IN DAYS  
LAUNCH COUNTDOWN PHASE  
ELAPSED TIME IS SHOWN IN  
HOURS
4. PARALLEL OPERATIONS  
ARE INDICATED BY P

TATION DATA

- START STEERING ENGINES

S

INTERNAL SUPPLY TO INTERNAL SOURCE)

ECKS

CKOUT VERIFYING INTERNAL OPERATION

RIENTATION INPUT DATA.

SPACECRAFT TO BLOCKHOUSE)

TER ABORT DETECTION SYSTEM ACTIVATED

The time phasing of tasks shown in Figure 3-65 and the man-hour requirements presented in Section 3.2.2 both reflect a basic underlying design philosophy assumed in the conceptual procedures. This philosophy is very similar to, and benefits from, the experience that NASA has obtained with the X-15 aircraft. This philosophy is characterized by several basic precepts which are (1) design for long critical life in subsystem components; (2) design subsystems for self check capability requiring no removal; and (3) design for a scheduled maintenance plan that makes maximum use of (1) and (2) above.

#### 3.2.1.3 Prelaunch and Launch Phase

The prelaunch phase covers that period after mating of the spacecraft and cargo module-adaptor to the launch vehicle and includes the all-systems checks that are made to confirm the flight readiness of the vehicle. This schedule is shown in Figure 3-66. Installation of ordnance items is accomplished in this period. It is estimated that a total of 13 days is required for these procedures.

Also shown in Figure 3-66 are the scheduled steps required in the final count-down. Currently-known requirements indicate that a 14-hour period is sufficient to cover all necessary steps. The concept of checkout employed for the Configuration I vehicle provides for a checkout crew to be onboard the spacecraft performing many of the checks normally accomplished in the blockhouse for current systems. The flight crew enters the spacecraft at about T-5 hours and takes over the remaining checkout tasks.

The number of personnel and the man-hour requirements are summarized in Table 3-16 for both prelaunch and countdown phases. The total calendar days required for pad occupancy is 32, compared to a projected Saturn IB requirement of 48 days in the 1969 time period.

#### 3.2.1.4 Spacecraft Recovery

This aspect of the use-cycle of the Configuration I spacecraft was confined to an investigation of the number of recovery sites required and the cost of these sites. The number of recovery sites required is a function of the inclination of the orbit from which the spacecraft is recovered, the maximum permissible wait time in orbit before deorbit is required, the orbital altitude, and the cross-range capability of the re-entering spacecraft.



Table 3-16  
HOURS REQUIRED DURING PRELAUNCH AND  
LAUNCH COUNTDOWN PHASES

Prelaunch phase tasks	Total Hours	Total Personnel
a. Mate spacecraft to booster	1,600	50
b. Connect umbilical (power and cool)	386	12
c. Post mate system checkout	4,000	50
d. RF and ordnance checks	960	20
e. Propulsion pressure checks	80	5
f. Service propulsion	480	30
g. Final propulsion system service	80	5
h. Install ordnance items	320	20
i. Blockhouse requirements	<u>6,240</u>	<u>30</u>
	14,146	222
Launch countdown phase hours (T-14 Hours)	<u>35,000</u>	2,500 personnel
Combined Total	49,146	

Assumptions:

1. Prelaunch phase is scheduled 2 shifts of 8 hours per day.
2. Tracking and range safety personnel are approximated at 1/4 of Gemini flights supporting personnel for the launch countdown phase.
3. Launch countdown phase starts at T-14 hours and has scheduled built-in holds of 1.5 hours.

Determination of this type of information was the objective of a study recently completed for NASA, Reference 4, and served as the basis for the recovery data used in this study. These data are summarized in Table 3-17 for orbital inclinations of 30, 57, and 90°, for an orbital wait time not to exceed 24 hours, and for spacecraft with re-entry cross-range capability of Configuration I, 600 nmi

Table 3-17  
CONFIGURATION I RECOVERY REQUIREMENTS

Cross-range capability = 600 nmi			Max. wait time before deorbit = 24 hours
Orbital altitude = 250 nmi			Primary landing site location = Z.I. plus daylight alternate
Orbital inclination (deg)	30	55	90
Number of recovery sites (normal operation)	3	4	4
Primary	2	2	2
Secondary	1	2	2
Number of ships (boost abort)	8	4	6
Number of ships (launch site abort)	0	0	0
Number of helicopters (launch site abort)	5	5	5
Rescue aircraft	3	3	3

Airfields were chosen in the zone of interior and were classified according to primary and secondary sites according to whether all-weather landing aids were made available or only daylight capabilities were provided. Airfields were also selected from a survey of existing sites having runway lengths equal to or greater than 8,000 ft.

For reasonable mission flexibility, it was concluded that refurbishment sites should not be located at the recovery sites since this could entail at least two and probably four sites.

The recovery site costs are presented in Table 3-18. These costs are also from Reference 1 and represent additional costs required to provide the unique facilities associated with this type of operation. As discussed previously, airfield site locations were chosen from a survey of existing airfields.

At the recovery site, the principal functions are shown in Figure 3-67. These events are based on normal operations. The phasing of these functions, together with some alternate handling procedures, are indicated in Figure 3-68. Basically, however, the major steps involve a crew debriefing, a post-flight inspection, posting of the vehicle's maintenance log, and disassembly and preparation for shipping. Shipping techniques are discussed in Section 3.2.1.1.

### 3.2.2 Refurbishment Analysis

The objectives of the refurbishment analysis were to identify major refurbishment tasks, to perform a first-order evaluation of the time required, and to project a first-order cost involved in these tasks.

The approach used in the accomplishment of these objectives was to define a refurbishment cost model to the level of major subsystems and, through the use of a set of refurbishment task assumptions, arrive at the cost of refurbishment and the time required. The assumptions used will, of course, imply a basic design philosophy which is discussed in a summarization of the refurbishment study results.

Table 3-18  
CONFIGURATION I RECOVERY OPERATIONS COSTS

(All Costs in Millions of Dollars)			
			Max. wait time before deorbit = 24 hour
			Flight frequency = 10/year
Cross-range capability = 600 nmi			
Orbital altitude = 250 nmi			
Orbital inclination (deg)	30	55	90
Operations cost, total	(0.9984)	(0.7251)	(0.9156)
Return from orbit	0.2892	0.3599	0.3784
Boost abort	0.6880	0.3440	0.5160
Launch site abort	0.0050	0.0050	0.0050
Air-sea rescue service	0.0162	0.0162	0.0162

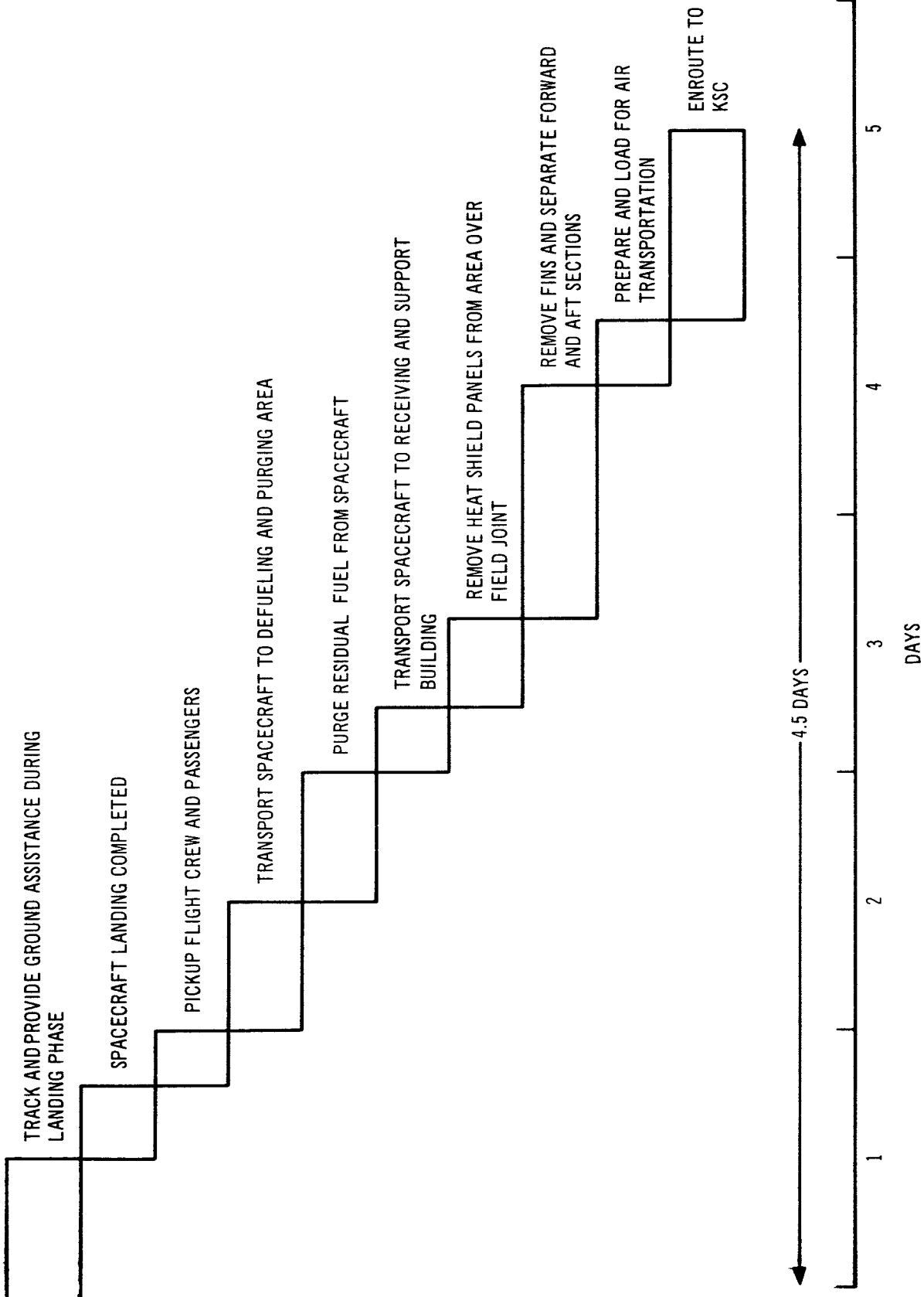


Figure 3-67. Recovery Site Key Sequence Time

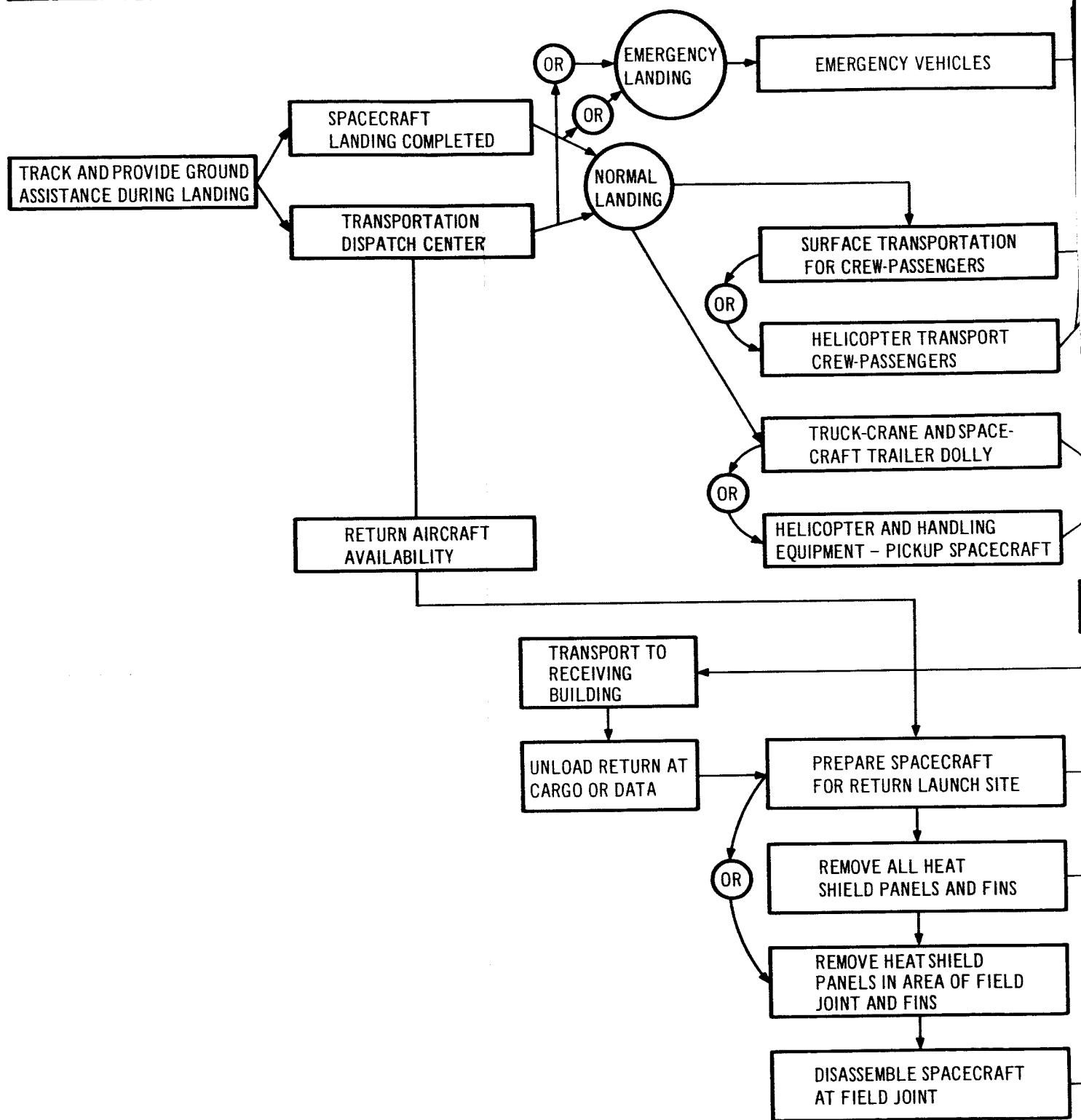
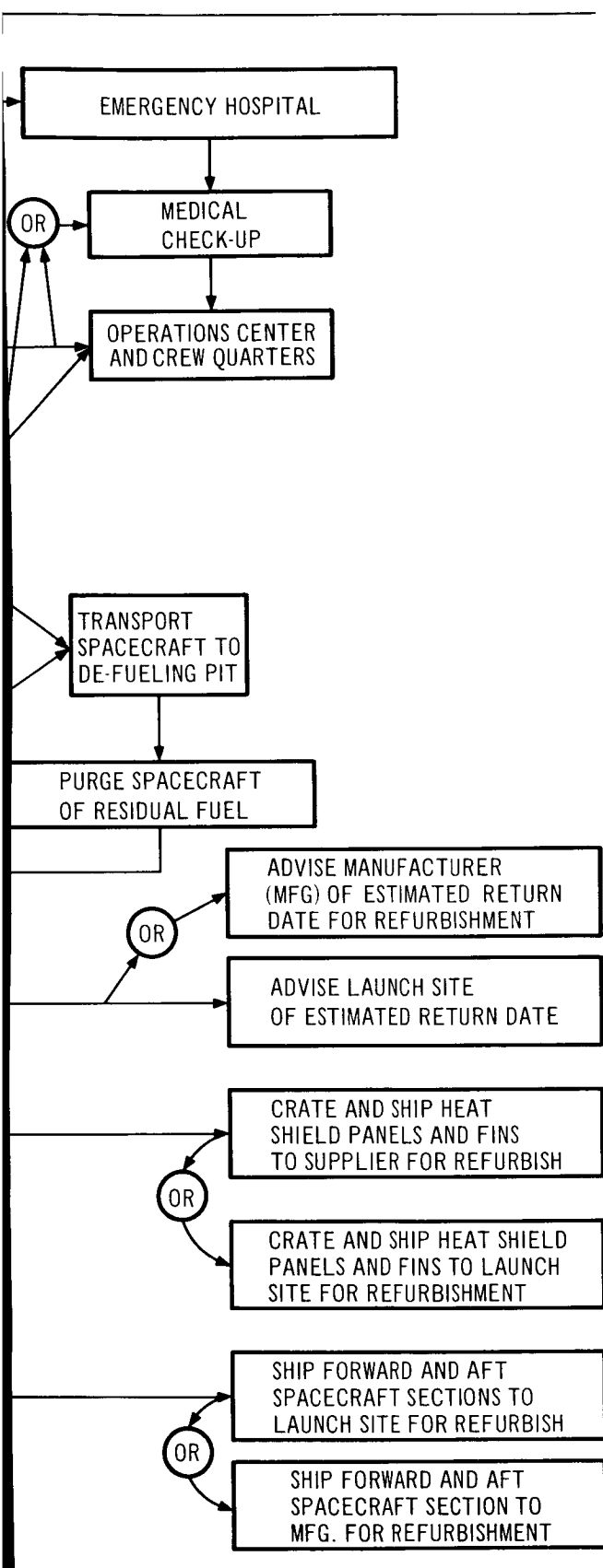


Figure 3-68. Recovery Site Events and Detail Operations-Configuration I Spacecraft



140-2

### 3.2.2.1 The Refurbishment Model

The key events involved in refurbishment of the Configuration I spacecraft are shown in Figure 3-69. Alternate paths indicate procedures available when system components fail to pass a particular test. Specific components, such as the landing gear skids and heat shield panels, are replaced after each flight. A live firing of the engines is scheduled after each flight. An assumed level of spares is included to replace time-life-limited items and as a backup for items that fail to pass critical checks. The model assumes no scheduled removal of subsystems except as previously noted.

### 3.2.2.2 The Refurbishment Schedule

The schedule of refurbishment tasks has been shown previously in Figure 3-65 for the environment of the normal processing tasks required of any vehicle, new or used. It will be noted that the total time for processing a used vehicle is only seven and one-half days longer than for a new vehicle (Figure 3-64). For instance, the removal of the exposed heat shield is unique to the used vehicle but the installation of new panels is common to both new and used vehicles.

### 3.2.2.3 Cost Assumptions

The cost assumptions are as follows and are consistent with costing guidelines used to project planning-type cost estimates for the hardware procurement of the entire Configuration I program:

1. Labor rates at \$20/hour.
2. Heat shield panel costs at \$840/ft<sup>2</sup> (all ablative, with fiberglass structure).
3. Quantity of panels based on wetted areas of spacecraft plus 10%.
4. Subsystem spares at 25%/year of total subsystem procurement.
5. Unscheduled structural repair at 5% of primary structure cost.
6. A 5-year program with 4 spacecraft and a total of 46 refurbishments.

### 3.2.2.4 Refurbishment Costs

The application of the costing assumptions to the refurbishment model, the Configuration I vehicle characteristics, and the projected refurbishment schedule resulted in the refurbishment cost breakdown shown in Table 3-19.



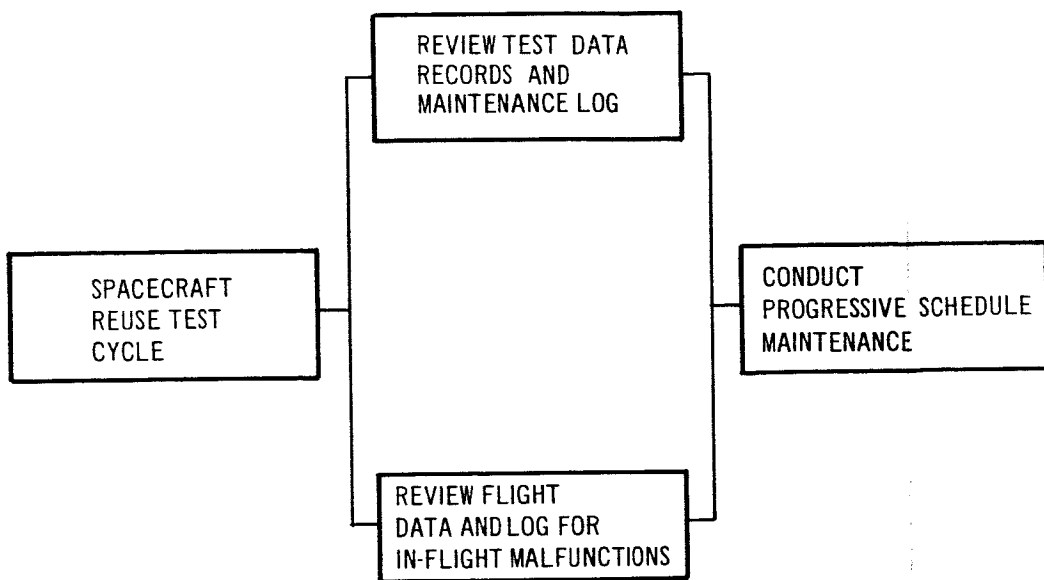
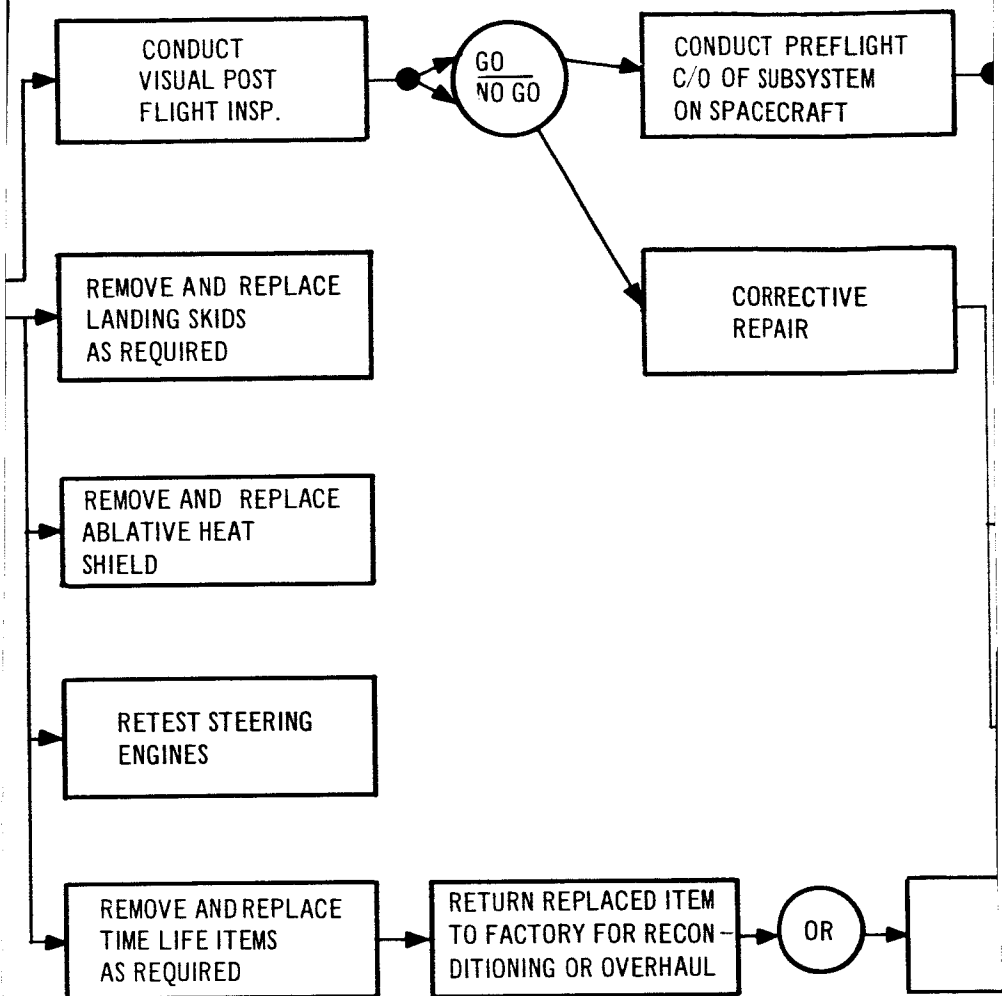
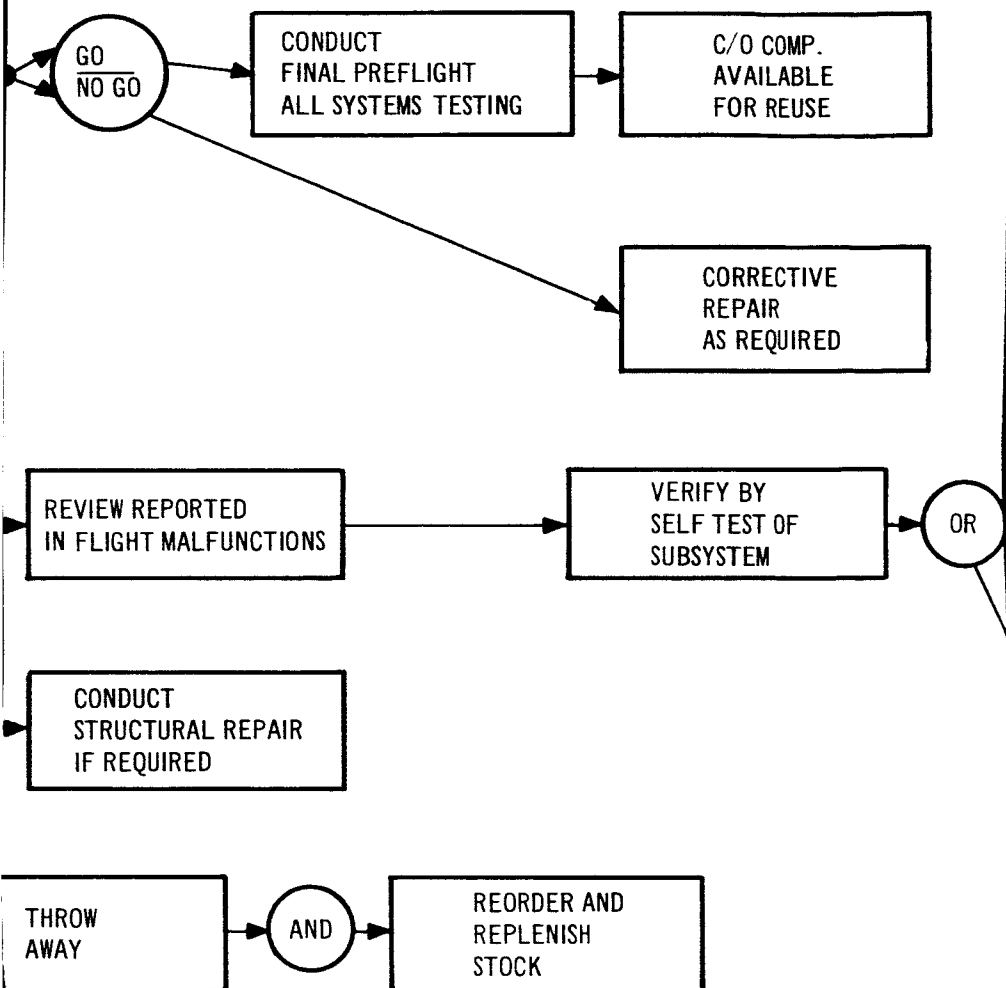


Figure 3-69. Refurbishment Model





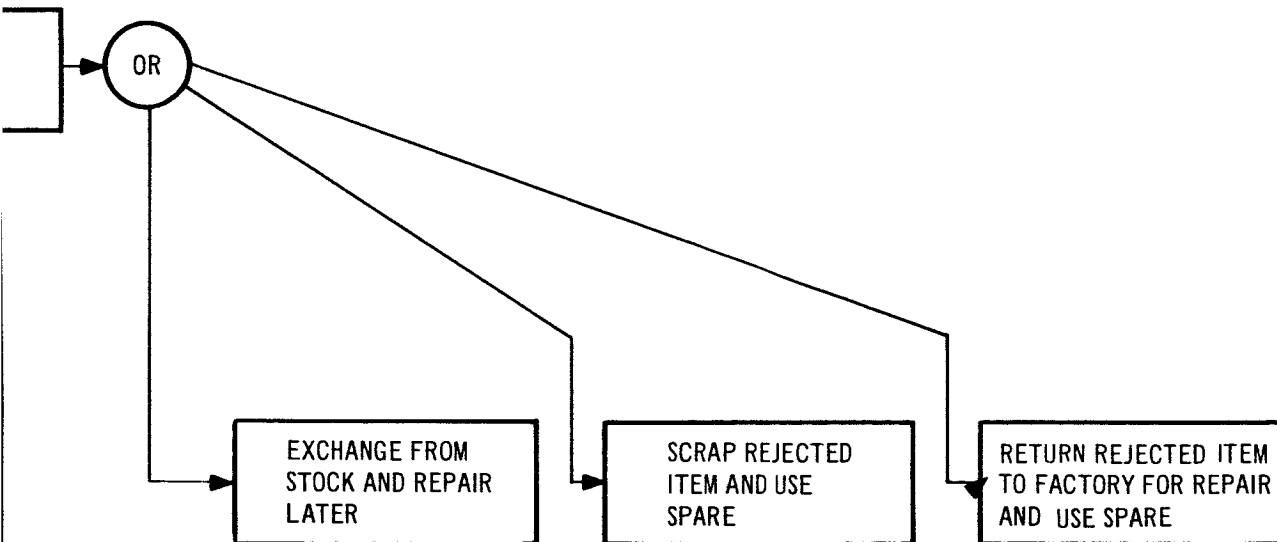
REPAIR AS  
REQUIRED ON  
SPACECRAFT

REMOVE FROM  
SPACECRAFT

MAKE IMMEDIATE  
REPAIRS AT KSC

TEST AND  
RE-INSTALL

142-4



142-5

Table 3-19  
REFURBISHMENT COSTS

Item	(\$ Millions)
Refurbishment labor costs	
10,400 hours at \$20/hr	0.208
Thermal heat-shield costs	1.960
Subsystems replacement and repair	1.590
Structure repair (material)	0.083
Preflight testing	
14,920 hr at \$20/hr	0.298
	\$4.139

It should be noted that these costs reflect the following additional factors:

1. Heat-shield panels are not refurbished after normal mission.
2. There is no salvage of components failing a postflight check.

These costs represent 10.7% of the Configuration I spacecraft procurement as discussed in Section 3.3.2.2.

### 3.2.3 Range Safety

To determine the minimum separation between hazardous facilities and inhabited buildings, a review of current solid-propellant safety data was made. Reference was made to the Solid Propellant Safety Handbook SP-4-45-S, dated 1 February 1965, prepared by the Kennedy Space Center NASA Safety Office, and Air Force Manual (AFM 127-100), Ground Safety Explosives Safety Manual, dated 20 April 1965. Because of the propellant quantities required for the study vehicle, the information available in these two documents cannot be directly applied for quantity-distance determination.

Minimum intraline separation distances were determined for the Configuration I vehicle. A free-air TNT equivalence of 20% was applied to the total loaded propellant weight of 5,121,800 lb, including the 5,016,500 lb of Class II solid

propellant and the 105,300 lb of storable liquid steering and maneuver propellant. For consideration of an on-pad abort situation, and the consequent reflected pressure wave, this TNT equivalence was doubled to obtain separation distances. This TNT equivalence is in agreement with values used by studies done by Douglas and Lockheed. Studies performed by Martin for NASA-Huntsville used a 10% TNT equivalence for the solid booster. Based on a 3-psi maximum overpressure limit for intraline distances, the Configuration I vehicle requires a separation distance of 1,961 ft. The distances associated with other overpressure levels are shown in Table 3-20.

#### 3.2.4 Summary

The study results, discussed in detail in Sections 3.2.1, 3.2.2, and 3.2.3, may be summarized as follows:

1. The use of head-end steering with fixed-nozzle, solid-propellant motor in Configuration I will result in a significant savings in launch-pad-occupancy time compared to all-liquid propulsion systems employing conventional steering.
2. Transportation of the spacecraft from recovery site to refurbishment site in the Super-Guppy aircraft is feasible.

Table 3-20  
CONFIGURATION I OVERPRESSURE CRITERIA

Total propellant weight = 5,121,800 lb	
Reflected TNT equivalence = 40%	
Overpressure (psi)	Distance (ft)
10	1,075
5	1,392
3	1,961
2	2,732
1	5,275
0.5	10,626

3. Primary refurbishment tasks would be accomplished at the launch-site location.
4. Refurbishment analyses made for the 44-ft HL-10 spacecraft employing an all-ablative, double-wall thermo-protection system resulted in costs slightly over 10% of spacecraft procurement costs per refurbishment. This cost is that required to bring the spacecraft to the same condition as a new spacecraft when received at Cape Kennedy.

### 3.2.5 Recommendations

The incorporation of reusability into space system hardware results in a closed loop type of operation. This requires that logistic paths be established for which there exists no precedent in current or past space system programs.

This study has shown the implications of vehicle refurbishment characteristics and costs on the total operations program. It is clear that much more study is required before reasonable tradeoff analyses can be made in the spacecraft design.

Specific task areas that are recommended for future study are as follows:

1. Effect of orbit dwell time on subsystems, including structure.
2. Evaluation of thermo-structural techniques on refurbishment time and cost.
3. In-depth study of surface flow paths for the determination of firm recommendations for facility size and arrangement as a function of spacecraft size and mission requirements.



### 3.3 COMPARATIVE STUDIES

#### 3.3.1 General Objectives

The objective of the comparative studies is to define and evaluate selected vehicle concepts on a consistent basis so as to determine the relative advantages and/or disadvantages associated with the use of (1) head-end steering, instead of conventional thrust vector control; (2) all-solid-propellant boosters, instead of liquid or combination liquid-solid booster's; (3) lifting body (HL-10) spacecraft, instead of ballistic (BALLOS) spacecraft; and (4) the overall head-end steering system concept, instead of a conventional system, such as Saturn IB-BALLOS.

The comparisons were to be based on the technical, operational, and economic characteristics of the vehicle systems defined during the course of the study. This portion of the Phase II study was intended to answer the question of whether or not any additional benefit accrued from using head-end steering over and above that derived from the utilization of solid-propellant boosters.

#### 3.3.2 Approach

The approach selected to attain this objective consisted of the following steps:

1. Select and define vehicle system concepts and mission characteristics to be investigated.
2. Establish comparison criteria and reliability and cost models.
3. Select a thrust vector control technique for use on those vehicles requiring conventional steering.
4. Size the selected boosters and payloads, as required.
5. Refine vehicle technical, operational, and economic characteristics.
6. Perform the comparative analyses and form appropriate conclusions.

##### 3.3.2.1 Vehicle and Mission Definition

The HES-2G vehicle which evolved from the Phase I studies was sized on the basis of the extended MORL mission. The characteristics of this mission, along with those of the LORL mission and a mission slightly modified from extended MORL, are listed in Table 3-21. These mission descriptions were used for sizing the spacecraft and vehicles described below.

Table 3-21  
COMPARATIVE STUDY GUIDELINES MISSION CHARACTERISTICS

	Extended MORL (9 man)	LORL (24 man)	Extended MORL Type (9 man)
Logistics Spacecraft Type	HL-10	BALLOS/HL-10	HL-10
Rendezvous Altitude (nmi)	300	260	300
Orbit Inclination (deg)	31	29.5	31
Mission Profile	Direct ascent to 300 nmi	105 nmi parking orbit Hohmann transfer to 260	105 nmi parking orbit Hohmann transfer to 300
Nominal Mission Requirements			
Crew replacement, number of men	6	12	6
Packaged cargo (lb)	5,000	13,455	5,000
Unallocated maneuver - capability @ rendezvous altitude (fps)	4,000	0	Dependent on configuration VII payload capability
Maximum Packaged Cargo Carrying Capability (lb)	23,750	13,455	23,750

The vehicle concepts selected for the comparative analyses are listed in Table 3-22. The intravehicle comparisons made to determine the effect of steering, booster, spacecraft, and overall concept are listed in Table 3-23 and described in the following paragraphs.

Configuration I is a refined version of the HES-2G vehicle system evolved in the Phase I study utilizing a head-end steered, three-stage, solid-propellant booster, with an HL-10 spacecraft sized for the extended MORL mission.

Configuration II is the HES-2G, or the Configuration I spacecraft on a conventionally controlled, three-stage, solid-propellant booster. The spacecraft is modified by the deletion of the steering system and the addition of a low-thrust, in-orbit maneuvering propulsion system. Liquid-injection thrust vector control systems, chosen on the basis of a thrust vector control technique selection study, were incorporated on each boost stage.

Configuration III is the BALLOS logistics vehicle sized for the LORL mission and as defined by Lockheed Aircraft Corporation without additional modification. This vehicle is described in Reference 2 .

Configuration IV is a BALLOS spacecraft and modified cargo adapter on a head-end steered, two-stage solid-propellant booster. This vehicle, as well as Configurations V and VI, were sized for the LORL mission.

Configuration V is a BALLOS spacecraft and modified cargo adapter on a two-stage, solid-propellant booster incorporating liquid-injection thrust vector control.

Configuration VI is a HL-10 lifting body spacecraft sized for the LORL mission and boosted by a head-end steered, two-stage solid-propellant boost vehicle.

Configuration VII uses the HES-2G spacecraft, as in Configuration I, with a slight off-loading of on-board maneuver propellant. This off-loading makes the payload consistent with the capabilities of a boost vehicle composed of an S-IVB second stage and a 260-in. diam, solid-propellant first stage, Reference 3. Head-end steering is provided for control during first-stage burning.

Table 3-22  
COMPARATIVE STUDY VEHICLE DESCRIPTION

Configurations	Spacecraft Type	Booster Type	Steering Technique	Mission Description
Group A				
I	HL-10	Solid	HES	Extended MORL
II	HL-10	Solid	PTVC	Extended MORL
Group B				
III	BALLOS	Liquid (Saturn IB)	PTVC	BALLOS-LORL
IV	BALLOS	Solid	HES	BALLOS-LORL
V	BALLOS	Solid	PTVC	BALLOS-LORL
VI	HL-10	Solid	HES	BALLOS-LORL
Group C				
VII	HL-10	Solid - First Stage Liquid - Second Stage	HES - First Stage PTVC - Second Stage	Extended MORL
VIII	HL-10	Solid	HES	Extended MORL

Table 3-23  
VEHICLE COMPARISONS

---

Effect of Steering Technique

HL-10 spacecraft

Configuration I versus Configuration II

Ballos-Type spacecraft

Configuration IV versus Configuration V

Effect of Booster Type

Ballos-type spacecraft

Configuration III versus Configuration V

HL-10 type spacecraft

Configuration VII versus Configuration VIII

Effect of Spacecraft Type

All-solid type booster

Configuration IV versus Configuration VI

Effect of General Concepts

Configuration I versus Configuration II

Configuration III versus Configuration IV

Configuration III versus Configuration VI

---

Configuration VIII is the HES-2G spacecraft with the same in-orbit maneuvering capability as the Configuration VII spacecraft. The booster is a head-end steered, three-stage, solid-propellant vehicle.

The spacecraft evolved from these vehicle concept and mission guidelines are depicted in Figures 3-70, 3-71, and 3-72. The vehicles are described in more detail in Section 3.3.3.

### 3.3.2.2 Comparison Criteria and Models

#### Comparison Criteria

The comparison criteria selected for use in the evaluation of the vehicle concepts selected are listed below:

1. Technical Considerations -- Vehicle length, vehicle weight, payload packaging efficiency, and design sensitivity.
2. Operational Considerations -- Launch vehicle reliability, number of subsystems required for launch vehicle control, complexity and time required for prelaunch checkout, and number of recovery sites required.
3. Economic Considerations -- Total operations cost and cost effectiveness.

Payload packaging efficiency is defined here as the ratio of useful load impulse to total weight above the upper stage of the launch vehicle, where useful load impulse is the product of packaged cargo mass plus the mass of personnel in pounds times the in-orbit maneuvering capability in feet per second. The sensitivity of boost impulsive velocity and payload carrying capability to incremental changes in stage specific impulse, propellant weight, and inert weight, were determined for each vehicle and used for comparison purposes.

#### Reliability Model

The model developed for determining reliability of the vehicle systems is shown in Figure 3-73.

Reliability estimates were developed for each configuration at two points in time. This was necessitated by the comparison of an existing launch vehicle and stage, Saturn IB and S-IVB, with launch vehicles that will not have a history of usage at the time of the first logistics mission flight. Consequently,

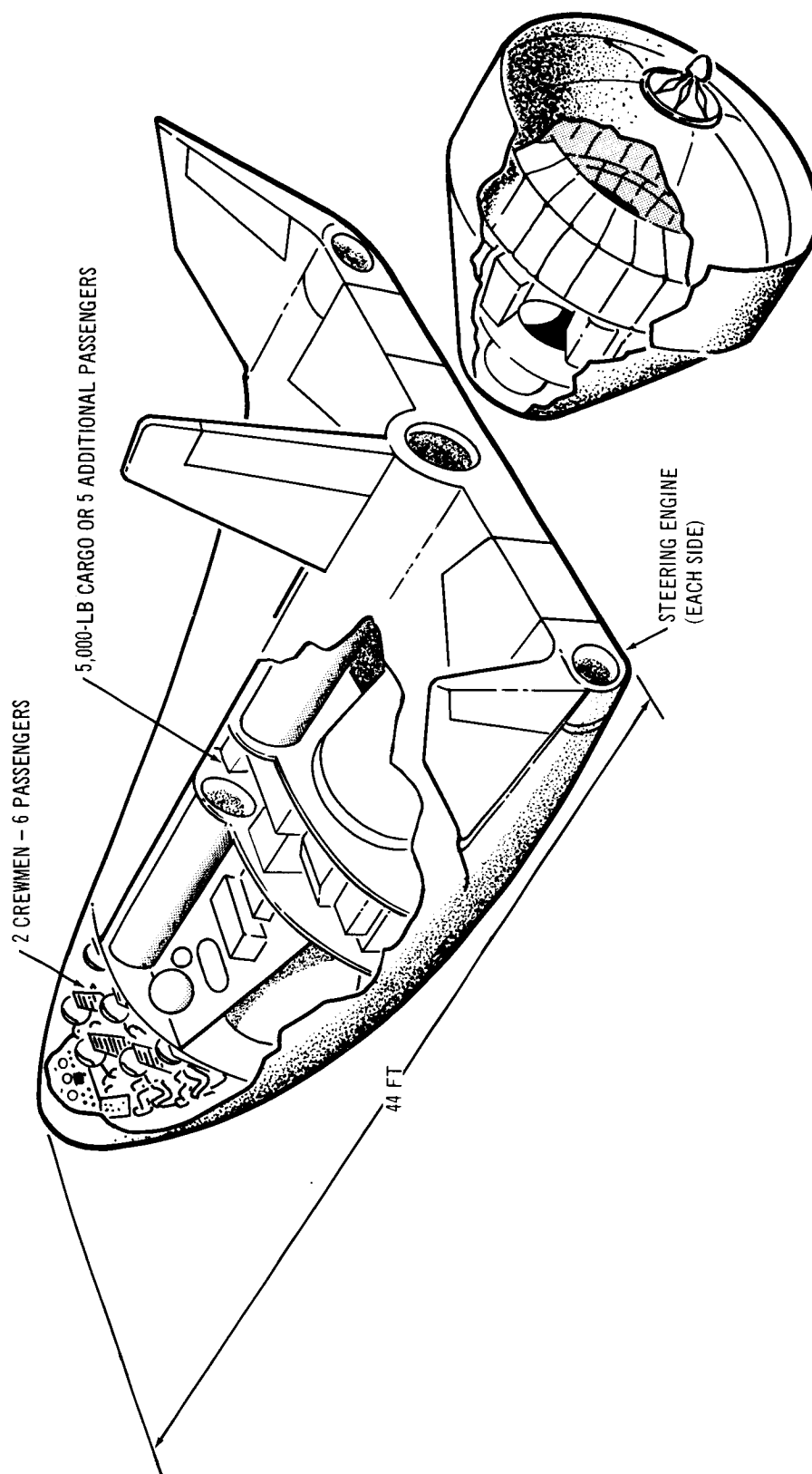


Figure 3-70. Spacecraft - Configurations I, II, VII, and VIII, - Extended MORL Mission

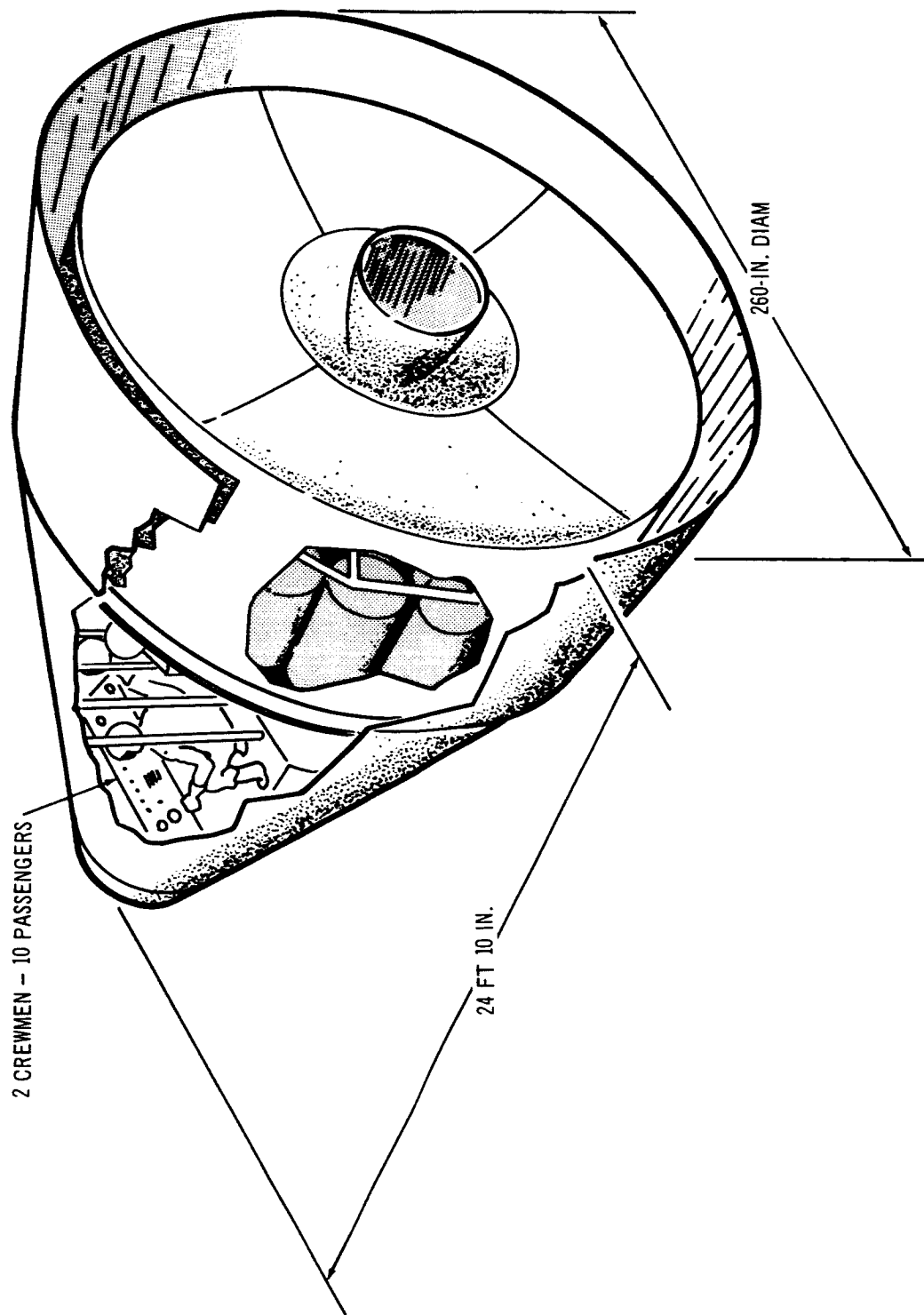


Figure 3-71. Spacecraft - Configurations III, IV, V, - LORL Mission



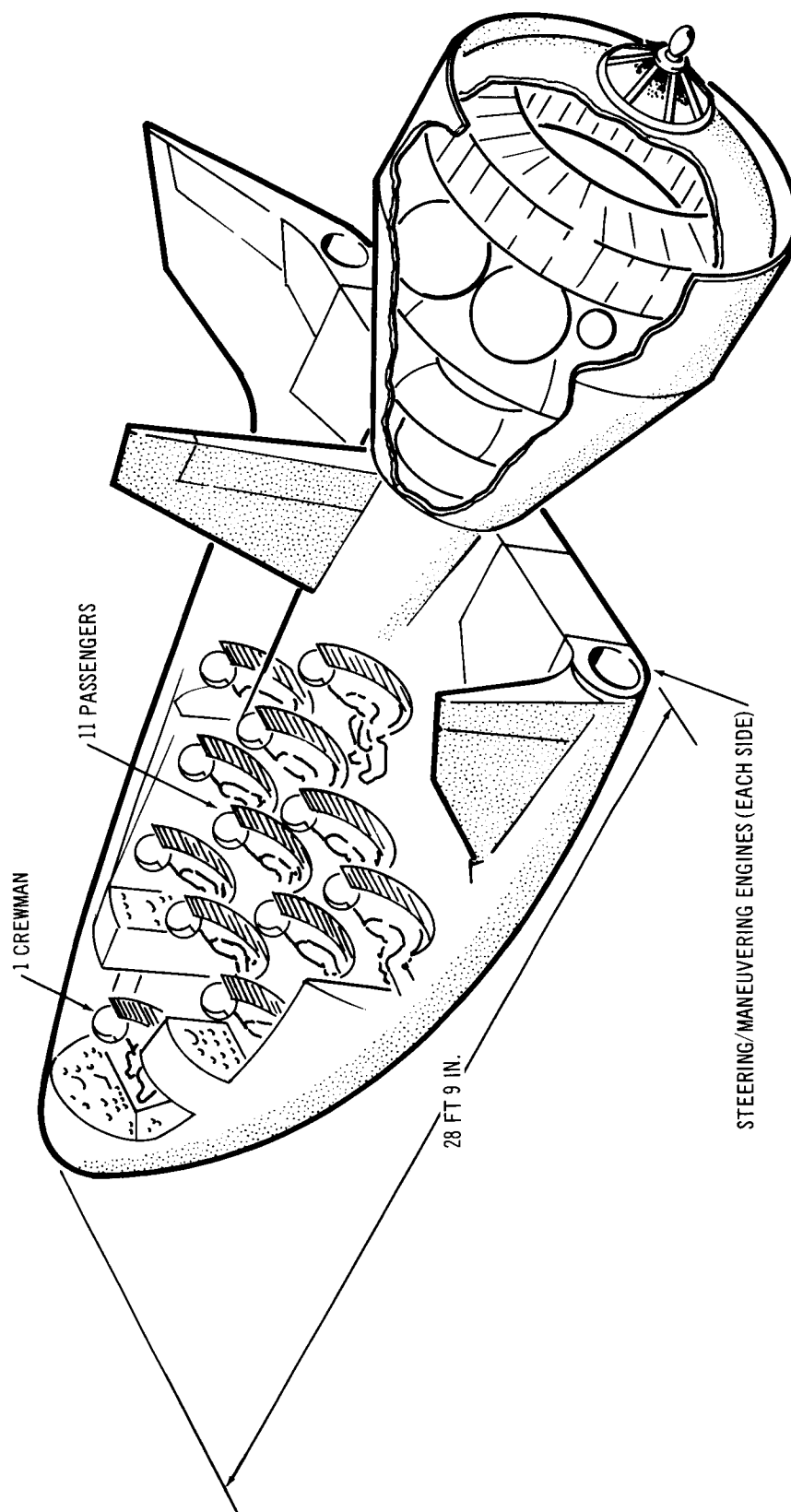


Figure 3-72. Spacecraft – Configuration VI -- LORL Mission

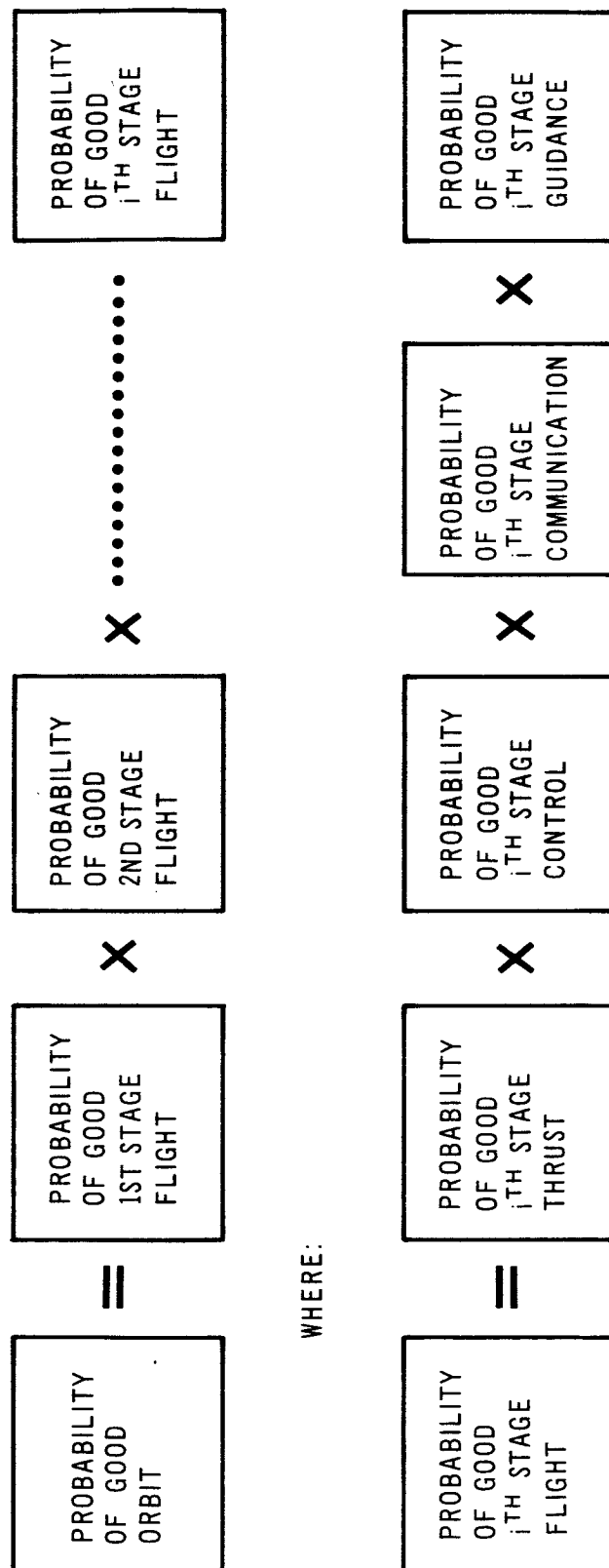


Figure 3-73. Reliability Model

two points in time were selected and designated Base A and Base B. Base A would correspond to the time of the first operational flight of the logistics vehicle. At this point in time, the Saturn IB vehicle and S-IVB stage are assumed to have reached their maximum reliability growth potential. Base B refers to that calendar point in time at which the solid-propellant vehicles would have reached their maximum reliability growth potential. The Saturn IB and S-IVB reliabilities would be the same for both time bases considered. The relative phasing of these bases are illustrated in Figure 3-74.

Reliability estimates were made for the major subsystems comprising the solid-propellant stages. These subsystems included the solid-propellant motor, with or without (1) thrust vector control, (2) flight control, (3) structure, (4) auxiliary power supply, (5) electrical, (6) separation, (7) range safety, (8) data acquisition, and (9) the steering system. It was assumed that after completion of the development flight program, solid-propellant motor reliability would be 0.995 without thrust vector control and 0.990 with it. Launch vehicle reliabilities quoted for the configurations investigated exclude the instrument unit reliabilities.

#### Comparative Cost Analyses

The objective of the comparative cost analyses was to obtain cost data which were as consistent as possible and which represented a level of accuracy that would permit reasonable comparisons. A simple cost model was formulated, the elements of which are shown in Figure 3-75.

Only operations costs are considered in the analyses of this study. Exploration of the differences in RDT&E costs between vehicle concepts was outside of the scope of the study. All system concepts which were compared in this study employed crew modules which incorporated reusability requirements in the basic approach to their design. All launch vehicles, including the cargo modules, are expendable.

The assumptions that were specified for the flight program were as follows:

1. A total of 50 successful launches.
2. A nominal flight frequency of 10 flights/year.
3. Spacecraft inventory determined by a cycle time capability of 80 days.
4. The probability of a successful launch of 0.95.

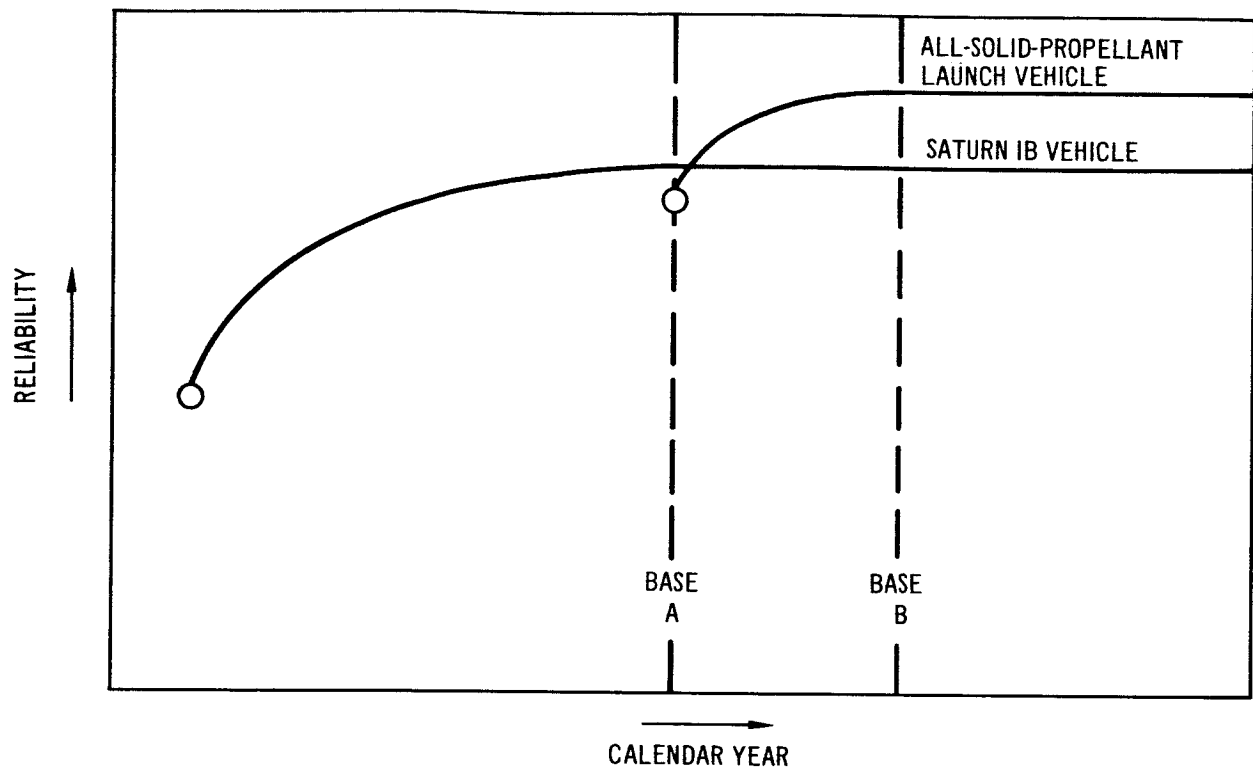


Figure 3-74. Reliability Time Bases

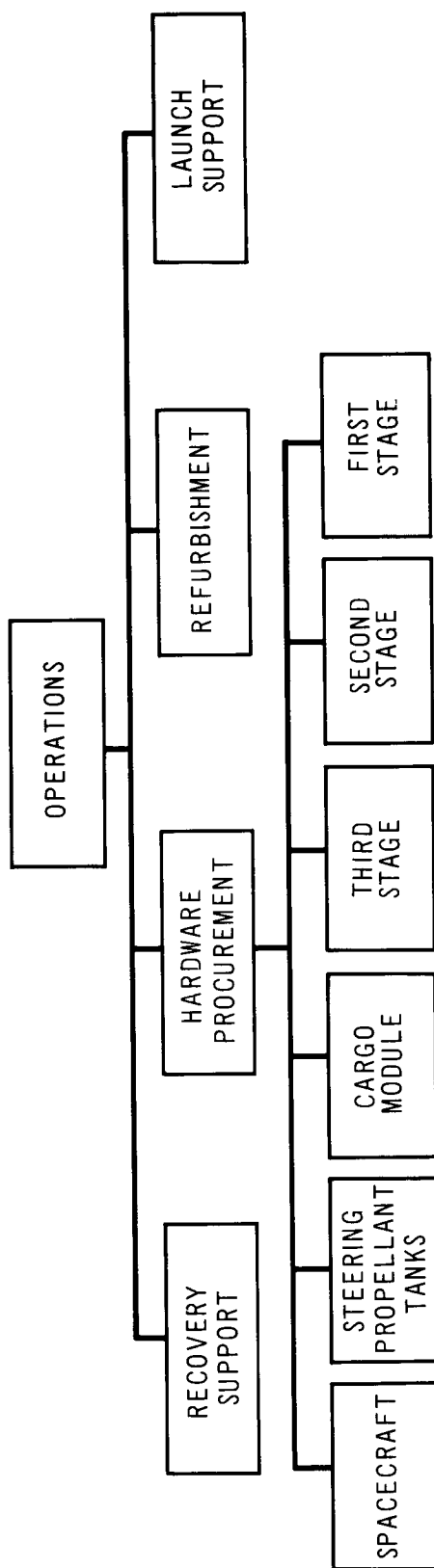


Figure 3-75. Cost Model

Since the spacecraft inventory in this study is determined by its time in the "pipe-line," and not on the basis of a specified mission life, flight costs remain nearly independent of flight frequency and are affected only by changes in the recovery and launch support costs.

The launch support costs were based on the assumption that essentially the same manpower requirements would apply to all the vehicles under consideration in this study. This manpower would remain at the same level throughout the operational program. Examination of current programs indicate an average expenditure of about \$2 million/flight for a program requiring 10 flights/year and vehicles similar to the Saturn IB.

The recovery support costs were obtained from a recently completed NASA study of recovery requirements for lifting vehicles (Reference 4 ). These data are summarized in Table 3-24 for recovery from an orbital altitude of 250 nmi and orbits whose inclinations are 30°, 55°, and 90°. The spacecraft configurations shown in this table are those defined in this study. Configurations III, IV, and V are of the ballistic type, with a crossrange capability of about 65 nmi. Configurations I, II, VI, VII, and VIII are of the lifting body type with a crossrange capability of 600 nmi.

Hardware procurement costs were categorized according to expendable hardware and reusable hardware procurement. The cost elements for the expendable hardware were made up of the various launch vehicle stages, the cargo module adapters, and the steering tankage section where applicable. The use of secondary liquid injection thrust vector control systems on the solid-propellant motors was analyzed in terms of the total cost of integrating the motor into a stage.

The solid-propellant launch vehicle stages were costed on the basis of the following elements:

1. Cost of delivered solid-propellant motor and nozzle assembly.
2. Cost of delivered subsystems for the stage.
3. Fabrication, assembly, and test of the primary interstage structure including skirts, fins, and so forth.
4. Raw material costs.
5. Tooling maintenance and sustaining engineering.

Table 3-24

## RECOVERY OPERATIONS AND COSTS COMPARISON

Saturn IB launch vehicle		ORBIT ALTITUDE = 250 NMI					
Land recovery mode		MAXIMUM WAIT TIME = 24 HOURS					
Orbit inclination (deg)		30		55		90	
Spacecraft Configurations		III, IV, V	I, II, VI, VII, VIII	III, IV, V	I, II, VI, VII, VIII	III, IV, V	I, II, VI VII, VIII
Recovery Sites (No.)		4	3	13	4	46	4
Primary		2	2	5	2	20	2
Secondary		2	1	8	2	26	2
Total operations costs per flight		2.31	1.00	2.64	0.73	8.29	0.92
(\$ millions)							
Return from orbit		0.65	0.29	2.02	0.36	7.48	0.38
Boost abort		1.63	0.69	0.60	0.34	0.77	0.52
Launch site abort		0.01	0.01	0.01	0.01	0.01	0.01
Air/sea rescue service		0.2	0.2	0.2	0.2	0.2	0.2

The costs of the delivered solid-propellant motors are shown in Figure 3-76. These data are based on a delivery of 63 units of both the 156-in. and 260-in. motor sizes, including an allowance of 10 units for development flight tests. The source of these data was an independent Douglas correlation of published cost data from Lockheed Propulsion, Aerojet, and Thiokol sources. The costs do not include additional fabrication and propellant processing facilities, which may be required at the manufacturers site.

The stage integration costs are based on generalized cost data obtained from Douglas experience with large launch vehicle components such as Saturn. The cargo module and the steering propellant-tank sections are fabricated with currently available materials, and manufacturing techniques, and reflect Douglas cost experience.

The costs for existing launch vehicle hardware such as the Saturn IB vehicle and the S-IVB second stage were obtained from published data with suitable qualification, as discussed in Sections 3.3.3.2 and 3.3.3.3.

The costing elements for the lifting body spacecraft configurations were (1) fabrication assembly and test of the primary spacecraft structure, (2) raw materials, (3) delivered subsystems, and (4) tooling maintenance and sustaining engineering.

The cost projections for the fabrication, assembly, and test of primary structure included allowances for the complexity of subsystem installation and checkout at the manufacturers site. Installation labor costs of the ablative heat-shield panels is included in the launch support costs for the concepts discussed herein. Delivered panel costs, however, are included in the delivered subsystems cost.

The cost of the ballistic spacecraft is based on a survey of industry experience and cost analyses and adjusted to guidelines of this study.

Refurbishment cost analyses were not performed in this study in any detail for the comparison study spacecraft, with the exception of Configuration I.

Douglas's experience indicates a refurbishment cost of the lifting body spacecraft using a double-wall, thermostructural design, with all-ablative panels, should be approximately 10% of the spacecraft hardware procurement cost.



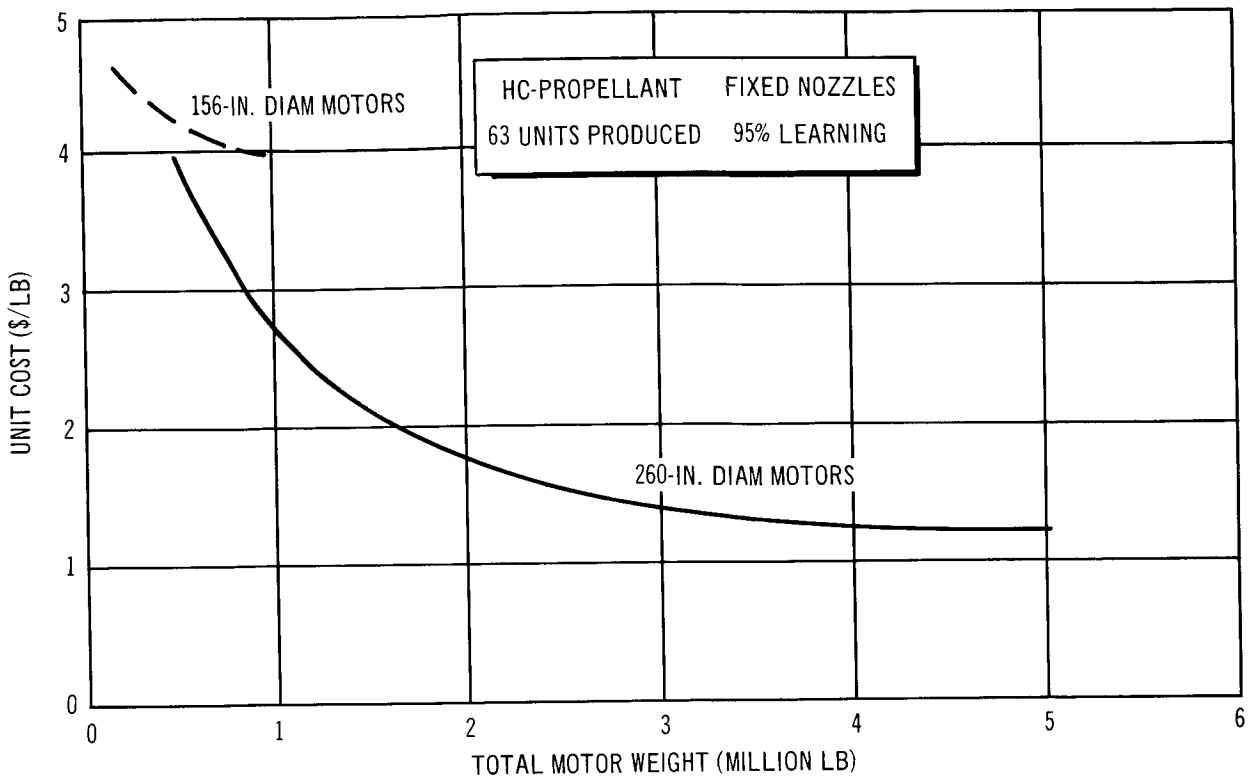


Figure 3-76. Average Cost of Solid-Propellant Motors

A survey of contractors performing design and manufacturing of ballistic spacecraft indicates that refurbishment cost should be approximately 25% of the ballistic spacecraft procurement.

Since the scope of this study precluded a refurbishment cost analysis for each spacecraft, two refurbishment cost bases were established and identified as Base A and Base B.

Refurbishment Base A is a refurbishment cost of 10% of spacecraft hardware procurement. When applied to a comparison of systems operations where both lifting body and ballistic types are involved, the comparative characteristics thus may be examined independently of refurbishment effects.

Refurbishment Base B uses the best available estimate of refurbishment costs and reflects projected cost differences between the lifting body types and the ballistic types. The actual refurbishment projection, as a percentage of spacecraft hardware procurement, is shown in the cost data for each configuration discussed in Section 3.3.3.

### Cost Effectiveness

Cost effectiveness was defined for the purposes of this study as the average flight cost divided by the useful load impulse. The average flight cost definition is discussed in the preceding section. The useful load impulse is a relatively new parameter adapted for use in this study and accounts for the effectiveness of maneuvering capability in the spacecraft. The useful load impulse is therefore defined as

$$U. L. I. = \frac{W_{U. L.} \times \Delta V}{g}$$

where

$W_{U. L.}$  = useful load in orbit (lb)

$\Delta V$  = maneuvering impulsive velocity (fps)

$g$  = acceleration due to gravity (fps<sup>2</sup>)

The useful load is considered to be the cargo weight carried in the spacecraft, plus the crew and passenger weights.

In the comparison of two systems having the same useful load and maneuvering capability, this definition of effectiveness does not serve as a particularly useful criterion, nor, for that matter, does the usual definition of payload cost effectiveness, that is, dollars per pound of payload in orbit. In establishing the effect of system size and mission requirements, this definition aids in evaluating the effectiveness, including maneuvering capability as well as useful load.

#### 3. 3. 2. 3 Thrust Vector Control Technique Selection

A number of techniques have been and are being used for thrust vector control of solid-propellant motors. These include jet tabs, jet vanes, gimbal nozzles, liquid injection, and warm- or hot-gas injection. Analytical and experimental investigation of the use of jet-tab and jet-vane techniques for large solid motors with long-burn durations have shown that these techniques are expensive with

regard to weight and cost as compared to the other techniques. They were, therefore not considered for the comparative study boost vehicles. While warm- and hot-gas injection offer attractive systems with respect to weight, development of thrust vector control subsystem components, such as hot-gas valves, has not reached the point where development risk would be satisfactorily low. Rather than use subsystems with questionable feasibility, the technique of gas injection was not considered.

Since both the gimbal-nozzle technique and the liquid-injection technique appeared competitive on a first look basis, a first order comparison of these techniques was performed to select the best technique for use on each stage. These thrust vector control techniques are illustrated in Figure 3-77. The sizing of the thrust vector control systems was based on the Configuration I launch vehicle and its required control moment history and trajectory. Liquid injection systems using nitrogen tetroxide or freon as injectant and helium, nitrogen, or warm gas as pressurant were investigated for all three stages. Of these, a system using nitrogen tetroxide as injectant and nitrogen as pressurant was selected for comparison with gimbal nozzles. Eight vehicles were set up with both thrust vector control techniques and impulsively sized to obtain total growth factors. These vehicle arrangements and their respective total growth factor are shown in Table 3-25. Growth factor is defined as the ratio of vehicle weight at liftoff to payload weight. It is apparent from these numbers that a vehicle utilizing liquid injection thrust vector control would have a lower gross weight at liftoff than any of the other combinations investigated. Based on available information, cost of the liquid-injection system and the gimbal-nozzle system appeared comparable and perhaps slightly lower for the liquid-injection system. Reliability seemed to be slightly higher for the gimbal nozzle system. On the basis of this information, the liquid-injection thrust vector control technique was selected for use on all vehicles requiring solid-propellant stages with thrust vector control. Those vehicles using the cryogenic liquid-propellant Saturn stages utilized the existing gimbal engines for control.

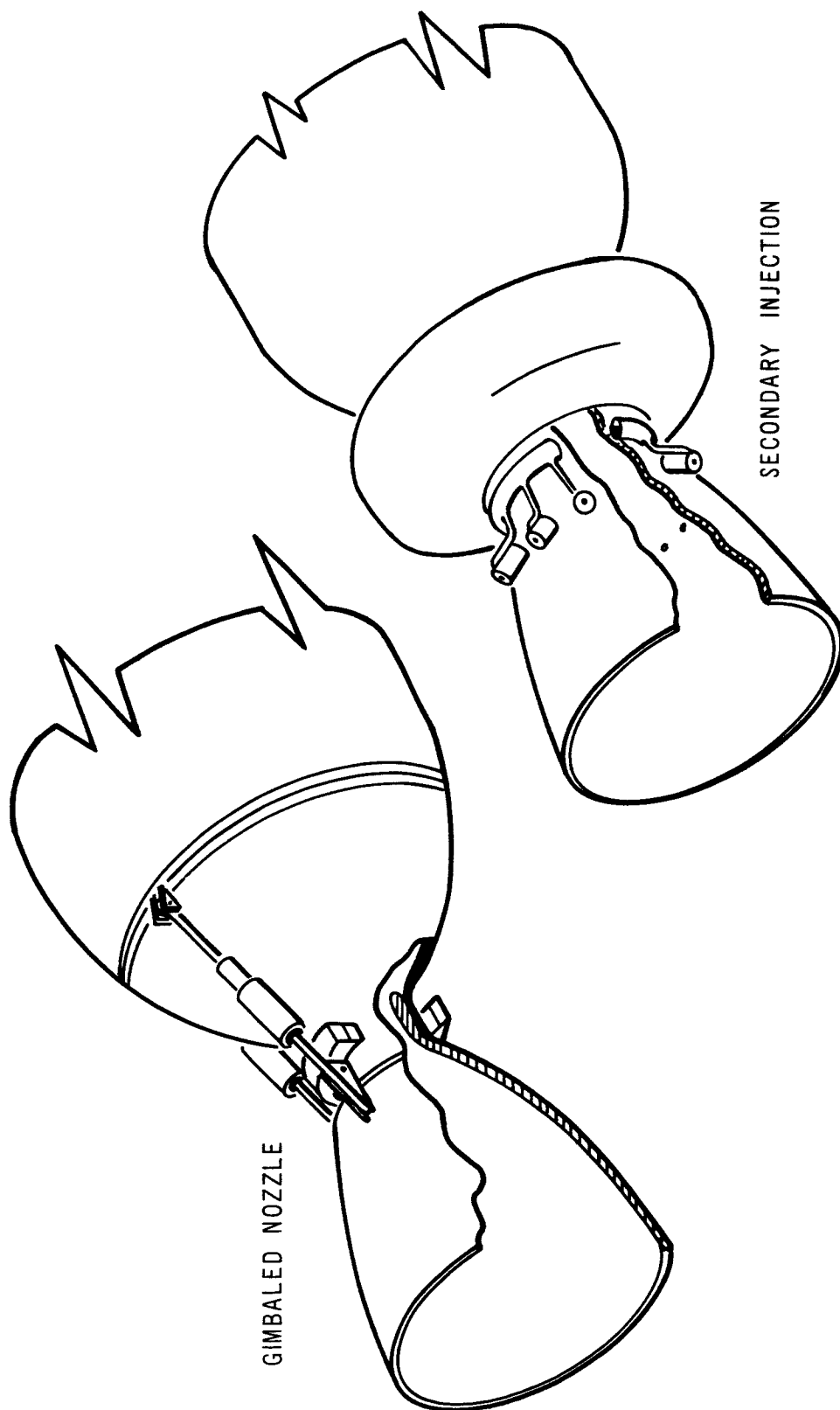


Figure 3-77. Primary Thrust Vector Control Techniques

Configuration designation	A	B	C	D	E	F	G	H
First-stage PTVC type	G	LI	G	G	LI	LI	G	LI
Second-stage PTVC type	G	G	LI	G	LI	G	LI	LI
Third-stage PTVC type	G	G	G	LI	G	LI	LI	LI
Total vehicle growth factor	67.0	65.9	65.7	64.9	64.5	64.1	63.5	62.6
Payload mass ratio	0.0149	0.0152	0.0152	0.0154	0.0155	0.0156	0.0157	0.0160
G = Gimbal nozzle								
LI = Liquid injection								

#### 3.3.2.4 Vehicle Sizing

The spacecraft were designed to fit mission requirements and vehicle concept descriptions for each configuration. Cargo modules for each configuration were designed according to cargo volume requirements and upper-stage booster diameter constraints. Steering propellant modules, as well as steering engines, were sized through an iterative process taking into account booster size and steering requirements and the consequent effect on payload and stage performance characteristics. Booster sizing was performed initially through impulsive sizing and then through detailed trajectory analysis of the resultant vehicle by means of the IBM 7090 computer program described in Reference 1. Sizing of steering requirements was accomplished through use of the steering simulation program described in Section 3.1.5.4. The vehicle configurations resulting from these analyses, along with the operational and economic characteristics of the configurations are described in Section 3.3.3. The comparisons made between these vehicles and the resultant conclusions are presented in Sections 3.3.4 and 3.3.5, respectively.

The use of head-end steering, therefore, is seen to produce a vehicle which may be operated at slightly lower total operation cost than one using secondary liquid-injection thrust-vector control.

### 3.3.3 Vehicle Description

#### 3.3.3.1 Extended MORL Mission

The extended MORL mission was used for sizing of the Phase I study HES-2G spacecraft and launch vehicle and is described in detail in Reference . The mission characteristics are summarized in Table 3-21. Configurations I and II were sized to meet these mission requirements and are directly comparable to determine the effect of steering technique with a launch vehicle using large solid-propellant boosters and a lifting-body spacecraft. These configurations are described in the following paragraphs.

#### Description of Configuration I

Configuration I consists of (1) an HL-10 spacecraft, (2) a cargo module, (3) a steering-propellant module, and (4) a three-stage, solid-propellant launch vehicle (Figure 3-78). The characteristics of this vehicle are summarized in Tables 3-26 and 3-27.

Spacecraft and Adapter -- The Configuration I spacecraft is identical to the Phase I study HES-2G spacecraft, as described in Reference 1 . The spacecraft carries two crewmen, six passengers, 5,000 lb of packaged cargo in a pressurized compartment, and 43,000 lb of usable propellant internally. This propellant is sufficient to provide 6,291 fps of impulsive velocity; however, 3,826 fps of this propellant is not allocated for any required maneuvers. Maneuvering capability is provided through use of the two steering engines mounted outboard along the trailing edge of the HL-10. These engines are located in pods which gimbal  $\pm 30^\circ$  in two planes for control.

The cargo module, or adapter, has a pressurized volume of approximately 1,000 ft<sup>3</sup>, which provides capability for 18,750 lb of packaged cargo and an aft docking station for rendezvous maneuvering. The nominal mission profile assumes that the cargo adapter is empty and would be separated from the spacecraft during third-stage separation.

Steering System -- As previously noted, boost steering thrust is provided by two engines located in the trailing edge of the HL-10 spacecraft. These

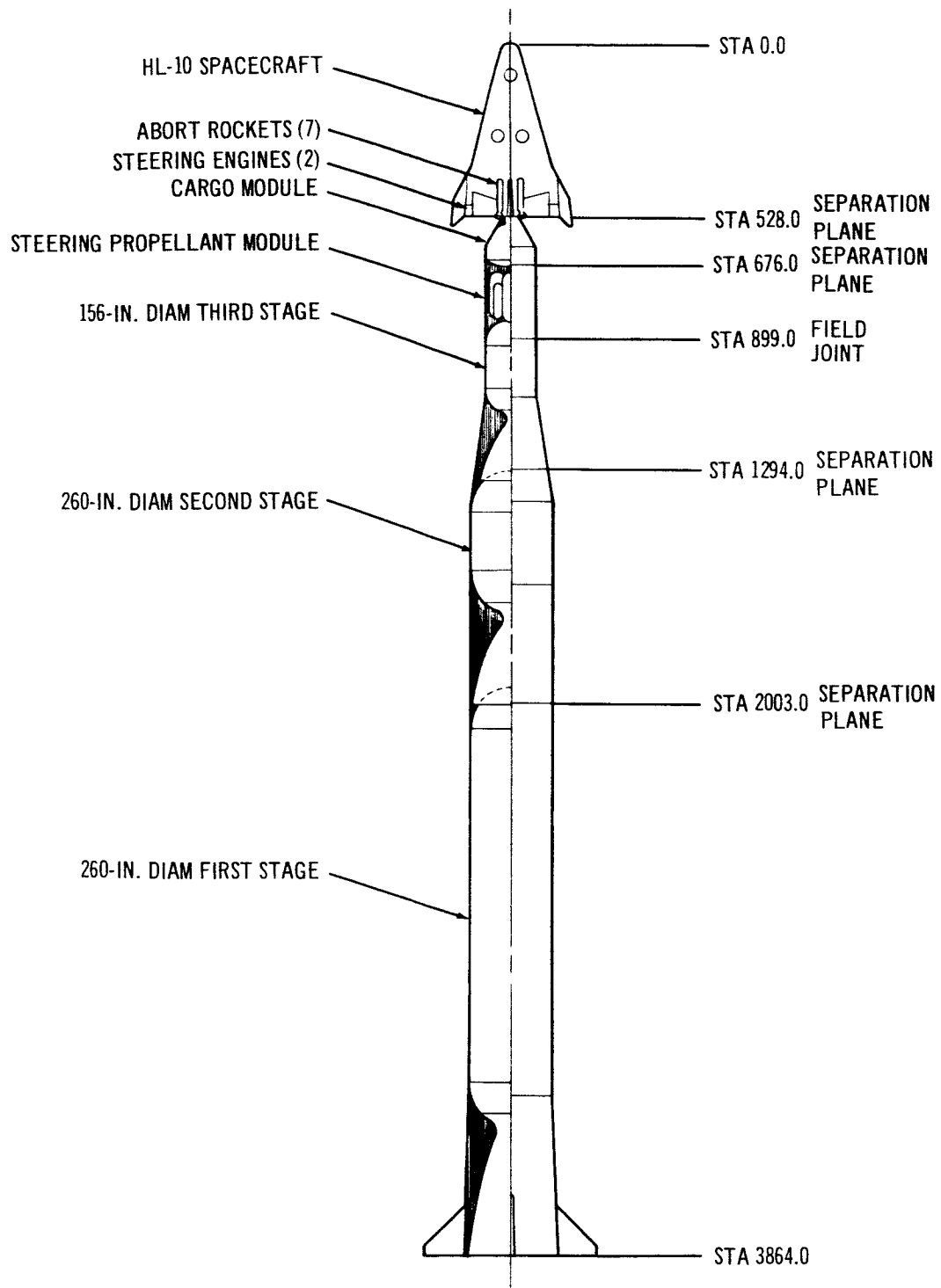


Figure 3-78. General Arrangement – Configuration I



Table 3-26  
SUMMARY OF CHARACTERISTICS OF CONFIGURATION I

---

General Characteristics

Number of crew	2 men
Number of Passengers	
Nominal (crew compartment)	6 men
Maximum (including cargo compartment)	9 to 11 men
Cargo carrying capability	
On-board HL-10 (packaged, Volume = 250 ft <sup>3</sup> )	5,000 lb
In cargo module (packaged, Volume = 938 ft <sup>3</sup> )	18,750 lb
Maximum vacuum thrust per engine	46,350 lb
Number of steering engines	2
Unallocated maneuver capability in orbit	3,826 fps

Dimensional Characteristics

HL-10 spacecraft	
Length	44.00 ft
Span	28.30 ft
Planform area	690 ft <sup>2</sup>
Adapter	
Cylindrical Diameter	156 in.
Cargo module total length	14.83 ft
Steering-propellant module length	18.58 ft
Overall length to field joint	30.92 ft
Third stage	
Diameter	156 in.
Cylindrical motor length	10.67 ft
Overall length	32.92 ft
Second stage	
Diameter	260 in.
Cylindrical motor length	16.67 ft
Overall length	59.08 ft
First stage	
Diameter	260 in.
Cylindrical motor length	103.42 ft
Overall length	155.08 ft
Overall booster length (to field joint)	247.08 ft
Total vehicle length	322.00 ft

---

Table 3-27  
WEIGHT SUMMARY FOR CONFIGURATION I

Item	Weight (lb)
<hr/>	
Spacecraft	
Structure and thermal protection	16,010
Electrical and mechanical subsystems	3,280
Propulsion system (dry)	3,540
Maneuver propellant (total)	43,900
Reaction-control system (dry)	750
RCS propellant	2,000
Landing provisions	2,840
Environmental control and life support	2,100
Crew and associated equipment	2,150
Growth contingencies	5,830
Cargo (packaged)	5,000
Abort rockets	6,300
Gross weight at liftoff	93,700
Adapter	
Cargo module (empty)	3,900
Cargo (baseline mission)	0
Gross cargo module at liftoff	3,900
Steering-propellant module (dry)	9,300
Steering propellant (total)	61,400
First-stage requirement	34,780
Second-stage requirement	9,610
Third-stage requirement	15,810
Gross steering module at liftoff	70,700
Launch Vehicle	
Third stage	291,930
Gross motor weight	287,990
Propellant weight	252,500
Inert motor weight	35,490
Inert stage weight	3,940
Second stage	1,137,300
Gross motor weight	1,124,800
Propellant weight	1,013,000
Inert motor weight	111,800
Inert stage weight	12,500
First stage	4,130,300
Gross motor weight	4,111,400
Propellant weight	3,751,000
Inert motor weight	360,400
Inert stage weight	18,900
Gross launch vehicle at liftoff	5,559,530
Gross Vehicle at Liftoff	5,727,830
<hr/>	

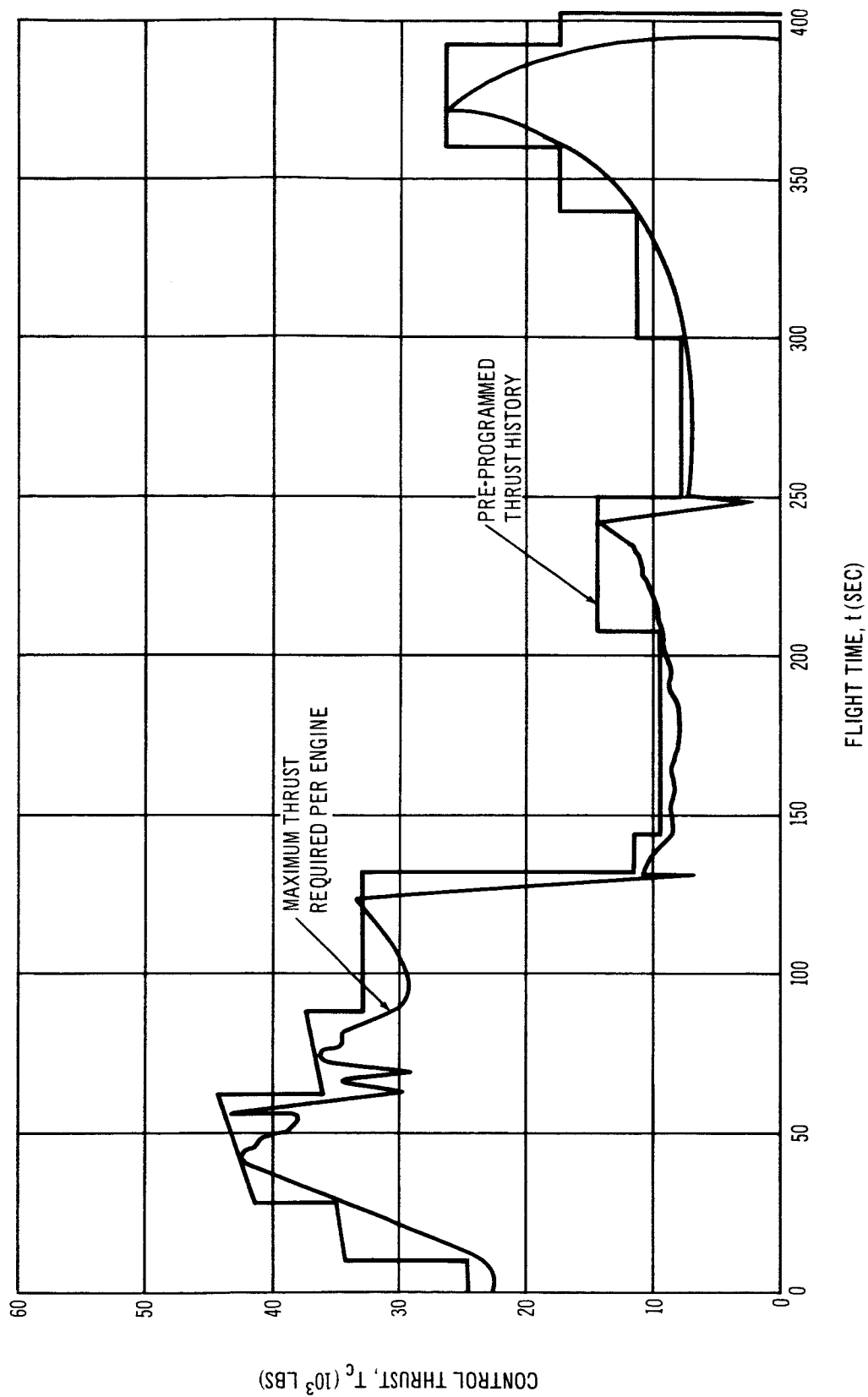


Figure 3-79. Configuration I Control Thrust History

The second stage consists of (1) a 260-in. diam motor loaded with 1,013,000 lb of propellant, (2) a fixed, contoured nozzle with an expansion ratio of 22:1, (3) a conical forward skirt, and (4) a cylindrical aft skirt. A neutral thrust-time curve for this motor can be obtained by using a four-by-four dendrite grain of the type used in the first-stage motor. A vacuum thrust of 2,548,000 lb and specific impulse of 286 sec is developed over a web burn time of 110 sec for this motor. The pyrogen igniter is mounted in the foredome of the motor.

The third stage consists of (1) a 156-in. diam motor, (2) a fixed, contoured nozzle with an expansion ratio of 40:1, (3) a cylindrical forward skirt, and (4) a conical aft skirt. The motor propellant grain weighs 252,500 lb and is a seven-pointed star design. This provides a highly regressive motor with good volumetric loading and low sliver fraction, as discussed in Section 3.1.2.3. Vacuum specific impulse is 303 sec with initial thrust of 914,400 lb, final thrust of 284,800 lb and a web burn time of 122.2 sec. Ignition is provided by a pyrogen-type igniter located in the forward dome.

Abort Requirements --The Configuration I abort system is sized to provide successful abort escape and land recovery of the HL-10 spacecraft throughout the flight duration, with or without the steering engines being operative. This is discussed in detail in Section 3.1.4. The resulting abort system which was used for sizing purposes consists of seven cylindrical, solid propellant motors located on the upper and lower aft surfaces of the HL-10. Total system weight is 6,300 lb, of which 4,620 lb is propellant. Total thrust is 308,000 lb at sea level and 336,000 lb at vacuum and is delivered over a 3.75-sec burn time. Launch vehicle trajectories flown for this configuration assume that five motors, or 4,500 lb, are jettisoned shortly after first-stage burn out.

Performance -- Configuration I is capable of rendezvousing with and delivering eight personnel and 5,000 lb of packaged cargo to an orbiting space station in a 300-n mi orbit in an inclination of  $31^{\circ}$ . It is also capable of providing 3,826 fps of impulsive velocity in orbit over and above that required to accomplish the mission profile. By offloading maneuver propellant, cargo carrying capability can be increased up to 23,750 lb. Horizontal landing on land is a design feature for both normal re-entry and abort conditions. Trajectory characteristics for this vehicle are shown in Figures 3-80 and 3-81. As

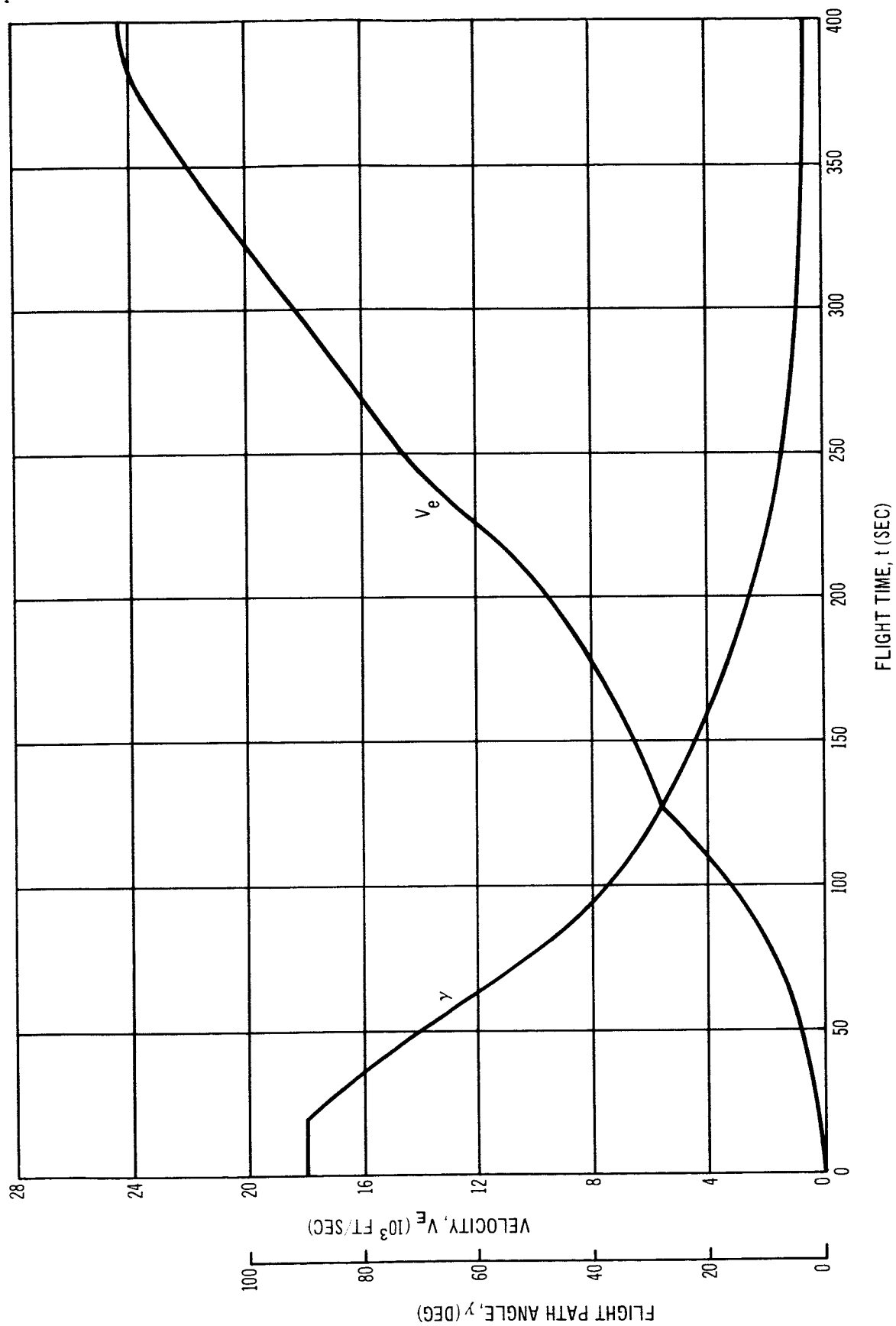


Figure 3-80. Configuration I Trajectory Characteristics

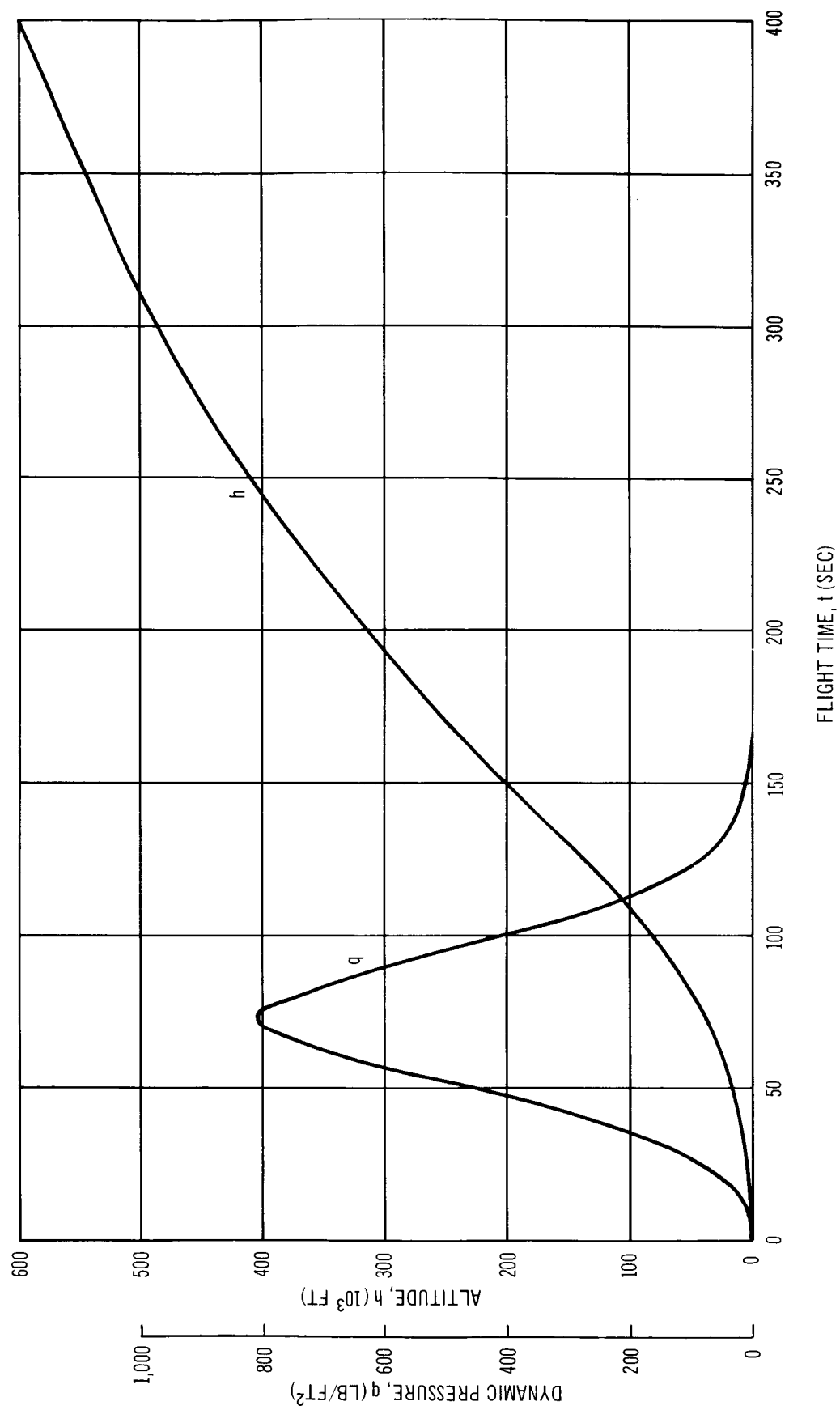


Figure 3-81. Configuration I Trajectory Characteristics

Table 3-28  
PERFORMANCE CHARACTERISTICS OF CONFIGURATION I

	First Stage	Second Stage	Third Stage
$T_i$	7, 138, 680	2, 548, 000	914, 410
$T_f$	8, 031, 014	2, 548, 000	284, 816
$I_{spSL}$	243.2	---	---
$I_{spVAC}$	273.6	286.3	302.7
$t_{Web}$	123.16	110.00	122.20
$t_{Act}$	132.43	117.64	144.30
$\lambda_M$	0.912	0.901	0.877
$\lambda'_{Eff}$	0.909	0.892	0.872
$(T/W)_i$	1.252	1.646	2.253
$a_{Max.}$	3.88	4.51	2.42
$GF_T$	55.29	---	---
$\eta_{PP}$	11.51	---	---

indicated, the maximum dynamic pressure experienced is 810 lb/ft<sup>2</sup>, which occurs 72 sec after launch. The maximum longitudinal acceleration occurs at the end of second-stage burn and is 4.5 g's. General vehicle performance characteristics are shown in Tables 3-28 and 3-29. An explanation of the symbols used is given in Table 3-30.

System Operation--This discussion will cover those key elements and associated time in preparation of the spacecraft and launch vehicle for operational use.

Configuration I prelaunch preparation processing time for a new spacecraft will be 32.5 days. During this phase of operation, receiving, shop processing, and preflight checkout will be accomplished. The three stages of the launch vehicle will also be processed in a time-phased parallel operation. It is

Table 3-29  
BOOSTER SENSITIVITIES OF CONFIGURATION I

X	$\frac{\partial \Delta V}{\partial X}$	$\frac{\partial W_{PL}}{\partial X}$	$\frac{\partial X}{\partial W_{PL}}$
First-Stage Specific Impulse	34.799 ft/sec/sec	605.71 lb/sec	0.001651 sec/lb
Second-Stage Specific Impulse	34.357 ft/sec/sec	598.02 lb/sec	0.001672 sec/lb
Third-Stage Specific Impulse	33.987 ft/sec/sec	591.57 lb/sec	0.001690 sec/lb
First-Stage Propellant Weight	0.001529 ft/sec/lb	0.02661 lb/lb	37.580 lb/lb
Second-Stage Propellant Weight	0.002897 ft/sec/lb	0.05042 lb/lb	19.833 lb/lb
Third-Stage Propellant Weight	0.008869 ft/sec/lb	0.15436 lb/lb	6.478 lb/lb
First-Stage Inert Weight	-0.002987 ft/sec/lb	-0.05198 lb/lb	-19.238 lb/lb
Second-Stage Inert Weight	-0.01423 ft/sec/lb	-0.24772 lb/lb	-4.037 lb/lb
Third-Stage Inert Weight	-0.05758 ft/sec/lb	-1.00000 lb/lb	-1.000 lb/lb
Payload Weight	-0.05745 ft/sec/lb	--	--



Table 3-30  
SYMBOL DEFINITIONS

---

$GF_T$	total vehicle growth factor, ratio between gross vehicle weight at liftoff to payload weight above third stage
$I_{spSL}$	delivered sea level specific impulse of motor or engine (sec)
$I_{spVAC}$	delivered vacuum specific impulse of motor or engine (sec)
$T_f$	delivered thrust at web burn-out (lb)
$T_i$	initial delivered thrust (lb)
$a_{Max.}$	maximum axial acceleration (g's)
$t_{Act}$	action time of motor or engine (sec)
$t_{Web}$	web burn time (sec)
$\lambda'_{Eff}$	effective stage mass fraction including steering propellant or thrust vector control system
$\lambda_M$	motor mass fraction excluding thrust vector control
$\eta_{PP}$	payload packaging efficiency - useful load impulse divided by weight above third stage (useful load impulse equals product of useful payload and propulsive velocity divided by 32.2 ft/sec. <sup>2</sup> )
$(T/W)_i$	initial stage thrust-to-weight ratio

---

estimated that 20 days will be required for the launch vehicle processing and erection at the launch pad. Major checkout tasks are required for the spacecraft, many of which may be accomplished before mating with the launch vehicle. Minimal checkout is required for the launch vehicle.

Upon completion of the launch vehicle erection and checkout, the spacecraft mating and countdown phase will commence and will be completed in 13 days. The final phase of this operation is the launch countdown phase which will take one day, consisting of 14 hours. Total pad time commences when the first stage arrives at the pad for erection and continues through third-stage erection and checkout.

This time consists of 14 days. Spacecraft/launch vehicle pad time is 14 days, making a total of 28 days. In summary, a total of 46.5 working days are required for this operation.

Recovery of the Configuration I spacecraft is on existing airfields. The number required and the associated costs are summarized in Section 3.3.2.2.

The recycle operations for this spacecraft will require a total of 44 days. Recovery site processing and transportation time of 4.5 days are included in the 44 days. The total recycle time through launch is expected to be 58 working days or 80 calendar days.

Cost of Operations -- Costs based on the assumptions and criteria presented in Section 3.3.2.2 were determined for Configuration I. The hardware procurement costs are summarized in Table 3-31, and the system operations costs summarized in Table 3-32. The effect of flight frequency on operations costs is shown in Table 3-33 for a 5-year program requiring 20, 50, and 100 flights.

Reliability Assessment -- Configuration I launch vehicle reliability and individual stage reliabilities are shown in Table 3-34. These are shown for both time bases, reflecting first-flight reliability and growth potential.

Table 3-31  
HARDWARE PROCUREMENT COSTS FOR CONFIGURATION I

Item	(\$ Millions)
Expendable hardware	(17.53)
First stage	8.09
Second stage	5.00
Third stage	1.89
Steering propellant tank section	0.97
Cargo module	1.58
Spacecraft	<u>38.54</u>
Total vehicle	56.07

Table 3-32  
OPERATIONS COST FOR 50 FLIGHTS OF CONFIGURATION I

Item		(\$ Millions)			
Orbit	30°		90°		
	A	B	A	B	
Refurbishment base <sup>1</sup>					
First flight	59.07	59.07	58.99	58.99	
Subsequent flight	25.43	25.70	25.35	25.62	
Average flight	28.20	28.45	28.12	28.37	
Total program cost	1,410	1,423	1,406	1,419	

<sup>1</sup>Refurbishment Base A: 10% of spacecraft hardware procurement

Refurbishment Base B: 10.7% of spacecraft hardware procurement

Table 3-33  
EFFECT OF FLIGHT FREQUENCY ON OPERATIONS COST FOR  
CONFIGURATION I

Item	(\$ Millions)		
Refurbishment base A*	Mission orbit = 30°		
Flight frequency per year	4	10	20
Average flight cost	28.74	28.20	27.35
Total program cost	575	1,410	2,735

\*Refurbishment Base A: 10% of spacecraft hardware procurement.

Table 3-34  
CONFIGURATION I RELIABILITY

Launch Vehicle	Base A	Base B
Launch vehicle	0.882	0.920
First stage	0.971	0.980
Second stage	0.978	0.986
Third stage	0.978	0.986
Steering system	0.950	0.966

#### Description of Configuration II

Configuration II consists of an HL-10 spacecraft, a cargo module, and a three-stage, solid-propellant launch vehicle (Figure 3-82). The vehicle characteristics are listed in Tables 3-35 and 3-36.

Spacecraft and Adapter -- This spacecraft is the same as the Configuration I, 44-ft HL-10, with some exceptions. Since this vehicle utilizes conventional thrust vector control for launch vehicle steering, the steering engines and their movable pods were removed. Two 4,000-lb thrust engines, with expansion ratios of 40:1 developing a vacuum specific impulse of 307 sec, are used to provide the same in-orbit maneuvering capability after circular orbit injection as Configuration I. This allows reduction of the amount of usable propellant required to 35,530 lb. This propellant provides 6,148 fps of impulsive velocity, 3,826 fps of which is not allocated.

The Configuration II cargo module is identical to that used for Configuration I, with the exception of the absence of steering-propellant transfer lines that are no longer required.

Launch Vehicle -- The launch vehicle is composed of three, large, solid-propellant booster motors incorporating liquid-injection thrust vector control for steering.

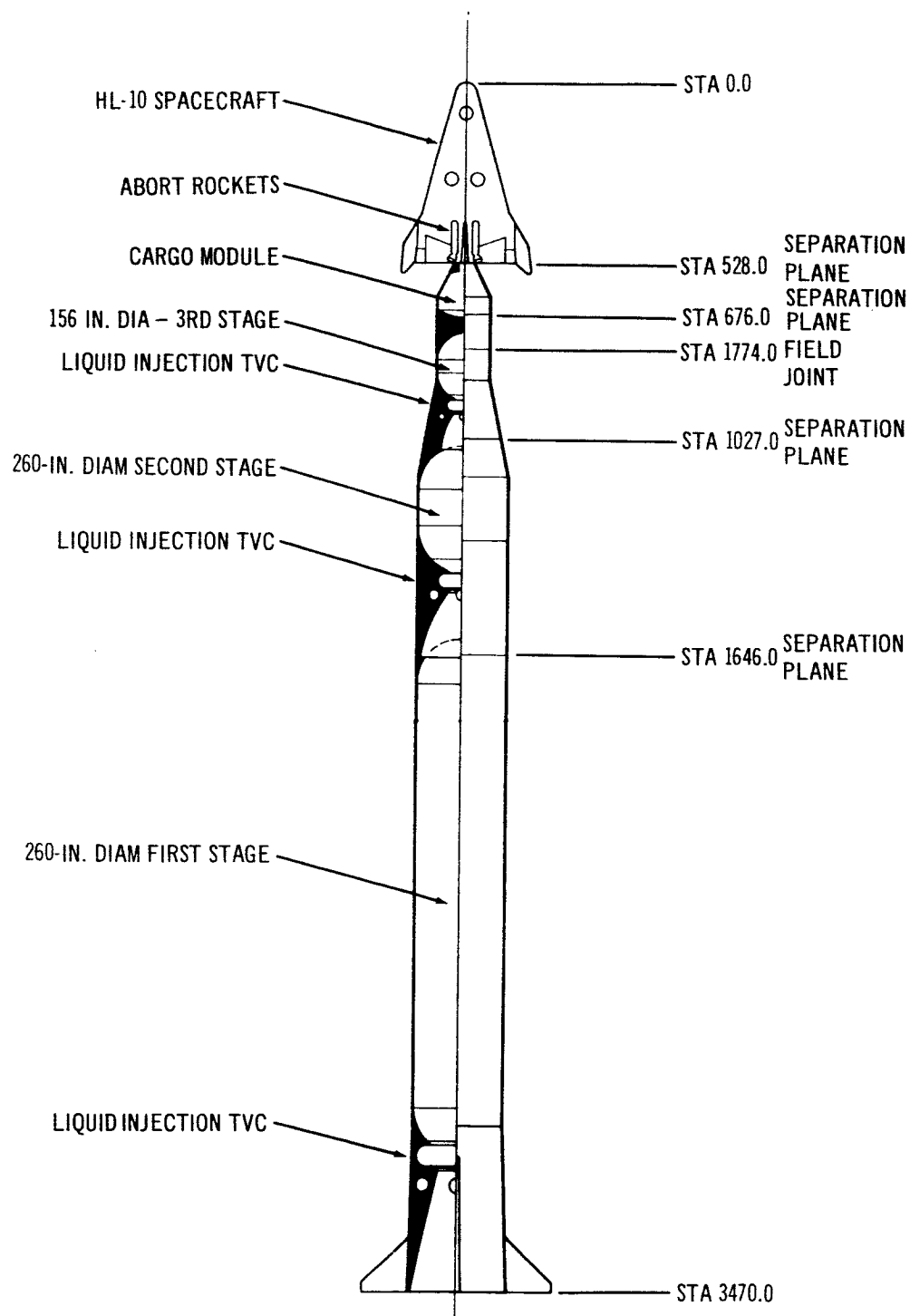


Figure 3-82. GeneralArrangement – Configuration II

Table 3-35  
SUMMARY OF DESCRIPTION OF CONFIGURATION II

<b>General Characteristics</b>	
Number of crew	2 men
Number of passengers	
Nominal (crew compartment)	6 men
Maximum (including cargo compartment)	9 to 11 men
Cargo carrying capability	
On-board HL-10 (packaged, volume = 250 ft <sup>3</sup> )	5,000 lb
In cargo module (packaged, volume = 938 ft <sup>3</sup> )	18,750 lb
Maneuver engine thrust level (2 engines)	4,000 lb/ engine
Unallocated maneuver capability in orbit	3,826 ft/sec
<b>Dimensional Characteristics</b>	
HL-10 Spacecraft	
Length	44.00 ft
Span	28.3 ft
Planform area	690 ft <sup>2</sup>
Adapter	
Cylindrical diameter	156 in
Cargo module total length	14.83 ft
Length to separation plane	12.33 ft
Third stage	
Diameter	156 in
Cylindrical motor length	3.00 ft
Overall length	21.08 ft
Second Stage	
Diameter	260 in
Cylindrical motor length	8.67 ft
Overall length	51.58 ft
First Stage	
Diameter	260 in
Cylindrical motor length	101.50 ft
Overall length	152.00 ft
Overall booster length (to field joint)	232.83 ft
Total vehicle length	289.17 ft

Table 3-36  
WEIGHT SUMMARY OF CONFIGURATION II

Item	Weight (lb)
Spacecraft	
Structure and thermal protection	15,510
Electrical and mechanical subsystems	2,970
Propulsion system (dry)	2,090
Maneuver propellant (total)	36,250
Reaction control system (dry)	700
RCS propellant	1,800
Landing provisions	2,650
Environmental control and life support	2,100
Crew and associated equipment	2,150
Growth contingencies	5,560
Cargo (packaged)	5,000
Deorbit rockets	7,000
Gross weight at liftoff	83,780
Adapter	
Cargo module (empty)	3,800
Cargo (baseline mission)	0
Adapter	1,100
Gross adapter at liftoff	4,900
Launch Vehicle	
Third stage	185,240
Gross motor weight	179,360
Propellant weight	152,300
TVC system	1,700
Liquid injectant* (usable)	900
Inert stage weight	4,180
Second stage	854,960
Gross motor weight	834,430
Propellant weight	744,300
TVC system	6,030
Liquid injectant* (usable)	3,450
Inert stage weight	14,500
First stage	4,166,100
Gross motor weight	4,116,530
Propellant	3,758,000
Thrust vector control system	28,170
Liquid injectant* (usable)	15,300
Inert stage weight	21,400
Gross launch vehicle at liftoff	5,206,300
Gross Vehicle at Liftoff	5,294,980
*Includes roll control propellant	

The first stage consists of (1) a 260-in. diam solid-propellant motor, (2) a fixed nozzle of expansion ratio 8.3:1, (3) a cylindrical forward skirt, and (4) a conical aft skirt. The 15,750 lb of liquid injectant,  $N_2O_4$ , which is required for control is stored in a toroidal tank mounted in the area between the aft skirt and the nozzle, along with the other thrust vector control and roll control hardware. The 3,758,000 lb of propellant contained in the motor provides a neutral thrust-time curve with a vacuum thrust of 7,445,500 lb over a web burn time of 133.2 sec. The vacuum specific impulse of the motor is 273 sec and liftoff thrust-to-weight ratio is 1.25:1. Fins mounted on the first-stage aft skirt were sized to minimize control requirements. The resulting pitch fins have an exposed semispan of 13.25 ft and an aspect ratio of 4.0. Yaw fins have an exposed semispan of 8.0 ft and an aspect ratio of 1.0. A 260-in. diam motor containing 744,300 lb of propellant, a contoured nozzle with an expansion ratio of 26:1, a liquid-injection thrust vector control system requiring 3,870 lb of  $N_2O_4$ , a conical forward skirt, and a cylindrical aft skirt comprise the second stage. Ignition of the motor is provided by a pyrogen-type igniter located in the motor forward dome. This motor develops a vacuum thrust of 1,903,250 lb and specific impulse of 290 sec over a web burn time of 110 sec. The thrust-time trace for this motor is neutral.

The third stage is composed of (1) a 156-in. diam motor containing 152,300 lb of propellant, (2) a contoured nozzle with an expansion ratio of 40:1, (3) a cylindrical forward skirt, and (4) a conical aft skirt. A liquid-injection system containing 960 lb of  $N_2O_4$  is located in the area surrounding the nozzle along with a four-thruster, bipropellant roll-control system similar to those existing on the first and second stage. A neutral burning propellant grain is used which provides 442,250 lb of vacuum thrust and a specific impulse of 302 sec over a web burn time of 100 sec.

Abort Requirements -- The Configuration II abort system was sized to provide essentially the same apogee velocity to the spacecraft on pad abort, as that achieved by the Configuration I spacecraft. This, in combination with the on-board maneuver system capability, will probably allow the land recovery of the spacecraft on pad abort. The low-altitude cruise capability of the Configuration II spacecraft, however, was not investigated in detail. The resulting abort system weighs 7,000 lb, 5,130 lb of which is propellant. Total sea level thrust



developed would be 342,000 lb with a burn time of 3.75 sec. Half of the abort motors, or 3,500 lb, would be jettisoned after first-stage burn out. The solid-propellant motors required to provide this impulse would be mounted on the aft end of the HL-10, as in Configuration I.

Performance -- Mission capabilities of the Configuration II spacecraft are identical to those of Configuration I, as indicated in Table 3-21. The total impulsive velocity capability of the on-board maneuver propulsion system is approximately 150 fps lower than that of Configuration I to allow for the difference in injection velocity required to attain a 300-nmi circular orbit. The unallocated velocity of 3,826 fps is the same as the Configuration I capability. Trajectory characteristics are shown in Figures 3-83 and 3-84. The maximum dynamic pressure of 830 psf is experienced 74 sec after launch. The maximum longitudinal acceleration of 4.7 g's occurs at the end of second-stage burn. Vehicle performance characteristics are summarized in Tables 3-37 and 3-38.

Table 3-37  
PERFORMANCE CHARACTERISTICS OF CONFIGURATION II

	First Stage	Second Stage	Third Stage
$T_i$	6,618,725	1,903,248	442,245
$T_f$	7,445,521	1,903,248	442,245
$I_{spSL}$	242.4	---	---
$I_{spVAC}$	272.7	289.9	301.7
$t_{Web}$	133.21	110.00	100.00
$t_{Act}$	143.20	117.78	108.99
$\lambda_M$	0.913	0.892	0.849
$\lambda'_{Eff}$	0.906	0.875	0.827
$(T/W)_i$	1.250	1.691	1.635
$a_{Max.}$	4.48	4.72	3.57
$GF_T$	62.16	---	---
$\eta_{PP}$	13.99	---	---

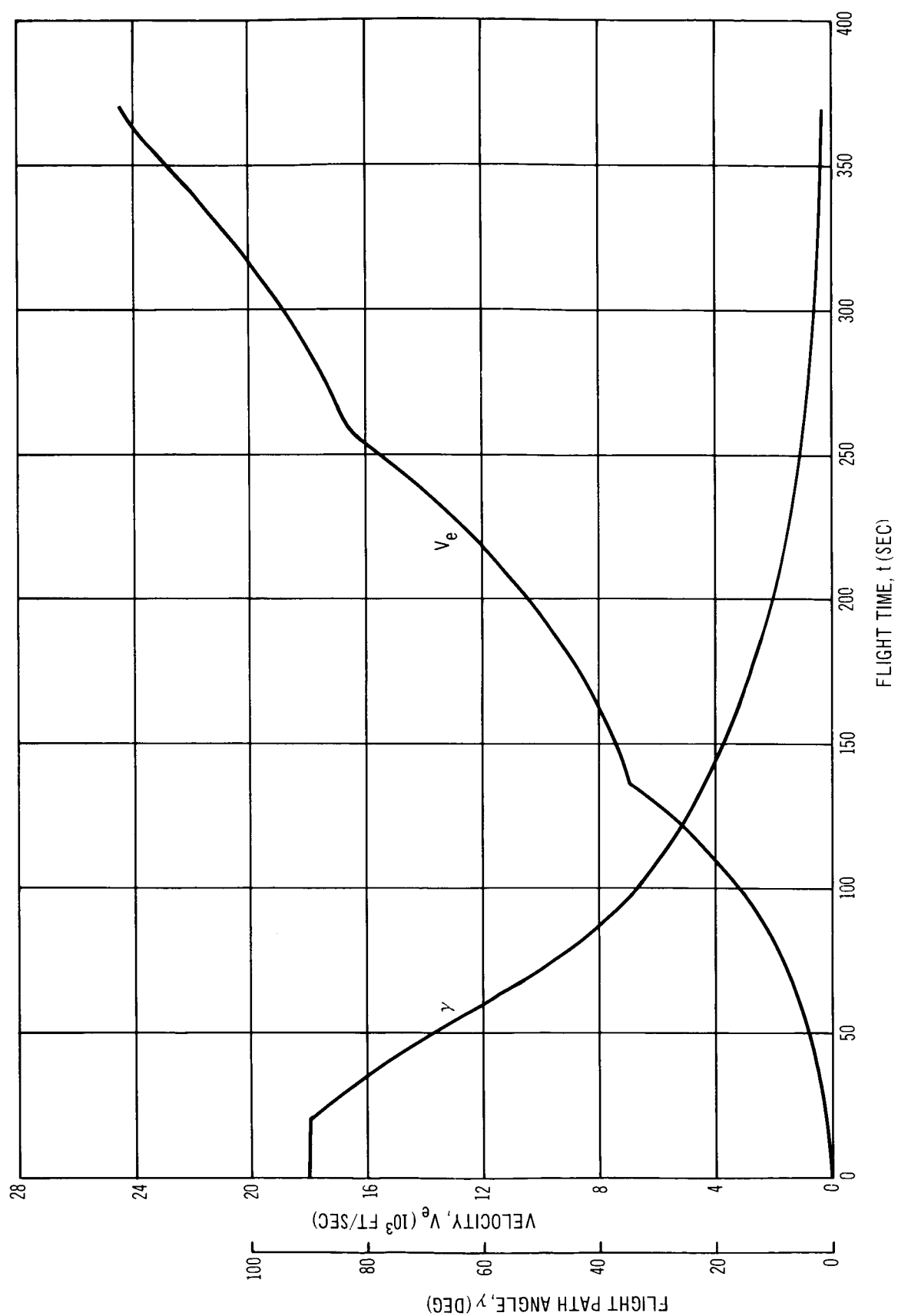


Figure 3-83. Configuration II Trajectory Characteristics

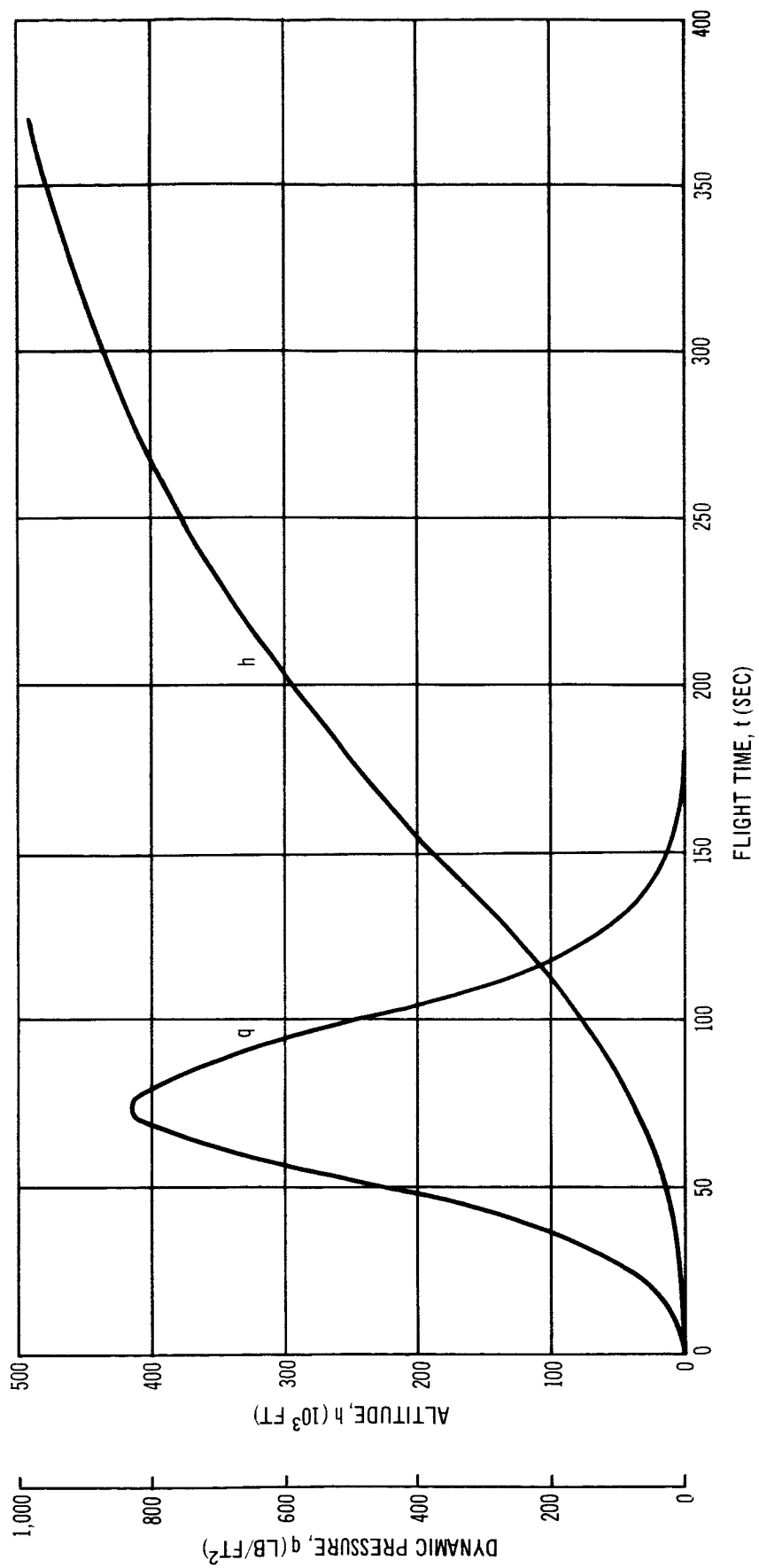


Figure 3-84. Configuration II Trajectory Characteristics

Table 3-38  
BOOSTER SENSITIVITIES FOR CONFIGURATION II

X	$\frac{\partial \Delta V}{\partial X}$	$\frac{\partial W_{PL}}{\partial X}$	$\frac{\partial X}{\partial W_{PL}}$
First-Stage Specific Impulse	40.119 ft/sec/sec	598.27 lb/sec	0.001671 sec/lb
Second-Stage Specific Impulse	35.113 ft/sec/sec	523.91 lb/sec	0.001909 sec/lb
Third-Stage Specific Impulse	26.895 ft/sec/sec	401.06 lb/sec	0.002493 sec/lb
First-Stage Propellant Weight	0.001651 ft/sec/lb	0.02462 lb/lb	40.617 lb/lb
Second-Stage Propellant Weight	0.004157 ft/sec/lb	0.06198 lb/lb	16.134 lb/lb
Third-Stage Propellant Weight	0.015288 ft/sec/lb	0.22797 lb/lb	4.387 lb/lb
First-Stage Inert Weight	-0.004102 ft/sec/lb	-0.06117 lb/lb	-16.348 lb/lb
Second-Stage Inert Weight	-0.020484 ft/sec/lb	-0.30545 lb/lb	-3.274 lb/lb
Third-Stage Inert Weight	-0.067280 ft/sec/lb	-1.00000 lb/lb	-1.000 lb/lb
Payload Weight	-0.067059 ft/sec/lb	--	--

System Operation -- Configuration II spacecraft processing time would be the same as Configuration I. The only exception to this would be a reduction in processing time by deleting the weight and balance fixture test of the steering propulsion tank module (SPTM). This would decrease the prelaunch processing time from 32.5 to 31.5 days.

It is estimated that the total launch vehicle processing time would increase from 20 days to 26 days. The deletion of the SPTM has no effect in the time span as time programmed for checkout and mating to the third stage is a parallel task operation. This increase of 6 days is caused by the added checkout of the thrust vector and roll control systems required, of which 3 days would be in the receiving and assembly area and 3 additional days at the launch pad. The additional 3 days of pad occupancy results in a total pad tie-up time of 31 days.

The recycle time for this configuration is projected to be 58 working days. The substitution of the fixed maneuver engines for the gimballed Configuration I steering engines might require less recycle time; however, this difference in time appeared to be negligible and, as such, was not considered in the refurbishment time hours. As for Configuration I, recovery is at existing airfields.

Cost of Operations -- Configuration II hardware procurement costs are summarized in Table 3-39. System operations costs are shown in Table 3-40.

Table 3-39  
HARDWARE PROCUREMENT COSTS FOR CONFIGURATION II

Item	(\$ Million)
Expendable hardware	(18.75)
First stage	9.54
Second stage	5.56
Third stage	2.10
Cargo Module	1.55
Spacecraft	36.04
Total vehicle	54.79

Table 3-40  
OPERATIONS COST FOR 50 FLIGHTS OF CONFIGURATION II

Item	(\$ Million)			
	30°		90°	
Refurbishment base*	A	B	A	B
First flight	57.79	57.79	57.71	57.71
Subsequent flight	26.48	26.59	26.40	26.51
Average flight	29.07	29.47	28.99	29.39
Total program cost	1,454	1,474	1,450	1,470

\*Refurbishment Base A: 10% of spacecraft hardware procurement

\*Refurbishment Base B: 11.2% of spacecraft hardware procurement

Reliability Assessment -- Configuration II launch vehicle reliability and individual stage reliabilities are shown in Table 3-41. These are shown for both time bases, reflecting first flight reliability and growth potential.

Table 3-41  
CONFIGURATION II RELIABILITY

Item	Base A	Base B
Launch vehicle	0.806	0.886
First stage	0.926	0.950
Second stage	0.933	0.966
Third stage	0.933	0.966

### 3.3.3.2 LORL Mission

The LORL Mission, as described in Reference 2, was used for determining the requirements and sizing of Configurations III, IV, V, and VI. Mission characteristics are summarized in Table 3-21. The four configurations listed above fulfill these mission requirements and are directly comparable so as to enable the determination of the separate effects of steering technique, launch vehicle type, spacecraft type, and the overall concept. These configurations are described in the following paragraphs.

#### Description of Configuration III

Configuration III is the BALLOS logistics vehicle studied by Lockheed Aircraft Company for use in the LORL space station logistics system. It consists of a crew module and cargo-maneuver module mounted on a Saturn IB launch vehicle. This vehicle is described in detail in Reference 2. The vehicle characteristics are summarized in Tables 3-42 and -43 and is pictured in Figure 3-85.

Spacecraft and Adapter -- The crew module is a 12-man ballistic spacecraft. It is conical in shape with a spherical segment base. The base diameter of the spacecraft is 190 in. The cargo-maneuver module is conical in shape and located immediately aft of the crew module. The conical shape adapts the 190-in. diam crew module to the 260-in. diam of the launch vehicle. This module is capable of carrying 13,455 lb of packaged cargo and 3,755 lb of maneuver propellant. This propellant is sufficient to meet the maneuvering impulsive velocity requirements of 1,050 fps which is provided by a modified LEM descent engine located in the module. Three solid-propellant retrorockets are located at the fore end of this module also.

Launch Vehicle -- The Configuration III launch vehicle is the Saturn IB vehicle consisting of a Saturn IB first stage, a S-IVB second stage, and the instrument unit. Both stages use high energy, cryogenic liquid propellants, liquid oxygen ( $\text{LO}_2$ ) and kerosene (RP-1) on the first stage and  $\text{LO}_2$  and liquid hydrogen ( $\text{LH}_2$ ) on the second stage.

The first stage is propelled by eight Rocketdyne H-1 engines which develop a total of about 1.6 million lb of thrust at liftoff. First stage usable propellant weight is approximately 882,400 lb. The outer ring of H-1 engines is hydraulically gimballed to provide thrust vector control during flight.

Table 3-42

## SUMMARY OF CHARACTERISTICS OF CONFIGURATION III

## General Characteristics

Number of crew	2 men
Number of passengers	10 men
Cargo carrying capability (packaged)	13,455 lb
Unallocated maneuver capability	--

## Dimensional Characteristics

## BALLOS Spacecraft:

Length (overall)	15.8 ft
Base diameter	190 in.
Launch escape system length	35.7 ft

## Adapter (cargo module):

Length	10.8 ft
--------	---------

## Second Stage (S-IVB)

Instrument Unit length	3.0 ft
Instrument Unit diameter	260 in.
Stage length (excluding instrument unit)	58.9 ft
Stage diameter	260 in.

## First Stage (Saturn IB)

Stage length	80.8 ft
Stage diameter	260 in.

Overall booster length	142.8 ft
Total vehicle length	193.3 ft

The second stage is powered by a single Rocketdyne J-2 engine producing 200,000 lb of thrust. Usable propellant loading on the S-IVB is approximately 228,700 lb. Restart capability on this stage is used to provide optimum trajectory profiles as well as injection capability. Pitch and yaw control is provided during flight by gimbaling the J-2 engine. Roll control during powered flight and coast, as well as pitch and yaw control during coast, is provided by two auxiliary propulsion system (APS) modules mounted on the side of the S-IVB stage.



Table 3-43  
WEIGHT SUMMARY OF CONFIGURATION III

Item	Weight (lb)
<b>Spacecraft</b>	
Structure and thermal protection	4,377
Electrical and mechanical systems	1,518
Reaction control system (dry)	235
RCS propellant	200
Landing provisions	840
Environmental control and life support	1,061
Crew and associated equipment	3,761
Growth contingencies	163
Deorbit rockets	1,010
Launch escape system	8,750
Gross weight at liftoff	21,915
<b>Adapter</b>	
Structure and subsystems	3,591
Maneuver propulsion system (dry)	804
Maneuver propellant (total)	3,835
Cargo and containers	13,455
Gross weight at liftoff	23,685
<b>Launch Vehicle</b>	
Instrument Unit	3,990
Second stage (S-IVB)	255,120
Propellant weight	230,670
First stage (Saturn IB) including interstage	1,009,930
Propellant weight	898,500
S-IVB/Saturn IB interstage	6,430
Gross launch vehicle at liftoff	1,269,040
Gross Vehicle at Liftoff	1,314,650

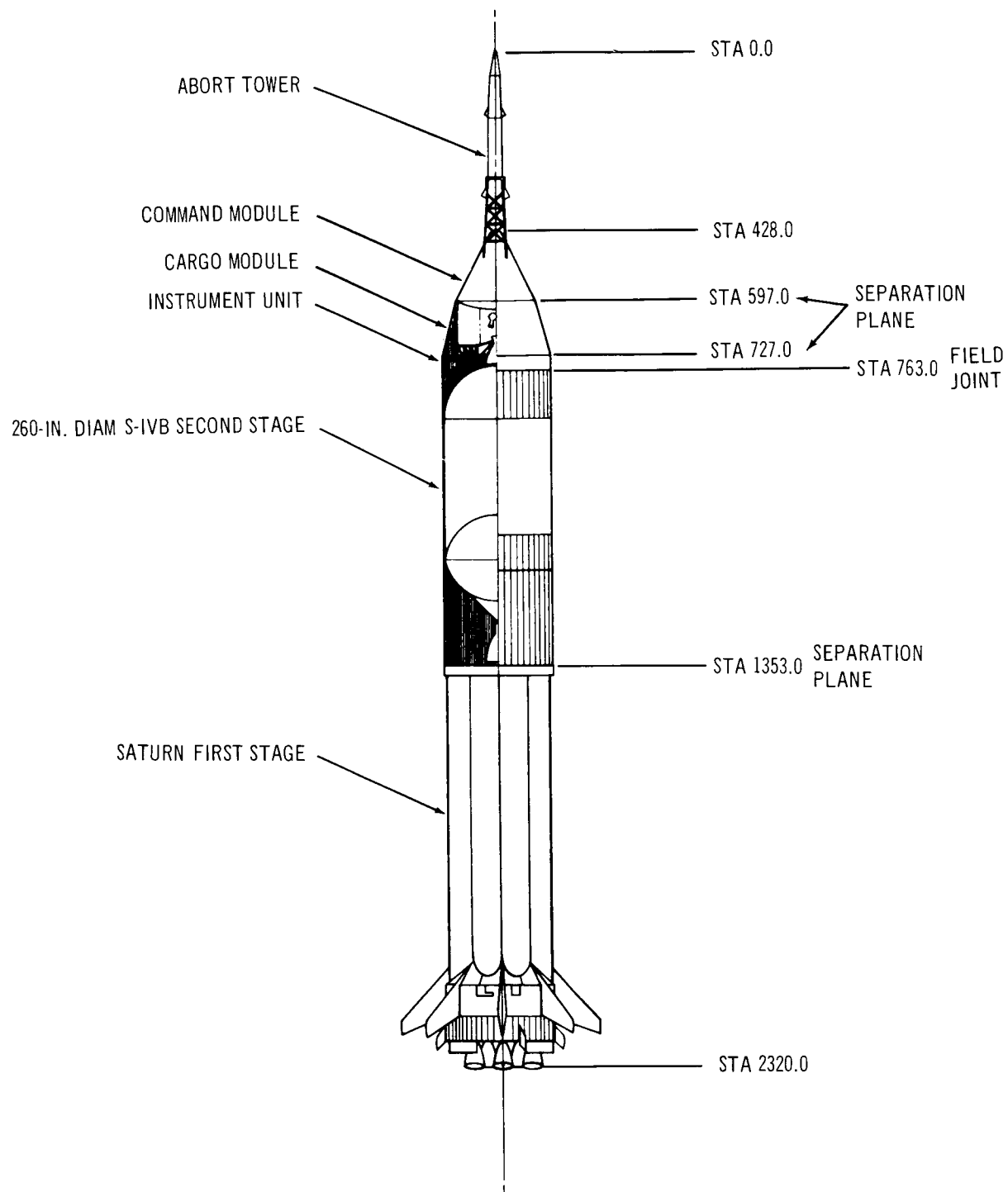


Figure 3-85. General Arrangement – Configuration III

The instrument unit houses the guidance and control systems and the flight instrumentation systems for the vehicle. It is a cylindrical section located just forward of the second stage and would be dropped with the expended S-IVB.

Abort System -- The Configuration III abort system is sized to meet both pad abort and abort during ascent requirements. It consists of a solid propellant abort motor, a tower, and a tower jettison motor which are located on the front end of the ballistic spacecraft. This system weighs 8,750 lb and provides sufficient impulse to take the spacecraft to an altitude of 5,000 ft on pad abort or to separate the spacecraft from the booster by 125 fps after firing at a condition of maximum dynamic pressure. The abort motor provides 360,000 lb of thrust for 3 sec and the tower jettison motor provides 40,000 lb of thrust for 2 sec. Approximate longitudinal acceleration during abort is 17 g's.

Performance -- This vehicle fulfills the mission requirements of delivering 12 men and 13,455 lb of packaged cargo to a space station orbiting at an altitude of 260 nmi and an inclination of  $29.5^{\circ}$ . The launch vehicle puts the spacecraft in a 105 nmi parking orbit from which a Hohmann transfer is used to reach the rendezvous altitude of 260 nmi. Impulse for the Hohmann transfer and injection into final orbit is provided for in the 1,050 fps of impulsive velocity capability of the maneuver propulsion system. Trajectory characteristics from launch to attainment of the 105-nmi parking orbit are shown in Figure 3-86. The maximum dynamic pressure of 525 psf is reached approximately 85 sec after launch. The maximum longitudinal acceleration during launch is approximately 4 g's. Performance characteristics are summarized in Tables 3-44 and 3-45.

System Operations -- On an operational basis, prelaunch preparation time for a new Configuration III spacecraft is 40 days. This time period includes receiving and shop processing prior to mating to the erected launch vehicle.

The projected 1968 to 1970 time period estimate for on-pad preparation time for the Saturn IB launch vehicle is 48 days. Of this, 23 days are allowed for payload mating and integrated vehicle checkout. The total prelaunch processing time required for the Configuration III vehicle, therefore, would be 63 days.

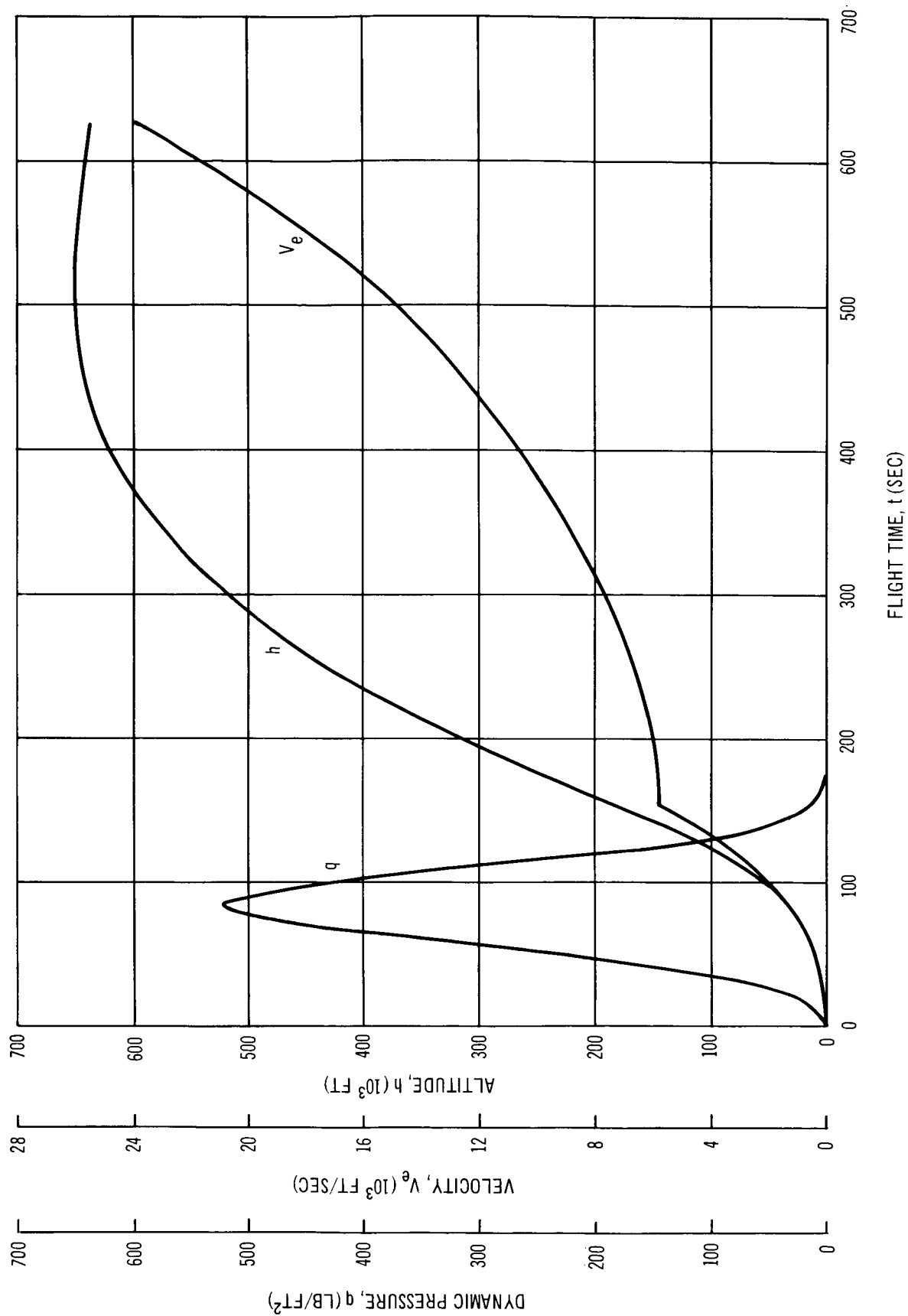


Figure 3-86. Configuration III Trajectory Characteristics

Table 3-44  
PERFORMANCE CHARACTERISTICS OF CONFIGURATION III

	First Stage	Second Stage
$T_i$	1,498,805	200,000
$T_f$	1,600,000	200,000
$I_{sp_{SL}}$	256	--
$I_{sp_{VAC}}$	291	426
$t_{Web}$	--	--
$T_{Act}$	154.0	490.0
$\lambda_M$	--	--
$\lambda_{Eff}$	0.893	0.891
$(T/W)_i$	1.153	0.658
$a_{Max}$	~ 4.0	NA
$GF_T$	35.27	--
$\eta_{PP}$	14.00	--

Recovery of the BALLOS spacecraft would be at prepared land recovery sites. The number required and associated costs are discussed in Section 3.3.2.2. Refurbishment of the recovered spacecraft requires an estimated 90 days. The total recycle time, including recovery, transportation, reprocessing, and prelaunch preparation, would be 117 days.

Cost of Operation -- Configuration III hardware procurement costs are summarized in Table 3-46. System operations costs are shown in Table 3-47.

Table 3-45  
BOOSTER SENSITIVITIES OF CONFIGURATION III

X	$\frac{\partial \Delta V}{\partial X}$	$\frac{\partial W_{PL}}{\partial X}$	$\frac{\partial X}{\partial W_{PL}}$
First-stage specific impulse	37.294 ft/sec/sec	208.955 lb/sec	0.004786 sec/lb
Second-stage specific impulse	48.668 ft/sec/sec	272.684 lb/sec	0.003667 sec/lb
First-stage propellant weight	0.007012 ft/sec/lb	0.039289 lb/sec	25.4524 lb/lb
Second-stage propellant weight	0.030718 ft/sec/lb	0.172115 lb/sec	5.8101 lb/lb
First-stage inert weight	-0.015364 ft/sec/lb	-0.086087 lb/lb	-11.616 lb/lb
Second-stage inert weight	-0.178553 ft/sec/lb	-1.00000 lb/lb	-1.000
Payload weight	-0.178476 ft/sec/lb	--	--

Table 3-46  
HARDWARE PROCUREMENT COSTS FOR CONFIGURATION III

Item	(\$ Millions)
Expendable hardware	(20.82)
Saturn IB	18.50
Cargo module	2.32
Spacecraft	19.55
Total vehicle	40.37

Table 3-47  
OPERATIONS COST FOR 50 FLIGHTS OF CONFIGURATION III

Item	(\$ Millions)			
Orbit	30°		90°	
Refurbishment base*	A	B	A	B
First flight	44.68	44.68	50.66	50.66
Subsequent flight	28.42	31.31	34.40	37.29
Average flight	29.82	32.98	35.80	38.46
Total Program Cost	1,491	1,624	1,790	1,923

\*Refurbishment Base A: 10% of spacecraft hardware procurement

\*Refurbishment Base B: 25% of spacecraft hardware procurement

Reliability Assessment--Configuration III launch vehicle reliabilities are based on available Saturn IB information and are based on the 1969 time period. The Saturn IB reliability goal is 0.90. Launch vehicle reliabilities consistent with the other configurations, excluding the instrument unit, are shown in Table 3-48.

Table 3-48  
CONFIGURATION III RELIABILITY

Item	Base A	Base B
Launch vehicle	0.918	0.918
First stage	0.950	0.950
Second stage	0.966	0.966

#### Description of Configuration IV

Configuration IV is designed to accomplish the LORL mission using the BALLOS spacecraft, head-end steering, and a solid-propellant launch vehicle. Configuration characteristics are listed in Tables 3-49 and 3-50 and the vehicle is shown in Figure 3-87.

Spacecraft and Adapter--The spacecraft is identical to that used on Configuration III. It is ballistic in type and carries 12 men, including the crew. The cargo adapter is redesigned such that its outer shell is cylindrical in shape rather than conical as is the BALLOS adapter. The 190-in. base diam of the crew module was used as the cylindrical diameter of the cargo module. Four steering engines are located around the circumference at the fore end of the cargo module at 90° intervals. These engines, rated at a maximum vacuum thrust of 21,080 lb/each, swivel  $\pm 30^\circ$  in one plane to provide pitch, yaw, and roll control during boost. The use of a steering engine nozzle expansion ratio of 18:1 results in a vacuum specific impulse of 296 sec. These engines are used to provide the 1,310 fps of impulsive velocity required for maneuvering and injection. The 5,440 lb of maneuver propellant required is carried in the forward section of the cargo adapter.

Steering System--The four engines described in the preceding paragraph are used for steering during boost. They are pump-fed engines with a chamber pressure of 800 psia. The 52,300 lb of propellant,  $N_2O_4$  and MMH, required for steering is stored in a conical adapter section located between the cargo module and the 156-in. diam second stage booster motor. The engines are



Table 3-49

## SUMMARY OF CHARACTERISTICS OF CONFIGURATION IV

## General Characteristics

Number of crew	2 men
Number of passengers	10 men
Cargo carrying capability (packaged)	13,455 lb
Unallocated maneuver capability	None
Steering engine thrust level (maximum)	21,080 lb
Number of steering engines	4

## Dimensional Characteristics

## BALLOS Spacecraft

Length (overall)	15.8 ft
Base diameter	190 in.
Launch escape system length	35.7 ft

## Adapter

Cargo-maneuver module length	17.5 ft
Cargo-maneuver module diameter	190 in.
Steering propellant module length	14.25 ft
Steering propellant module base diameter	156 in.

## Second Stage

Motor diameter	156 in.
Motor cylindrical length	14.2 ft
Stage length (to separation plane)	37.42 ft

## First Stage

Motor diameter	260 in.
Motor cylindrical length	82.9 ft
Stage length	131.50 ft
Overall booster length	168.92 ft
Total vehicle length	250.42 ft

Table 3-50  
CONFIGURATION IV WEIGHT SUMMARY

Item	Weight (lb)
<b>Spacecraft</b>	
Structure and thermal protection	4,377
Electrical and mechanical systems	1,518
Reaction control system (dry)	235
RCS propellant	200
Landing provisions	840
Environmental control and life support	1,061
Crew and associated equipment	3,761
Growth contingencies	163
Deorbit rockets	1,010
Launch escape system	8,750
Gross weight at liftoff	21,920
<b>Cargo-maneuver Module</b>	
Structure and subsystems	5,635
Maneuver propulsion system (dry)	5,800
Maneuver propellant (total)	5,540
Cargo and containers	13,455
Gross weight at liftoff	32,430
<b>Steering Propellant Module</b>	
Inert weight	7,450
Propellant (total)	53,400
First stage requirement	43,900
Second stage requirement	8,400
Gross weight at liftoff	60,850
<b>Launch Vehicle</b>	
Second stage	353,430
Gross motor weight	349,630
Propellant	306,340
Inert stage weight	3,800
First stage	3,643,120
Gross motor weight	3,613,950
Propellant	3,302,500
Inert stage weight	29,170
Gross launch vehicle weight at liftoff	3,996,550
Gross Vehicle Weight at Liftoff	4,111,750

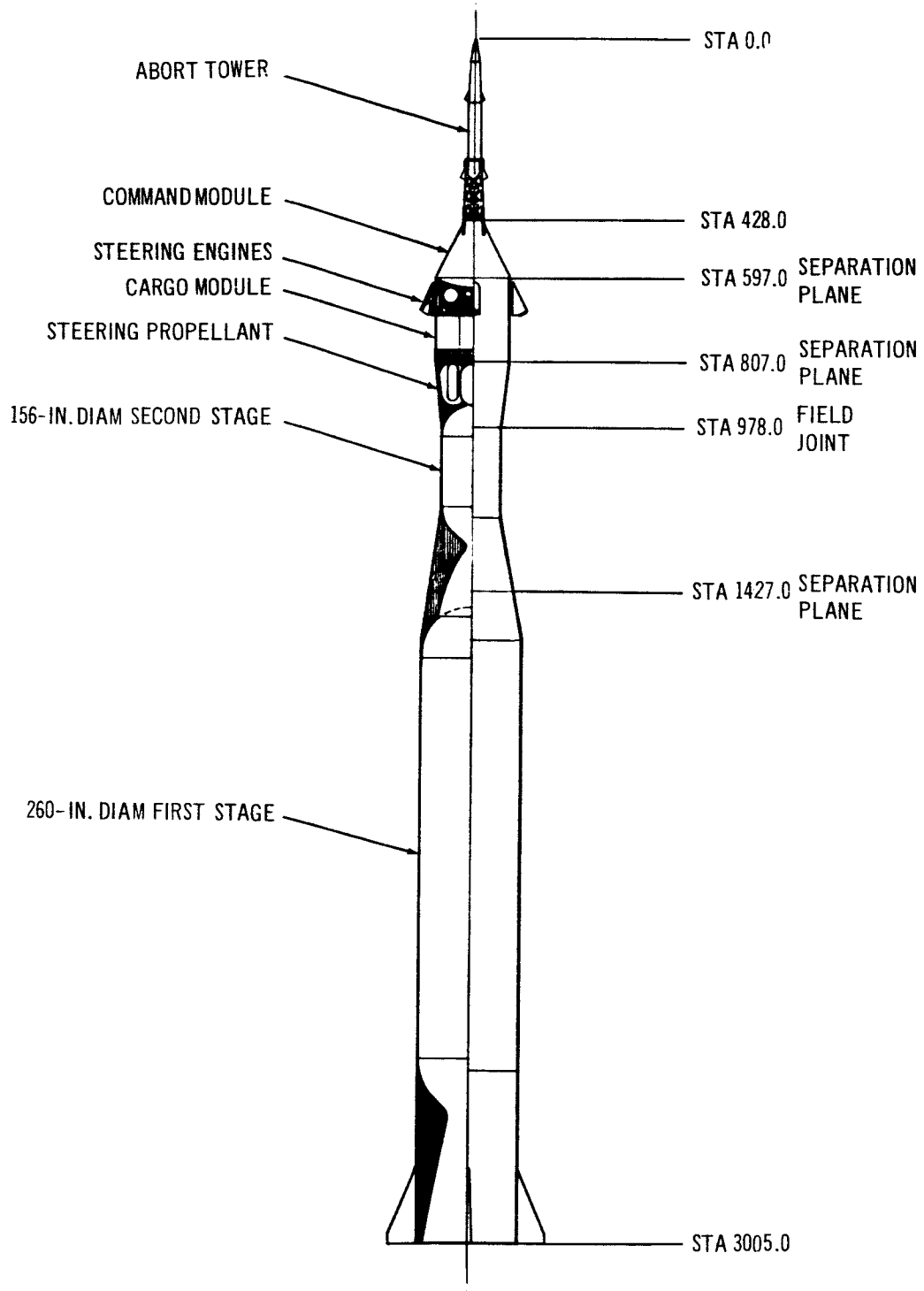


Figure 3-87. General Arrangement Configuration IV

symmetrically step throttled to meet maximum steering requirements throughout boost as shown in Figure 3-88.

Because of the symmetry of the BALLOS vehicle, minimum control thrust requirements were achieved with identical pitch and yaw fins, each having an exposed semi-span of 7.20 ft and an aspect ratio of 1.9. It will be noted from Figures 3-79 and 3-88 that the peak occurring near the end of second and third stage burn for Configuration I is not present at the end of second stage burn for Configuration IV. This is because the limitation in yaw effectiveness of Configuration I, discussed in Section 3.1.3.3, is not present when the pitch and yaw engines are separate and have equal travel. Also, the loss in effectiveness common to pitch and yaw control from forward motion of the center of gravity is compensated for by regressive burn of the second stage, as discussed in Section 3.1.2.3.

Launch Vehicle--The Configuration IV launch vehicle is composed of solid-propellant stages without steering capability.

The first stage consists of a 260-in. diam solid motor; a fixed, conical nozzle with a 10:1 expansion ratio; a conical forward skirt and a cylindrical aft skirt. The motor contains 3,302,500 lb of propellant which is designed to produce a neutral thrust-time curve with a vacuum thrust of 6,290,150 lb and a web burn time of 152 sec. A vacuum specific impulse of 274 sec is delivered by this motor.

The second stage is composed of a 156-in. solid-propellant motor, a fixed, contoured nozzle with an expansion ratio of 40:1, a conical forward skirt, and a conical aft skirt. The 306,340-lb propellant grain is tailored to provide a regressive thrust-time curve. As in Configuration I, regressivity in the upper boost stage yields a decreased disturbing moment towards the end of motor burn time, thereby decreasing the amount of control propellant required. Initial thrust is 765,700 lb and final thrust is 688,600 lb, resulting in an initial-to-final thrust ratio of 1:11:1. This regressivity ratio was found to provide for a neutral second-stage control thrust history, as was shown in Figure 3-88. Motor burn time is 122 sec and the vacuum specific impulse is 302.6 sec.

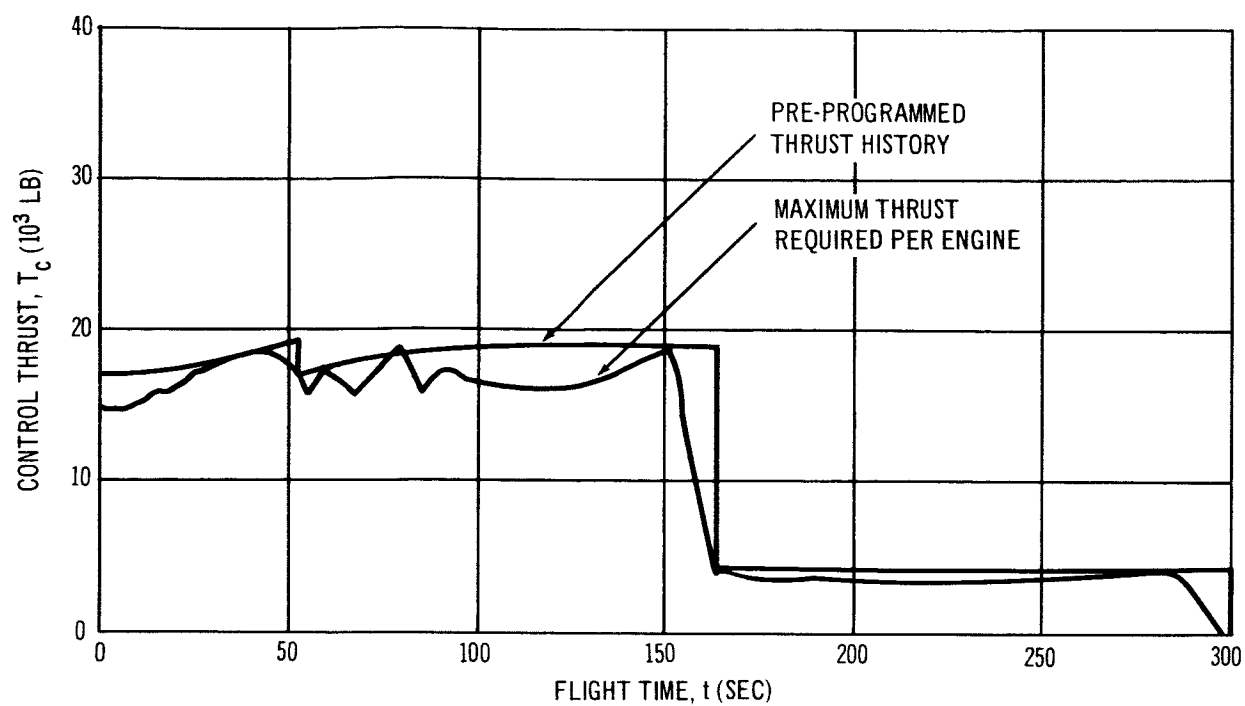


Figure 3-88. Configuration IV Control Thrust History

Abort System--A detailed investigation of the abort requirements for Configuration IV was not undertaken because of study scope limitations. Because of the similarity between the spacecraft used for Configurations III and IV, however, the same abort system weight of 8,750 lb was assumed for sizing purposes. Depending on the TNT equivalence assumed for the Configuration IV solid propellant booster, the size of the booster could necessitate a small change in abort system weight. This abort system would enable deployment of parachutes and subsequent water recovery on pad abort as did the Configuration III system.

Performance--The Configuration IV vehicle fulfills the same mission requirements as Configuration III. It delivers 2 crewmen and 10 passengers and 13,455 lb of packaged cargo to a space station in a 260-nmi circular orbit at an inclination of  $29.5^\circ$  and subsequently re-enters for a land recovery. The Configuration IV mission profile is essentially the same as Configuration III. The booster provides an apogee altitude of 105 nmi. The on-board maneuver propulsion system injects the space craft into a parking orbit and then provides impulse for a Hohmann transfer, plane change, and injection into a 260-nmi circular orbit. The trajectory characteristics are shown in Figures 3-89 and 3-90. The maximum dynamic pressure of  $940 \text{ lb/ft}^2$  is experienced 76 sec after launch. The maximum longitudinal acceleration of  $6.5 \text{ g's}$  occurs at first-stage burnout. Vehicle performance characteristics are summarized in Tables 3-51 and 3-52.

System Operations--The Configuration IV spacecraft is identical to that of Configuration III and prelaunch preparation time is also 40 days for receiving and shop processing. Checkout of the cargo-maneuver and steering propellant modules would be accomplished by parallel, time-phased operations. Mating of the spacecraft to the erected launch vehicle would occur 14 days prior to launch. Total launch vehicle processing time from receiving to launch requires 17 days, of which 11 days are required for erection and on-pad checkout. Total pad tie-up time is, therefore, 25 days and total on-site processing time for spacecraft and launch vehicle is 57 days.

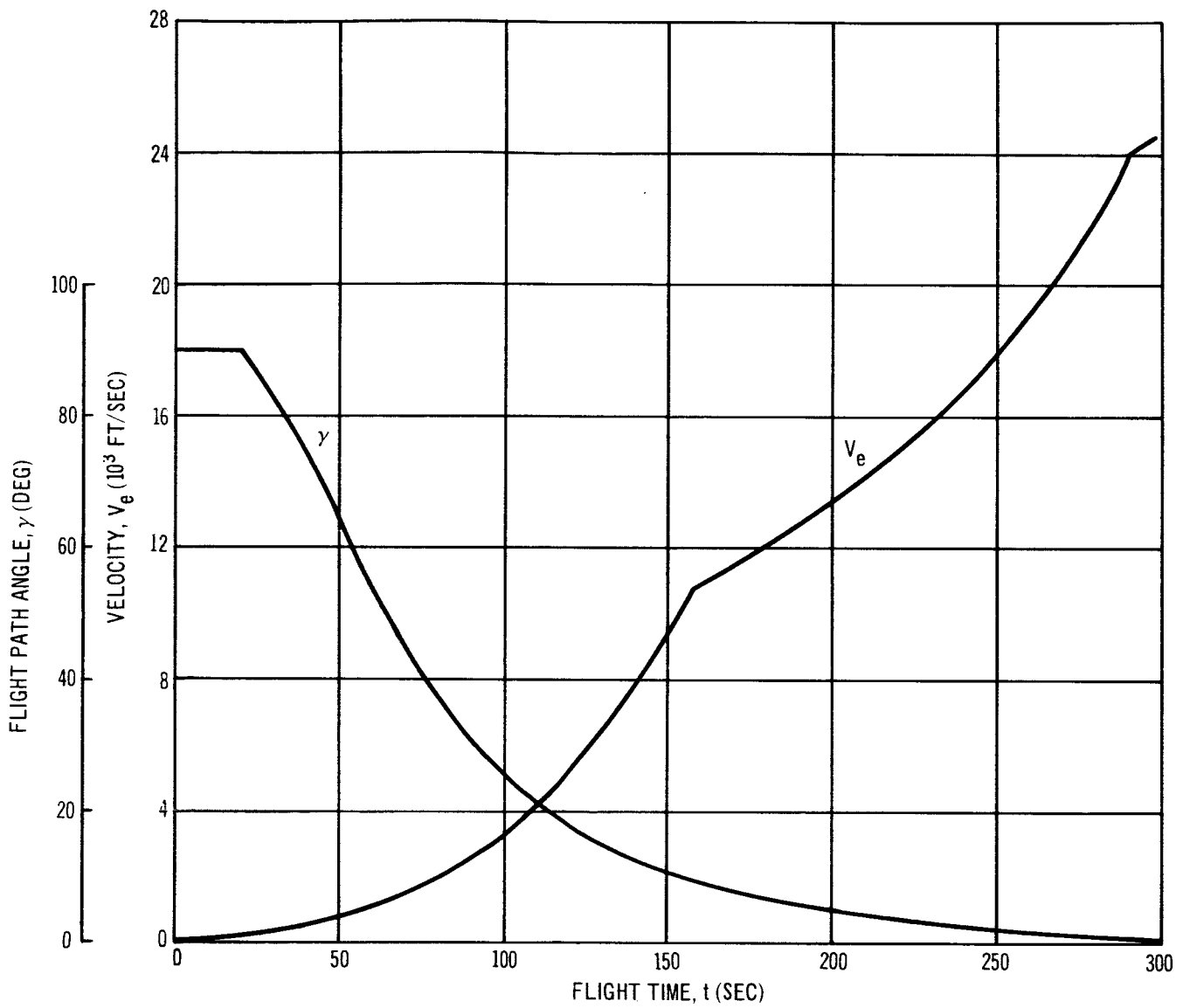


Figure 3-89. Configuration IV Trajectory Characteristics

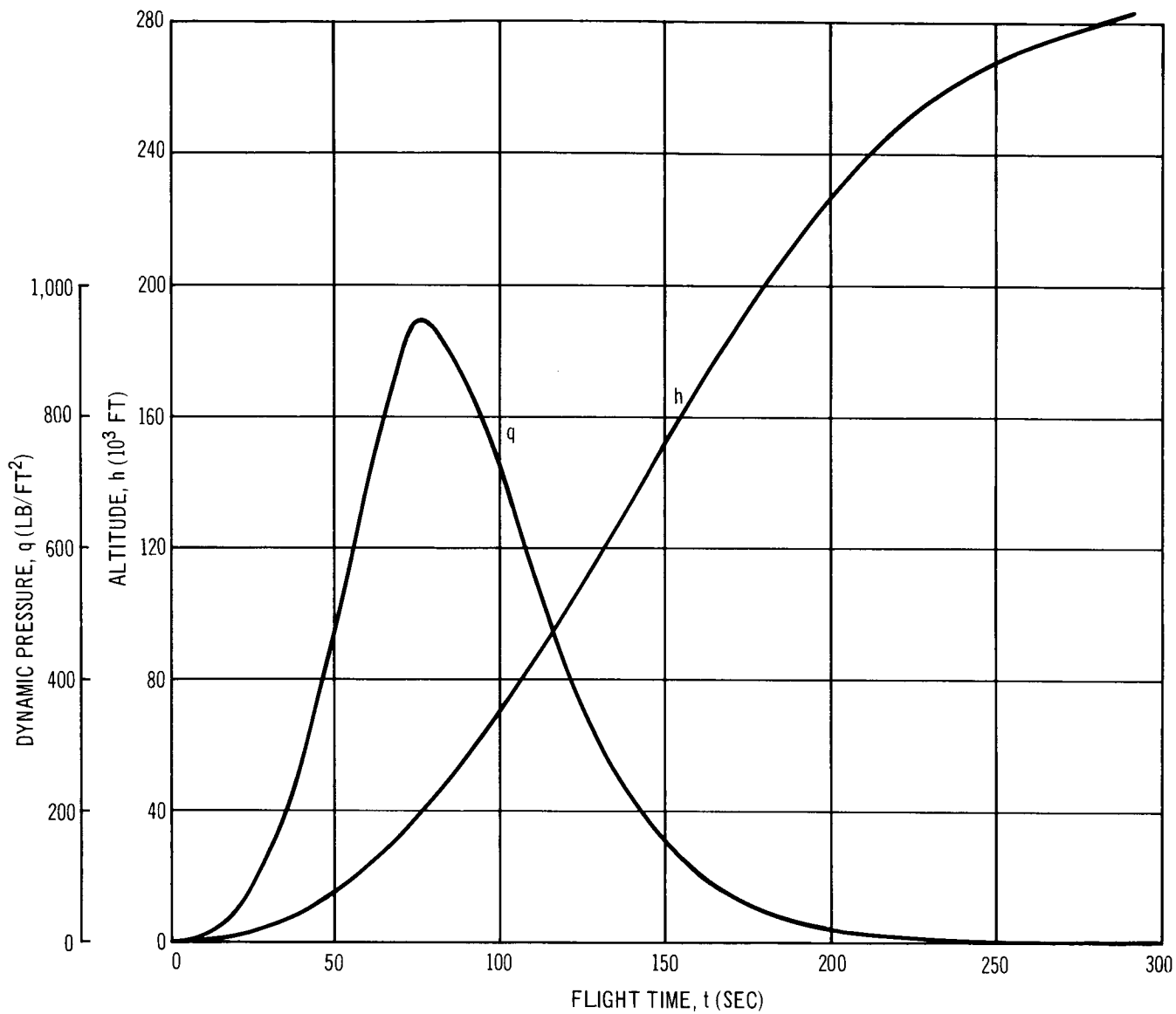


Figure 3-90. Configuration IV Trajectory Characteristics



Table 3-51  
PERFORMANCE CHARACTERISTICS OF CONFIGURATION IV

	First Stage	Second Stage
$T_i$	5,092,490	765,722
$T_f$	5,729,055	688,610
$I_{spSL}$	243.2	--
$I_{spVAC}$	273.6	302.6
$t_{Web}$	152.04	122.00
$t_{Act}$	163.39	133.61
$\lambda_M$	0.914	0.876
$\lambda'_{Eff}$	0.908	0.870
$(T/W)_i$	1.251	1.873
$a_{Max}$	6.50	6.10
$GF_T$	75.93	--
$\eta_{PP}$	9.53	--

Spacecraft recovery is accomplished at prepared land recovery sites. The total recycle time required for the recovered spacecraft is 108 days including recovery, reprocessing, and launch. Refurbishment time is estimated to be 90 days.

Cost of Operations--The estimated costs of hardware procurement for Configuration IV are shown in Table 3-53. System operations costs are summarized in Table 3-54.

Reliability Assessment--Configuration IV launch vehicle reliability, as well as individual stage reliabilities, are shown in Table 3-55. These are shown for both time bases, reflecting first-flight reliability and growth potential.

Table 3-52  
BOOSTER SENSITIVITIES OF CONFIGURATION IV

X	$\frac{\partial \Delta V}{\partial X}$	$\frac{\partial W_{PL}}{\partial X}$	$\frac{\partial X}{\partial W_{PL}}$
First-stage specific impulse	54.097 ft/sec/sec	669.24 lb/sec	0.001494 sec/lb
Second-stage specific impulse	45,457 ft/sec/sec	562.36 lb/sec	0.001778 sec/lb
First-stage propellant weight	0.002116 ft/sec/lb	0.02617 lb/lb	38.212 lb/lb
Second-stage propellant weight	0.013749 ft/sec/lb	0.17009 lb/lb	5.879 lb/lb
First-stage inert weight	-0.009263 ft/sec/lb	-0.11460 lb/lb	-8.726 lb/lb
Second-stage inert weight	-0.080833 ft/sec/lb	-1.00000 lb/lb	-1.000 lb/lb
Payload weight	-0.080833 ft/sec/lb	--	--

Table 3-53  
HARDWARE PROCUREMENT COSTS FOR CONFIGURATION IV

Items	(\$ Millions)
Expendable hardware	(14.40)
First stage	6.70
Second stage	2.34
Steering propellant tank section	0.713
Cargo module	4.61
Launch escape system	0.04
Spacecraft	19.55
Total vehicle	33.95

Table 3-54  
OPERATIONS COST FOR 50 FLIGHTS OF CONFIGURATION IV

Item	(\$ Millions)			
Orbit	30°		90°	
Refurbishment base*	A	B	A	B
First flight	38.26	38.26	44.24	44.24
Subsequent flight	21.57	24.46	27.55	30.44
Average flight	22.97	25.63	28.95	31.61
<u>Total Program Cost</u>	1,149	1,282	1,488	1,581
*Refurbishment Base A: 10% of spacecraft hardware procurement				
*Refurbishment Base B: 25% of spacecraft hardware procurement				

#### Description of Configuration

The Configuration V vehicle is composed of the BALLOS spacecraft, a cargo module, and a two-stage, solid-propellant booster with thrust vector control on each stage. This vehicle is shown in Figure 3-91 and the characteristics are listed in Tables 3-56 and 3-57.

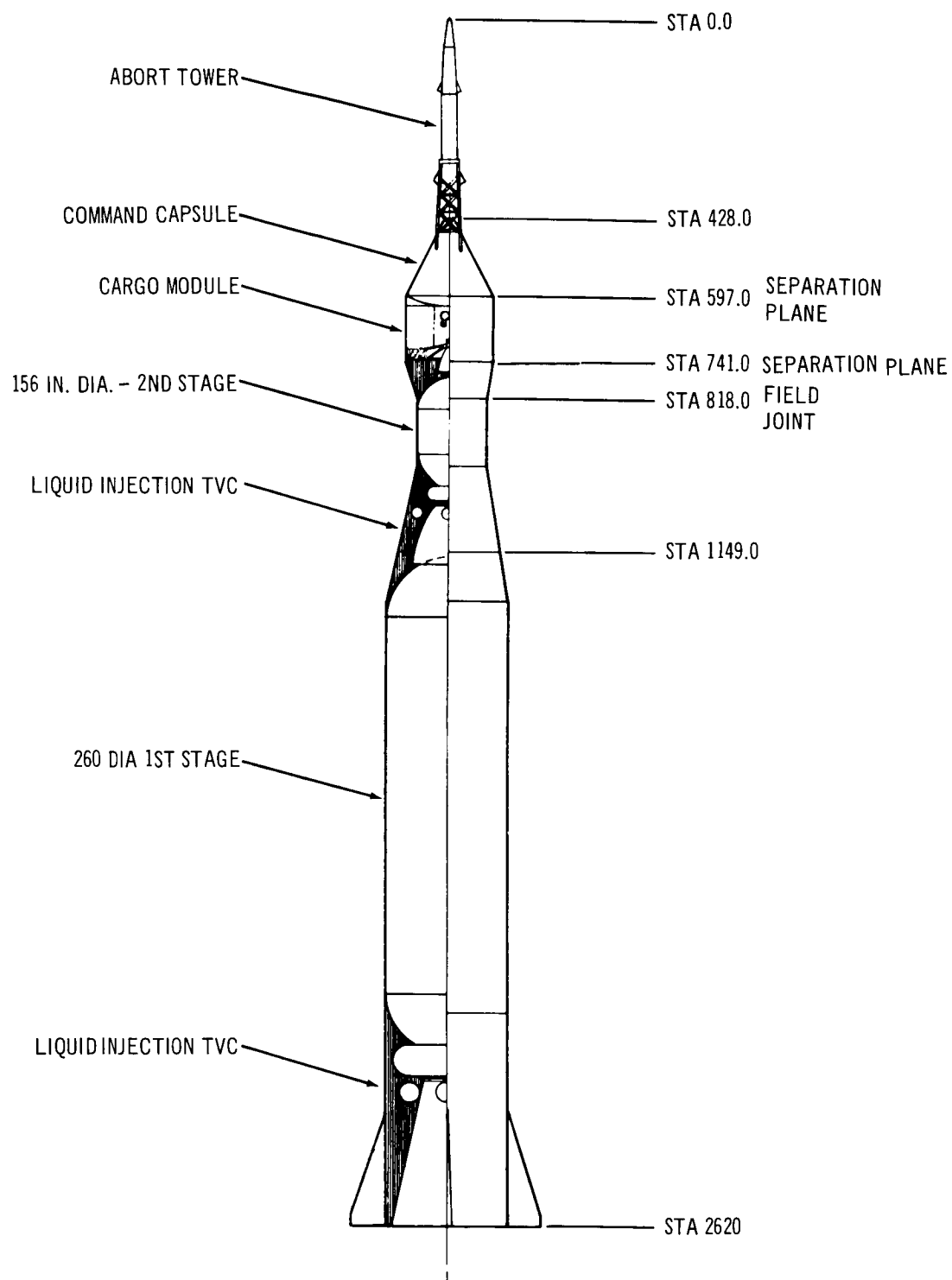


Figure 3-91. General Arrangement – Configuration V

Table 3-55  
CONFIGURATION IV RELIABILITY

Item	Base A	Base A
Launch vehicle	0.893	0.913
First stage	0.971	0.980
Second stage	0.978	0.986
Steering system	0.940	0.945

Spacecraft and Adapter--The BALLOS crew module, as used in Configurations III and IV, is used for this configuration. The cargo module differs from that used for Configuration IV in that the steering engines are eliminated and the maneuver engine used by Configuration III has been added. The 190-in. base diam of the crew module is the cylindrical diameter of the cargo module. A conical skirt is used to adapt the cargo module to the 156-in. diam of the second-stage booster.

Launch Vehicle--The Configuration V launch vehicle is a two-stage solid propellant vehicle incorporating a liquid injection thrust vector control system and a storable liquid, bipropellant roll control system on each stage.

The first stage is a 260-in. diam motor with a 10:1 expansion ratio conical nozzle, a conical forward skirt, and a cylindrical aft skirt. The neutral burning propellant grain weighs 2,857,300 lb and has a web burn time of 152 sec. Delivered vacuum thrust is 5,027,960 lb and vacuum specific impulse is 277 sec. The weight of the expendable liquid injectant ( $N_2O_4$ ) is 9,500 lb and 750 lb of  $N_2O_4$  and MMH is required for roll control. Both control systems are located in the free volume between the nozzle and aft skirt. Because of the symmetry of the BALLOS vehicle, minimum control requirements were achieved with identical pitch and yaw fins, each having an exposed semispan of 6.05 ft and an aspect ratio of 1:2. Optimization of the fin size was accomplished by minimizing the area under the curve of equivalent engine gimbale angle as a function of time. This area is a measure of the control fuel required.

Table 3-56  
SUMMARY OF CHARACTERISTICS OF CONFIGURATION V

General characteristics	
Number of crew	2 men
Number of passengers	10 men
Cargo carrying capability	13,455 lb
Unallocated maneuver capability	--
Dimensional characteristics:	
BALLOS spacecraft	
Length (overall)	15.8 ft
Base diameter	190 in.
Launch escape system length	35.7 ft
Adapter	
Cargo-maneuver module diameter	190 in.
Cargo-maneuver module length	12.00 ft
Overall adapter length	18.42 ft
Second stage	
Motor diameter	156 in.
Motor cylindrical length	8.2 ft
Overall stage length	27.58 ft
First stage	
Motor diameter	260 in.
Motor cylindrical length	68.4 ft
Overall stage length	122.58 ft
Overall booster length	150.17 ft
Total vehicle length	218.33 ft

The second stage is a 156-in. motor, with a contoured nozzle of 40:1 expansion ratio, and conical forward and aft skirts. The 225,450-lb propellant grain is tailored to provide constant thrust over a 120-sec web burn time. Vacuum thrust for this motor is 546,100 lb and the delivered vacuum specific impulse is 301 sec. The thrust vector control system requires 1,900 lb of expendable injectant and the roll control system requires 230 lb of expendable propellant.

Abort System--The Configuration V abort system, as used for vehicle sizing, is the same as those for Configurations III and IV. Because of the study scope limitations, Configuration V abort requirements were not investigated in detail; however, the similarity in spacecraft provided the rationale for use of

Table 3-57  
WEIGHT SUMMARY OF CONFIGURATION V

Item	Weight (lb)
Spacecraft	
Structure and thermal protection	4,377
Electrical and mechanical systems	1,518
Reaction control system (dry)	235
RCS Propellant	200
Landing provisions	840
Environmental control and life support	1,061
Crew and associated equipment	3,761
Growth contingencies	163
Deorbit rockets	1,010
Launch escape system	8,750
Gross weight at liftoff	21,915
Adapter	
Structure and subsystems	3,908
Maneuver propulsion system (dry)	857
Maneuver propellant (total)	4,650
Cargo and containers	13,455
Aft adapter	600
Gross weight at liftoff	23,470
Launch Vehicle	
Second stage	267,610
Gross motor weight	260,520
Propellant	225,450
Thrust vector control system	3,410
Liquid injectant* (usable)	2,130
Inert stage weight	3,680
First stage	3,178,300
Gross motor weight	3,130,050
Propellant	2,857,300
Thrust vector control	18,850
Liquid injectant* (usable)	10,250
Inert-stage weight	29,400
Gross launch vehicle weight at liftoff	3,445,910
Gross vehicle at liftoff	3,493,300

---

\*Includes roll-control propellant.

---

the 8,750-lb BALLOS abort system. Although the amount of propellant contained in the booster motors is less than that of Configuration IV, the maximum dynamic pressure is slightly higher; consequently, a detailed study would be necessary to adjust the abort system weight used. This was not felt to be justified. As for Configurations III and IV, this abort system must provide sufficient altitude on pad abort to allow parachute deployment and adequate separation velocity at maximum dynamic pressure abort.

Performance--This vehicle performs the BALLOS mission of resupplying the LORL space station. As with Configurations III and IV, 12 men and 13,455 lb of packaged cargo are delivered to a 260 nmi circular orbit at 29.5° inclination with subsequent reentry and land recovery. The mission profile is also the same as that of Configuration IV. Boost to a 105-nmi apogee altitude is accomplished by the launch vehicle with injection, Hohmann transfer, and plane-change impulse being supplied by the on-board propulsion system located in the cargo-maneuver module. Trajectory characteristics are shown in Figures 3-92 and 3-93. The maximum dynamic pressure of 970 lb/ft<sup>2</sup> is experienced 77 sec after launch. The maximum longitudinal acceleration of 6.9 g's occurs at first-stage burnout. Vehicle performance characteristics are shown in Tables 3-58 and 3-59.

Systems Operations--The new Configuration V spacecraft, identical to those of Configurations III and IV, requires 40 days for receiving and shop processing operations. Spacecraft mating to the erected launch vehicle will occur 14 days prior to launch. Prelaunch preparation time for the launch vehicle requires a total of 21 days, 13 days of which requires pad tie-up. Additional time required for checkout of the TVC and roll control systems was estimated at 2 days in the receiving and assembly area and 2 days on the pad. The resultant total processing time for the spacecraft and launch vehicle is 61 days. Total pad occupancy time is 29 days.

Recovered spacecraft recycle time requires 110 days from recovery at land sites through processing and launch. Refurbishment of the spacecraft requires 90 days.

Cost of Operations--Configuration V hardware procurement costs are summarized in Table 3-60. The costs of system operations are summarized in Table 3-61.



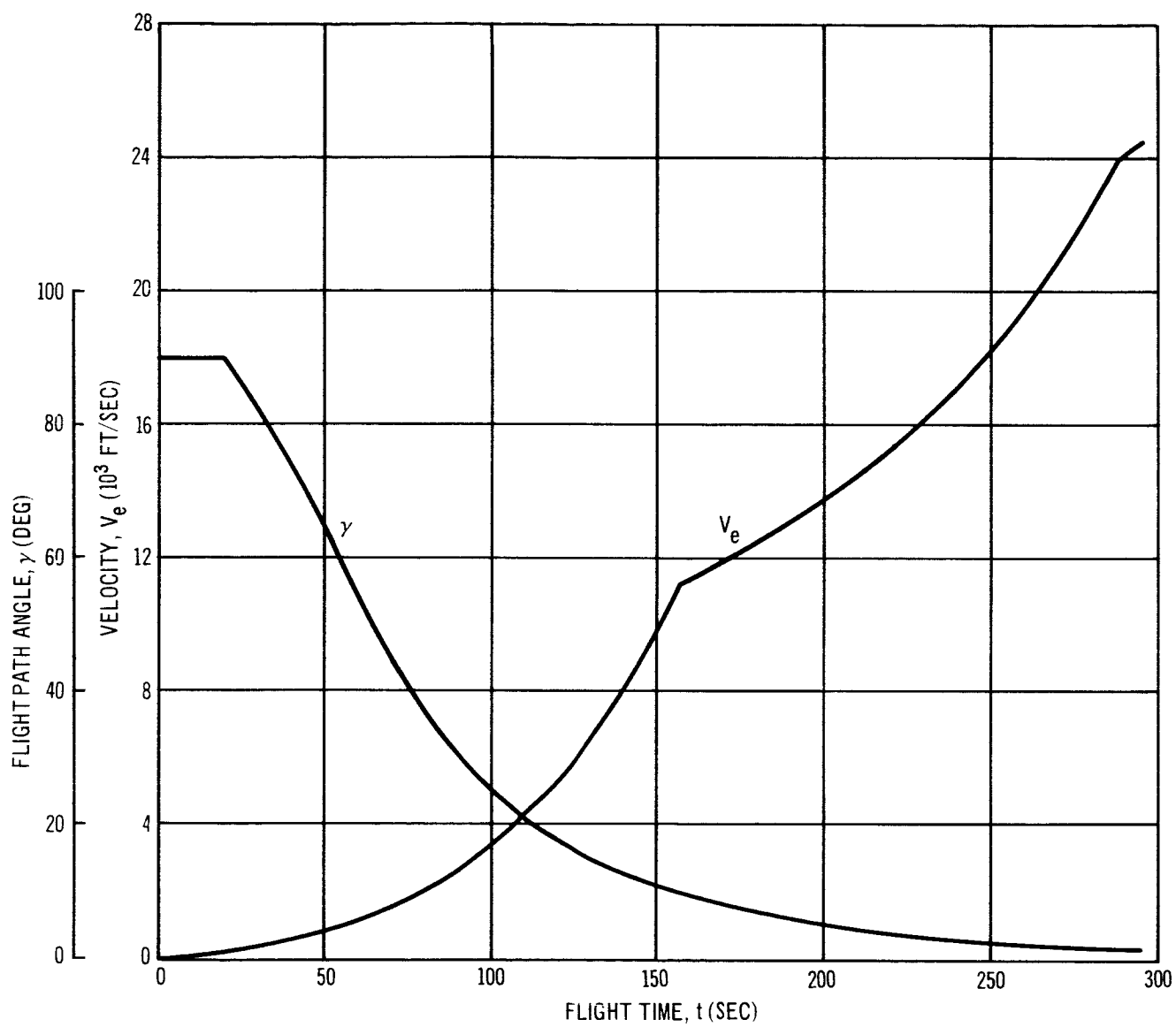


Figure 3-92. Configuration V Trajectory Characteristics

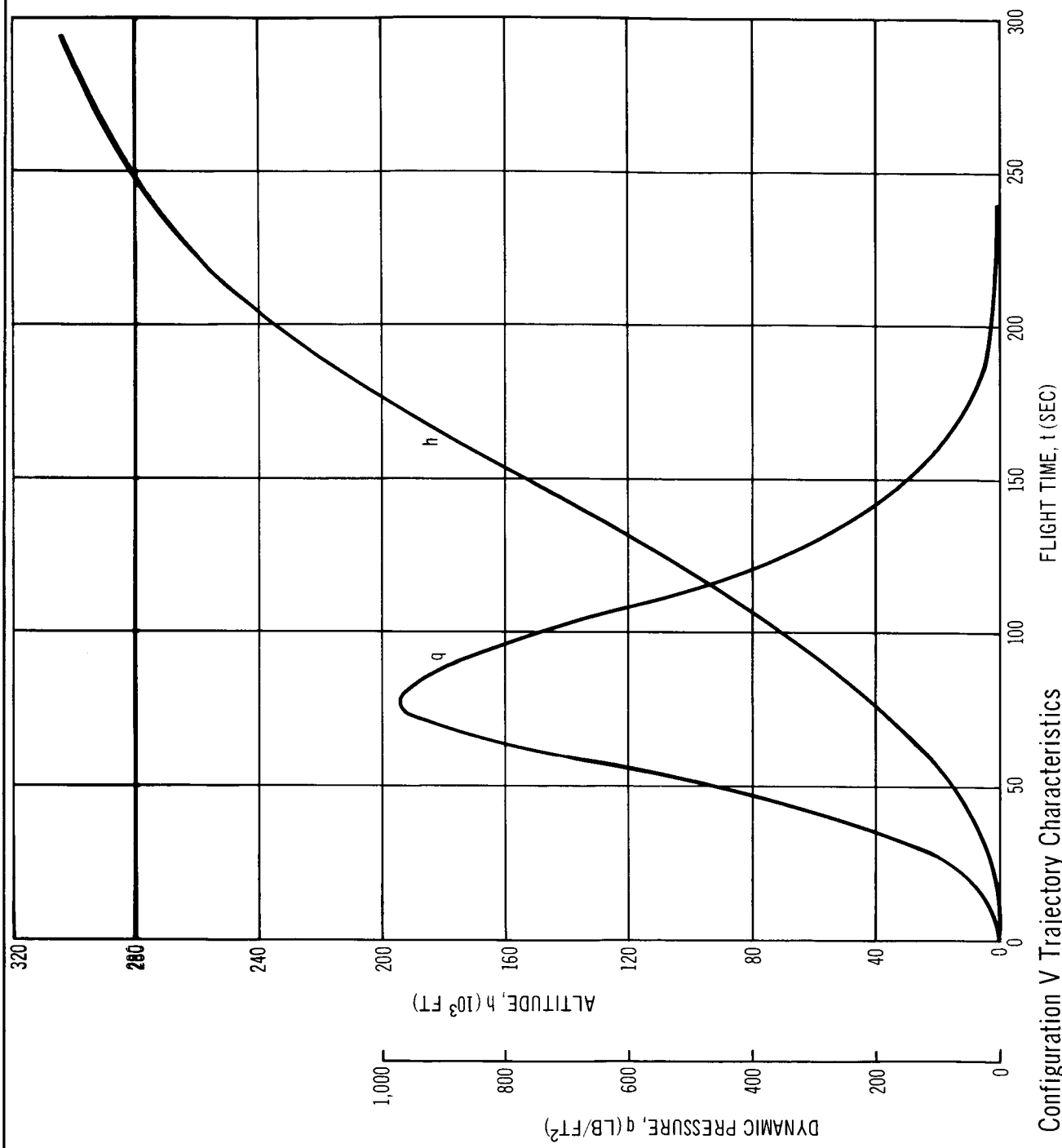


Figure 3-93. Configuration V Trajectory Characteristics

Table 3-58  
PERFORMANCE CHARACTERISTICS OF CONFIGURATION V

	First Stage	Second Stage
$T_i$	4,366,625	546,086
$T_f$	5,027,960	546,086
$I_{spSL}$	240.5	--
$I_{spVAC}$	276.9	301.0
$t_{Web}$	152.22	120.00
$t_{Act}$	163.59	130.79
$\lambda_M$	0.913	0.865
$\lambda'_{Eff}$	0.902	0.850
$(T/W)_i$	1.250	1.783
$a_{Max.}$	6.86	6.16
$GF_T$	90.41	--
$\eta_{PP}$	13.35	--

Reliability Assessment--Configuration V launch vehicle and stage reliabilities are shown in Table 3-62. These are shown for both time bases, reflecting first flight reliability levels and growth potential.

Table 3-59  
BOOSTER SENSITIVITIES OF CONFIGURATION V

X	$\frac{\partial \Delta V}{\partial X}$	$\frac{\partial W_{PL}}{\partial X}$	$\frac{\partial X}{\partial W_{PL}}$
First-stage specific impulse	55.328 ft/sec/sec	538.24 lb/sec	0.001858 lb/lb
Second-stage specific impulse	43.729 ft/sec/sec	425.40 lb/sec	0.002351 lb/lb
First-stage propellant weight	0.002539 ft/sec/lb	0.02470 lb/lb	40.486 lb/lb
Second-stage propellant weight	0.019813 ft/sec/lb	0.19274 lb/lb	5.188 lb/lb
First-stage inert weight	-0.011651 ft/sec/lb	-0.11334 lb/lb	-8.823 lb/lb
Second-stage inert weight	-0.102795 ft/sec/lb	-1.00000 lb/lb	-1.000 lb/lb
Payload weight	-0.102795 ft/sec/lb	--	--

Table 3-60  
HARDWARE PROCUREMENT COSTS FOR CONFIGURATION V

Item	(\$ Millions)
Expendable hardware	(12.86)
First stage	7.87
Second stage	2.42
Cargo module	2.57
Spacecraft	19.55
Total vehicle	32.41

Table 3-61  
OPERATIONS COST FOR 50 FLIGHTS OF CONFIGURATION V

Item	(\$ Millions)			
Orbit	300		900	
Refurbishment base*	A	B	A	B
First flight	36.72	36.72	42.70	42.70
Subsequent flight	19.98	22.87	25.96	28.85
Average flight	21.38	24.04	27.36	30.02
Total Program Cost	1,069	1,202	1,368	1,501

\*Refurbishment Base A: 10% of spacecraft hardware procurement

\*Refurbishment Base B: 25% of spacecraft hardware procurement

Table 3-62  
CONFIGURATION V RELIABILITY

Item	Base A	Base B
Launch vehicle	0.864	0.918
First stage	0.926	0.950
Second stage	0.933	0.966

## Description of Configuration VI

The Configuration VI vehicle consists of an HL-10 type lifting body spacecraft, a cargo module, a steering propellant module, and a two-stage, solid-propellant launch vehicle. The vehicle incorporates the head-end steering concept for control during boost. The launch vehicle is shown in Figure 3-94 and its characteristics are listed in Tables 3-63 and 3-64.

Spacecraft and Adapter -- The Configuration VI crew module was designed as the minimum sized HL-10 spacecraft which would carry 2 crewmen and 11 personnel. This resulted in a 28-ft, 9-in. spacecraft as shown in Figure 3-73. The HL-10 is not designed to carry cargo or maneuver propellant internally. However, two steering engines are incorporated in the outboard sections of the HL-10 trailing edge. These engines are located in pods which can gimbal in two planes when the fins are rotated forward similar to the steering engine arrangement on the Configuration I spacecraft. The steering engines are also to provide thrust for in-space maneuvering.

Maneuver propellant and cargo are carried in a module located immediately aft of the HL-10. This cargo-maneuver module is also shown in Figure 3-73. The 4,980-lb of maneuver propellant,  $N_2O_4$  and MMH, are located in the conical, forward section of the module in common bulkhead tanks. The 13,455 lb of packaged cargo required for the LORL logistics mission is carried in the aft section of this module. Egress is permitted from the HL-10 through the module and through a hatch at the aft end of the module by means of a cylindrical, 30-in. dia tunnel. A docking station is located at this hatch to facilitate the rendezvous and docking maneuver.

Steering System -- As indicated in the preceding paragraphs, two steering engines are located in the HL-10 spacecraft. These engines have a maximum vacuum thrust of 21,050 lb/engine and can be gimbaled  $\pm 30^\circ$  in two planes. The symmetrical, step throttling history required, shown with the boost steering thrust requirements in Figure 3-95 assumes throttling capacity to 16% of full thrust. The engines are turbo-pump fed and operate at a chamber pressure of 800 psia. The nozzle expansion ratio of 18:1 results in a delivered vacuum specific impulse of 296 sec.

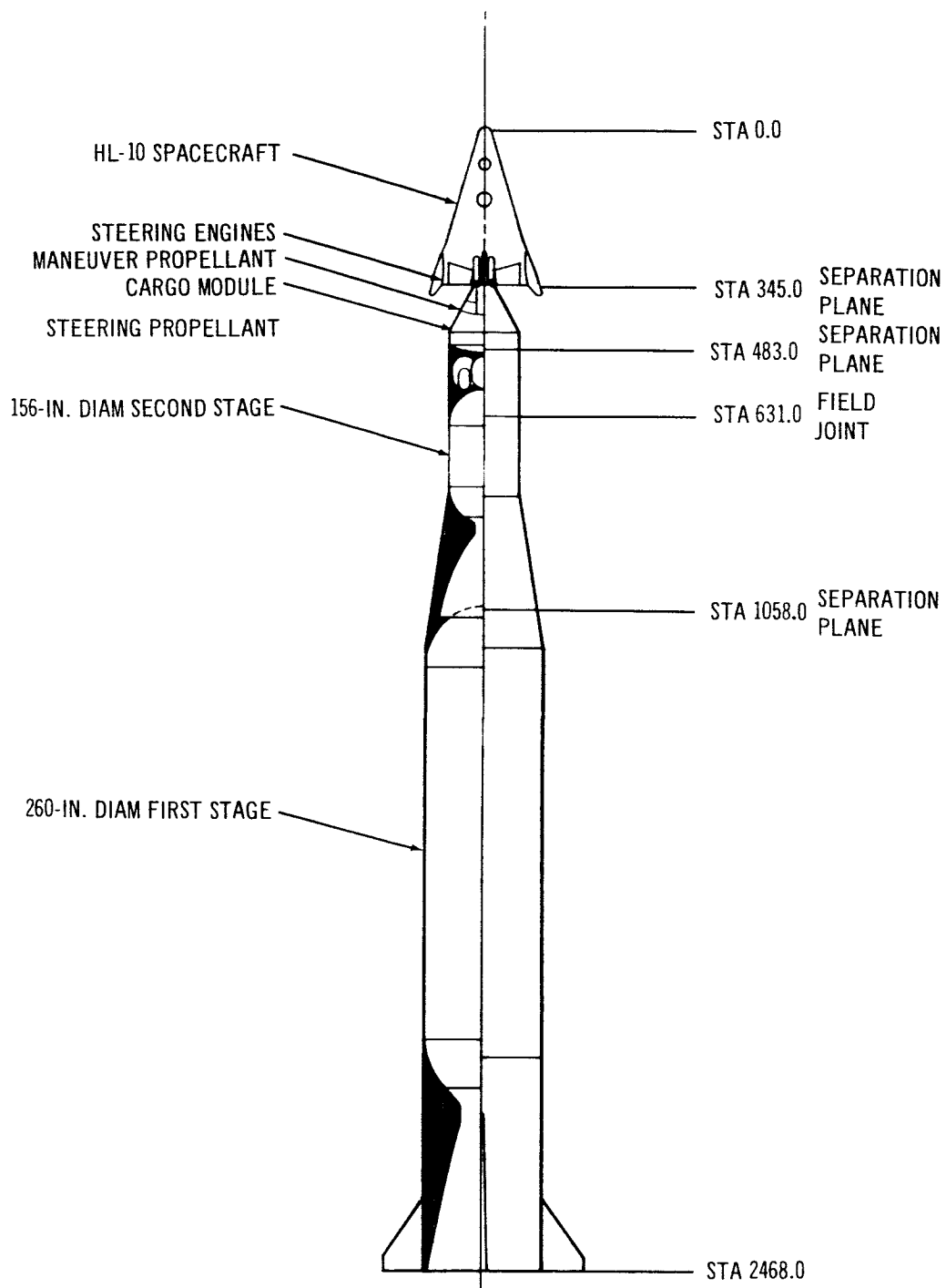


Figure 3-94. General Arrangement - Configuration VI

Table 3-63

## SUMMARY OF CHARACTERISTICS OF CONFIGURATION VI

## General characteristics

Number of crew	1 man
Number of passengers	11 men
Cargo carrying capability (packaged)	13,455 lb
Unallocated maneuver capability	--
Steering engine thrust level (maximum)	21,050 lb
Number of steering engines	2

## Dimensional characteristics

## HL-10 spacecraft:

Length	28.67 ft
Span	18.44 ft
Planform area	293 sq ft

## Adapter

Cylindrical diameter	156 in.
Cargo-maneuver module total length	14.0 ft
Steering propellant module length	12.33 ft
Overall length to field joint	23.83 ft

## Second stage

Diameter	156 in.
Cylindrical motor length	11.0 ft
Overall length	35.58 ft

## First stage

Diameter	260 in.
Cylindrical motor length	65.5 ft
Overall length	117.50 ft

Overall booster length	153.08 ft
Total vehicle length	205.67 ft

The 25,400 lb of steering propellant required by this configuration is contained in a module located between the cargo-maneuver module and the second-stage booster motor. The  $N_2O_4$  and MMH is carried in four cylindrical tanks which are plumbed through the cargo module to the steering engines which operate throughout boost.



Table 3-64  
WEIGHT SUMMARY OF CONFIGURATION VI

Item	Weight (lb)
<b>Spacecraft</b>	
Structure and thermal protection	5,510
Electrical and mechanical subsystems	1,410
Reaction control system (dry)	150
RCS propellant	70
Propulsion system (dry)	800
Landing provisions	870
Environmental control and life support	580
Crew and associated equipment	3,070
Growth contingencies	790
Deorbit rockets	1,480
Abort rockets (additional)	740
Gross weight at liftoff	15,470
<b>Cargo-maneuver module</b>	
Structure and subsystems	5,355
Maneuver propellant (total)	5,080
Cargo (packaged)	13,455
Gross weight at liftoff	23,890
<b>Steering propellant module</b>	
Structure and subsystems	4,280
Steering propellant (total)	25,900
First stage requirement	20,800
Second stage requirement	4,600
Gross weight at liftoff	30,180
<b>Launch vehicle</b>	
Second stage	299,560
Gross motor weight	295,880
Propellant	257,550
Inert stage weight	3,680
First stage	3,051,950
Gross motor weight	3,026,550
Propellant	2,761,950
Inert stage weight	25,400
Gross launch vehicle weight at liftoff	3,351,510
Gross vehicle weight at liftoff	3,423,050

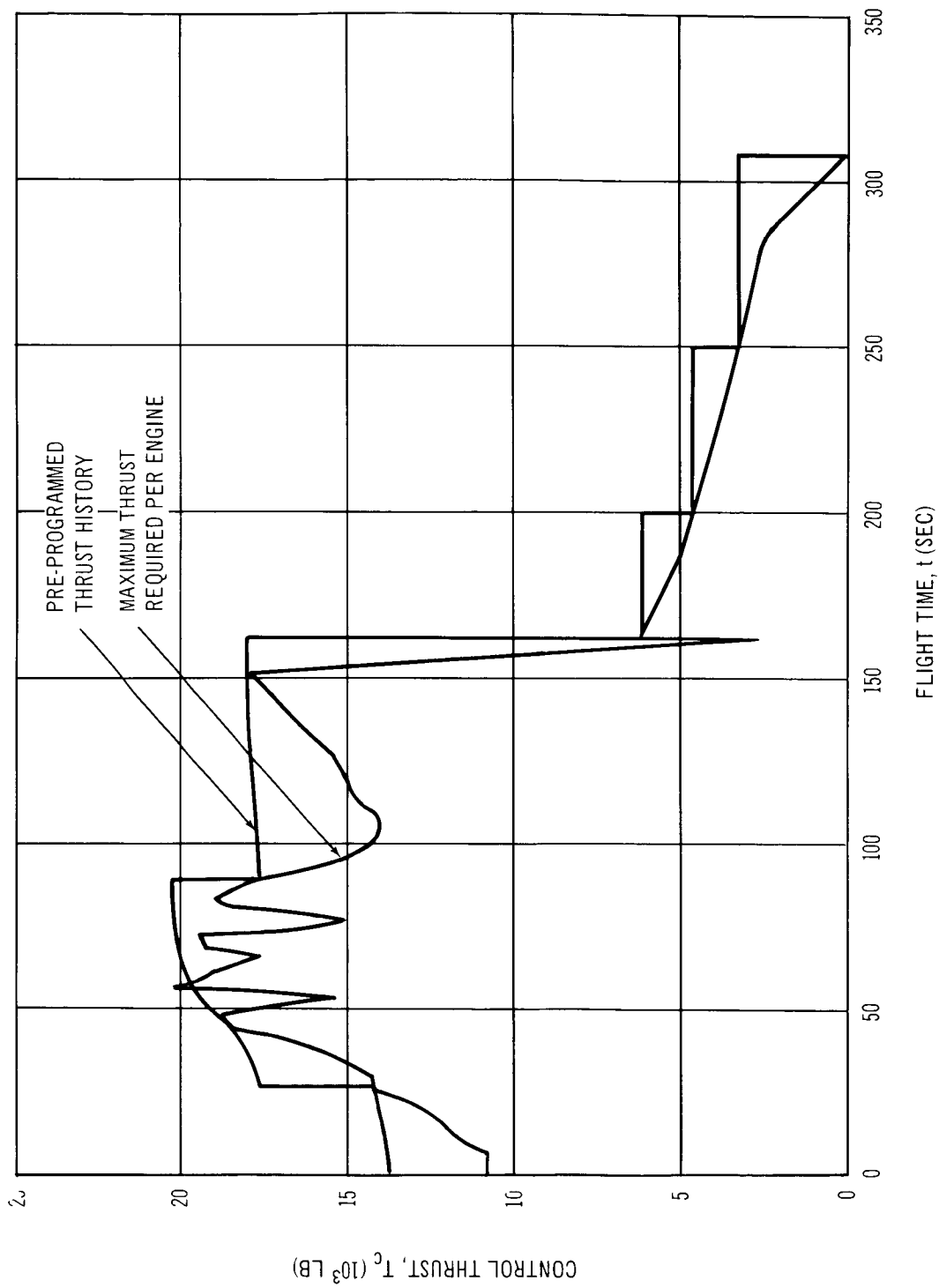


Figure 3-95. Configuration VI Control Thrust History

Aerodynamic fins mounted on the first stage skirt were sized to minimize control requirements during boost. Minimum control thrust requirements were achieved with pitch fins having an exposed semispan of 9.5 ft and an aspect ratio of 2.875 and yaw fins having an exposed semispan of 7.0 ft and an aspect ratio of 1.0. The control thrust requirements are shown in Figure 3-95. It will be noted that the peak occurring near the end of second- and third-stage burn for Configuration I is not present at the end of second-stage burn for Configuration VI. In fact, the control thrust requirement continuously decreases throughout second stage because of two factors. First, the CG remains relatively far aft, so the yaw control effectiveness does not decrease in the same degree as for Configuration I. Secondly, the second-stage engine regressivity is so great that the moment requirements due to engine misalignment and eccentricity decrease more than the control effectiveness. The regressivity could be changed to flatten out the required thrust curve for second stage; however, the total area under the curve would not change appreciably. Thus, there would be little, if any, decrease in control fuel requirements.

Launch Vehicle -- The Configuration VI launch vehicle consists of two solid-propellant vehicle stages which utilize head-end steering for control.

The first stage is composed of a 260-in. diam motor with a 10:1 expansion ratio, fixed, conical nozzle, a conical forward skirt, and a cylindrical aft skirt. The motor contains 2,761,950 lb of propellant which is designed into a neutral burning grain. The motor produces 4,902,150 lb of thrust at vacuum conditions for a web burn time of 150.7 sec. The vacuum specific portion of flight requires 20,800 lb of steering propellant.

The second stage consists of (1) a 156-in. diam motor with a 40:1 expansion ratio, fixed, contoured nozzle, (2) a cylindrical forward skirt, and (3) a conical aft skirt. The 257,550-lb propellant grain is tailored to produce a regressive thrust-time history over the 122-sec web burn time. Initial thrust is 932,170 lb and final thrust is 290,400 lb. As can be seen from Figure 3-95, this regressivity ratio of 3.2:1 results in a regressive control thrust requirement history. Tailoring of the second-stage propellant grain to produce less regressivity should result in a neutral control thrust history and a slight reduction in the steering propellant quantity required. Vacuum specific impulse developed by this motor is 303 sec.

Abort System -- The Configuration VI abort system was sized to provide an adequate thrust-to-weight ratio and apogee altitude for a 4-sec warning time escape from a detonation of the booster on the pad. With subsequent optimization and resizing of the launch vehicle, the abort system weight of 2,200 lb, which was used for all sizing, has become quite conservative. This abort system consists of six cylindrical, solid-propellant rocket motors mounted on the aft upper and lower surfaces of the HL-10. Two of these motors will be jettisoned shortly after first-stage booster burnout and the remaining four used to provide deorbit impulse prior to re-entry or high-altitude abort impulse.

Because of the relatively high lift-to-drag ratio of the HL-10 spacecraft, a vertical ascent abort trajectory with subsequent glide away from the pad area can be used to minimize the abort impulse required.

Performance -- Although the Configuration VI spacecraft is of the lifting body rather than ballistic type, the mission performed is identical. The vehicle is capable of delivering 2 crewmen and 10 passengers and 13,455 lb of packaged cargo to a space station orbiting at an altitude of 260 nmi and an inclination of 29.5°. The mission profile consists of a boost to an apogee altitude of 105 nmi, injection into a parking orbit with subsequent Hohman transfer, plane change, and injection at 260 nmi. Booster burnout and drop would occur prior to attainment of the 105-nmi apogee with subsequent impulse requirements provided by the maneuver propulsion system. Trajectory characteristics are shown in Figures 3-96 and 3-97. Maximum dynamic pressure for this vehicle is 1,020 lb/ft<sup>2</sup>, and occurs 78 sec after launch. The maximum longitudinal acceleration of 6.4 g's occurs at first stage burn-out. Vehicle performance characteristics are shown in Tables 3-65 and 3-66.

System Operations -- New spacecraft prelaunch preparation time was estimated to be the same as Configuration I. Although the Configuration VI spacecraft does not have the on-board maneuver propellant tankage system of Configuration I (consequently requiring less system checkout time) the same extent of parallel checkout on Configuration I is not possible because of the lack of capability to split the spacecraft. The estimated receiving and shop processing time requirement is 32.5 days. Spacecraft mating and on-pad checkout time required is 14 days.

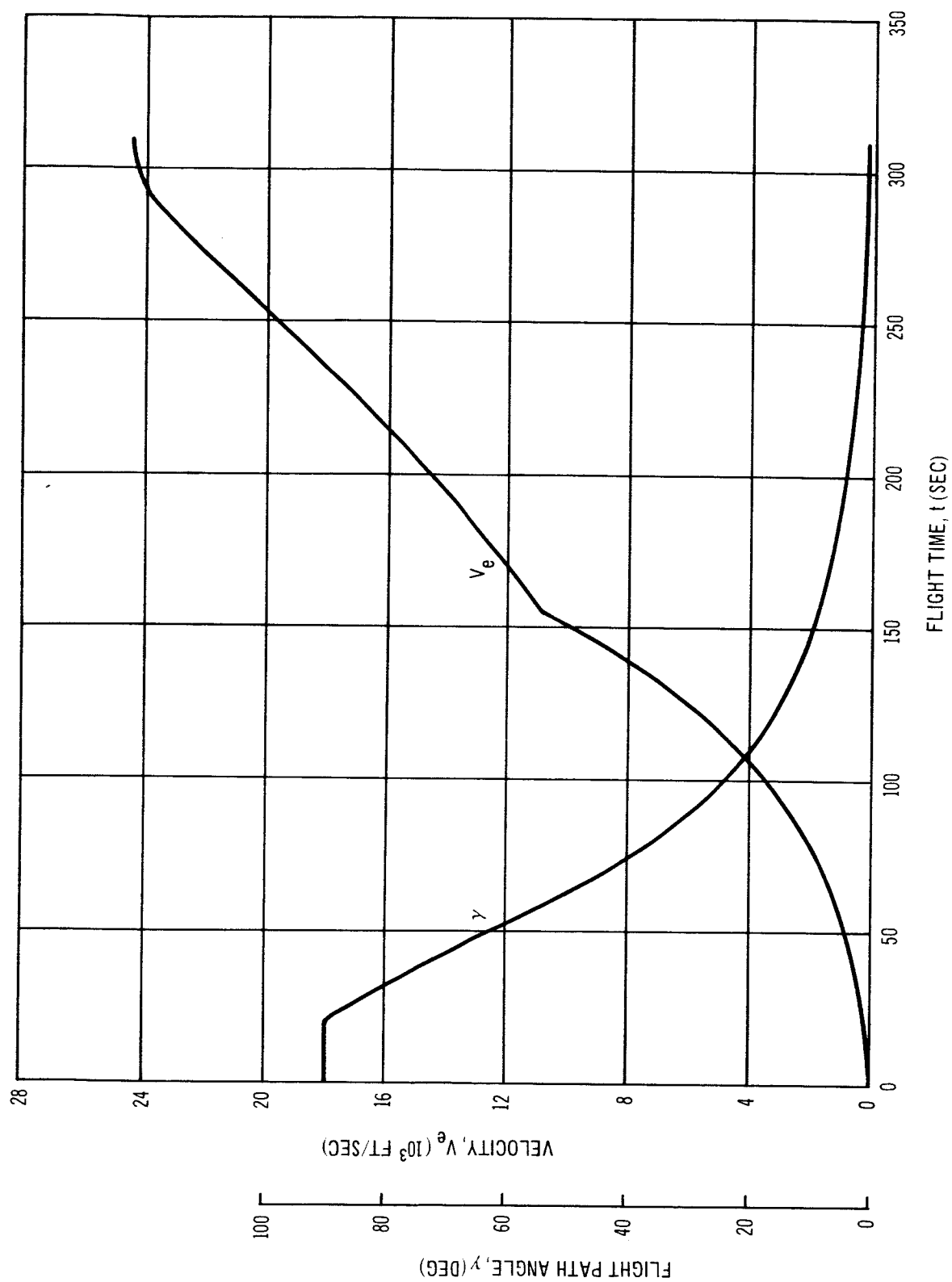


Figure 3-96. Configuration VI Trajectory Characteristics

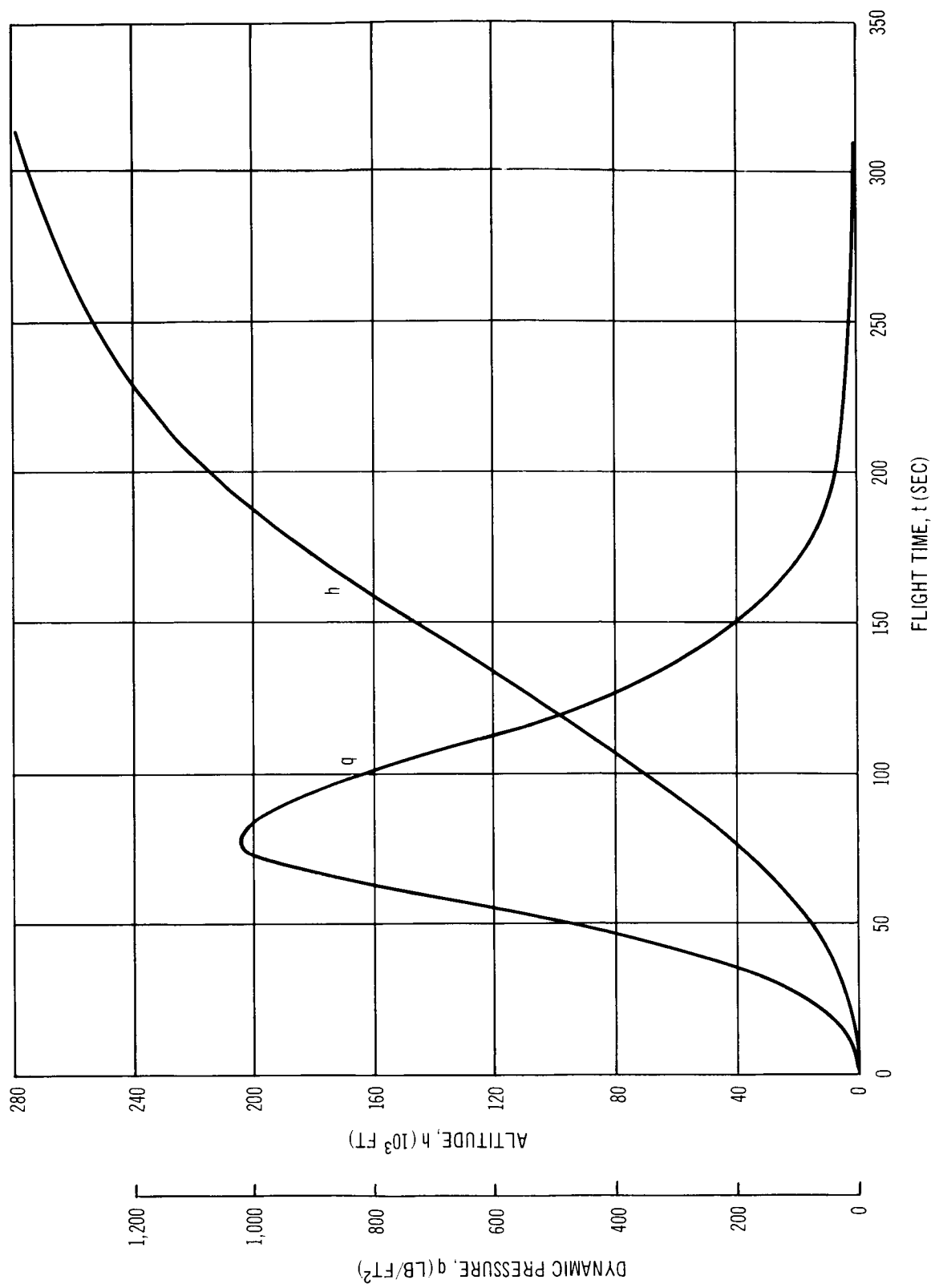


Figure 3-97. Configuration VI Trajectory Characteristics

Table 3-65  
PERFORMANCE CHARACTERISTICS OF CONFIGURATION VI

	First Stage	Second Stage
$T_i$	4, 257, 366	932, 171
$T_f$	4, 902, 153	290, 396
$I_{spSL}$	241.0	302.6
$I_{spVAC}$	277.5	302.6
$t_{Web}$	150.72	122.00
$t_{Act}$	161.98	145.20
$\lambda_M$	0.913	0.870
$\lambda'_{Eff}$	0.906	0.862
$(T/W)_i$	1.250	2.702
$a_{Max.}$	6.62	3.34
$GF_T$	75.40	--
$n_{PP}$	11.37	--

Launch vehicle preparation time is 16 days, of which 10 days would require pad occupancy. Total spacecraft and launch vehicle prelaunch preparation is 48.5 days, and total pad occupancy time would be 24 days for this configuration.

As for Configuration I, recycle time of the Configuration VI spacecraft is 44 days, 4.5 days of which is required for recovery site processing and transportation. Recovery is accomplished at existing airfields. The total recycle time through launch is 54 days, of which pad occupancy requires 24 days.

Table 3-66  
BOOSTER SENSITIVITIES OF CONFIGURATION VI

X	$\frac{\partial \Delta V}{\partial X}$	$\frac{\partial W_{PL}}{\partial X}$	$\frac{\partial X}{\partial W_{PL}}$
First-stage specific impulse	53.942 ft/sec/sec	583.21 lb/sec	0.001715 sec/lb
Second-stage specific impulse	44.721 ft/sec/sec	483.50 lb/sec	0.002068 sec/lb
First-stage propellant weight	0.002541 ft/sec/lb	0.02747 lb/lb	36.403 lb/lb
Second-stage propellant weight	0.015936 ft/sec/lb	0.17230 lb/lb	5.804 lb/lb
First-stage inert weight	-0.011062 ft/sec/lb	-0.01196 lb/lb	-8.361 lb/lb
Second-stage inert weight	-0.092551 ft/sec/lb	-1.00000 lb/lb	-1.000 lb/lb
Payload weight	-0.0929931 ft/sec/lb	--	--



Cost of Operations -- Configuration VI hardware procurement costs are summarized in Table 3-67. The costs of system operations are shown in Table 3-68.

Table 3-67  
HARDWARE PROCUREMENT COSTS FOR CONFIGURATION VI

Item	(\$ Million)
Expendable hardware	(10.83)
First stage	5.87
Second stage	2.03
Steering propellant tank section	.484
Cargo module	2.45
Spacecraft	23.04
Total vehicle	33.87

Table 3-68  
OPERATIONS COST FOR 50 FLIGHTS OF CONFIGURATION VI

Orbit	30°		90°	
Refurbishment base*	A	B	A	B
First flight	36.87	36.87	36.79	36.79
Subsequent flight	16.78	17.25	16.70	17.17
Average flight	18.44	18.87	18.36	18.79
Total program cost	922	944	918	940

\*Refurbishment Base A: 10% of spacecraft hardware procurement

\*Refurbishment Base B: 12% of spacecraft hardware procurement

Reliability Assessment -- Configuration VI launch vehicle and stage reliabilities are shown in Table 3-69. These are shown for both time bases, reflecting first flight reliability and growth potential.

Table 3-69  
CONFIGURATION VI RELIABILITY

Item	Base A	Base B
Launch vehicle	0.903	0.933
First stage	0.971	0.980
Second stage	0.978	0.986
Steering system	0.950	0.966

### 3.3.3.3 Extended MORL Type Mission

This mission is essentially identical to that of extended MORL. As indicated in Table 3-21, orbital altitude, inclination, and other characteristics are the same, with the exception of the unallocated maneuver capability available after injection. This is necessitated by the slight reduction in performance capability of the Configuration VII vehicle, which is based on the studies reported in Reference 3. The Configuration VIII payload was designed to satisfy the same mission requirements as Configuration VII.

#### Description of Configuration VII

Configuration VII consists of a 44-ft HL-10 spacecraft, a cargo module, a steering propellant module, a Saturn S-IVB second stage with instrumentation unit, and a solid-propellant first stage. This vehicle is similar, but not identical, to the vehicle studied by Douglas for NASA-Marshall and reported on in Reference 3. This vehicle is shown in Figure 3-98 and its characteristics are listed in Tables 3-70 and 3-71.

Spacecraft and Adapter -- The spacecraft is the 44 ft HL-10 used for Configuration I. The maneuver propellant tanks on board the spacecraft are off-loaded to carry 39,500 lb of usable propellant instead of 43,000 lb for the nominal mission. The two steering engines would have a maximum thrust at vacuum conditions of 35,800 lb each.

The cargo module is designed to the same volume and load requirements as Configurations I and II. The available pressurized volume provides capability for carrying 18,750 lb of packaged cargo, access through the cargo module from the HL-10 to the space station, and a docking station to facilitate rendezvous and docking. This module differs from the Configuration I cargo module in that its entire length is conical in order to provide an adapter between the HL-10 spacecraft and the 260-in. diam of the S-IVB stage.

Steering System -- Although this vehicle incorporates head-end steering, the gimbal engine capability of the S-IVB is used for pitch and yaw control during second-stage operation. Second-stage roll control capability is provided by the existing S-IVB auxiliary propulsion system.

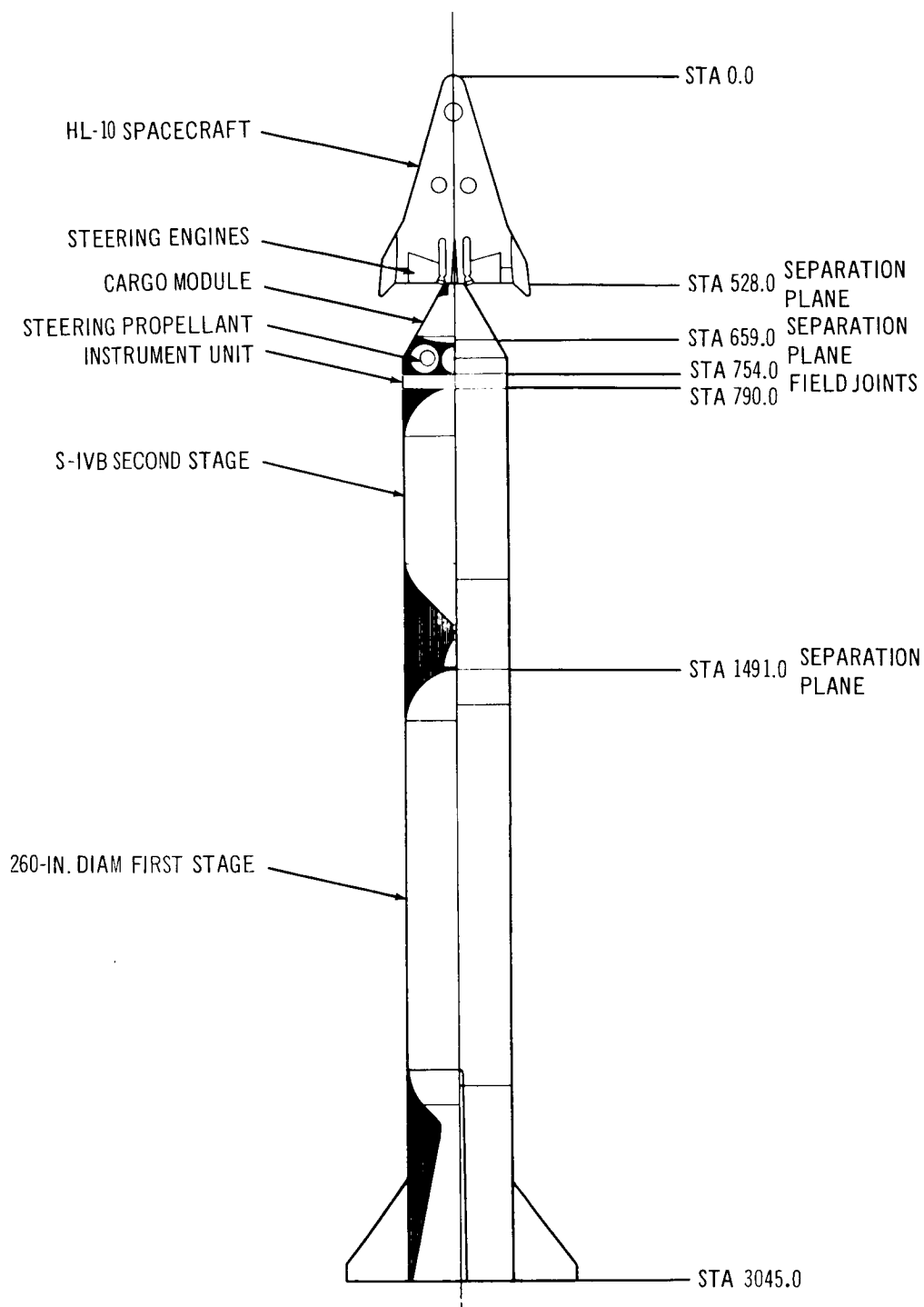


Figure 3-98. General Arrangement – Configuration VII

Table 3-70

## SUMMARY OF CHARACTERISTICS OF CONFIGURATION VII

## General characteristics:

Number of crew	2 men
Number of passengers:	
Nominal (crew compartment)	6 men
Maximum (including cargo compartment)	9-11 men
Cargo carrying capability:	
On-board HL-10 (packaged, Vol. = 250 ft. <sup>3</sup> )	5,000 lb
In cargo compartment (packaged, Vol. = 938 ft. <sup>3</sup> )	18,750 lb
Maneuver engine thrust level (2 engines)	35,800 lb
Unallocated maneuver capability in orbit	3,320 fps

## Dimensional characteristics:

## HL-10 spacecraft:

Length	44.0 ft
Span	28.3 ft
Planform area	690 sq ft

## Adapter:

Cylindrical diameter	260 in.
Cargo module total length	13.42 ft
Steering propellant module length	7.91 ft
Overall length to field joint	18.83 ft

## Second stage (S-IVB):

Instrument Unit diameter	260 in.
Instrument Unit length	3.0 ft
Stage diameter	260 in.
Stage length (excluding instrument unit)	49.2 ft

## First stage:

Diameter	260 in.
Cylindrical motor length	74.9 ft
Stage length	129.5 ft

Overall booster length	190.92 ft
Total vehicle length	253.75 ft

Table 3-71  
WEIGHT SUMMARY OF CONFIGURATION VII

Item	Weight (lb)
Spacecraft:	
Structure and thermal protection	16,010
Electrical and mechanical subsystems	3,280
Propulsion system (dry)	3,540
Maneuver propellant (total)	40,400
Reaction control system (dry)	750
RCS propellant	2,000
Landing provisions	2,840
Environmental control and life support	2,100
Crew and associated equipment	2,150
Growth contingencies	5,830
Cargo (packaged)	5,000
Abort rockets	6,300
Gross weight at liftoff	90,200
Adapter:	
Cargo module (empty)	3,600
Cargo (baseline mission)	0
Gross cargo module at liftoff	3,600
Steering propellant module (dry)	5,770
Steering propellant (total)	27,150
First stage requirement	26,350
Second stage requirement	0
Gross steering module at liftoff	32,920
Launch vehicle:	
Instrument Unit	3,990
Second stage (S-IVB)	258,650
Propellant	229,155
First stage (including interstage)	3,305,430
Gross motor weight	3,274,000
Propellant	2,990,000
Inert stage weight	31,430
Gross launch vehicle at liftoff	3,568,070
Gross vehicle at liftoff	3,694,790

Control during first stage is provided by the head-end steering system. The 26,350 lb of usable propellant required is carried in four spherical tanks located between the cargo module and the second stage. The propellants used are  $N_2O_4$  and MMH. These tanks would be plumbed through the cargo module to the pump-fed engines located on the spacecraft. These engines would be capable of gimbaling  $\pm 30^\circ$  in two planes when the fins are rotated forward. Throttling capability of 56% of full thrust would be provided to meet the symmetrical step throttling curve shown in Figure 3-99. The control-thrust history required during first-stage operation is also shown in this figure. Control thrust requirements were minimized by utilizing pitch fins having an exposed semispan of 15.5 ft and an aspect ratio of 3:0 and yaw fins with an exposed semispan of 11.0 ft and an aspect ratio of 1.0.

Launch Vehicle -- As previously discussed, the launch vehicle consists of a S-IVB second stage and instrument unit and a solid-propellant first stage.

The first stage is composed of a 260-in. dia solid-propellant motor with a 10:1 expansion ratio; a fixed, conical nozzle; a cylindrical forward skirt; and a cylindrical aft skirt. The 2,940,000-lb propellant grain is tailored to provide a neutral thrust-time history over the 131.6-sec web burn time. The vacuum thrust developed is 5,975,000 lb and the vacuum specific impulse is 278 sec.

The second stage consists of the S-IVB stage, a cylindrical aft skirt which is separated with the first stage, and an instrumentation unit. The 229,150 lb of  $LO_2$  and  $LH_2$  used as propellant provides both second-stage boost impulse to a 105 nmi parking orbit and impulse for injection into a transfer orbit to and circularization at 300 nmi. The gimbal engine and auxiliary propulsion system provide control during boost and coast phases.

Abort System -- The Configuration VII abort requirements were assumed to be essentially the same as those for Configuration I and, consequently, the same abort system was used for sizing purposes. This system consists of seven cylindrical solid-propellant motors mounted on the upper and lower aft surfaces of the HL-10. These motors, along with the steering engines, would provide sufficient impulse on pad abort to reach a cruising altitude which would enable horizontal land recovery. Under abort conditions at the time of maximum

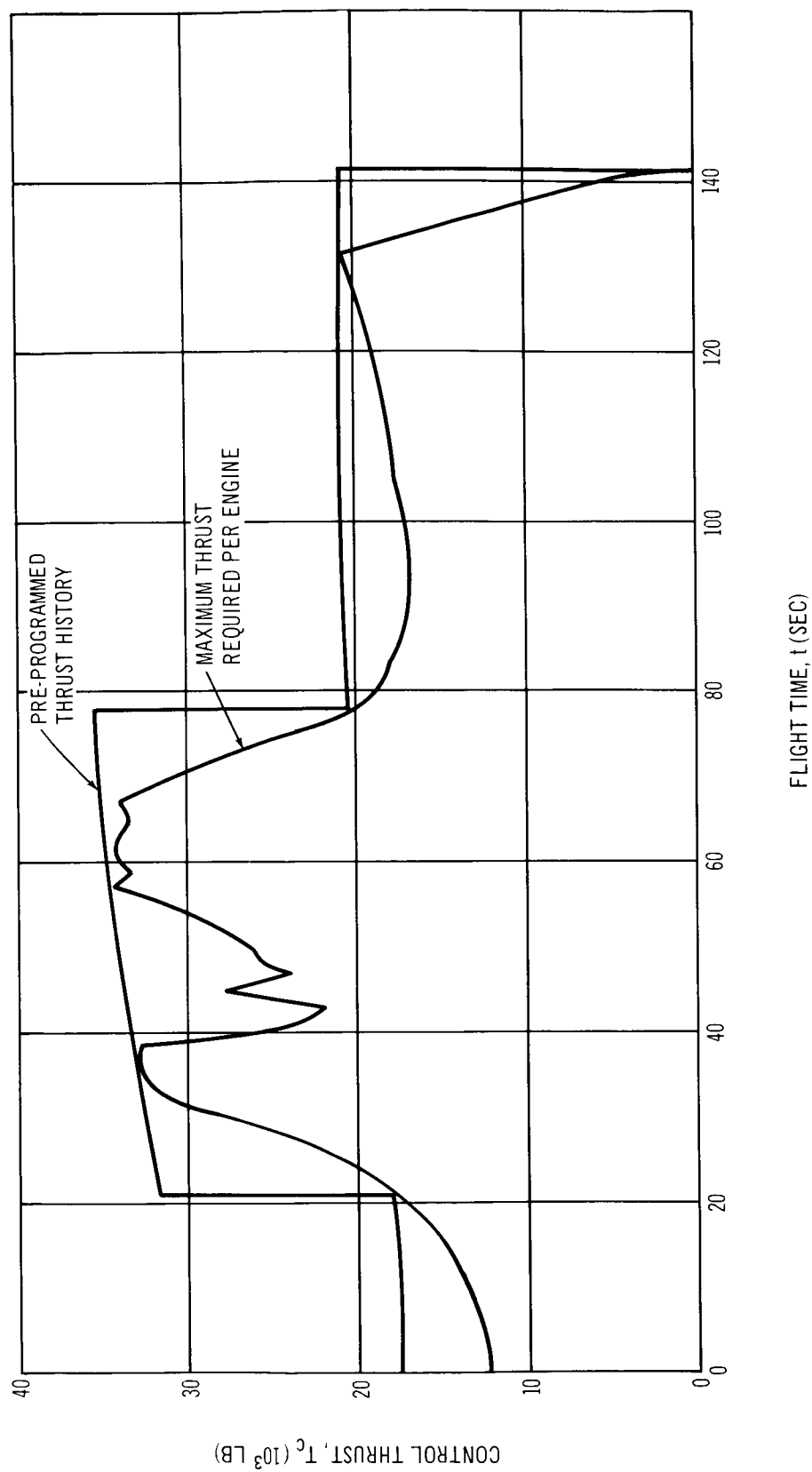


Figure 3-99. Configuration VII Control Thrust History (First Stage)



dynamic pressure, these motors can operate with or without the steering engines to provide adequate separation from the booster. Of the seven rocket motors required for pad abort, five motors, with a total weight of 4,500 lb, are dropped shortly after the end of first-stage burning.

Performance -- This vehicle is capable of delivering 8 men and 5,000 lb of packaged cargo to a space station in a 300-nmi circular orbit at an inclination of  $31^{\circ}$ . With this cargo loading, an unallocated maneuver capability in orbit of 3,320 fps is available. By off-loading maneuver propellant and decreasing this maneuver capability, cargo-carrying capability can be increased up to 23,750 lb. The mission profile includes boost to and injection into a 105-nmi parking orbit. A Hohmann transfer to and injection into a 300-nmi circular orbit is subsequently accomplished using the on-board maneuver propulsion system. The trajectory characteristics for this vehicle are shown in Figures 3-100 and 3-101. The maximum dynamic pressure of 1,190 psf is experienced 61 sec after launch. The maximum longitudinal acceleration of 7.7 g's occurs at first-stage burn-out. The Configuration VII performance characteristics are summarized in Tables 3-72 and 3-73.

System Operation -- Configuration VII prelaunch preparation requires 32.5 days, as for Configuration I, for receiving and shop-processing operations. Prelaunch preparation of the cargo and steering propellant modules takes place in parallel to spacecraft checkout. Mating of the spacecraft to the erected launch vehicle occurs 14 days prior to launch.

Launch vehicle preparation for the solid-propellant first stage and S-IVB second stage requires a total of 17 days. First-stage processing and erection requires 9 days, erection and mating of the S-IVB to the first stage requires 4 days, and launch-vehicle checkout an additional 4 days. The 11-day launch-vehicle-pad occupancy time required prior to mating of the spacecraft results in a total pad occupancy time of 25 days. Total processing time for the vehicle is 46.5 working days.

Recovered spacecraft recycle time is 44 days, of which 4.5 days is required for recovery site processing and transportation. The total recycle time through launch is 58 working days.

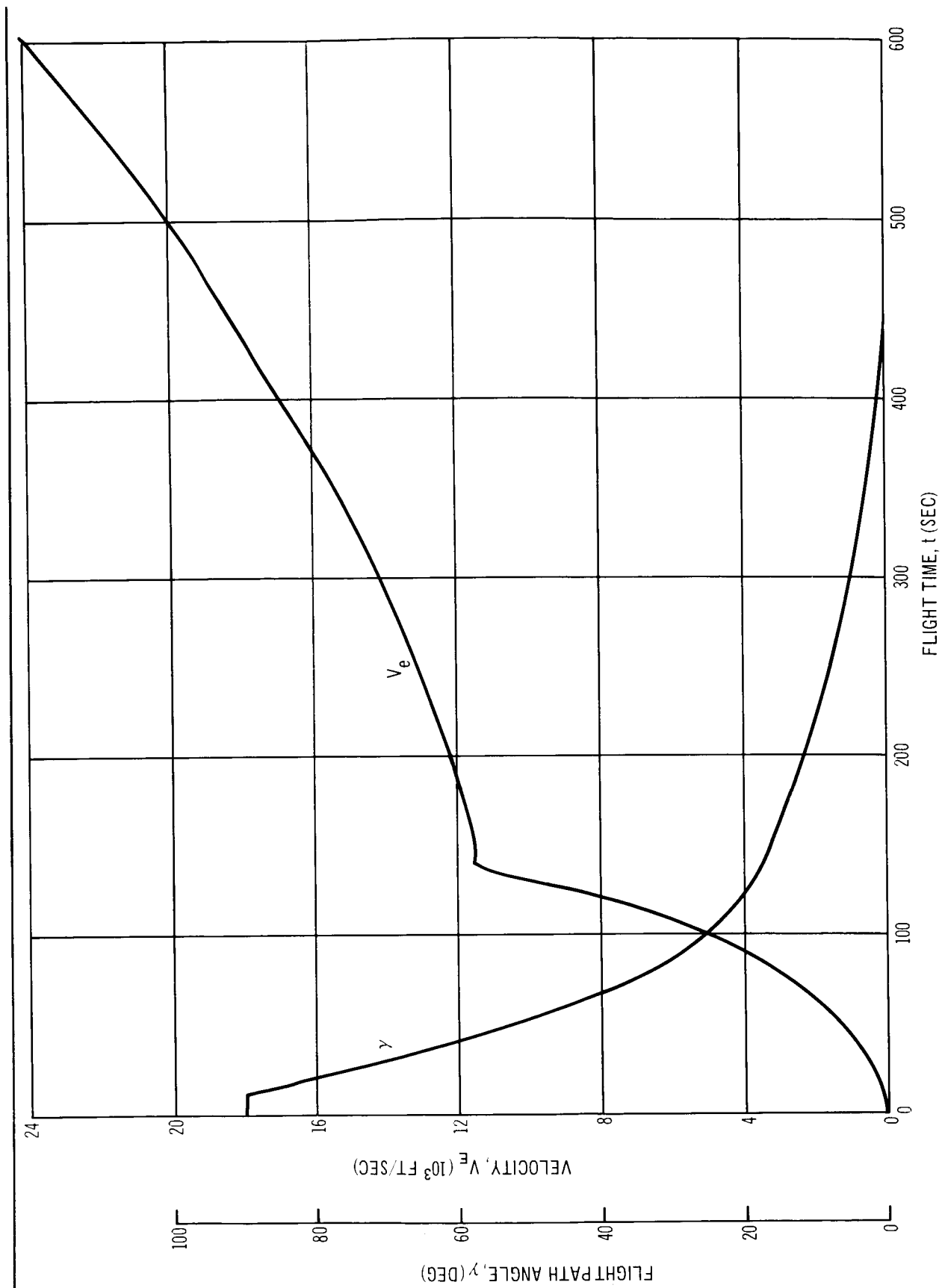


Figure 3-100. Configuration VII Trajectory Characteristics

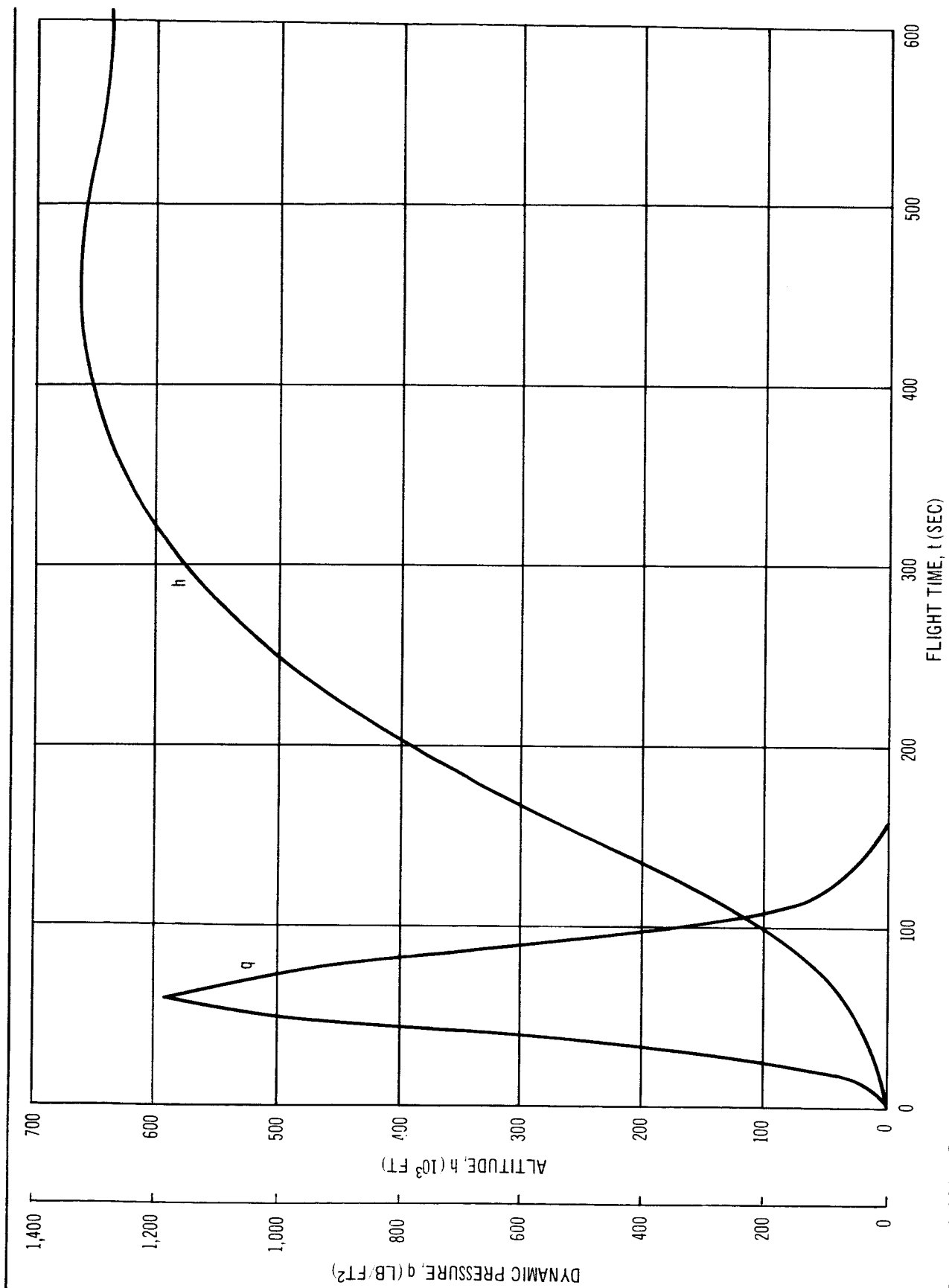


Figure 3-101. Configuration VII Trajectory Characteristics

Table 3-72

## PERFORMANCE CHARACTERISTICS OF CONFIGURATION VII

	<u>First Stage</u>	<u>Second Stage</u>
$T_i$	5,279,000	205,000
$T_f$	6,078,517	205,000
$I_{spSL}$	241.0	--
$I_{spVAC}$	277.5	426
$t_{Web}$	131.59	--
$t_{Act}$	141.41	462.6
$\lambda_M$	0.913	--
$\lambda'_{Eff}$	0.905	0.873
$(T/W)_i$	1.435	0.572
$a_{Max}$	7.74	~1.48
$GF_T$	38.54	
$\eta_{AP}$	11.28	

Cost of Operations -- Configuration VII hardware procurement costs are summarized in Table 3-74. The cost of 4.5 million dollars for the S-IVB was based on a fixed-production configuration and has a minimum of instrumentation and telemetry equipment. In addition, this cost projection assumes that the S-IVB hardware is delivered directly to the Kennedy Space Center and will not be processed through a hot-firing checkout at the Douglas-Sacramento facility. The costs of system operations are shown in Table 3-75.

Table 3-73  
BOOSTER SENSITIVITIES OF CONFIGURATION VII

X	$\frac{\partial \Delta V}{\partial X}$	$\frac{\partial W_{PL}}{\partial X}$	$\frac{\partial X}{\partial W_{PL}}$
Specific impulse, first stage	54.751 ft/sec/sec	706.223 lb/sec	0.001416 sec/lb
Specific impulse, second stage	32.676 ft/sec/sec	421.480 lb/sec	0.002373 sec/lb
Propellant weight, first stage	0.002406 lb/sec	0.03103 lb/sec	32.2269 lb/lb
Propellant weight, second stage	0.027137 lb/sec	0.35004 lb/lb	2.8568 lb/lb
Inert weight, first stage	-0.10803 lb/sec	-0.13934 lb/lb	-7.1767 lb/lb
Inert weight, second stage	-0.077760 lb/sec	-1.00000 lb/lb	-1.000 lb/lb
Payload weight	-0.077527 lb/sec	--	--

Table 3-74  
HARDWARE PROCUREMENT COSTS FOR  
CONFIGURATION VII (\$ Millions)

Expendable Hardware	(13.30)
First Stage	6.37
Second Stage	4.5
Steering Propellant Tank Section	0.86
Cargo Module	1.57
Spacecraft	38.38
Total Vehicle	\$51.68

Table 3-75  
OPERATIONS COST FOR CONFIGURATION VII  
(\$ Millions)

(50 FLIGHTS)

ORBIT (DEG)	30		90	
Refurbishment Base <sup>1</sup>	A	B	A	B
First Flight	54.68	54.68	54.60	54.60
Subsequent Flight	20.95	21.14	20.87	21.06
Average Flight	23.71	23.89	23.63	23.81
TOTAL PROGRAM COST	1,186	1,195	1,182	1,191

<sup>1</sup> Refurbishment Base A: 10% of spacecraft hardware procurement

Refurbishment Base B: 10.5% of spacecraft hardware procurement

Reliability Assessment -- Configuration VII launch-vehicle and stage reliabilities are shown in Table 3-76. These are shown for both time bases, reflecting first-flight reliability and growth potential. The instrument unit reliability has been excluded from these estimates.

Table 3-76  
CONFIGURATION VII RELIABILITY

	Base A	Base B
Launch Vehicle	0.891	0.914
First Stage	0.971	0.980
Second Stage	0.966	0.966
Steering System	0.950	0.966

#### Description of Configuration VIII

Configuration VIII is designed as an all-solid-propellant launch vehicle utilizing head-end steering for comparison with Configuration VII. It consists of an HL-10 spacecraft, a cargo module, a steering propellant module, and a three-stage, solid-propellant launch vehicle. This vehicle is shown in Figure 3-102, and its characteristics are described in Tables 3-77 and 3-78.

Spacecraft and Adapter -- The Configuration VIII spacecraft is a 44-ft HL-10 identical in design to the Configurations I and VII spacecraft. The maneuver propellant tanks are off-loaded to 42,200 lb of propellant to provide the same unallocated maneuver capability as Configuration VII after injection into a 300-nmi orbit. This maneuver capability is 5,915 fps and is produced by the two steering engines located in the trailing edge of the spacecraft. These engines have a maximum vacuum thrust of approximately 45,200 lb each.

The cargo module used on Configuration VIII is identical to those of Configurations I and II. For the nominal mission, it is empty and serves solely as the adapter between the spacecraft and the 156-in. diam steering propellant module and third-stage motor.

Steering System -- The head-end steering concept is used on this vehicle. The two steering engines are located on the spacecraft, are pump-fed with storable propellants ( $N_2O_4$  and MMH), can be gimballed  $\pm 30^\circ$  in two planes and are throttleable. The 58,700 lb of usable steering propellant required is carried in four cylindrical tanks located between the cargo module and the third stage.

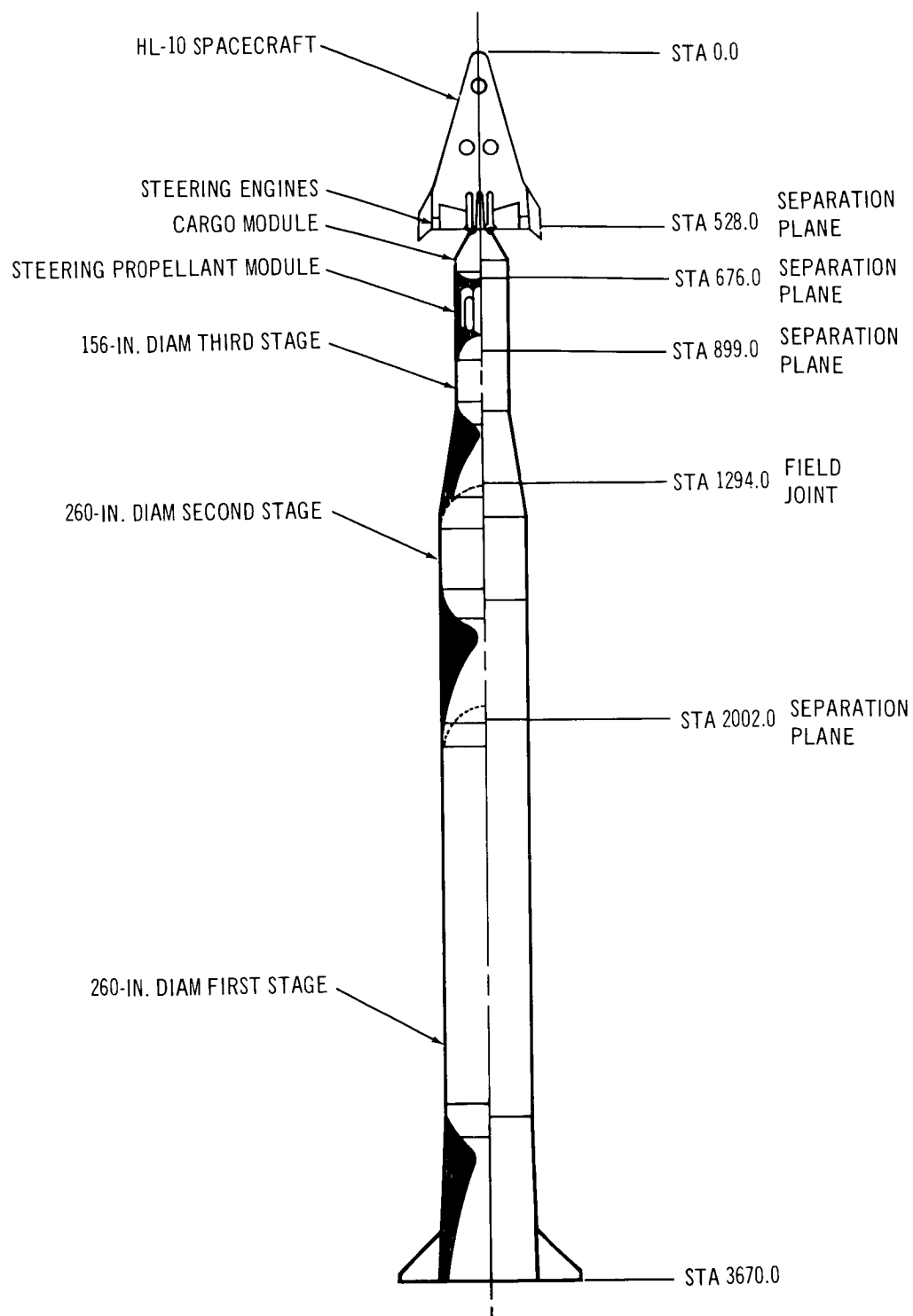


Figure 3-102. General Arrangement – Configuration VIII



Table 3-77

## SUMMARY OF CHARACTERISTICS OF CONFIGURATION VIII

## General characteristics:

Number of crew	2 men
Number of passengers:	
Nominal (crew compartment)	6 men
Maximum (including cargo compartment)	9-11 men
Cargo carrying capability:	
On-board HL-10 (packaged, Vol. = 250 ft. <sup>3</sup> )	5,000 lb
In cargo module (packaged, Vol. = 938 ft. <sup>3</sup> )	18,750 lb
Vacuum thrust (maximum) per engine	~45,000
Number of steering engines	2
Unallocated maneuver capability in orbit	3,320 ft/sec

## Dimensional characteristics:

## HL-10 Spacecraft:

Length	44.00 ft
Span	28.30 ft
Planform area	690 sq ft

## Adapter:

Cylindrical diameter	156 in.
Cargo module total length	14.83 ft
Steering propellant module length	18.58 ft
Overall length to field joint	30.92 ft

## Third stage:

Diameter	156 in.
Cylindrical motor length	10.67 ft
Overall length	32.92 ft

## Second stage:

Diameter	260 in.
Cylindrical motor length	14.6 ft
Overall length	59.00

## First stage:

Diameter	260 in.
Cylindrical motor length	88.7 ft
Overall length	139.0 ft

Overall booster length (to field joint)	230.92 ft
Total vehicle length	305.83 ft

Table 3-78  
WEIGHT SUMMARY OF CONFIGURATION VIII

Item	Weight (lb)
Spacecraft:	
Structure and thermal protection	16,010
Electrical and mechanical subsystems	3,280
Propulsion system (dry)	3,540
Maneuver propellant (total)	43,100
Reaction control system (dry)	750
RCS propellant	2,000
Landing provisions	2,840
Environmental control and life support	2,100
Crew and associated equipment	2,150
Growth contingencies	5,830
Cargo (packaged)	5,000
Abort rockets	6,300
Gross weight at liftoff	92,900
Adapter:	
Cargo module (empty)	3,900
Cargo (baseline mission)	0
Gross cargo module at liftoff	3,900
Steering propellant module (dry)	9,090
Steering propellant (total)	59,870
First stage requirement	33,730
Second stage requirement	9,130
Third stage requirement	15,810
Gross steering module at liftoff	68,960
Launch Vehicle:	
Third Stage	291,930
Gross motor weight	287,990
Propellant weight	252,500
Inert motor weight	35,490
Inert stage weight	3,940
Second stage	1,061,500
Gross motor weight	1,049,340
Propellant weight	944,400
Inert motor weight	104,940
Inert stage weight	12,160
First stage	3,697,500
Gross motor weight	3,661,100
Propellant weight	3,344,000
Inert motor weight	317,100
Inert stage weight	36,400
Gross launch vehicle at liftoff	5,050,930
Gross vehicle at liftoff	5,216,700

Because of the similarity between Configurations VIII and I, no steering analysis was performed on Configuration VIII. Optimum fin sizes would compare closely with Configuration I. Since the vehicle is shorter, the control moment arm decreases; however, the effective moment arm resulting from thrust misalignment and the moment arm for aerodynamic forces decrease as well. Also, the booster thrust and aerodynamic forces decrease, thus resulting in a net decrease in control thrust requirements. These considerations led to an estimated decrease in first-stage steering propellant requirements of 3% and 5% in second-stage requirements with respect to Configuration I. No adjustment was made to third-stage requirements since both vehicles utilize the same third stage. These steering propellant weight adjustments were felt to be conservative in light of the information available.

Launch Vehicle -- The launch vehicle is a three-stage, solid-propellant vehicle which utilizes head-end steering for control throughout the boost phase.

The first stage consists of a 260-in. diam solid-propellant motor with a fixed, conical, 8.3:1 expansion ratio nozzle, a cylindrical forward skirt, and a conical aft skirt. The 3,344,000-lb propellant grain develops a neutral thrust-time curve over a 120.7-sec web burn time. The vacuum thrust of this motor is 7,299,600 lb and the vacuum specific impulse is 273 sec.

The second stage is also a 260-in. diam solid-propellant motor. It has a fixed, contoured, 26:1 expansion-ratio nozzle, a conical forward skirt, and a cylindrical aft skirt. The propellant loading of 944,400 lb provides a neutral thrust-time curve with a vacuum thrust of 2,410,230 lb and a web burn time of 110 sec. A vacuum specific impulse of 291 sec is developed by the motor.

The third-stage consists of a 156-in. diam solid-propellant motor which is identical to that used on Configuration I. This motor has a 40:1 expansion-ratio, fixed, contoured nozzle and has a cylindrical forward skirt and a conical aft skirt attached to complete the stage. A motor-propellant grain weighing 252,500 lb produces a highly regressive thrust-time history over a web burn time of 122.2 sec. Initial thrust is 914,400 lb and final thrust is 284,800 lb. The delivered vacuum specific impulse of the motor is 303 sec.

Abort System -- The similarity between Configuration VIII and I resulted in the use of the same abort system on both. This system, consisting of seven solid-propellant rocket motors with a total weight of 6,300 lb, was used on Configuration VII also. This provides sufficient impulse on pad abort to enable the spacecraft to fly to and land at one of several possible recovery strips as discussed in Section 3.1.4. Five of the seven motors would be dropped after first stage burn-out and the remaining two used for high-altitude abort.

Performance -- This vehicle can fulfill the same mission requirements and is directly comparable to Configuration VII. It is capable of delivering 8 men and 5,000 lb of packaged cargo to a 300-nmi orbit at an inclination of  $31^\circ$  and can provide 3,320 fps of unallocated maneuver capability in orbit. With reduced maneuver capability, the cargo-carrying capability can be increased up to 23,750 lb. The mission profile consists of boost to an apogee altitude of 100 nmi. Injection into a 105-nmi parking orbit, Hohmann transfer, plane change, and injection into a 300-nmi circular orbit is accomplished through use of the on-board maneuver system. Trajectory characteristics are as shown in Figures 3-103 and 3-104. The maximum dynamic pressure of 1,020 psf is reached 77 sec after launch. The maximum longitudinal acceleration of 4.3 g's occurs at second-stage burn-out. Configuration VIII performance characteristics are summarized in Tables 3-79 and 3-80.

System Operations -- System operation requirements for Configuration VIII are identical to those of Configuration I as discussed previously. The prelaunch preparation times are summarized here. A total of 46.5 working days are required for new vehicle prelaunch preparation. Spacecraft receiving and processing prior to launch-vehicle mating requires 32.5 days with 14 additional days required for mating and on-pad checkout. Launch-vehicle processing, erection, and checkout prior to spacecraft mating requires a total of 20 days of which 14 days of pad occupancy are required.

Recycle time for a recovered spacecraft is 44 days, of which 4.5 are required for recovery site processing and transportation. Total recycle time through launch is 58 working days.

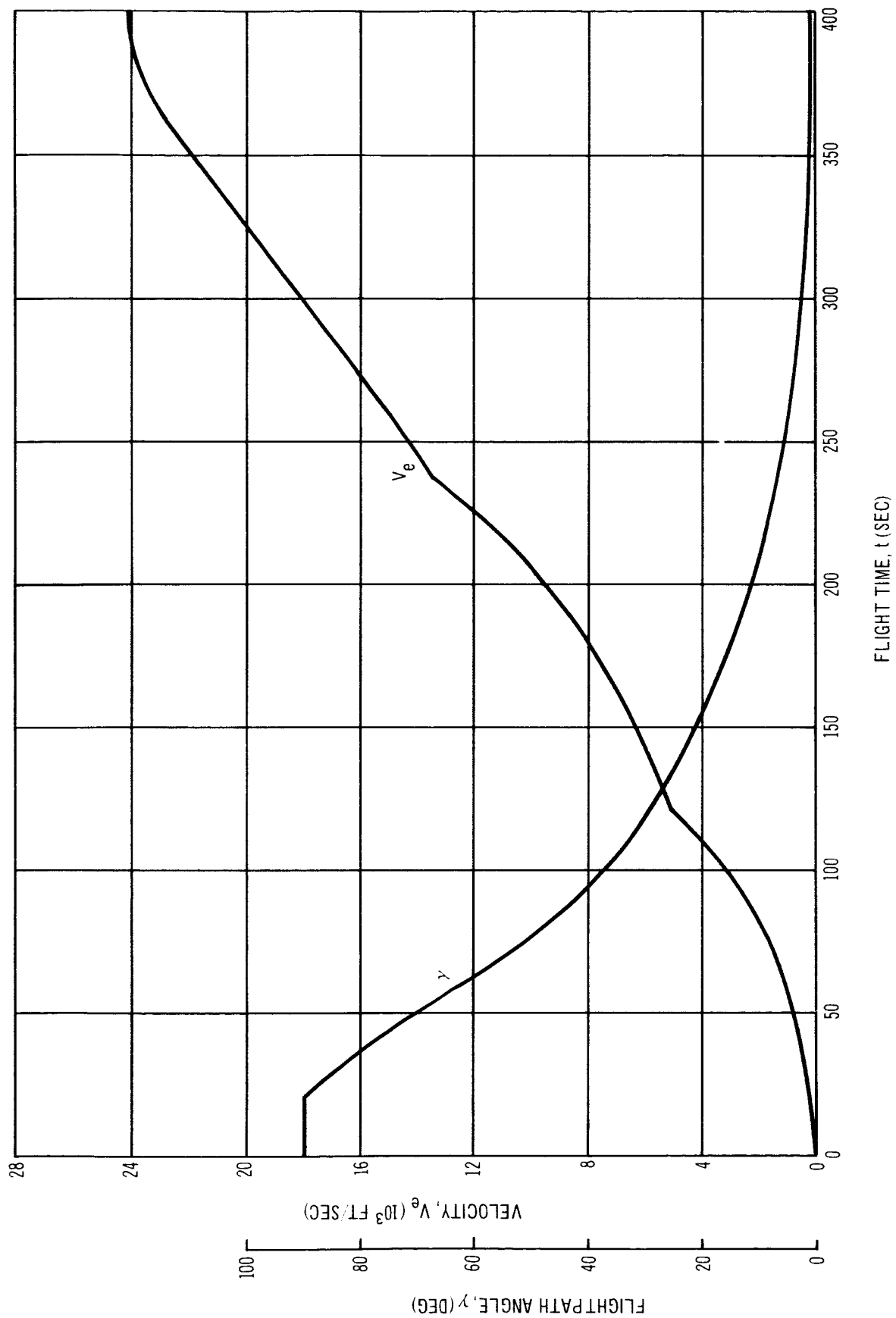


Figure 3-103. Configuration VIII Trajectory Characteristics

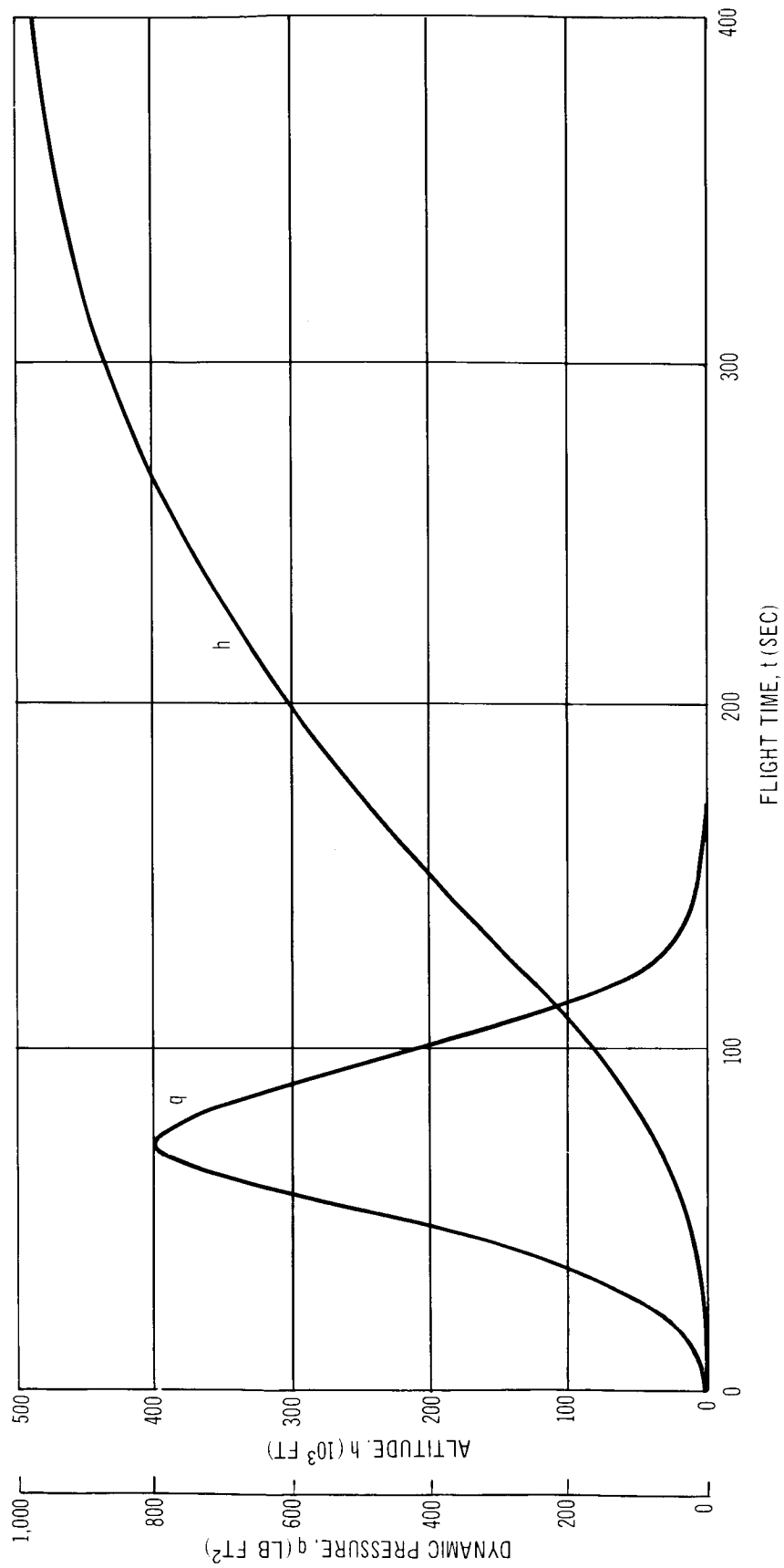


Figure 3-104. Configuration VIII Trajectory Characteristics

Table 3-79  
CONFIGURATION VIII PERFORMANCE CHARACTERISTICS

	First Stage	Second Stage	Third Stage
$T_i$	6,489,000	2,410,230	914,410
$T_f$	7,299,591	2,410,230	284,816
$I_{spSL}$	243.0	--	--
$I_{spVAC}$	273.4	290.6	302.7
$t_{Web}$	120.74	110.00	122.20
$t_{Act}$	129.76	117.74	144.30
$\lambda_M$	0.913	0.900	0.877
$\lambda'_{Eff}$	0.905	0.891	0.872
$(T/W)_i$	1.251	1.639	2.258
$a_{Max}$	3.74	4.33	2.43
$GF_T$	50.85		
$\eta_{PP}$	10.54		

Cost of Operations -- Configuration VIII hardware procurement costs are shown in Table 3-81. System operations costs are summarized in Table 3-82.

Table 3-80

## CONFIGURATION VIII BOOSTER SENSITIVITIES

X	$\frac{\partial \Delta V}{\partial X}$	$\frac{\partial W_{PL}}{\partial X}$	$\frac{\partial X}{\partial W_{PL}}$
Specific impulse, first stage	33.547 ft/sec/sec	577.49 lb/sec	0.001732 sec/lb
Specific impulse, second stage	33.217 ft/sec/sec	571.82 lb/sec	0.001749 sec/lb
Specific impulse, third stage	34.135 ft/sec/sec	587.62 lb/sec	0.001702 sec/lb
Propellant weight, first stage	0.001678 ft/sec/lb	0.02889 lb/lb	34.614 lb/lb
Propellant weight, second stage	0.003198 ft/sec/lb	0.05505 lb/lb	18.165 lb/lb
Propellant weight, third stage	0.003695 ft/sec/lb	0.14967 lb/lb	6.681 lb/lb
Inert weight, first stage	-0.003087 ft/sec/lb	-0.05314 lb/lb	-18.818 lb/lb
Inert weight, second stage	-0.014463 ft/sec/lb	-0.24897 lb/lb	-4.017 lb/lb
Inert weight, third stage	-0.058223 ft/sec/lb	-1.00000 lb/lb	-1.000 lb/lb
Payload weight	-0.058090 ft/sec/lb	--	--



Table 3-81  
HARDWARE PROCUREMENT COSTS FOR CONFIGURATION VIII

Item	(\$ Million)
Expendable hardware	(15.76)
First stage	7.04
Second stage	4.28
Third stage	1.91
Steering propellant tank section	0.944
Cargo module	1.59
Spacecraft	38.54
Total vehicle	\$54.30

Table 3-82  
OPERATIONS COST FOR CONFIGURATION VIII, 50 FLIGHTS

(\$ Million)				
ORBIT - DEGREES	30		90	
	A	B	A	B
Refurbishment base <sup>1</sup>				
First flight	57.30	57.30	57.22	57.22
Subsequent flight	23.56	23.83	23.48	23.75
Average flight	26.33	26.58	26.25	26.50
TOTAL PROGRAM COST	1,317	1,329	1,313	1,325

<sup>1</sup> Refurbishment Base A: 10% of spacecraft hardware procurement  
Refurbishment Base B: 10.7% of spacecraft hardware procurement

Reliability Assessment -- Configuration VIII launch vehicle and stage reliabilities are shown in Table 3-83. These are shown for both time bases, reflecting first-flight reliability and growth potential.

Table 3-83  
CONFIGURATION VIII RELIABILITY

	Base A	Base B
Launch vehicle	0.882	0.920
First stage	0.971	0.980
Second stage	0.978	0.986
Third stage	0.978	0.986
Steering system	0.950	0.966

### 3.3.4 Comparative Analyses

The purpose of the comparative analyses is to apply the comparison criteria described in Section 3.3.2.2 to the system definitions for each of the models developed in Section 3.3.3. These comparison criteria will be evaluated specifically in those system comparisons enumerated in Table 3-23, which were designed to isolate the separate effects of steering technique, launch-vehicle propulsion-system type, and spacecraft configuration. Finally, the total system concept will be analyzed and the effects shown.

#### 3.3.4.1 Effect of Steering Technique

The effect of steering technique is isolated in the comparisons of Configuration I with II and of Configuration IV with V. The comparisons involve all-solid-propellant motors for the launch vehicles. The comparison of Configurations I and II is made in the context of lifting body spacecraft in the 100,000-lb payload class and performing the extended MORL mission with the flexibility of accomplishing other missions requiring up to 3,800 fps of in-orbit maneuvering capability. The comparison of Configurations IV and V is made in the context of a ballistic type of spacecraft in the 40,000-lb payload class performing the LORL mission.

#### Comparison of Configurations I and II

Both system concepts for Configurations I and II were constrained to perform the extended MORL mission described in Section 3.3.2.1. This results in the same useful load, the same number of personnel, and the same maneuvering capability in orbit. The ascent trajectories used in the sizing of the launch vehicles were selected to produce nearly the same apogee velocity at the design-orbit altitude, 300 nmi. Ballistic-type flight profiles were used for both vehicles.

Vehicle Size Comparison--A gross size comparison is shown in Figure 3-105. Configuration II, employing secondary fluid injection for steering control in each of the three solid stages, is approximately 33 ft shorter than Configuration I. This is due primarily to the absence of any steering propellant tankage at the top of the third-stage motor as required for the head-end steered vehicle (Configuration I). Some reduction in length for Configuration II is also realized due to the smaller solid-motor propellant loadings required, particularly in the two upper stages.

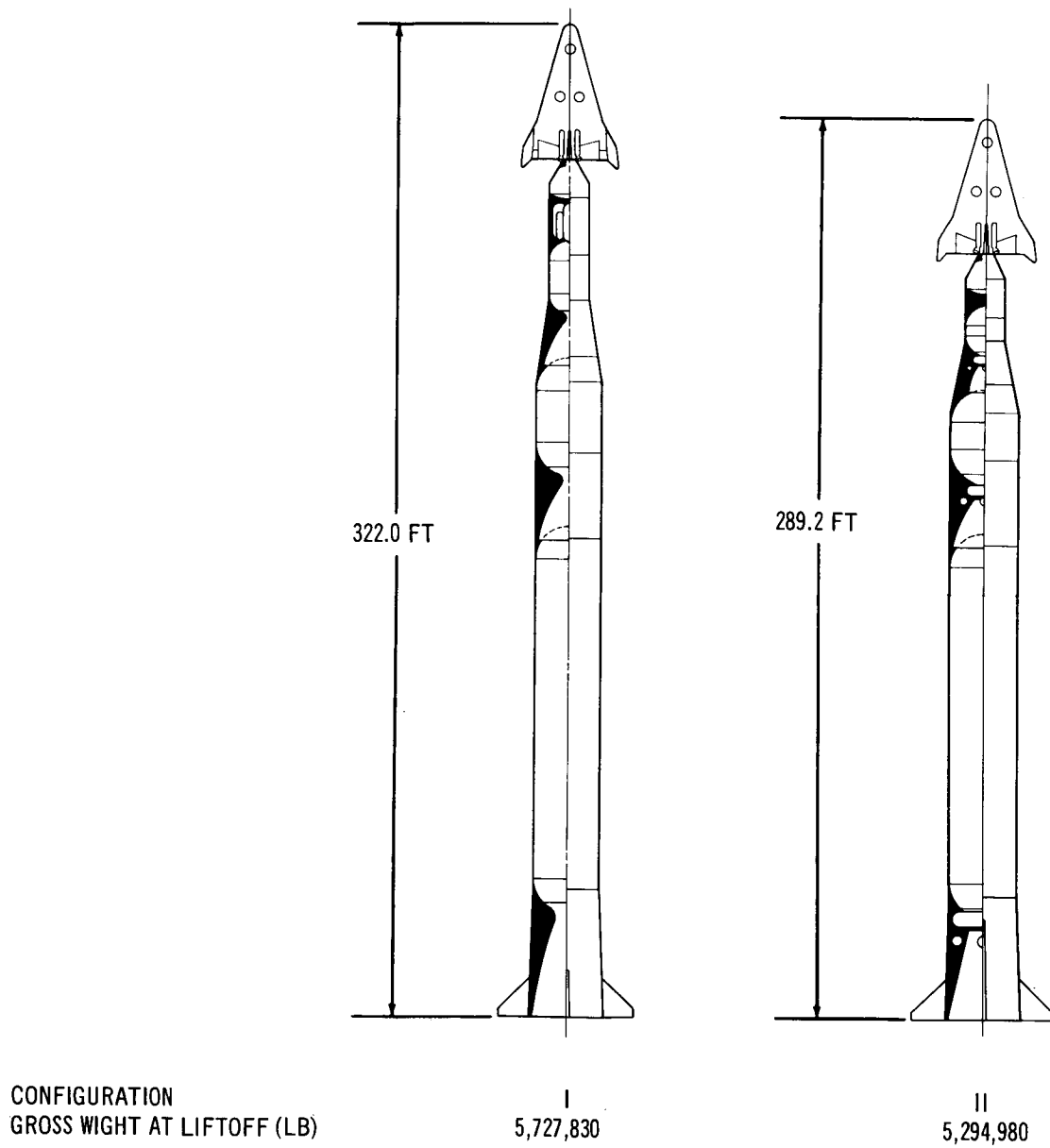


Figure 3-105. Effect of Steering Technique on Gross Vehicle Size – Extended MORL Mission

Table 3-84 shows a more detailed weight breakdown for the two vehicles.

Vehicle II weighs less than I by 432,850 lb due primarily to the smaller payload weight above the third stage. The payloads shown in Table 3-84 consist of all the weight above the third-stage motor at liftoff but not including the steering propellants in the case of Configuration I. It should be pointed out that the propellant distribution for Configuration I is non-optimum since steering control requirements limit the minimum size of the third-stage motor to about 308,000 308,000 lbs as discussed in Section 3.1.4.2.

The steering systems are compared in Table 3-85. The inert weight for the head-end steering system is 10,500 lb and is carried entirely in the third stage. The inert weight of the secondary liquid injection system is 16,250 lb but is distributed throughout all three stages.

Table 3-84

EFFECT OF STEERING TECHNIQUE ON VEHICLE WEIGHTS  
EXTENDED MORL MISSION  
(ALL WEIGHTS IN POUNDS)

Configuration	I	II
Gross Vehicle at Lift-Off	5,727,830	5,294,980
Gross Payload at Lift-Off	108,100	88,680
Crew Module	87,400	76,780
Cargo Module	3,900	3,800
Steering Module	70,700	NA
Launch Escape System	6,300	7,000
Gross Third Stage	307,740*	185,240
Propellant	252,500	152,300
Gross Second Stage	1,146,910*	854,960
Propellant	1,013,000	744,300
Gross First Stage	4,165,080*	4,166,100
Propellant	3,751,000	3,758,000

\*Includes steering propellant.

Table 3-85

# EFFECT OF STEERING TECHNIQUE ON STEERING SYSTEM CHARACTERISTICS

## EXTENDED MORL MISSION

Configuration	I	II
Steering Technique	HES	LITVC
Steering System Location	Above Third Stage	Nozzle Area Each Stage
Steering Propellant/ TVC Injectant	N <sub>2</sub> O <sub>4</sub> /MMH	N <sub>2</sub> O <sub>4</sub>
Steering System Weight		
Total at Launch, all stages (lb)	70,700	35,900
Total Expendables, all stages (lb)	60,200	19,650
Maximum Vac. Steering Thrust (lb) or Effective Gimbal Angle (deg) Required		
First Stage	46,350	0.36
Second Stage	14,500	0.41
Third Stage	26,510	0.51
Number of Systems Required for Control	1	6

The mass fraction of the head-end steering system is 0.851 while the average mass fraction of the secondary liquid system is on the order of 0.547. The higher mass fraction of the head-end steering system is due to the large size and concentration of the function in one location. The net effect of stage location, mass fraction, and control characteristics of the steering system on total vehicle size is that the secondary fluid-injection steering technique produces a smaller overall vehicle size by some 8.4%.

A comparison of trajectory characteristics is shown in Table 3-86. It is quite clear that the choice of steering technique would make an insignificant difference in these characteristics.

Table 3-86

EFFECT OF STEERING TECHNIQUE ON TRAJECTORY CHARACTERISTICS  
EXTENDED MORL MISSION

Configuration	I	II
Thrust/ Weight @ Liftoff	1.25	1.25
Maximum Dynamic Pressure (lb/ft <sup>2</sup> )	801	816
Maximum Axial Acceleration (g's)	4.51	4.72
Apogee Altitude (nmi)	300	300
Injection Velocity Required at Apogee (fps)	565	421

Vehicle Cost Comparison--Table 3-87 shows the hardware procurement costs for Configurations I and II. These data show that the spacecraft for Configuration I costs \$2,495,000 more than Configuration II. This is primarily due to the cost of steering system integration into the spacecraft primary structure. This larger spacecraft cost is offset by the lower cost of the launch vehicle. The Configuration I launch vehicle costs \$1,215,000 less than the Configuration II vehicle. Although the motor sizes of the Configuration II vehicle are smaller than I and there is no steering propellant tank section, the increased cost of integrating the secondary liquid injection system results in a larger unit cost for expendable components.

This effect is shown on first unit costs, subsequent flight cost, and on average flight cost in Table 3-88. The significance of the reusability of the spacecraft is seen here. Even though the spacecraft costs are higher for I, the savings made in the expendable launch vehicle produces a net savings of \$1,050,000 per subsequent flight or \$870,000 per flight on an average flight basis for the case of a 50-flight program. There is no change in the relative cost position for Configurations I and II in programs involving 20 and 100 total flights (Table 3-88).

Table 3-87

EFFECT OF LAUNCH VEHICLE PROPULSION ON HARDWARE  
PROCUREMENT COST, EXTENDED MORL MISSION

(ALL COSTS IN MILLIONS OF DOLLARS)

Configuration	I	II
Spacecraft	38.54	36.04
Cargo Module-Adapter	1.58	1.55
Steering Propellant Tank Section	0.96	--
First Stage	7.95	9.68
Second Stage	4.98	5.66
Third Stage	2.06	1.87
Recoverable Hardware Total	38.54	36.04
Non-Recoverable Hardware Total	17.53	18.75
First Flight Hardware Total	56.07	54.79

Table 3-88

EFFECT OF STEERING TECHNIQUE ON OPERATIONS COSTS

30° ORBIT RECOVERY

REFURBISHMENT BASE A

PROBABILITY OF SUCCESSFUL LAUNCH = 95%

(ALL COSTS IN MILLIONS OF DOLLARS)

Total Successful Flights	20	50	100
Inventory, Spacecraft	2	4	6
Inventory, Expendable Hardware	21	53	105

Configuration	I	II	I	II	I	II
First Flight Cost	59.07	57.79	59.07	57.79	59.07	57.79
Subsequent Flight Cost	25.43	26.48	25.43	26.48	25.43	26.48
Average Flight Cost	28.74	29.54	28.20	29.07	27.35	27.88
Total Program Cost	575	591	1410	1454	2735	2788



Vehicle Cost Effectiveness--As discussed in Section 3.3.2.2, the vehicle cost effectiveness is based on average costs per flight and on the useful load impulse. For two vehicles possessing the same crew size, the same useful load, and the same maneuver capability in orbit, the average flight cost would be an adequate basis for comparison. If it is desired to show the effects of mission requirements on the vehicle cost effectiveness, the incorporation of crew size, useful load and maneuvering capability is required to produce a more useful criteria. For the purpose of examining the effect of mission requirements, the cost effectiveness parameters are presented in Table 3-89.

Qualitative Reliability Assessment--The approach to a comparison of concepts on the basis of their relative reliabilities is discussed previously in Section 3.3.2.2. The individual concept reliabilities are developed for Configurations I and II in Section 3.3.3.1. This section will compare these reliabilities and discuss the salient reasons for their differences.

Table 3-90 presents the reliabilities of Configurations I and II and shows these data for two different bases. As would be expected, the reliability is higher in

Table 3-89

COST EFFECTIVENESS

50 Flights	Refurbishment Base A	30° Orbit Recovery
Configuration	I	II
Average Flight Cost (\$ millions)	28.20	29.07
Useful Load (lb)	6,600	6,600
In-orbit Maneuvering Capability, V (ft/sec)	5,820	5,820
Useful Load Impulse ( $10^6$ lb-sec)	1.192	1.192
Cost Effectiveness (\$ per lb-sec)	23.6	24.4

Table 3-90

## EFFECT OF STEERING TECHNIQUE ON LAUNCH VEHICLE RELIABILITY

Configuration	I		II	
	A	B	A	B
Reliability Base*				
First Stage	0.971	0.980	0.926	0.945
Second Stage	0.978	0.986	0.933	0.952
Third Stage	0.978	0.986	0.933	0.952
HES System	0.950	0.966	--	--
Total Launch Vehicle	0.882	0.920	0.806	0.856

\* Two reliability bases are shown: "A" is based on the first flight date, "B" is based on the date the vehicle achieves its full reliability potential as discussed in Section 3.3.2.2.

each stage for Configuration I because of the fixed nozzle configuration and absence of any steering control hardware. This difference is 0.045 in each stage for the vehicle at the time of the first flight, reliability base "A". At the time when full reliability potential is achieved, the difference in reliability per stage is slightly less or 0.035. This stage reliability advantage is offset by the reliability of the head-end steering system. The total launch vehicle reliability, however, still favors Configuration I by 0.076 at the time of first flight and 0.064 at the time reliability is fully developed. This situation points out the significance of small improvements in reliability made in each stage of a three-stage vehicle. The net effect, including the addition of a pseudo fourth-stage system of reasonably high reliability, is an increase in reliability.

Evaluation of Operational Characteristics--Configurations I and II are discussed separately with respect to operational characteristics in Section 3.3.3.1. Since the recoverable spacecraft are the same size and type and have similar functional characteristics, there is very little difference except in the area of prelaunch preparation. Table 3-91 summarizes the similarities and differences in operations.

Table 3-91

## EFFECT OF STEERING TECHNIQUE ON SYSTEM OPERATIONS

Configuration	I	II
Abort System Weight (lb)	6,300	7,000
Number of Steering Systems Requiring Pre-Launch Checkout In:		
First Stage	0	2
Second Stage	0	2
Third Stage	0	2
Payload	1	0
Launch Pad Tie-Up Time, Calendar Days	32	36
Steering Checkout Independent of Boost Stages	Yes	No
Number of Recovery Sites Required From Orbits at 250 nmi Inclined at		
30°	3	3
55°	4	4
90°	4	4

The abort characteristics are similar since the abort systems were sized to the same requirements. The abort system for Configuration II is larger than for Configuration I since it does not have the contribution of the thrust of the steering engines for pad abort escape.

The recovery requirements are the same since the lift/drag ratios of the two spacecraft are identical. The return of the spacecraft to the refurbishment site is identical for both Configurations I and II since the construction techniques and the sizes are the same.

It is estimated that Configuration II will tie up the launch pad complex about four days more than Configuration I. This additional time will result from the

more extensive and complex all-system checks that will be required when the secondary fluid injection TVC systems are incorporated in all three stages. The spacecraft must be mated prior to making these checks.

#### Comparison of Configurations IV and V

The effect of steering technique was isolated also in the differences between Configurations IV and V. The mission constraints for these two vehicles were the LORL mission requirements as performed by the BALLOS vehicle in Reference 2. Thus, the crew size, useful load, and in-orbit maneuvering capability are the same. The ascent trajectories used in sizing these two vehicles were selected to produce the same, or nearly the same, apogee velocities at the design parking orbit altitude of 105 nmi. Ballistic-type flight profiles were used for both vehicles.

Vehicle Size Comparison--A gross size comparison is shown in Figure 3-106. Configuration V, which employs secondary fluid injection for steering control in each stage, is 32.1 ft shorter than Configuration IV which uses head-end steering. As for the case of Configuration I, the additional length of Configuration IV is partially due to the steering propellant-tank section. Unlike Configuration I, however, IV has a longer cargo module section since this section also carries the steering engines. The balance of the additional length of IV is due to the somewhat heavier weight above the second stage as shown in Table 3-92. This difference amounts to 15,510 lb of which 7,560 lb is attributable to the heavier cargo-maneuver module and 8,550 lb to the inert weight of the steering propellant tank section. This results in the large size of the first- and second-stage motors for Configuration IV. Thus, the gross weight of IV is heavier than V by 618,450 lbs.

The steering systems are compared in Table 3-93. The inert weight for the head-end steering system is made up of the 8,550 lb of the steering propellant tank section plus an amount, contained in the cargo-maneuver module weight, associated with the steering engine installation. The entire steering system weight is, however, charged to the second stage and has a one-to-one equivalence to payload. The inert steering system weight for Configuration V is 9,880 lb and is distributed between the first and second stages with the major portion in the first stage. The average mass fraction for the steering system of Configuration V is 0.556.

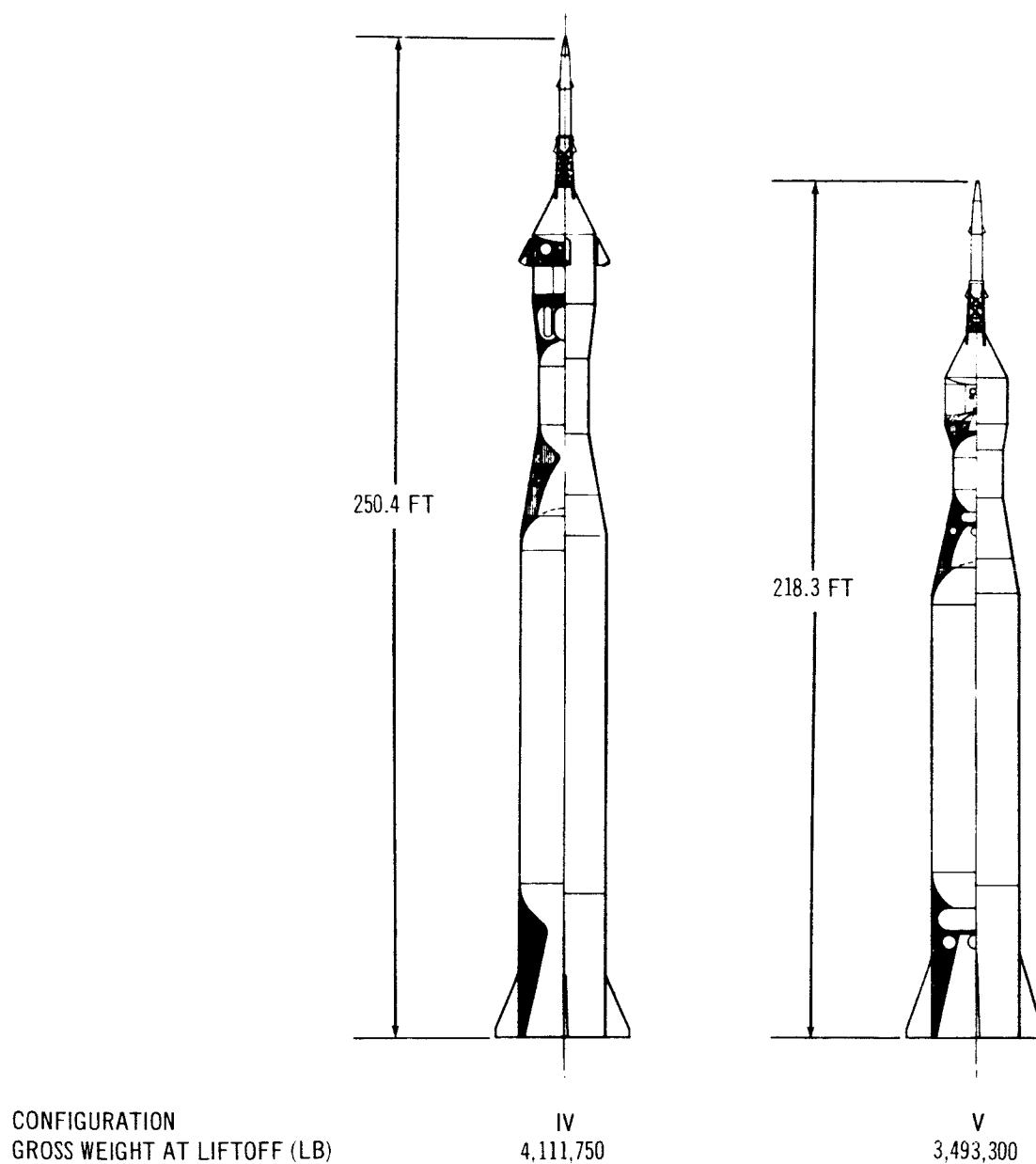


Figure 3-106. Effect of Steering Technique on Gross Vehicle Size – LORL Mission

Table 3-92  
EFFECT OF STEERING TECHNIQUE ON VEHICLE WEIGHTS,  
LORL MISSION  
(All weights in pounds)

Configuration	IV	V
Gross Vehicle at Lift-off	4,111,750	3,493,300
Gross Payload at Lift-off	62,900	46,790
Crew Module	13,170	13,170
Cargo Maneuver Module	32,430	24,870
Steering Module	60,850	NA
Launch Escape System	8,750	8,750
Gross Second Stage	361,830*	267,610
Propellant	306,340	225,450
Gross First Stage	3,687,020*	3,178,300
Propellant	3,302,500	2,857,300

\*Includes steering propellant.

Table 3-93  
EFFECT OF STEERING TECHNIQUE ON STEERING SYSTEM  
CHARACTERISTICS, LORL MISSION

Configuration	IV	V
Steering Technique	HES-4 Engines	LITVC
Steering System Location	Above Second Stage	Nozzle Area Each Stage
Steering Propellant/TVC Injectant	N <sub>2</sub> O <sub>4</sub> /MMH	N <sub>2</sub> O <sub>4</sub>
Steering System Weight		
Total at Launch, Lb (all stages)	60,850	22,260
Total Expendables, Lb (all stages)	52,300	12,380
Maximum Vac. Steering Thrust (Lb) or Effective Gimbal Angle (Deg) Required		
First Stage	21,080	0.28
Second Stage	4,300	0.69
Number of Systems Required for Control	1	4

Vehicle Performance Comparison--The trajectory characteristics of Configurations IV and V are compared in Table 3-94. Very little difference is apparent from these data. Vehicle V requires about 38 fps more injection velocity from the spacecraft than does IV.

Vehicle Cost Comparison--The hardware procurement costs for Configurations IV and V are shown in Table 3-95.

Table 3-94  
TRAJECTORY CHARACTERISTICS

Configuration	IV	V
Thrust/Weight	1.25	1.25
Maximum Dynamic Pressure (Lb/Ft) <sup>2</sup>	934	974
Maximum Axial Acceleration (g's)	6.5	6.9
Apogee Altitude (nmi)	105	105
Injection Velocity Required at Apogee (fps)	163	201

Table 3-95  
EFFECT OF STEERING TECHNIQUE ON HARDWARE  
PROCUREMENT COSTS  
(All costs in millions of pounds)

Configuration	IV	V
Spacecraft	19.55	19.55
Cargo Module Adapter	4.55	2.56
Steering Propellant Tanks Section	0.71	--
First Stage	6.77	7.86
Second Stage	2.37	2.44
Reusable Hardware Total	19.55	19.55
Non-Recoverable Hardware Total	14.40	12.86
First Flight Hardware Total	33.95	32.41

Since the spacecraft cost the same, the difference in first flight hardware cost is entirely due to the expendable components. This difference is 1.54 million dollars favoring Configuration V. In this case, the higher cost of the cargo module adapter and the steering propellant tank section is not completely offset by the higher stage cost of Configuration V. Incorporating the steering engines into the cargo module adapter results in a completely expendable steering system which, of course, reflects the significant effect on average flight costs of a partially reusable system.

A summary of first flight costs, subsequent flight costs, and average flight costs is shown in Table 3-96. These data include the recovery costs from and refurbishment costs from Section 3.3.3.2. For the case of the ballistic body spacecraft, head-end steering does not show a cost advantage. In fact, it is more expensive than Configuration V which uses secondary liquid injection thrust vector control. The difference is \$1,590,000 per flight on an average cost basis for a 50 flight program. This would result in a difference of 80 million dollars for the total program of 50 flights.

Table 3-96  
EFFECT OF STEERING TECHNIQUE ON OPERATIONS COSTS

30 Degree Orbit Recovery		Refurbishment Base A	
Probability of Successful Launch = 0.95%			
Total Successful Flights		50	
Inventory, Spacecraft		4	
Inventory, Expendable Hardware		53	
Configuration		IV	V
First Flight Cost		38.26	36.76
Subsequent Flight Cost		21.57	19.98
Average Flight Cost		22.97	21.38
Total Program Cost		1149	1069



Vehicle Cost Effectiveness--The cost effectiveness data for Configurations IV and V appear in Table 3-97. Both spacecraft are the 12-man BALLOS configuration. The useful load and in-orbit maneuvering capability were also kept constant. Hence, the results of the payload effectiveness evaluation do not alter the basic cost analysis results.

Qualitative Reliability Assessment--The approach for evaluating relative reliability of the system concepts is discussed in Section 3.3.2.2. The individual reliabilities developed for Configurations IV and V are presented in Section 3.3.3.2. This section will compare the relative reliabilities of Configurations IV and V and emphasize the reasons for their differences.

Table 3-98 presents the reliabilities of Configurations IV and V and shows these data for two different bases for prediction. As would be expected, the reliability is higher for each stage of Configuration IV due to the fixed nozzle configuration and absence of any steering control hardware.

The higher-stage reliability of Configuration IV is not sufficient, however, to offset the effect of the separate steering-system reliability. The steering-system reliability is lower than for Configuration I because of the four engines required. Configuration IV shows a higher reliability at first flight and would

Table 3-97  
EFFECT OF STEERING TECHNIQUE ON COST EFFECTIVENESS

50 Flights	Refurbishment Base A	30° Orbit Recovery
Configuration	IV	V
Average Flight Cost (\$ millions)	22.97	21.38
Useful Load (lb)	15,855	15,855
In-orbit Maneuvering Capability $\Delta V$ (fps)	1,050	1,050
Useful Load Impulse ( $10^6$ lb/sec)	0.516	0.516
Cost Effectiveness (\$ per lb-sec)	44.5	41.4

Table 3-98  
EFFECT OF STEERING TECHNIQUE ON LAUNCH  
VEHICLE RELIABILITY

Reliability Base*	A		B	
Configuration	IV	V	IV	V
First Stage	0.971	0.926	0.980	0.950
Second Stage	0.978	0.933	0.986	0.966
HES System	0.940	--	0.945	--
Total, Launch Vehicle	0.893	0.864	0.913	0.918

\*Two reliability bases are shown: "A" is based on the time of the first flight; "B" is based on the date the vehicles achieve full potential reliability.

achieve full potential in a shorter period of time than would be experienced with Configuration V. This is due to the longer development time required for two separate, secondary fluid-injection systems which also require a separate roll control system for each stage.

Evaluation of Operational Characteristics -- The operational characteristics of Configurations IV and V are discussed separately in Section 3.3.3.2. The spacecraft and the abort system configurations are identical and would differ only in detail. Recovery characteristics would also be identical and determined by the ballistic shape of the spacecraft.

Some differences do appear, as summarized in Table 3-99, in the checkout required and the resulting launch pad tie-up time. Since each stage of Configuration V contains two steering systems which would require an all-system check with the spacecraft in place, V would require an additional four days on the pad compared to Configuration IV. The cargo module for IV contains the steering engines which are mated to the spacecraft and checked out prior to mating to the launch vehicle. Some merit must therefore be given to Configuration IV in terms of response time.

Table 3-99  
EFFECT OF STEERING TECHNIQUE ON SYSTEM  
OPERATIONS LORL MISSION

Configuration	IV	V
Abort System Weight (lb)	8,750	8,750
Checkout In:		
First Stage	0	2
Second Stage	0	2
Payload	1	0
Launch Pad Tie-Up Time, Calendar Days	29	33
Steering Checkout Independent of Boost Stages	Yes	No
Number of Recovery Sites Required from Orbits at 250 nmi Inclined at		
30°	4	4
55°	13	13
90°	46	46

#### 3.3.4.2 Effect of Launch Vehicle Propulsion

The effect of launch vehicle propulsion characteristics is isolated in the comparisons of Configurations III and V. With some minor qualifications, this effect is also isolated in comparisons of Configurations VII and VIII.

#### Comparison of Configurations III and V

The comparisons of III and V are made in the framework of an all-liquid-propellant two-stage vehicle, the Saturn IB, and an all-solid-propellant two-stage vehicle, Configuration V. Both vehicles are in the 40,000-lb payload classification and both perform the LORL logistics mission. Hence the spacecraft configurations are the same, and the same crew complements, useful loads, and in-orbit maneuvering capability are employed for both vehicles. Both launch vehicles employ primary thrust vector control techniques.

The ascent trajectories used in sizing these two vehicles were selected to produce nearly the same apogee velocities at the design parking orbit altitude of 105 nmi. A ballistic type flight profile was used for Configuration V where no attempt was made to modify the trajectory for Configuration III, the BALLOS-Saturn IB, as presented in Reference 2.

Vehicle Size Comparison -- A gross size comparison is presented in Figure 3-107. The Saturn IB, with its BALLOS payload is 15 ft shorter than the all-solid-propellant counterpart, Configuration V. It is evident from this sketch that the larger size of Configuration V is due to the much larger first stage. The hammer-head payload shape for Configuration V is due to the predetermined base diameter of the BALLOS spacecraft and the desirability of using a 156-in. second stage.

The weight characteristics of Configurations III and V are summarized and compared in Table 3-100. As indicated, the gross payloads at liftoff are very similar. This is true also in the second stage. The first stages differ by a large margin, the solid-propellant first stage of Configuration V weighing over 3 times greater than the first stage of Configuration III.

Table 3-100  
EFFECT OF LAUNCH VEHICLE PROPULSION ON VEHICLE WEIGHTS  
LORL MISSION  
(all weights in pounds)

Configuration	III	V
Gross vehicle at liftoff	1,314,650	3,493,300
Gross payload at liftoff	45,610	46,790
Crew module	13,170	13,170
Cargo maneuver module	23,690	24,870
Steering module	--	--
Launch escape system	8,750	8,750
Gross second stage	265,540	267,610
Propellant	230,670	225,450
Gross first stage	1,003,500	3,178,300
Propellant	902,160	2,857,300

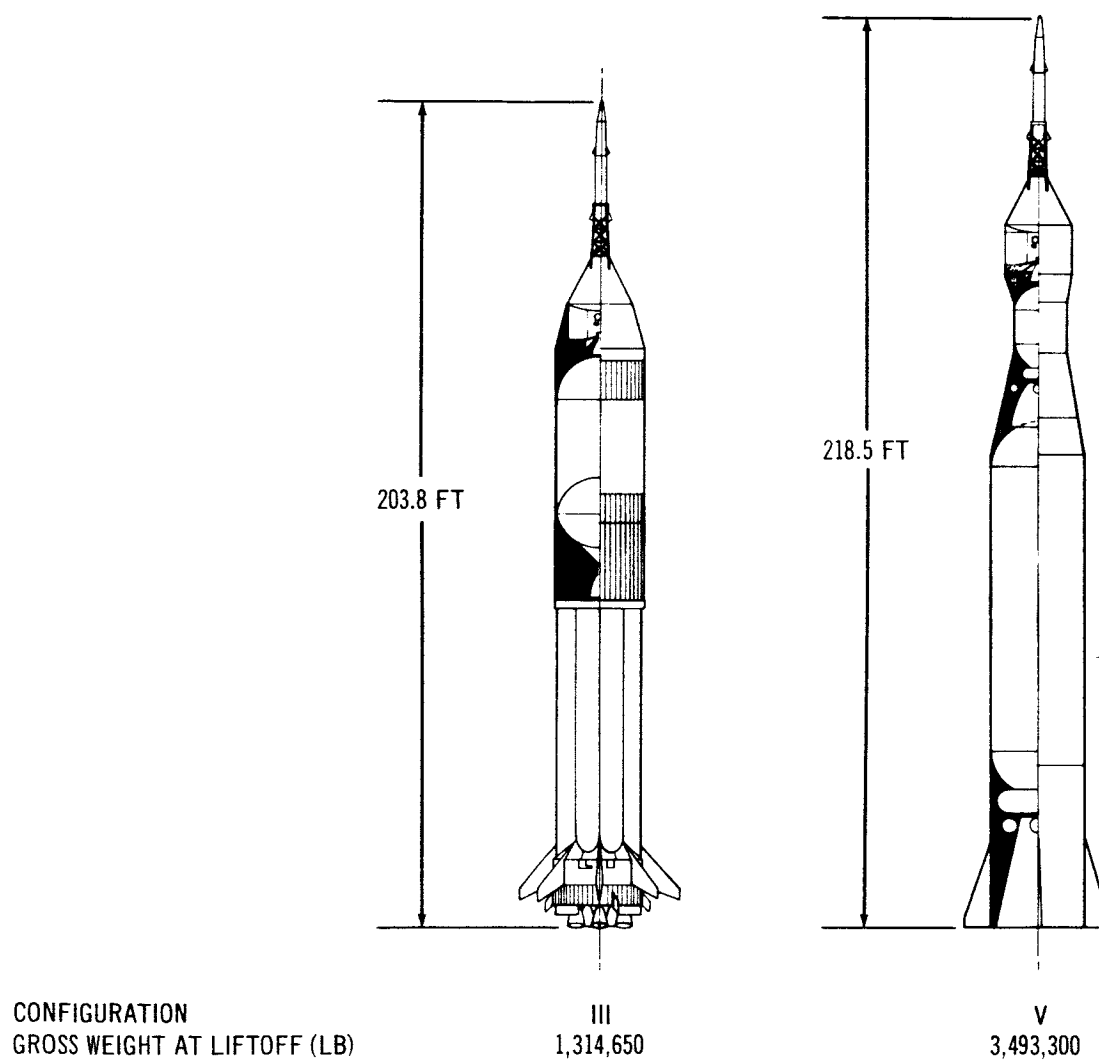


Figure 3-107. Effect of Launch Vehicle Propulsion on Gross Vehicle Size – LORL Mission

The steering systems for Configurations III and V are compared in Table 3-101. Although one more system is required for control of Configuration V first-stage roll control than for Configuration III, no significant qualitative or quantitative conclusions can be made from this chart since steering control alternatives for Configuration III were not examined in this study.

Table 3-101  
EFFECT OF LAUNCH VEHICLE PROPULSION  
ON STEERING SYSTEM CHARACTERISTICS  
LORL Mission

Configuration	III	V
Steering technique	Gimbal engine TVC	LITVC
Steering system location	Engine--each stage	Nozzle area-- each stage
Steering propellant/TVC injectant	1st stage-LO <sub>2</sub> /RP-1 2nd stage-LO <sub>2</sub> /LH <sub>2</sub>	N <sub>2</sub> O <sub>4</sub>
Steering system weight		
Total at launch (lb) (all stages)	NA	22,260
Total expendables (lb) (all stages)	NA	12,380
Maximum vacuum steering thrust (lb) or effective gimbal angle (deg) required		
First stage	--	0.28
Second stage	--	0.69
Number of systems required for control	3	4

Vehicle Performance Comparison--The trajectory characteristics of Configurations III and V are compared in Table 3-102. Higher dynamic pressures and axial accelerations are encountered in the trajectory of Configuration V due primarily to the shorter burn times and thrust levels of the all-solid-propellant stages. The S-IVB second stage of Configuration III has a restart capability and provides injection velocity at the design orbit altitude. The injection velocity of Configuration V is obtained from the spacecraft propulsion system.

Vehicle Cost Comparison--The hardware procurement costs of Configurations III and V are compared in Table 3-103. In this case as with Vehicles IV and V, the cost differences arise entirely because of differences in expendable hardware. The launch vehicle of Configuration V without the cargo module is slightly more than one-half the cost of the launch vehicle for Configuration III.

The cost difference in expendable hardware has a direct effect on total operations cost as shown in Table 3-104. These data are shown for the case of recovery from a 30° orbit, a refurbishment base of 10%, and for a probability of a successful launch of 95%. The difference in the average per flight cost is \$8,440,000 for a 50-flight program or \$422 million for the total operations cost.

There is very little difference in cost because of the total number of flights in the program as long as the inventory is determined by turn-around time requirements rather than by mission life limitations.

Table 3-102

EFFECT OF LAUNCH VEHICLE PROPULSION  
ON TRAJECTORY CHARACTERISTICS  
LORL Mission

Configuration	III	V
Thrust/weight at liftoff	1.15	1.25
Maximum dynamic pressure (psf)	525	974
Maximum axial acceleration (g's)	~4.0	6.9
Apogee altitude (nmi)	105	105
Injection velocity required at apogee (fps)	0	201

Table 3-103

EFFECT OF LAUNCH VEHICLE PROPULSION ON HARDWARE  
PROCUREMENT COST  
LORL Mission  
(all costs in millions of dollars)

Configuration	III	V
Spacecraft	19.55	19.55
Nonrecoverable hardware	20.82	12.86
Cargo module adapter	2.32	2.56
First stage	18.50	7.86
Second stage		2.44
Total, first flight hardware	40.37	32.41

Table 3-104

EFFECT OF LAUNCH VEHICLE PROPULSION ON  
OPERATIONS COSTS  
(all costs in millions of dollars)

30° Orbit Recovery

Refurbishment Base A

Probability of Successful Launch = 95%

Total Successful Flights	50	
Inventory, Spacecraft	4	
Inventory, Expendable Hardware	53	
Configuration	III	V
First flight cost	44.72	36.76
Subsequent flight cost	28.42	19.98
Average flight cost	29.82	21.38
Total program cost	1,491	1,069



Vehicle Cost Effectiveness--Since both spacecraft for Configurations III and V are the same in terms of crew size, useful load, and in-orbit maneuvering capability, the cost effectiveness data suggest the same conclusions as in the preceding section. These data are shown in Table 3-105. Configuration III requires \$16.3 more per lb-sec of useful load impulse than for Configuration V. This represents a 39% increase.

Qualitative Reliability Assessment--At the time that Configuration V would make its first flight, Configuration III should have achieved its full reliability potential as shown in Table 3-106. At that time the total launch vehicle reliability of Configuration V is 0.864 or 0.054 below the projected reliability of Configuration III. However, in about 1-1/2 years after first flight time, Configuration V should achieve at least the level of Configuration III because of the inherent high reliability of the fixed-nozzle solid-propellant motors. The degree to which the solid motor with LITVC could exceed an all-liquid system of the Saturn IB type would require a more detailed reliability analysis than was possible in this study.

Evaluation of Operational Characteristics--The data of Table 3-107 are presented to emphasize the similarities and differences of Configurations III and V from the standpoint of operational characteristics.

Table 3-105

EFFECT OF LAUNCH VEHICLE PROPULSION ON COST EFFECTIVENESS

50 Flights	Refurbishment Base A	30° Orbit Recovery
Configuration	III	V
Average flight cost (\$ millions)	29.82	21.38
Useful load (lb)	15,855	15,855
In-orbit maneuvering capability $\Delta V$ (fps)	1,050	1,050
Useful load impulse ( $10^6$ lb-sec)	0.516	0.516
Cost effectiveness (\$/lb-sec)	57.7	41.4

Table 3-106

EFFECT OF LAUNCH VEHICLE PROPULSION ON  
LAUNCH VEHICLE RELIABILITY

Reliability Base Configuration	A		B	
	III	V	III	V
First stage	0.950	0.926	0.950	0.950
Second stage	0.966	0.933	0.966	0.966
HES system	--	--	--	--
Total, launch vehicle	0.918	0.864	0.918	0.918

The abort escape requirements are very similar. Those requirements resulting from the spacecraft configuration would be the same. Some difference may exist in abort system weight because of the differences in explosive hazard levels of the two launch vehicles. Because of the difficulty in reaching a compatible equivalence in hazard level, this was omitted in the study and the BALLOS abort escape system was used for all vehicles using BALLOS spacecraft.

The number of steering systems requiring checkout is four for Configuration V, exceeding those required for Configuration III by one. An all-system checkout cannot be made for either vehicle until assembly and erection has been completed.

Since the spacecraft for both Configurations III and V are identical, the recovery site requirements are the same. Ground support for launch, rendezvous, and re-entry phases are the same.

#### Comparison of Configurations VII and VIII

Vehicles VII and VIII represent concepts which differ in upper-stage propulsion types. The upper stage of Configuration VII is a high-energy liquid-propulsion system, the S-IVB. Both upper stages of Configuration VIII are solids. The first stages of both vehicles are 260-in. solid motors.

Table 3-107

## EFFECT OF LAUNCH VEHICLE PROPULSION ON SYSTEM OPERATIONS

Configuration	III	V
Abort system weight (lb)	8,750	8,750
Number of steering systems requiring prelaunch checkout in:		
First stage	1	2
Second stage	2	2
Payload	0	0
Launch pad tie-up time, calendar days	48	33
Steering checkout independent of boost stages	No	No
Number of recovery sites required from orbits at 250 nmi inclined at		
30°	4	4
55°	13	13
90°	46	46

The steering for both vehicles is from the head-end during first stage. During second-stage flight of Configuration VII, the existing gimballed engine technique is retained and the head-end steering engines are shut down. Head-end steering is employed throughout the burning of all three stages of Configuration VIII.

The missions for these two vehicles are identical and meet the extended MORL requirements used for Configurations I and II except for reduced in-orbit maneuvering capability. These two vehicles are described individually in more detail in Section 3.3.3.3.

Vehicle Size Comparison--A comparison of gross size characteristics is depicted in Figure 3-108. Configuration VII, benefiting from its high energy S-IVB second stage is 48 ft shorter than Configuration VIII and smaller in gross liftoff weight by 1,574,460 lb. Of some influence on the shorter length of Configuration VII was

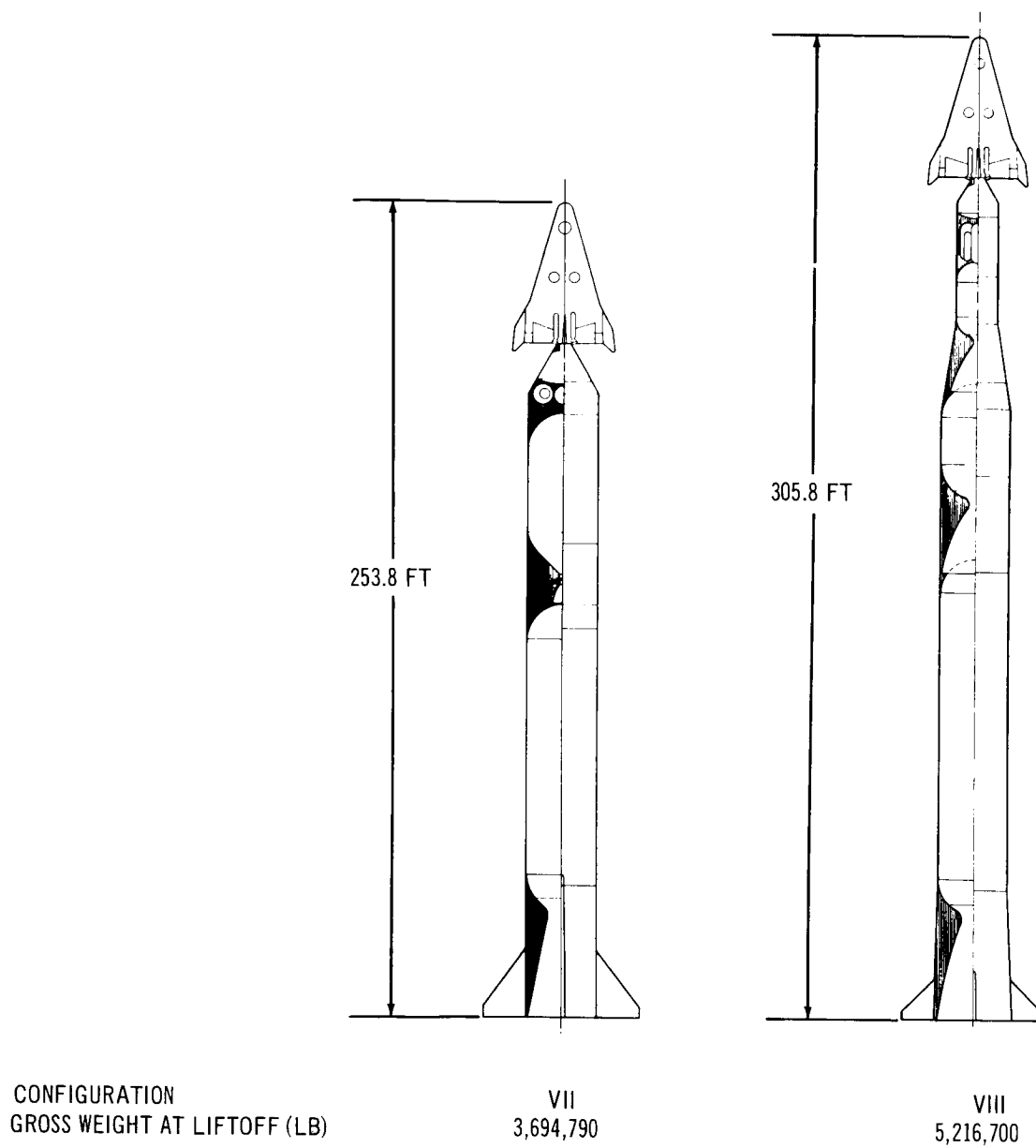


Figure 3-108. Effect of Launch Vehicle Propulsion on Gross Vehicle Size— Extended MORL Mission

the more usable volume afforded for steering tankage because of the 260-in. diameter of the S-IVB. Contributing to this effect was the smaller steering propellant requirements of Configuration VII.

A summary comparison of vehicle weights is shown in Table 3-108. The gross payload data reflect a somewhat smaller total weight at liftoff for Configuration VII because of a lighter spacecraft cargo module and inert steering propellant tank section. The smaller steering engines required for Configuration VII permit a better nozzle expansion ratio for in-orbit maneuvering and, thus, a small amount of propellants is required for the maneuvering impulse. The Configuration VII cargo module is lighter than Configuration VIII because of its shorter length and better structural configuration for transmitting the lifting-body spacecraft loads into the launch vehicle structure.

Additional data on the steering system are presented in Table 3-109. The steering system weight (excluding steering engines in the spacecraft) of Configuration VII is only 48% of the steering system of Configuration VIII, in part attributable to the fact that the weight for Configuration VIII includes steering requirements for second- and third-stage control. The lower first-stage steering thrust required by Configuration VII is because of the shorter coupled launch vehicle and the lower first-stage motor thrust levels.

In spite of the higher thrust/weight ratio for Configuration VII at liftoff, as indicated by the performance data of Table 3-110, the thrust of Configuration VII is some 1,200,000 lb less than for Configuration VIII resulting in much smaller thrust misalignment disturbances. As would be expected, the employment of a relatively high thrust/weight ratio produces a high maximum dynamic pressure, some 368 psf more than for Configuration VIII. Maximum axial accelerations are also higher for Configuration VII by 3.31 g's. Configuration VII also utilizes the restart capability of the S-IVB second stage to inject into orbit, thus requiring no injection impulse from the spacecraft.

Vehicle Cost Comparison--The differences in hardware procurement costs are presented in Table 3-111. These data indicate very little difference in spacecraft cost. The major differences are reflected in the launch vehicles. The cost of the S-IVB second stage of Configuration VII reflects a minimum cost program and involves certain qualifications as discussed in Section 3.3.2.2.

Table 3-108

EFFECT OF LAUNCH VEHICLE PROPULSION ON VEHICLE WEIGHTS (LB)  
Extended MORL Mission

Configuration	VII	VIII
Gross vehicle at liftoff	3,694,790	5,216,700
Gross payload at liftoff	100,370	107,100
Crew module	83,900	86,600
Cargo module	3,600	3,900
Steering module	32,920	68,970
Launch escape system	6,300	6,300
Gross third stage	NA	307,740
Propellant	NA	252,500
Gross second stage*	269,070	1,070,630
Propellant	229,155	944,400
Gross first stage*	3,325,350	3,731,230
Propellant	2,990,000	3,344,000

\*Includes steering propellant

Since the difference in hardware procurement costs is almost entirely in the expendable components, it would be expected that Configuration VII should also show lower total operations costs. This is, in fact, borne out as shown in Table 3-112. The average flight cost for Configuration VII is \$2.62 million less than for Configuration VIII for a 50-flight program.

Without cost data supplied to specific program requirements, it is difficult to show a more refined cost comparison of Configurations VII and VIII. It is clear, however, that the high-energy liquid upper-stage launch vehicle is a cost effective vehicle. Other characteristics of these two vehicles will be compared in the following sections.

Table 3-109

EFFECT OF LAUNCH VEHICLE PROPULSION ON STEERING  
SYSTEM CHARACTERISTICS  
Extended MORL Mission

Configuration	VII	VIII
Steering technique	First stage - HES	HES
	Second stage - Gimbal engine TVC	
Steering system location	First stage - above S-IVB	Above third stage
	Second stage - engine	
Steering propellant	First stage - $N_2O_4/MMH$	$N_2O_2/MMH$
	Second stage - $LO_2/LH_2$	
Steering system weight (excluding S-IVB)		
Total at launch, all stages (lb)	32,920	68,970
Total expendables, all stages (lb)	26,350	58,670
Maximum vacuum steering thrust (lb) or effective gimbal angle (deg) required		
First stage	35,800	44,960
Second stage	~3.6°	13,780
Third stage	NA	26,510
Number of systems required for control	3	1

Table 3-110

EFFECT OF LAUNCH VEHICLE PROPULSION ON TRAJECTORY  
CHARACTERISTICS  
Extended MORL Mission

Configuration	VII	VIII
Thrust/weight at liftoff	1.44	1.25
Maximum dynamic pressure (psf)	1,166	798
Maximum axial acceleration (g's)	7.74	4.33
Apogee altitude (nmi)	105	105
Injection velocity required at apogee (fps)	0	291

Table 3-111

EFFECT OF LAUNCH VEHICLE PROPULSION ON HARDWARE  
PROCUREMENT COST (\$ MILLIONS)  
Extended MORL Mission

Configuration	VII	VIII
Spacecraft	38.38	38.54
Nonrecoverable hardware	13.30	15.76
Cargo module adapter	1.58	1.58
Steering propellant tank section	0.85	0.94
First stage	5.70	6.99
Second stage	5.17	4.18
Third stage	--	2.07
Total, first flight hardware	51.68	54.30



Table 3-112

EFFECT OF LAUNCH VEHICLE PROPULSION ON  
OPERATIONS COSTS (\$ MILLIONS)

30° Orbit Recovery		Refurbishment Base A	
Probability of Successful Launch = 95%			
Total Successful Flights		50	
Inventory, Spacecraft		4	
Inventory, Expendable Hardware		53	

Configuration	VII	VIII
First flight cost	54.68	57.30
Subsequent flight cost	20.95	23.56
Average flight cost	23.71	26.33
Total program cost	1,186	1,317

Vehicle Cost Effectiveness--Both Configurations VII and VIII carry the same useful load, crew size, and have the same in-orbit maneuvering capability. These data are shown in Table 3-113. The useful load impulse is therefore 1.081 million pps in orbit. This results in \$2.4/pps less for Configuration VII than for Configuration VIII. This is the same trend developed in the preceding comparison based on cost alone.

Qualitative Reliability Assessment--The first flight of Configuration VIII has been assumed to be at the time the S-IVB stage of Configuration VII has reached its full reliability potential. At this time the reliability of Configuration VIII would be 0.882 or 0.009 lower than for Configuration VII. These data are presented in Table 3-114. This reliability difference results primarily from the inherent advantage of a fewer number of stages. At the time when full reliability is achieved for Configuration VIII, the advantage of a two-stage vehicle should be overcome by the

Table 3-113

## EFFECT OF LAUNCH VEHICLE PROPULSION ON COST EFFECTIVENESS

50 Flights	Refurbishment Base A	30° Orbit Recovery
Configuration	VII	VIII
Average flight cost (\$ millions)	23.71	26.33
Useful load (lb)	6,600	6,600
In-orbit maneuvering capability $\Delta V$ (fps)	5,270	5,270
Useful load impulse ( $10^6$ lb-sec)	1.081	1.081
Cost effectiveness (\$/lb-sec)	21.9	24.3

Table 3-114

EFFECT OF LAUNCH VEHICLE PROPULSION ON  
LAUNCH VEHICLE RELIABILITY

Reliability Base	A		B	
Configuration	VII	VIII	VII	VIII
First stage	0.971	0.971	0.980	0.980
Second stage	0.966	0.978	0.966	0.986
Third stage	--	0.978	--	0.986
HES system	0.950	0.950	0.966	0.966
Total, launch vehicle	0.891	0.882	0.891	0.920

inherent higher reliability of the fixed-nozzle solid motors. This difference then shifts to the advantage of Configuration VIII by 0.029.

Evaluation of Operational Characteristics--The abort escape requirements for Configurations VII and VIII are very similar. The abort system weights, as indicated in Table 3-115, are the same and are based on analyses performed on Configuration I. The spacecraft, since they are nearly identical, would possess land recovery capability from aborted flights up to and slightly beyond the maximum dynamic pressure point in the ascent trajectory.

Table 3-115

EFFECT OF LAUNCH VEHICLE PROPULSION ON SYSTEM OPERATIONS

Configuration	VII	VIII
Abort system weight (lb)	6,300	6,300
Number of steering systems requiring prelaunch checkout in:		
First stage	0	0
Second stage	2	0
Third stage	NA	0
Payload	1	1
Launch pad tie-up time, calendar days	30	32
Steering checkout independent of boost stages	Yes (first stage)	Yes
Number of recovery sites required from orbits at 250 nmi, inclined at		
30°	3	3
55°	4	4
90°	4	4

Configuration VII would require three major steering systems to be checked out prior to launch while Configuration VIII requires only one. However, Configuration VII requires that only two stages be assembled while Configuration VIII requires three. The estimate of resultant launch pad tie-up time indicates 2 days longer for Configuration VIII.

The number of recovery sites required for the two vehicles is the same since both possess the same aerodynamic configuration and hence, the same cross-range capability.

#### 3.3.4.3 Effect of Spacecraft Type

The effect of spacecraft configuration on total system characteristics has been isolated through a comparison of Configurations IV and VI. These vehicles have been previously discussed separately in Section 3.3.3.2. The scope of the Phase II study permitted the comparison to be made for only one type of steering system. Both Configurations IV and VI, therefore, use head-end steering adapted to the unique requirements of the ballistic spacecraft type, Configuration IV, and of the lifting body type, Configuration VI. It is possible, however, to obtain a first-order evaluation of the effect of the spacecraft shape independent of the steering and this will be discussed in Section 3.3.5.

#### Comparison of Configurations IV and VI

Both vehicles, Configurations IV and VI, were designed to accomplish the LORL logistics mission and therefore have the same crew size, useful load, and in-orbit maneuvering capability. All-solid-propellant motors are used with fixed nozzles for both vehicles. Steering is accomplished at the head-end of both vehicles though it is not feasible to install the steering engines on the ballistic type of spacecraft of IV. Consequently, these engines are located on the cargo-adaptor module and are not recoverable.

The spacecraft for Configuration VI is the HL-10 sized for 12 passengers but, unlike Configurations I, II, VII, and VIII, does not have a complete on-board propulsion system. It is therefore much smaller, having a length of 28.75 ft.

The BALLOS spacecraft is used for Configuration IV and is identical to the ballistic type of spacecraft used for Configurations III and V.

Vehicle Size Comparison--A gross size comparison of Configurations IV and VI is shown in Figure 3-109. The shorter length of Configuration VI is quite apparent. In terms of overall length this difference is 44.8 ft. Without the escape tower required for the ballistic spacecraft of Configuration IV, Vehicle VI is still shorter by 9.1 ft. The shorter length of Configuration VI results from shorter stage motor lengths, a shorter cargo module section and a shorter steering propellant tank section. Shorter lengths in these regions offset the longer spacecraft of Configuration VI.

The gross weight at liftoff is smaller for vehicle VI by 688,700 lb. A more detailed weight comparison is shown in Table 3-116. These data reveal that the gross payload at liftoff is heavier for Configuration IV by 16,760 lb due mostly to a heavier cargo module adapter section and a heavier steering propellant tank section.

The relative inefficiency of the four steering engines of Configuration IV may be seen in the data of Table 3-117. It will be noted that while the individual steering engine maximum thrust requirements are almost the same, the four-engine arrangement of Configuration IV requires over twice the propellant weight of Configuration VI. Since the steering system weights for both Configurations IV and VI are carried as upper-stage payload, the launch vehicle of Configuration IV is significantly larger.

The steering thrust required for Configuration VI during second-stage flight is higher than for Configuration IV. This is due to the lower inert second-stage weight of Configuration VI causing the control moment arm to approach closer to the control point than for Configuration IV.

Comparison of Vehicle Performance--The design ascent trajectories are discussed separately for both Configurations IV and VI in Section 3.3.3.2. These data are summarized and compared in Table 3-118. Very little difference exists. Vehicle VI encounters a somewhat higher maximum dynamic pressure than Vehicle IV but the difference is only 83 psf.

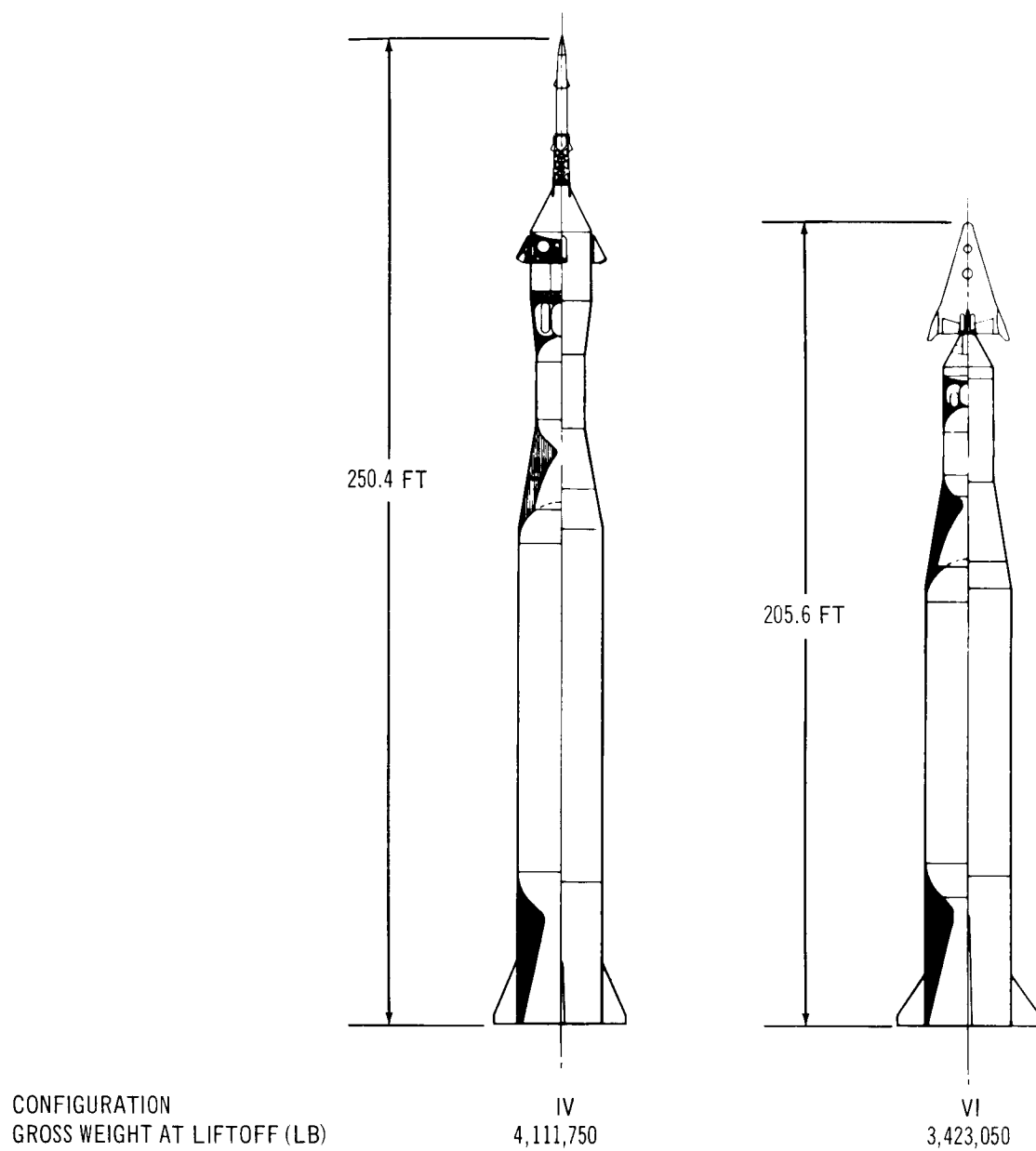


Figure 3-109. Effect of Spacecraft Configuration on Gross Vehicle Size – LORL Mission

Table 3-116

EFFECT OF SPACECRAFT CONFIGURATION ON VEHICLE WEIGHTS (LB)  
LORL MISSION

Configuration	IV	VI
Gross vehicle at liftoff	4,111,750	3,423,050
Gross payload at liftoff	62,900	46,140
Crew module	13,170	13,250
Cargo-maneuver module	32,430	25,890
Steering module	60,850	30,180
Launch escape system	8,750	2,220
Gross second stage*	361,830	304,160
Propellant	306,340	257,550
Gross first stage*	3,687,020	3,072,750
Propellant	3,302,500	2,761,950

\*Includes steering propellant.

Vehicle Cost Comparison--The hardware procurement costs are presented in Table 3-119. Total hardware procurement costs for the first flight are almost the same differing by only 0.2% of 1%. The higher cost of the spacecraft for Configuration VI is balanced by the higher expendable hardware cost of Configuration IV. As discussed in a previous section, the larger payload size of Configuration IV, resulting from a larger steering propellant requirement, demands a larger launch vehicle and, hence, a costlier launch vehicle. The cargo module is almost a factor of 2 higher in cost than the cargo module for Configuration VI because of the steering engine installation and bulkier size.

Despite the nearly identical first flight procurement costs, the effect of reusability produces a lower total operations cost for Configuration VI. This may be seen in Table 3-120, where the operations costs are summarized. These data show the effect

Table 3-117

EFFECT OF SPACECRAFT CONFIGURATION ON STEERING  
SYSTEM CHARACTERISTICS

## LORL MISSION

Configuration	IV	VI
Steering technique	HES-4 engines	HES-2 engines
Steering system location	Above second stage	Above second stage
Steering propellant/TVC injectant	N <sub>2</sub> O <sub>4</sub> /MMH	N <sub>2</sub> O <sub>4</sub> /MMH
Steering system weight		
Total at launch (lb) (all stages)	60,850	30,180
Total propellant (lb) (all stages)	52,300	25,400
Maximum vacuum steering thrust (lb) of effective gimbal angle (deg) required		
First stage	21,080	21,050
Second stage	4,300	6,090
Number of systems required for control	1	1

of spacecraft configuration on operations cost. While the significance of cross-range capability of the spacecraft on the number of recovery sites and their costs has been discussed in Section 3.2.1.4, these data show the effect of the recovery characteristics in terms of the total operation. Another factor introduced in the data presented in Table 3-120, is the refurbishment cost base for the spacecraft.

Refurbishment base A indicates refurbishment costs based on 10% of spacecraft hardware procurement cost for each refurbishment. In this case no differentiation is made in refurbishment costs between ballistic types and lifting-body,



Table 3-118

EFFECT OF SPACECRAFT CONFIGURATION ON TRAJECTORY  
CHARACTERISTICS

## LORL MISSION

Configuration	IV	VI
Thrust/weight at liftoff	1.25	1.25
Maximum dynamic pressure (psf)	934	1017
Maximum axial acceleration (g's)	6.5	6.4
Apogee altitude (nmi)	105	105
Injection velocity required at apogee (fps)	163	204

Table 3-119

EFFECT OF SPACECRAFT CONFIGURATION ON HARDWARE  
PROCUREMENT COST (\$ MILLIONS)

## LORL MISSION

Configuration	IV	VI
Spacecraft	19.55	23.04
Nonrecoverable hardware	14.40	10.83
Cargo module adapter	4.55	2.45
Steering propellant tank section	0.71	0.48
First stage	6.77	5.84
Second stage	2.37	2.06
Total, first flight hardware	33.95	33.87

Table 3-120

EFFECT OF SPACECRAFT CONFIGURATION ON OPERATIONS COSTS  
(\$ millions)

50 Flights				4 Spacecraft				
Probability of Successful Launch = 95%				53 Units of Expendable Hardware				
Orbit (deg)	30				90			
Refurbishment base	A		B		A		B	
Configuration	IV	VI	IV	VI	IV	VI	IV	VI
First flight cost	38.26	36.87	38.26	36.87	44.24	36.79	44.24	36.79
Subsequent flight cost	21.57	16.78	24.46	17.25	27.55	16.70	30.44	17.17
Average flight cost	22.97	18.44	25.63	18.87	28.95	18.36	31.61	18.79
Total program cost	1149	922	1282	944	1448	918	1581	940

horizontal-landing types. Refurbishment base B is based on estimates made for specific spacecraft configurations in other NASA-funded industry studies, References 5 and 6. In the case of the ballistic spacecraft, Configuration IV, the refurbishment Base B corresponds to 25% of the spacecraft hardware procurement for each refurbishment. For Configuration VI, the heat shield definition is similar to that described for Configuration I and consists of an all-ablative heat shield. Refurbishment Base B in this case is 12% of spacecraft hardware procurement cost for each refurbishment. Section 3.2.2 presents a discussion of an analysis made in this study for an all-ablative heat shield technique applied to the Configuration I spacecraft which results in a refurbishment cost of about 10% of spacecraft hardware procurement. The slightly higher percentage used for Configuration VI is because of the smaller size of the spacecraft.

Referring to Table 3-120, a comparison of the average flight costs of Configurations IV and VI indicates that Configuration VI is less expensive by from \$4 to \$7 million/flight for missions requiring a 30° orbital recovery. The range in cost results from the use of either of the two refurbishment cost bases. When missions require a polar-orbit recovery, the average cost per flight is less for Configuration VI by from \$10 to almost \$13 million depending on the refurbishment base.

Vehicle Cost Effectiveness--Table 3-121 interprets these costs in terms of cost effectiveness. These data show that Configuration VI is less costly by from \$9 to over \$13/lb-sec of useful load impulse for missions requiring recovery from a 30° orbit. For polar-orbit recoveries, Configuration VI is less costly by from \$20 to \$25/lb-sec of useful load impulse.

Qualitative Reliability Assessment--While Vehicles IV and VI are identical in terms of the complexity of the launch vehicle stages, the two additional steering engines required for Configuration IV produce a lower reliability than for Configuration VI. The probabilities of successful subsystem operation are shown in Table 3-122. It should be noted that a single engine failure of either configuration, resulting in either loss of thrust or in thrust vector orientation, would result in a mission abort.

Table 3-121

## EFFECT OF SPACECRAFT CONFIGURATION ON COST EFFECTIVENESS

50 Flights

Useful load = 15,855 lb

 $\Delta V$  In-orbit = 1050 fps

Useful load impulse = 516,000 lb-sec

Orbit (deg)	30				90			
Refurbishment base	A		B		A		B	
Configuration	IV	VI	IV	VI	IV	VI	IV	VI
Average flight cost (\$ millions)	22.97	18.44	25.63	18.87	28.95	18.36	31.61	18.79
Cost effectiveness (\$/lb-sec)	44.6	35.8	49.6	36.6	56.1	35.6	61.4	36.6

Table 3-122

EFFECT OF SPACECRAFT CONFIGURATION ON LAUNCH  
VEHICLE RELIABILITY

Reliability Base	A		B	
Configuration	IV	VI	IV	VI
First stage	0.971	0.971	0.980	0.980
Second stage	0.978	0.978	0.986	0.986
HES system	0.940	0.950	0.945	0.966
Total, launch vehicle	0.893	0.903	0.913	0.933

Evaluation of Operational Characteristics--A comparison of the operational characteristics of Configurations IV and VI is shown in Table 3-123. The use of head-end steering and all-solid-propellant motors with fixed nozzles in both vehicles assures very similar procedures in assembly checkout and erection procedures. An exploration of procedural practices resulted in the recommendation that the cargo module adapter for either configuration be mated with the spacecraft prior to assembly to the launch vehicle. A significant amount of system checkout could be accomplished, therefore, prior to mating of the spacecraft and cargo module adapter to the launch vehicle.

Table 3-123  
EFFECT OF SPACECRAFT CONFIGURATION  
ON SYSTEM OPERATIONS

Configuration	IV	IV
Abort system weight (lb)	8,750	2,220
Number of steering systems requiring Prelaunch checkout in:		
First stage	0	0
Second stage	0	0
Payload	1	1
Launch pad tie-up time, calendar days	29	29
Steering checkout independent of boost stages	Yes	Yes
Number of recovery sites required from orbits at 250 nmi inclined at		
30°	4	3
55°	13	4
90°	46	4

The abort system of Configuration VI is over 6,500 lb lighter than for Configuration IV because of the lack of any tower requirements. Sufficient altitude for parachute deployment is assured for Configuration VI after a pad abort. Lateral range are developed during and after the escape acceleration phase through aerodynamic lift.

Significant differences arise between Configurations IV and VI because of the differences in cross-range capability during the recovery phase and the differences in landing modes. The limited cross-range capability of Configuration IV requires, for a vertical landing on land, cleared sites of suitable topographical characteristics where none now exist. On the other hand, the lifting-body spacecraft landing horizontally would be able to utilize a high percentage of existing airfields in the zone of interior. This is particularly significant for recovery from orbits inclined more than  $30^\circ$  as shown in Table 3-123. Recovery from polar orbits would require 42 more recovery sites for Configuration IV than for Configuration VI. The number of sites required for Configuration VI is essentially independent of orbit inclination.

#### 3.3.4.4 Effect of Total System Concept

The sum-total effect of steering technique, launch vehicle propulsion, and spacecraft configuration is indicated by the comparison of Configurations III and VI.

#### Comparison of Configurations III and VI

These two vehicles have been described in preceding discussions of this report both individually and in comparison with other vehicles. They were both required to perform the LORL logistics mission and, hence, possess the same capability for resupply of crew and cargo and for in-orbit maneuvering. The launch vehicle for Configuration III is the Saturn IB. Liquid oxygen and RP-1 propellants are burned in the first-stage propulsion system and liquid oxygen and liquid hydrogen are the propellants for the S-IVB second stage. Steering is by gimballing of the rocket engines of each stage with the S-IVB stage requiring a separate roll-control system. The BALLOS spacecraft for Configuration III is the ballistic type, similar to APOLLO in shape, but carrying 12 passengers. Cargo is carried in a module which also serves as the structural adapter between the spacecraft and the second stage.

The Configuration VI launch vehicle employs a two-stage all-solid-propellant booster system with fixed nozzles. The first stage is a 260-in. motor and the second stage is a 156-in. motor. Head-end steering propellants are carried in a tank section at the upper end of the second stage. The two steering engines are installed in the outer trailing-edge extremities of the HL-10 spacecraft and are fully gimballed. The HL-10 spacecraft of Configuration VI is of the lifting body type and carries no independent propulsion, the steering engines being entirely dependent on the propellants from the steering tank section and the in-orbit maneuvering propellants located in the cargo module adapter section.

Vehicle Size Comparison--The two vehicles, III and VI, are compared side by side in Figure 3-110. There is very little difference in overall length but the launch vehicle of Configuration III is significantly shorter. As would be expected, the all-solid-propellant launch vehicle for Configuration VI is considerably heavier, weighing 2 million lb more than the Saturn IB of Configuration III. Additional weight comparisons are presented in Table 3-124. The gross payload at liftoff for the two vehicles differ by only 530 lb. This is because the heavier launch escape system of Configuration III balances out the heavier crew module, cargo-maneuver module, and dry-steering module of Configuration VI. The payload weight in orbit for Configuration III is significantly lower than Configuration VI since most of the launch escape systems are dropped during or at the end of first stage.

Table 3-124  
EFFECT OF TOTAL SYSTEM CONCEPT ON VEHICLE WEIGHTS (lb)  
LORL MISSION

Configuration	III	VI
Gross vehicle at liftoff	1, 314, 650	3, 423, 050
Gross payload at liftoff	45, 610	46, 140
Crew module	13, 170	13, 250
Cargo-maneuver module	23, 690	25, 890
Steering module	NA	30, 180
Launch escape system	8, 750	2, 220
Gross second stage	265, 540	304, 160
Propellant	230, 670	257, 550
Gross first stage	1, 003, 500	3, 072, 750
Propellant	920, 160	2, 761, 950

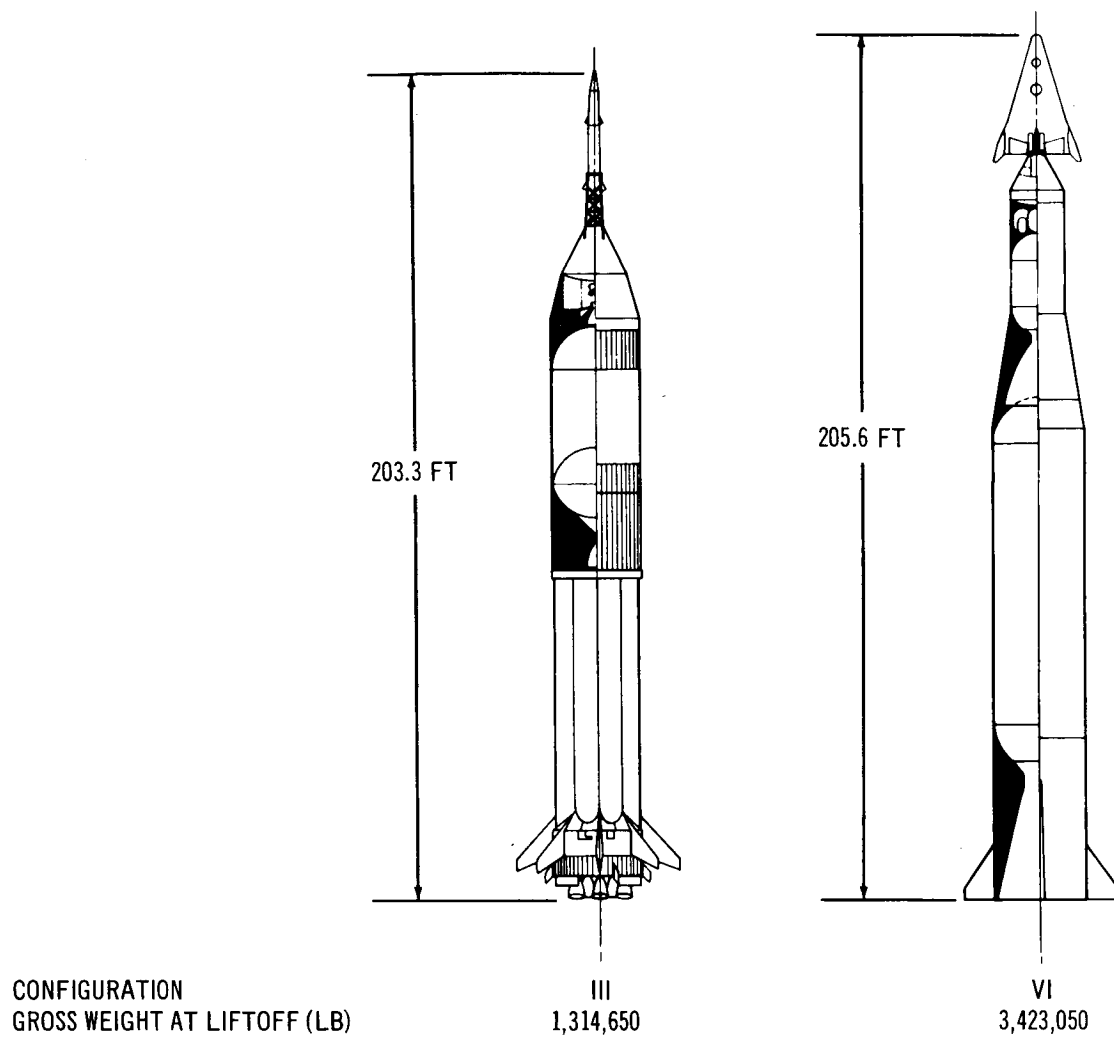


Figure 3-110. Effect of Total System Concept on Gross Vehicle Size – LORL Mission



The data of Table 3-125 are presented to highlight the differences in the steering system characteristics. Three steering systems are required for controlling Configuration III compared to one system required for Configuration VI.

Configuration VI is flown with a higher thrust/weight ratio at liftoff and consequently would experience a higher maximum dynamic pressure and higher maximum axial accelerations. The S-IVB second stage utilizes a restart capability in the BALLOS study of Reference and provides the required injection velocity at apogee conditions. The injection requirement for Configuration VI is obtained from the steering engines using propellants from tanks located in the cargo module.

Table 3-125  
EFFECT OF TOTAL SYSTEM CONCEPT ON STEERING  
SYSTEM CHARACTERISTICS  
LORL MISSION

Configuration	III	VI
Steering technique	Gimbal engine TVC	HES 2 engine
Steering system location	Engine each stage	Above second stage
Steering propellant/TVC injectant	first stage-LO <sub>2</sub> RP-1 second stage-LO <sub>2</sub> /LH <sub>2</sub>	N <sub>2</sub> O <sub>4</sub> /MMH
Steering system weight		
Total at launch, all stages (lb)	NA	30, 180
Total expendable, all stages (lb)	NA	25, 400
Maximum vacuum steering thrust (lb) or effective gimbal angle (deg) required		
First stage	--	21, 050
Second stage	--	6, 090
Number of systems required for control	3	1

A comparison of the trajectory characteristics is shown in Table 3-126.

Table 3-126  
EFFECT OF TOTAL SYSTEM CONCEPT  
ON TRAJECTORY CHARACTERISTICS  
LORL MISSION

Configuration	III	VI
Thrust/weight at liftoff	1.15	1.25
Maximum dynamic pressure (psf)	525	1,017
Maximum axial acceleration (g's)	~4.0	6.4
Apogee altitude (nmi)	105	105
Injection velocity required at apogee (fps)	0	204

Vehicle Cost Comparison--The hardware procurement cost comparison presented in Table 3-127 indicates a significant difference, particularly in expendable components. The launch vehicle of Configuration III without the cargo module is over twice the cost of the launch vehicle for Configuration VI. Despite the lower spacecraft cost for Configuration III, the influence of the launch vehicle cost produces almost the same 2:1 factor in total operations cost. These data are presented in Table 3-128. Cost data are presented for two refurbishment cost bases and for missions requiring recovery from 30° and 90° orbits. In the comparison of Configurations IV and VI, the spacecraft configuration may influence strongly both refurbishment and recovery costs. If one chooses to ignore the effect of refurbishment differences, the average flight cost for Configuration VI is still some \$11.4 million less than for Configuration III. Incorporating the refurbishment base B, the average flight cost for Configuration VI is almost \$20 million less than Configuration III for missions requiring a recovery from a polar orbit.

Vehicle Cost Effectiveness--Both Configurations III and VI have the same crew size, cargo capability, and in-orbit maneuvering requirement. The useful load impulse for both vehicles is thus the same. Table 3-129 presents a comparison of cost effectiveness analyses based on useful load impulse. These data follow the same trends shown in the cost comparisons. Using the same refurbishment cost percentage for both Configurations III and VI, base A, an average flight would

Table 3-127  
EFFECT OF TOTAL SYSTEM CONCEPT ON HARDWARE  
PROCUREMENT COST (\$ millions)

LORL MISSION

Configuration	III	VI
Spacecraft	19.55	23.04
Nonrecoverable hardware	20.82	10.83
Cargo module adapter	2.32	2.45
Steering propellant tank section	--	0.48
First stage	18.50	5.84
Second stage		2.06
Total, first flight hardware	40.37	33.87

Table 3-128  
EFFECT OF TOTAL SYSTEM CONCEPT  
ON OPERATIONS COSTS

50 Flights  
Probability of Successful Launch = 95%

(\$ millions)

4 Spacecraft  
53 Units of Expendable Hardware

Orbit, (deg)	30				90			
Refurbishment Base*	A		B		A		B	
Configuration	III	VI	III	VI	III	VI	III	VI
First flight cost	44.68	36.87	44.68	36.87	50.66	36.79	50.66	36.79
Subsequent flight cost	28.42	16.78	31.31	17.25	34.40	16.70	37.29	17.17
Average flight cost	29.82	18.44	32.48	18.87	35.80	18.36	38.46	18.79
Total program cost	1491	922	1624	944	1790	918	1923	940

\*Refurbishment Base A: Refurbishment costs at 10% of spacecraft hardware procurement costs. Refurbishment Base B: Refurbishment costs at 12% for Configuration VI and 25% for Configuration III.

Table 3-129  
EFFECT OF TOTAL SYSTEM CONCEPT  
ON COST EFFECTIVENESS

50 Flights

Useful Load = 15,855 lb

$\Delta V$  In-Orbit = 1,050 fps

Useful Load Impulse = 516,000 lb-sec

Orbit (deg)	30				90			
Refurbishment Base	A		B		A		B	
Configuration	III	VI	III	VI	III	VI	III	VI
Average flight cost (\$ millions)	29.82	18.44	32.48	18.87	35.80	18.36	38.46	18.79
Cost effectiveness (\$/lb-sec)	57.8	35.8	63.0	36.6	69.6	35.6	74.5	36.4

cost \$22/lb-sec more of useful load impulse for Configuration III than for Configuration VI when performing missions in a 30° orbit. For a 90° orbit mission and using refurbishment base B, the average flight cost is \$38/lb-sec more of useful impulse for Configuration III than for Configuration VI.

Qualitative Reliability Assessment--The reliability projections for Configurations III and VI are presented in Table 3-130. The two reliability bases A and B are defined, and the individual reliability characteristics are discussed separately for Configurations III and VI in Section 3.3.3.2.

At the time of the first flight of Configuration VI, it is estimated that the launch vehicle reliability will be 0.015 less than for the fully developed Configuration III. Configuration VI should however surpass Configuration III by 0.015 when its full potential is reached. The potential reliability of the fixed-nozzle solid-propellant stages of Configuration VI is sufficiently high to offset the pseudo-third-stage effect of the head-end steering system.

Table 3-130  
EFFECT OF TOTAL SYSTEM CONCEPT ON  
LAUNCH VEHICLE RELIABILITY

Reliability Base	A		B	
Configuration	III	VI	III	VI
First stage	0.950	0.971	0.950	0.980
Second stage	0.966	0.978	0.966	0.986
HES system	--	0.950	--	0.966
Total, launch vehicle	0.918	0.903	0.918	0.933

Evaluation of Operational Characteristics--The individual operational characteristics of Configurations III and VI are discussed in Section 3.3.3.2. A summary comparison of these characteristics is presented in Table 3-131. The differences in abort characteristics are the same differences that exist between Configurations IV and VI and has been discussed in Section 3.3.4.3.

The total number of steering systems requiring checkout prior to launch for Configuration III is three compared with the single head-end steering system for Configuration VI. These systems, with the interstage connections required, result in a rather lengthy all-systems checkout time for Configuration III with a fully erected launch vehicle and payload. The launch pad tie-up time for Configuration VI is estimated to be 19 days less than for Configuration III due primarily to shorter stage erection times and the pre-erection checkout that can be accomplished on the head-end steering system.

The normal recovery site requirements shown in Table 3-131 are those determined by the cross-range capability and landing mode characteristics of the spacecraft. In this comparison as in the comparison with Configuration IV, there is a significant advantage for Configuration VI in both cost and complexity of recovery operations.

Table 3-131

EFFECT OF TOTAL SYSTEM CONCEPT  
ON SYSTEM OPERATIONS

Configuration	III	VI
Abort system weight (lb)	8,750	2,220
Number of steering systems requiring prelaunch checkout in:		
First stage	1	0
Second stage	2	0
Payload	0	1
Launch pad tie-up time, calendar days	48	29
Steering checkout independent of boost stages	No	Yes
Number of recovery sites required from orbits at 250 nmi inclined at		
30°	4	3
55°	13	4
90°	46	4

### 3.3.5 Summary

The eight vehicles designed around the three mission profiles were investigated to the depth required to afford a comparative analysis of the head-end steering concept. The relative economic, technical, and operational advantages, as well as the disadvantages, were determined for the overall concept and for the separate design features comprising the concept, that is, lifting body spacecraft, solid-propellant launch vehicle, and the head-end steering technique. The resulting vehicles and their characteristics are shown in Figure 3-111 for those designed around the Extended MORL logistics mission and Figure 3-112 for the LORL logistics mission.

Vehicle Configurations I and II were compared to isolate the effects of using head-end steering rather than conventional liquid-injection thrust vector control on a solid-propellant launch vehicle with a lifting body spacecraft. Both vehicles were designed to satisfy the same mission. This comparison showed that, although the use of head-end steering resulted in a higher vehicle liftoff weight and greater overall length, it provided a more cost effective vehicle with a higher reliability. Launch pad tie-up time and vehicle turnaround time were shorter for the head-end steered vehicle.

A comparison of Configurations IV and V also isolated the effects of using head-end steering, but for a solid-propellant launch vehicle with a ballistic spacecraft. The use of a ballistic spacecraft necessitated a four-engine steering system which resulted in not only a heavier and longer head-end steered vehicle, but also a less cost effective vehicle. Reliability, however, was greater and turnaround time shorter for the head-end steered vehicle.

The isolated effect of launch vehicle propulsion was shown by a comparison of Configurations III and V. This showed the effect of using a solid-propellant launch vehicle rather than the cryogenic liquid-propellant Saturn IB, with both vehicles incorporating ballistic spacecraft and conventional thrust vector control techniques. The higher-energy liquid propellants results in a smaller and much lighter vehicle; however, the solid-propellant launch vehicle is more cost effective and requires a much shorter turn around time. The launch vehicle reliabilities are essentially the same.

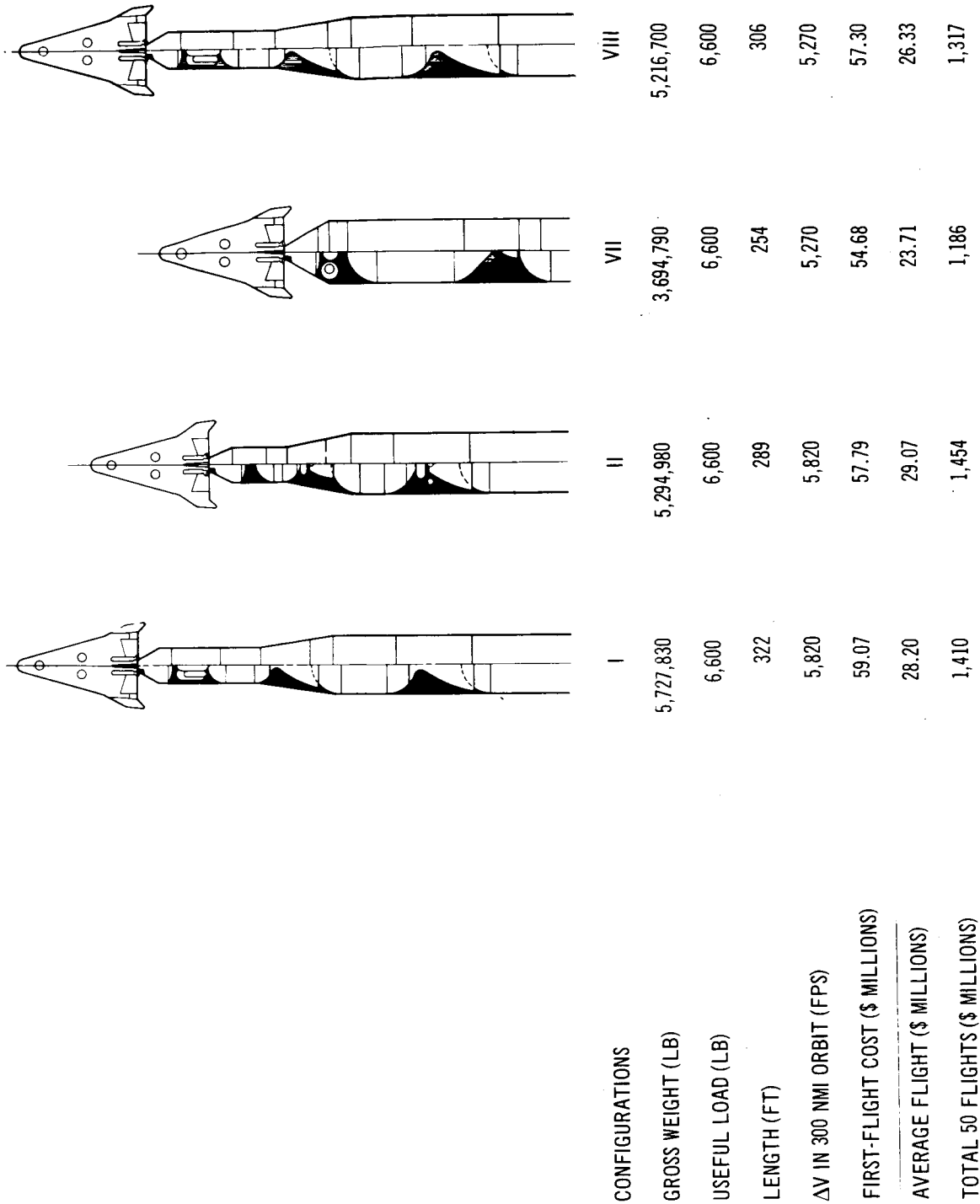


Figure 3-111. Summary - Phase II, Extended MORL Mission Vehicles



CONFIGURATIONS	III	IV	V	VI
GROSS WEIGHT (LB)	1,314,650	4,111,750	3,493,300	3,423,050
USEFUL LOAD (LB)	15,855	15,855	15,855	15,855
LENGTH (FT)	203	250	218	206
$\Delta V$ IN 105 NMI ORBIT (FPS)	1,050	1,050	1,050	1,050
FIRST-FLIGHT COST (\$ MILLIONS)	44.72	38.26	36.76	36.87
AVERAGE FLIGHT (\$ MILLIONS)	29.82	22.97	21.38	18.44
TOTAL 50 FLIGHTS (\$ MILLIONS)	1,491	1,149	1,069	922

Figure 3-112. Summary – Phase II, LORL Mission Vehicles

A comparison of a three-stage, solid-propellant launch vehicle with one using a solid-propellant first stage and a high-energy liquid-propellant S-IVB second stage was provided by Configurations VIII and VII. The hybrid launch vehicle of Configuration VII resulted in shorter vehicle length, lower vehicle weight, and greater cost effectiveness. The use of two stages rather than three resulted in a shorter pad tie-up time for the hybrid vehicle. The reliability potential of the all-solid-propellant vehicle, however, is greater.

Vehicle Configurations IV and VI showed the isolated effect of using a lifting body spacecraft rather than a ballistic spacecraft for a solid-propellant, head-end steered launch vehicle. Because of the effect of the spacecraft on steering system requirements, the magnitude of the variation in vehicle characteristics would not necessarily correspond to a comparison using a conventionally steered, solid-propellant launch vehicle although the direction of the changes would probably be the same. This comparison showed that use of a lifting body spacecraft results in a shorter, lighter, and much more cost effective logistics system. Reliability of the vehicle with the lifting body spacecraft was slightly higher, primarily because of the smaller number of steering engines required, while pad tie-up time was the same.

The effect of the total system concept is provided by a comparison of Configurations III and VI. The use of the head-end steering concept rather than the conventional BALLOS-Saturn IB system resulted in a heavier vehicle with essentially the same overall length. The head-end steering concept provided, however, a vehicle which was twice as cost effective, had a higher reliability potential, and required a much shorter turnaround time.

As stated in Section 3.3.1, an objective of the comparative studies portion of the Phase II study was to determine what portion of the benefits attributed to the head-end steering concept accrued because of (1) the use of a solid-propellant launch vehicle and (2) the use of head-end steering. Individual vehicle comparison of technical, operational, and economic characteristics were presented in the preceding sections. An attempt was made to summarize these comparisons into a single cost breakdown of the effects of using head-end steering, a solid-propellant launch vehicle, and a lifting body spacecraft. This comparison is discussed herein.

Two composite comparisons can be made with the vehicles investigated:

(1) determination of the contribution to cost savings of head-end steering using vehicles with ballistic spacecraft and (2) determination of the contribution using vehicles with lifting body spacecraft. The configurations selected for study lend themselves most directly to the first comparison.

The effect of using a solid-propellant launch vehicle instead of a cryogenic liquid-propellant launch vehicle with a ballistic spacecraft and conventional methods of thrust vector control is shown by comparing Configurations V and III (Table 3-132). The effect of using head-end steering instead of thrust vector control with a solid-propellant launch vehicle and ballistic spacecraft is shown by comparing Configurations IV and V. The effect of using a lifting body spacecraft instead of a ballistic spacecraft with a solid-propellant launch vehicle and head-end steering is shown by comparing Configurations VI and IV. The effect of using the head-end steering concept rather than the more conventional Saturn IB, ballistic spacecraft approach is shown by comparing Configurations VI and III. The cost parameter used for comparison is the average total operations cost based on a 50-flight, 5-year program.

As is indicated, this comparison shows that of the 42.8% net reduction in average flight cost, 24.1% stems from using a lifting body spacecraft, 24.7% from using solid-propellant launch vehicle, while the use of the head-end steering results in a 6.0% increase. Therefore, 56.3% of the reduction is attributed to the spacecraft, 57.8% to the launch vehicle, with an offsetting 14.1% increase to the steering technique. Although this comparison shows a cost disadvantage resulting from the steering technique, it must be remembered that the Configuration IV vehicle requires four steering engines because of the ballistic spacecraft and, because of this, was not a desirable application of the head-end steering concept. Vehicles utilizing lifting body spacecraft and conventional steering with liquid- and solid-propellant vehicles were not configured and a direct comparison of the more favorable head-end steered vehicles could not be made. An attempt to afford this comparison with the vehicle configurations studied is discussed below.

Table 3-132  
EFFECT OF CONCEPTUAL CHANGES ON COST  
(Direct Comparison)

Configurations			Weighted Reduction (%)	Contribution to Reduction (%)
Overall concept				
$\frac{\text{VI}}{\text{III}}$	$= \frac{\$18.87 \times 10^6}{\$32.98 \times 10^6}$	$= 0.572$	42.8	100.0
Spacecraft type				
$\frac{\text{VI}}{\text{IV}}$	$= \frac{\$18.87 \times 10^6}{\$25.63 \times 10^6}$	$= 0.736$	24.1	56.3
Launch vehicle type				
$\frac{\text{V}}{\text{III}}$	$= \frac{\$24.04 \times 10^6}{\$32.98 \times 10^6}$	$= 0.729$	24.7	57.8
Steering technique				
$\frac{\text{IV}}{\text{V}}$	$= \frac{\$25.63 \times 10^6}{\$24.04 \times 10^6}$	$= 1.066$	-6.0	-14.1

For this composite comparison, the effect caused by using a solid-propellant launch vehicle rather than one using liquid propellants is shown by comparing Configurations V and III (Table 3-133). Because the ballistic spacecraft unduly penalized the steering technique comparison, a comparison of Configurations I and II will be used to show the effect of steering, assuming that the differences in mission characteristics will not result in a change in magnitude of the effect. To isolate the effect of spacecraft type, an adjusted comparison is made. Configuration VI is compared to Configuration IV as a base. The comparisons of Configurations IV and V and Configurations I and II are then used to adjust

Table 3-133  
EFFECT OF CONCEPTUAL CHANGES ON COST  
(Adjusted Comparison)

Configurations	Weighted Reduction (%)	Contribution to Reduction (%)
Overall concept		
$\frac{\text{VI}}{\text{III}} = \frac{\$18.87 \times 10^6}{\$32.98 \times 10^6} = 0.572$	42.8	100.0
Spacecraft type		
$\left(\frac{\text{VI}}{\text{IV}}\right) \left[\frac{(\text{IV}/\text{V})}{(\text{I}/\text{II})}\right] = \frac{18.87}{25.63} \left[\frac{(25.63/24.04)}{(28.45/29.47)}\right]$	16.2	
$= 0.813$		
Launch vehicle type		
$\frac{\text{V}}{\text{III}} = \frac{\$24.04 \times 10^6}{\$32.98 \times 10^6} = 0.729$	23.6	55.0
Steering technique		
$\frac{\text{I}}{\text{II}} = \frac{\$28.45 \times 10^6}{\$29.47 \times 10^6} = 0.965$	3.0	7.0

the value to simulate a comparison of spacecraft type for a vehicle using thrust vector control rather than head-end steering. The adjusted comparison is

$$\left(\frac{\text{VI}}{\text{IV}}\right) \left[\frac{(\text{IV}/\text{V})}{(\text{I}/\text{II})}\right]$$

By this comparison, of the 42.8% overall reduction in average flight cost, 16.2% is attributed to the spacecraft, 23.6% to the launch vehicle, and 3.0% to the steering technique. Thus, 38% of the net reduction is attributed to the lifting body spacecraft, 55% to the solid-propellant launch vehicle, and 7% to head-end steering.

As shown by both of these comparisons, the predominant contributing factors to the reduction in average flight cost are the solid-propellant launch vehicle and the lifting body spacecraft. The effect of head-end steering on reducing costs does appear to be significant but only when used with the lifting body spacecraft. The incorporate head-end steering in a vehicle concept would result in operational advantages which could not be shown in terms of cost in this study.

### 3.3.6 Recommendations for Further Study

As discussed in the previous section, a complete isolation of the influence of the spacecraft on the net advantage of the head-end steering concept could not be made with the vehicles selected for investigation. The addition of a conventionally steered (thrust vector control), solid-propellant launch vehicle with a lifting body spacecraft sized for the LORL logistics mission to the matrix of vehicles studied would satisfy this comparison. This additional configuration would be compared to Configuration V. An alternative approach would be to size a conventionally steered, cryogenic liquid-propellant launch vehicle with the Configuration VI spacecraft for comparison to Configuration III. However, this would not provide as desirable a comparison as the first approach. The investigation of a vehicle configuration similar to Configuration VII, but using thrust vector control for first-stage control rather than head-end steering, would also appear to be desirable. This vehicle would be sized to the same mission requirements and sizing criteria and be directly comparable to Configurations VII and VIII.

The approach used to select a thrust vector control technique for those configurations requiring it was discussed in Section 3.3.2.3. As stated therein, the liquid-injection approach was selected from those techniques felt to be within existing technology. This qualification eliminated hot-gas and warm-gas injection systems from consideration. Available empirical data and analytical studies indicate, however, that use of these systems would improve vehicle performance and that these systems would be state-of-the-art technology in the likely operational time period of the logistics systems considered. A study of the application of a hot-gas injection thrust vector control system to the extended MORL logistics requirements, as defined and investigated herein, and its technical, operational, and economic ramifications would, therefore, appear to be warranted.

Some of the vehicles investigated appear to lend themselves to a building block approach to progressive payload capability increase with a minimum number of different stages required. An example of this would be a systematic advance from a Configuration VI vehicle to a Configuration VII vehicle and from there to a modified Configuration VIII vehicle. These vehicles are shown schematically, along with the similarity in stages, in Figure 3-1 13. It would appear that a single 260-in. solid-propellant first stage could be sized for common application to all three vehicles. Configuration VI, then, would require a 156-in. solid-propellant second stage to boost approximately 50,000 lb of payload into orbit. The second step would be to add the S-IVB to the existing 260-in. solid-propellant first stage, eliminating the 156-in. solid-propellant stage, to create a Configuration VII vehicle. This would increase payload capability to approximately 100,000 lb. The third step is the insertion of a 260-in. solid-propellant second stage, using the S-IVB as a third stage to create a modified Configuration VIII. The present Configuration VIII third stage weight corresponds closely to the S-IVB weight. Although this configuration has not been investigated, it is apparent that it would offer a sizable payload capability increase. This, therefore, warrants study as a means of providing a minimized cost approach to a stepped increase in payload capability through stage commonality.

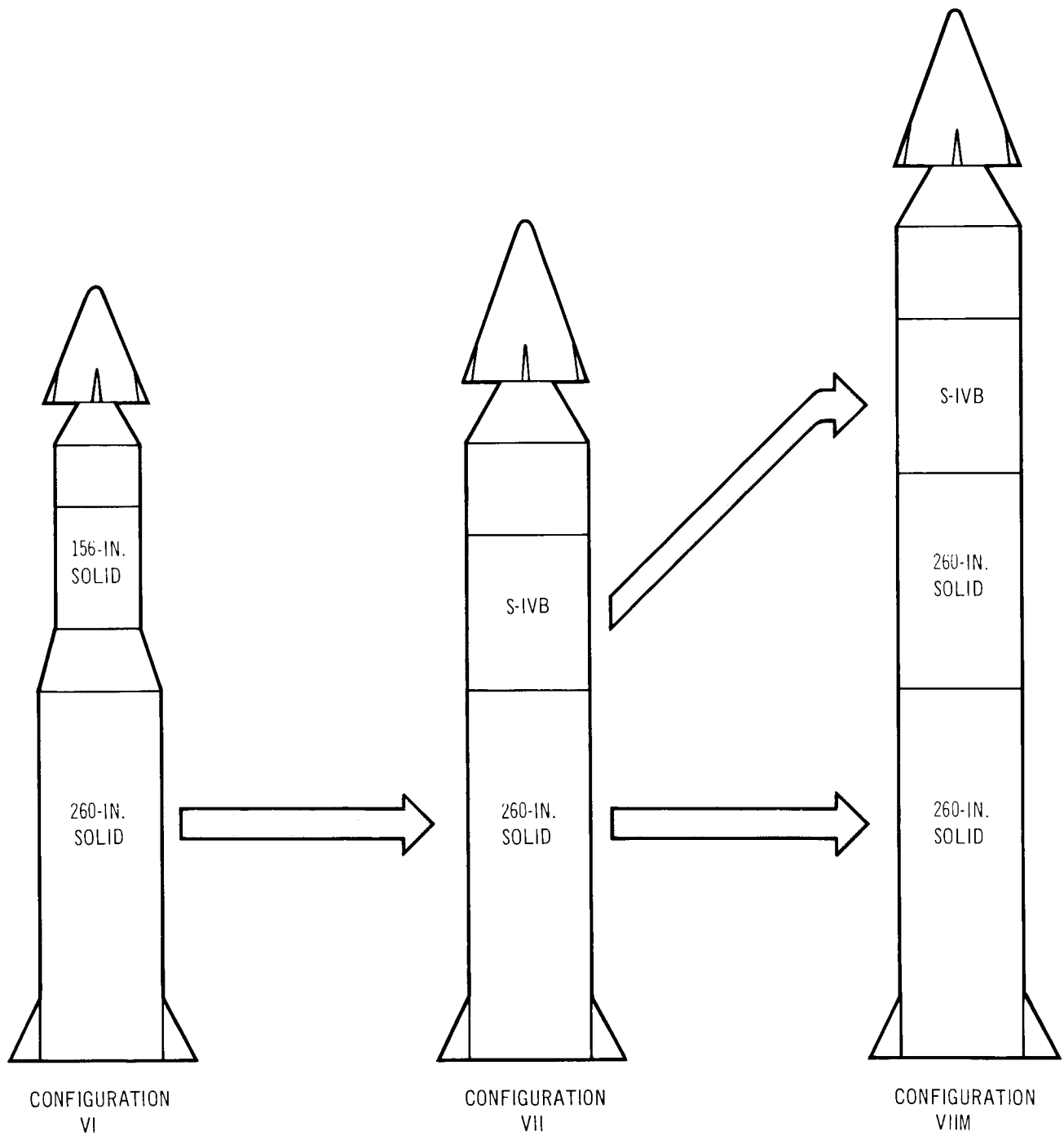


Figure 3-113. Building Block Approach to Payload Increase



## Section 4

### CONCLUSIONS

This section brings together in one location the conclusions independently reported in discussions of each of the three major task areas. The same task grouping is retained, however, for easier reference to the particular section in which the study results are presented.

#### 4.1 VEHICLE REFINEMENT AND OPTIMIZATION (SECTION 3.1)

1. The use of a regressive thrust-time profile in the third stage, together with an improved step throttling program for the steering engines, resulted in an overall reduction of 900,000 lb, or 14%, with reference to the vehicle defined at the end of the Phase I study.
2. Selection of the launch vehicle tail fin size for producing minimum steering control moments proved to be sensitive to fin planform shape in the transonic and supersonic regimes of the ascent trajectory.
3. Control system design requirements are state-of-the-art. Satisfactory gain and phase margins are characteristic of the techniques examined in this study. The first bending mode frequency at the most critical time in the flight (at liftoff) is slightly less than 1 cps or approximately the same as Saturn V.
4. The particular level of TNT equivalence specified for abort escape design analyses did not produce significant abort escape system weight penalties.
5. Escape from incipient first-stage motor failures on the launch pad is feasible, and the spacecraft may be recovered with a normal horizontal landing at Patrick AFB.
6. Escape from incipient first-stage motor failures at the condition of maximum dynamic pressure is feasible, and the spacecraft may be recovered with a normal horizontal landing at Patrick AFB. This is true also for the case of a steering system failure.
7. Recovery from a high-altitude abort situation produces the most severe dynamic pressure and normal acceleration environment for the spacecraft. Mission ascent profiles used in these analyses for vehicle optimization, however, result in abort recovery dynamic pressures which are less than 1,200 lb/ft<sup>2</sup> and, in normal accelerations less, than 6 g's.

#### 4.2 SYSTEM DEFINITION (SECTION 3.2)

1. The use of the solid-propellant launch vehicle propulsion with head-end steering will result in significant savings in launch pad occupancy times when compared to all-liquid-propulsion types employing conventional steering.
2. Transportation of the spacecraft from recovery site to refurbishment site in the Super-Guppy aircraft is feasible.
3. Primary refurbishment tasks would be accomplished at the launch site location.
4. Refurbishment analyses made for the 44-ft HL-10 spacecraft employing an all-ablative, double wall, thermo-protection system resulted in costs slightly over 10% of spacecraft procurement costs per refurbishment. This cost is that required to bring the spacecraft to the same condition as a new spacecraft when received at Cape Kennedy.

#### 4.3 COMPARISON STUDIES (SECTION 3.3)

1. The performance and cost effectiveness of the head-end steering technique were found to be sensitive to the spacecraft configuration employed.
  - A. Head-end steering integrated with a lifting-body type of spacecraft results in a vehicle which is more cost effective, reliable, and has quicker launch response time than a vehicle which uses conventional thrust vector control techniques.
  - B. Head-end steering, when used with a ballistic type of spacecraft, results in a vehicle which is less cost effective and less reliable than when conventional steering techniques are employed.
2. The use of lifting body spacecraft significantly reduces space recovery costs for missions requiring high orbit inclinations.
3. Launch vehicles employing all-solid-propellant stages are more cost effective than those employing all-liquid propulsion.
4. A high-energy liquid upper stage when used with a solid-propellant first stage results in a launch vehicle that is competitive in cost and performance with a vehicle which incorporates solid-propellant motors in all stages.
5. The combined effect of all-solid-propellant booster motors, head-end steering, and a lifting body spacecraft results in a vehicle that is twice as cost effective as one which uses all-liquid propulsion, conventional steering, and a ballistic type spacecraft.

## Section 5

### RECOMMENDATIONS FOR FUTURE STUDY

Specific recommendations for future study have been presented and discussed at the end of each major task area in this report with the exception of significant areas suggested as building-block additions to the Phase I and Phase II studies. Selected recommendations are summarized below, grouped according to their relationship to this study.

#### 5.1 VEHICLE REFINEMENT AND OPTIMIZATION (SECTION 3.1)

1. Refinement and optimization of the spacecraft including:
  - A. Tradeoff studies of thermo-structural techniques.
  - B. Tradeoff studies of the performance and cost characteristics of steering and in-orbit maneuvering propulsion systems.
  - C. Steering engine integration requirements.
2. A study of system cost and performance tradeoffs associated with the distribution of separation energy requirements between the crew module and the solid-propellant booster stages for high-altitude abort situations.
3. Tradeoff studies of vehicle performance versus steering-system weight when flying reduced wind profiles.

#### 5.2 SYSTEM DEFINITION (SECTION 3.2)

An in-depth study of refurbishment requirements as related to system operations and vehicle design.

#### 5.3 COMPARISON STUDIES (SECTION 3.3)

1. A comparative study of more advanced thrust-vector-control techniques in the context of specific system applications.
2. A systems study of the use of launch vehicle stage interchangeability to obtain payload-size flexibility using Configurations VI, VII, and VIII described in this report as basic models.

#### 5.4 ADDITIONAL STUDY STEPS

Preliminary design analysis for a specific mission and launch vehicle, and incorporating head-end steering on a lifting body spacecraft.

Section 6  
REFERENCES

1. G. M. Fuller. A Feasibility Study of Head-End Steering for a Simplified Manned Space Vehicle. Douglas Aircraft Company Report SM-48152. December 1964 (NAS 1-4149).
2. Study of a Ballistics Re-entry-Type Logistics Spacecraft. Lockheed California Company Report LR 17477, 12 February 1964 (NAS 9-1666).
3. Saturn IB Improvement Study (Solid First Stage) Phase II. Second Quarter Report. Douglas Aircraft Company Report SM-51816 dated 11 January 1966. (NAS 8-20242).
4. Mission Requirements of Lifting Systems - Operational Aspects. Boeing Company Report D2-82531-1,2,3,4, August 1965 (NAS 9-3522).
5. Mission Requirements of Lifting Systems - Engineering Aspects. McDonnell Aircraft Corporation Report No. 3832, 18 August 1965. (Final Oral Briefing - NAS 9-3562. )
6. Modified Apollo Logistics Spacecraft Study - Final Report. North American Aviation, Inc. Report SID 63-1461-7, 30 December 1963 (NAS 9-1506)